SHEAR REINFORCEMENT IN REINFORCED CONCRETE COLUMN HEADS

by

Narayani Narasimhan
B.E.(Hons), D.I.C.

A thesis submitted for the Degree of
Doctor of Philosophy
in the Faculty of Engineering of the University of London.

Concrete Structures and Technology
Civil Engineering Department,
Imperial College of Science and Technology,
London.

February 1971

BIBL. LONDON. UNIV

ABSTRACT

Laboratory tests were carried out to study the behaviour of flat slabs supported on columns. The effects of varying amounts of shear reinforcement, and eccentricity of the applied load transmitted to the column, on the ultimate load were of special interest. A method of predicting the ultimate load for concentrically loaded column-slab connections without shear reinforcement is outlined and extended to slabs with shear reinforcement and slabs subjected to combined load. The proposed solutions take into account the strength of materials and the dimensional characteristics of slab.

ACKNOWLEDGEMENTS.

The research work presented in this thesis was carried out in the Imperial College, Concrete Structures and Technology section, under the supervision of Prof. A.L.L. Baker, D.Sc., F.I.C.E., F.I.Struct.E., Hon.A.C.G.E. The author is indebted to him for his valuable discussions and guidance.

Sincere gratitude is due to Dr. P.E. Regan for his help, encouragement and tolerance throughout the work.

The author acknowledges the help received from all laboratory staff and Mr. Stan Finch in particular.

Sincere thanks are due to the Imperial College for the grant of a Bursary made available from C.I.R.I.A. funds in order to achieve this project, and to C.I.R.I.A. for this and its support of the experimental programme.

CONTENTS

PAGE NO.

Abstract. 2

Acknowledgements. 3

Contents. 4

List of Tables. 8

List of Figures. 11

Notations. 16

Chapter I. 19

1.1. Introduction. 19

1.2. Critical part of the slab structure. 19

1.3. Definitions. 19

Flat slab. 19

Column head. 19

Concentric loads. 19

Eccentric or combined loads. 19

Punching shear. 20

1.4. Need for Research. 20

1.5. Object and scope. 20

Chapter II Literature Study. 21

2.1. Introduction. 21

2.2. Early Empirical formulae. 21

Talbot. 21

Graf. 21

Elsner and Hognestad. 21

Keefe. 22

Whitney,. 22

Base. 23

Rosenthal. 23

Yitzhaki. 23

2.3. Elastic Theories. 24

Distasio and Van Buren. 24

Beresford. 25

Long and Bond. 25

Chapter II (contd) PAGE NO.

2.4. Inclined Compression theories. 26
Kinnunen and Nylander. 26
Kinnunen. 27
Anderson 27
Anis 28
2.5. Interaction theories. 31
Moe. 32
Stamenković. 33
Hanson and Hanson. 36
2.6. Design Specifications. 36
British Code 36
A.C.I. 37
Australian Code. 38
Swedish Code. 39

Chapter III Experimental Investigation. 51

3.1. Outline of tests. 51
3.1.1. Series L. 51
3.1.2. Series ES. 51
3.1.3. Corner column. 52
3.2. Materials used. 52
3.2.1. Concrete. 52
3.2.2. Reinforcing steel. 54
3.3. Fabrication and curing. 55
3.4. Testing. 55
3.5. Details of measurements. 56
3.5.1. Deflection. 56
3.5.2. Strains. 56
3.5.3. Cracks and ultimate load. 56

Chapter IV Presentation of Test Results. 65

4.1. Introduction. 65
4.2. Deflection. 65
4.2.1. Series L 65
4.2.2. Series ES 67

Chapter IV (Contd) PAGE NO.

4.3 Strain in shear reinforcement 67
4.3.1. Series L 67
4.3.2. Series ES. 68
4.4. Strain in main steel 68
4.5. Concrete strains on the surface of the slab. . . 69
4.5.1. Series L 69
4.5.2. Series ES. 69
4.5.3. Corner column CS. 70
4.6. Crack patterns 70
4.6.1. Series L. 70
4.6.2. Series ES. 71
4.6.3. Corner column CS 72
4.7. Ultimate load. 72

Chapter V Theory of shear failure in slabs. 123
5.1 General behaviour of slabs. 123
5.2. Vertical shear stresses in the compressive zone. . 124
5.3. Failure criterion for concrete compression zone. . 125
5.4. Dowel action. 126

Chapter VI Proposed Solution. 145
6.1. Introduction 145
6.2. Elastic neutral axis factor n_e 146
6.3. Calculation of Load P_T 147
6.4. Calculation of P_o and the corresponding neutral axis factor n_o. 153
6.4.1. Introduction. 153
6.4.2. Forces in Flexural steel 153
6.4.3. Tangential forces in concrete. 156
6.4.4. Radial force in concrete 158
6.4.5. Conditions of equilibrium 158
6.4.6. Variation of neutral axis depth from n_e to n_o. . 159
6.5. Calculation of P_{YL} and neutral axis factor n_{YL} . . 161
6.6. Calculation of failure load. 161
6.7. Combined load. 163
6.8. Shear reinforcement. 164

Chapter VI (contd.) PAGE NO.

6.9. Analysis of existing data. 166

6.10 Simplified formula.. 174

6.11. Edge Columns with normal moments. 174

6.12 Edge Columns with tangential moments. 186

6.13 Corner columns. 187

Chapter VII Analysis of Test results using proposed solution. 205

7.1. Introduction.. 205

7.1.1. Effect of eccentricity of the load. 206

7.1.2. Effect of column size to slab depth. 206

7.1.3. Effect of main reinforcement. 206

7.1.4. Effect of openings. 207

7.1.5. Effect of shear reinforcement. 207

7.2. Comparison with existing formulae. Internal columns. 244

7.2.1. Introduction. 244

7.2.2. Slabs with concentric loading and no shear reinforcement. 244

7.2.3. Slabs with combined loading and no shear reinforcement. 248

7.2.4. Slabs with concentric loading and shear reinforcement. 250

7.2.5. Slabs with combined loading and shear reinforcement. 252

7.3. Comparison with existing formulae - edge columns. 254

Chapter VIII Conclusions and suggestions for future research. 256

8.1. Conclusions. 256

8.2. Recommendations for design. 257

8.3. Suggestion for future research. 259

References. 260

LIST OF TABLES.

Table No.		Page No.
III-1	Details of control tests - concrete.	53
III-2	Details of reinforcing bars.	54
IV-1	Details of shear reinforcement.	66
V-1	Values of dowel constant K_d for various types of bar.	130
VI-1	Values of n_e for various values of U_w and r_{st}. . .	148
VI-2	Values of m_r and m_t for various values of B/L. . .	151
VI-3	Values of k_T for square columns.	154
VI-4	Values of n_o for various values of $r_{st}.f_y$ and U_w.	160
VI-5	Values of n_{YL} for various values of $r_{st}.f_y$ and U_w.	162
VI-6	Values of ALPHA 1 for various values of B/L and n_e.	168
VI-7	Values of ALPHA 2 and ALPHA 3 for various values of n.	171
VI-8	Comparison between actual loads and calculated loads - using accurate solution.	175
VI-9	Edge columns with normal moment - Comparison. . .	184
VI-10	Corner columns.	189
	Comparison of actual and calculated loads using simplified formula - Internal columns.	
VII-1	Slabs tested by Hognestad - concentric load. . .	212
VII-2	Slabs tested by Ivy - concentric load.	213
VII-3	Slabs tested by Kinnunen and Nylander - concentric load.	214
VII-4	Slabs tested by Mowrer and Vanderbelt - concentric load.	215
VII-5	Slabs tested by Manterola - concentric load. . .	216
VII-6	Slabs tested by Hognestad, Elsner and Hansen - concentric load.	217
VII-7	Slabs tested by Moe - combined load.	218
VII-8	Slabs tested by Stamenković - combined load. . .	219
VII-9	Slabs tested by Anis - combined load.	220
VII-10	Slabs tested by Hognestad - concentric load + shear reinforcement.	221

LIST OF TABLES (Contd)

Table No.		Page No.
VII-11	Slabs tested by Anderson - concentric load + shear reinforcement.	222
VII-12	Slabs tested by Moe - concentric load + shear reinforcement.	224
VII-13	Slabs tested by Wenthur - concentric load + shear reinforcement.	225
VII-14	Slabs tested by Author - combined load + shear reinforcement.	227
VII-15	Slabs tested by Graf - concentric load + shear reinforcement.	228
VII-16	Slabs tested by Moe - concentration of reinforcement near the column.	230
VII-17	Slabs tested by Moe - holes near the column. . .	232
	Slabs tested by Mowrer and Vanderbelt - holes near the column.	234
VII-18	Slabs tested by Hognestad - supports on two sides only.	236
VII-19	Slabs tested by Richart and Kluge - isolated loads.	237
VII-20	Slabs tested by Stamenković and Moe - rectangular columns.	239
VII-21	Footings tested by Richart.	240
VII-22	Edge columns with moments perpendicular to free edge Slabs tested by the Author. Slabs tested by Anderson. Slabs tested by Stamenković. Slabs tested by Tankut.	241
VII-23	Edge columns with tangential moments. . . . . . Slabs tested by Stamenković Slabs tested by Tankut.	243

LIST OF TABLES (CONTD)

Table No. Page No.

Comparison with existing formulae - Internal Columns

VII-24 Slabs with concentric load and no shear reinforcement-using formulae given by Hognestad, Moe, ACI, Anis, C.P.114 and proposed solution. 245

VII-25 Slabs with combined load and no shear reinforcement - using formulae given by Hognestad, Moe, ACI, Anis, C.P.114 and proposed solution. 249

VII-26 Slabs with concentric load and shear reinforcement - using formulae given by Hognestad, Moe, ACI and proposed solution. 251

VII-27 Slabs with combined load and shear reinforcement - using formulae given by Hognestad, Moe, ACI and proposed solution. 253

Comparison with existing formulae - Edge Columns.

VII-28 Edge columns with moments perpendicular to free edge - using formula given by Anderson, ACI and proposed solution. 255

LIST OF FIGURES.

FIGURE NUMBER		PAGE NO.
1	Shear stress distribution - according to Distasio and Van Buren.	41
2	Idealised model - Kinnunen and Nylander.	42
3	Idealised model - Anderson.	43
4	Idealised model - Anis.	44
5	Category 1 and 2 according to Stamenković.	45
6	Idealised model for internal column (bending resistance) - Stamenković.	46
7a	Interaction diagram - Category 1.	47
7b	Interaction diagram - Category 2.	48
8a	Shear reinforcement details - Australian Code.	49
8b	Shear reinforcement details - Swedish Code.	50
9	Details of main reinforcement - Series L.	57
10	Details of main reinforcement - Series ES.	58
10a	Details of reinforcement - Slab CS.	59
11	Stress strain diagram for steel.	60
12	Details of shear reinforcement.	61
13a	Testing arrangement.	62
13b	Details of test rig.	63
14	Location of dial gauges - Series L and ES.	64
15a	Deflection profile of slabs L_9 and L_7.	74
15b	Deflection profile of slabs L_1, L_4, L_3 and L_5.	75
15c	Deflection profile of slabs L_2, L_8 and L_{11}.	76
16	Load V_s deflection - slabs L_2, L_8 and L_{11}.	77
17	Deflection profile - parallel to free edge - Series ES.	78
18	Deflection profile - perpendicular to free edge - Series ES.	79
19	Load V_s deflection - Series ES.	80

LIST OF FIGURES (Contd.)

FIGURE NUMBERS		PAGE NO.
20	Load V_s strain in shear reinforcement - Slab L_5 (ϕ_v = 13 mm, EC = 305 mm).	81
21	Load V_s strain in shear reinforcement - Slab L_4 (ϕ_v = 6.5 mm, EC - 305 mm).	82
22	Load V_s strain in shear reinforcement - Slab L_6 (ϕ_v = 8.0 mm, EC = 152.5 mm θ - 45°).	83
23	Load V_s strain in shear reinforcement - Slab L_{10} (ϕ_v = 8.0 mm, EC = 152.5 mm, θ = 30°).	84
24	Load V_s strain in shear reinforcement - Slab L_{11} (2 layers of shear reinforcement, EC = 152.5 mm). . .	85
25	Tearing of reinforcement showing dowel action. . .	86
26	Slab after failure - showing anchorage of shear reinforcement.	86
27	Slab after failure - showing NO crushing.	87
28	Slab after failure indicating a flat crack.	87
29	Applied load V_s shear carried by shear hat.	88
30	Load V_s strain in shear reinforcement - Slab ES3 (ϕ_v = 6.5 mm, EC = 228.5 mm).	89
31	Load V_s strain in shear reinforcement - Slab ES_4 (ϕ_v = 9.5 mm, EC = 228.5 mm).	90
32	Load V_s strain in shear reinforcement - Slab ES_6 (ϕ_v = 6.5 mm, EC = 0).	91
33	Load V_s strain in shear reinforcement - Slab ES_7 (ϕ_v = 6.5 mm, EC = - 228.5 mm).	92
34	Applied load V_s load carried by shear hat - Series ES.	93
35a	Load V_s strain in main steel - Slab L_1.	94
35b	Load V_s strain in main steel - Slab L_3.	95
35c	Load V_s strain in main steel - Slab L_4.	96
35d	Load V_s strain in main steel - Slab L_5.	97

LIST OF FIGURES (Contd.)

FIGURE NUMBER.		PAGE NO.
35e	Load V_s strain in main steel - Slab L_6.	98
36a	Load V_s strain in main steel - Slab ES_1..	99
36b	Load V_s strain in main steel - Slab ES_2.	100
36c	Load V_s strain in main steel - Slab ES_3.	101
36d	Load V_s strain in main steel - Slab ES_4.	102
37	Tangential and radial concrete strains across the slab.	103
38a	Load V_s strain in concrete - Slab L_1.	104
38b	Load V_s strain in concrete - Slab L_3.	105
38c	Load V_s strain in concrete - Slab L_4.	106
38d	Load V_s strain in concrete - Slab L_5.	107
38e	Load V_s strain in concrete - Slab L_{11}.	108
39a	Load V_s strain in concrete - Slab ES_1.	109
39b	Load V_s strain in concrete - Slab ES_3.	110
39c	Load V_s strain in concrete - Slab ES_5.	111
40	Load V_s strain in concrete - Slab CS.	112
41	Crack pattern of slabs L_9 and L_1 - Bottom surface. . .	113
42	Crack pattern of slabs L_3 and L_4 - Bottom surface. .	114
43	Crack pattern of slab L_{11} - Bottom surface.	115
44	Special support details.	116
45	Crack pattern of slabs - Top surfaces, ES_6, ES_3 and ES_7.	117
46	Crack pattern of slabs - Bottom surfaces, ES_1, ES_2 and ES_5.	118
47	Crack pattern of slabs - Bottom surface, ES_6, ES_3 and ES_7.	119
48	Corner slab CS after failure.	120
49	Torsional crack on edges - Series ES	121
50	Shear cracks at the free edge - Series ES.	122

LIST OF FIGURES (Contd.)

FIGURE NUMBER.		PAGE NO.
51	Types of failures that can occur.	135
52	Distribution of shear stress across the depth. . .	136
53	Theoretical distribution of moments and shear around the column - according to Moe.	137
54	Actual distribution of shear around the column. . .	138
55	Idealised concrete element and isometric of Tetrahedral model - Baker.	139
56	Failure criteria for concrete - Test results. . . .	140
57	Dowel action.	141
58	Relation between tensile splitting and compressive strength of concrete.	142
59	Dowel specimen used by Roy and Baumann.	143
60	Dowel specimen used by Arroyo and Krefeld and Thurston.	144
61	Assumed model when the slab is in an elasto-plastic state.	190
62	Neutral axis depth V_s load.	191
63	Stress-strain diagram for concrete.	192
64	$n_e V_s \quad {}^{n_e^2}/_{1-n_e}$	193
65	Systems 1 and system 2.	194
66	$m \; V_s \; P$ for calculation of P_T	194
67	Simplified stress-strain diagram for concrete. . .	195
68	$n_o V_s \left(\frac{0.50 \, n_o^2}{1-n_o} \cdot C_4 + 0.714 \, n_o \frac{B}{L}\right)$	196
69	$n \; V_s \; \frac{r_{st} \cdot f_y}{\sigma_{CT}}$ for various values of ${}^{r_s}/_{L}$.	197
70	$n \; V_s \; P$	198
71	$n \; V_s$ ALPHA.	199

LIST OF FIGURES (Contd.)

FIGURE NUMBERS		PAGE NO.
72	Graphical solution for calculation of Q - Sheet 1.	200
72	Graphical solution for calculation of Q - Sheet 2.	201
73	Perimeters to be used for various shapes of column.	202
74	Edge column subjected to combined load (eccentricity perpendicular to the free edge). . . .	203
75	Interaction diagram for edge columns (eccentricity perpendicular to the free edge) Q/Q_{CAL} V_s M/M_{CAL}. .	204
76	Effect of eccentricity on edge columns with tangential moment.	208
77	Effect of eccentricity on internal column with combined loading.	209
78	Effect of column size to slab depth on calculated failure load.	210
79	Effect of openings.	211
80	Details of shear reinforcement - Hognestad.	223
81	Details of shear reinforcement - Anderson.	223
82	Details of shear reinforcement - Wanthur.	226
83	Details of shear reinforcement - Graf.	229
84	Reinforcement layout - Moe.	231
85	Details of holes - Moe.	233
86	Details of holes - Mowrer and Vanderbelt.	235
87	Location of loads - Richart and Kluge.	238
88	Division of slab panels.	258

NOTATIONS.

A_{st} - Area of main steel provided over width L.

A_{sq} - Area of shear reinforcement.

B - Diameter of a circular column.

b - Side length of a square column or breadth in general.

b_x - Side length of a column parallel to the free edge, in the case of an external column-slab connection.

b_y - side length of a column perpendicular to the free edge in the case of an external column-slab connection.

b_{col} - perimeter of the column.

b_c - concrete perimeter.

b_d - dowel perimeter.

$C_R . \Delta \phi$ - Radial compressive force in the compression zone in a sector element with a centre angle $\Delta \phi$.

$C_T . \Delta \phi$ - Radial resultant of the tangential forces in concrete, in a sector element with a central angle $\Delta \phi$.

C_{pl} - Radius of the slab area in which the tangential compressive strain in the concrete at the bottom surface of the slab is greater than e_{pl} at failure.

d - Total depth of the slab.

d_1 - Effective depth of the slab.

e_s - Strain in reinforcement.

e_c - Extreme fibre strain in concrete at the bottom surface of the slab.

e_{pl} - Concrete strain at which state of plastification is reached.

EC - Eccentricity of the load to be transferred across the potentially critical crack measured from centre of the column.

f_{av} - Average compressive stress in a fully developed concrete block.

f_y - Yield point stress of flexural reinforcement.

f_{yq} - Yield point stress of shear reinforcement.

I - Moment of inortia.

K_d - Dowel constant.

L - Theoretical span length of a test slab (side of a square slab or diameter of the slab).

l - span length of a panel in a flat slab.

M_{CAL} - Calculated ultimate resisting moment.

M - Ultimate resisting moment at failure.

m - moment per unit length.

n_e - neutral axis factor when the slab system is elastic.

n_o - neutral axis factor corresponding to the stage when all the tangential steel has yielded.

n_{YL} - neutral axis factor corresponding to the yield line load.

$n.d_1$ - neutral axis depth at failure.

P_T - Load corresponding initial tangential steel yield.

P_o - Load corresponding to all tangential steel yielding.

P_{YL} - Load corresponding to yield line failure.

Q - Vertical load.

Q_d - Calculated dowel force.

Q_c - Calculated shear force carried by the concrete compressive zone.

Q_v - Force carried by the shear reinforcement

Q_{CAL} - Calculated failure load.

Q_u, Q_{TEST} - Actual failure load.

q - Shear stress.

r_s - Radius of the slab area in which yield point stress f_y is reached in the tangential reinforcement at failure.

r_{st} - ratio of reinforcement $(\frac{A_{st}}{L.d_1})$.

T_r - Resisting moment in torsion.

$T.\Delta\phi$ - Radial resultant of the forces in the flexural reinforcement in a sector element with a central angle $\Delta\phi$.

U_w - Cube strength of concrete.

U_{cyl} - Cylinder strength of concrete.

U_t - Concrete tensile strength (split cylinder)

V_{max} - Maximum shear stress around the periphery of the slab specimen.

V_{avg} - Average shear stress around the periphery of the slab specimen.

w - Deflection.

X,Y - Side lengths of an external column-slab connection as defined in Fig. 74.

ϕ_M - Diameter of main steel.

ϕ_v - Diameter of shear reinforcement.

θ - Inclination of shear reinforcement.

ψ - Angle of rotation of the sector element.

$\Delta\phi$ - Central angle of a sector element of the slab over the column.

v - Poissons ratio.

CHAPTER I.

1.1 Introduction:-

The ultimate flexural theory of slabs has been developed in considerable detail during recent years. A fundamental assumption of this theory is that the slabs are designed so that sudden shear failures do not occur before the full flexural capacity of the slab is reached. Hence a deeper knowledge regarding the characteristics of shear failures, particularly punching failures in flat slabs, is urgently needed, so that effective measures, such as the provision of shear reinforcement, may be taken in their design.

1.2 Critical part of the Slab Structure:

The junctions between the slab and the supporting columns are the critical areas as far as the strength of a flat slab structure is concerned. The stress distribution in the slab portion around a column is very complex due to concentrations of high bending moments and shear forces, but it is essential that the strength of the connection is computed accurately.

1.3 Definitions:

Some of the terms which are used in the text repeatedly are defined below.

Flat slab: A flat slab structure without drops or column capitals. The term 'slab' should be taken to represent flat slabs throughout this work.

Column head: Area of the slab common to both slab and column.

Concentric loads: Loads applied concentric with the centre line of the column. In the case of internal column connections this type of load produces no unbalanced moments at the connection.

Eccentric or Combined Load: Load applied eccentric to the centre line of column producing shear and unbalanced moments at the connection.

Combined loading occurs in practice under the following circumstances:

a. Due to uneven distribution of live loads (i.e.) one bay more heavily loaded than the adjacent ones.

b. Uneven spacing of columns.

c. Lateral forces caused by wind in combination with vertical loads.

Punching Shear: In the present study, a punching of column stub through the slab is regarded as punching shear failure unless such punching takes place after the full flexural capacity of the slab has developed by inelastic action.

1.4 Need for Research:

Over the years a number of experimental studies have been carried out by various investigators.

Many have proposed equations, empirical and theoretical (see chapter II), applicable to axially loaded internal columns. The majority of the results published are from tests of column heads with no shear reinforcement. Such connections generally fail by Punching Shear, which means that the strength of the whole structure would be limited by the localized shear effect. A natural reaction to this is to consider the use of shear reinforcement to raise the punching strength and to study the effectiveness of such shear reinforcement by tests.

None of the existing methods seem to predict the ultimate load of connections subjected to eccentric loading accurately. This lack of data on combined loading and on external columns is reflected in the British Code C.P.114[22] which refers neither to combined loads nor to columns with differing locations.

1.5 Object and Scope:

The present investigation was taken up in order to establish simple design equations to predict the ultimate loads of column heads under concentric or eccentric loads.

The main object of the research was:-

a) To study the mechanism of failure in shear of reinforced concrete column heads.

b) To study the effectiveness of shear reinforcement as a means of preventing punching failures.

c) To propose simple design equations to predict Ultimate Strengths of slabs with reasonable accuracy.

CHAPTER II

Literature Study.

2.1 Introduction.

Numerous tests of "Punching shear" in reinforced concrete slabs have been made in different parts of the world and the majority of them has resulted in empirical formulae, and some in theoretical ones. The available literature is broadly classified here, under the following headings: Early empirical formulae, Elastic theories, Compression theories, Interaction theories and Specifications.

2.2 Early Empirical Formulae.

In 1913 Talbolt[1] presented the results of his extensive tests carried out on wall and column footings. Based on a number of shear failures which occurred during the investigation, he computed the shear stress q with the following formula:

$$q = \frac{Q}{4b.jd} \leq q \text{ allowable} \quad \ldots\ldots\ldots\ldots (1)$$

where 4b, jd and Q are the perimiter of the column footing, distance from the centre of the reinforcing bars to the centre of the compressive stresses and the shear force respectively. The generally allowable value of q for punching shear for 1:2:4 concrete is specified as 120 psi (working stress).

In 1933 Graf[2] carried out a series of shear tests on three slabs loaded near the supports. He computed the shearing stresses by the formula,

$$q = \frac{Q}{4.b.d} \leq q \text{ allowable} \quad \ldots\ldots\ldots\ldots (2)$$

where d is the total depth of the slab. He concluded that the shear capacity decreased as the load moved away from the support. A series of eight slabs was tested in 1938[3] to study the effect of shear reinforcement.

In 1953 Elstner and Hognestad[4] reported shear tests of twenty-four slabs supported on all four sides and again in 1956[5] of another thirty-eight square slabs. This time the effect of the various

variables such as concrete strength, amount of flexural tension and compression reinforcement, shear reinforcement, size of column and eccentricity of the applied load were studied. Based on their results they proposed the formula,

$$q = \frac{Q}{\frac{7}{8}.4.bd_1} = 333 + .046\ U_{cyl}/\phi_o \text{(in psi)} \quad \ldots\ldots (3)$$

for slabs with no shear reinforcement.

$$\text{and} \quad q = \frac{333 + .046\ U_{cyl}}{\phi_o} + U_{cyl} \times \left[\frac{A_{sq}.f_{yq}.\sin\theta}{\frac{7}{8}.4.bd_1\ U_{cyl}} - .05\right] \text{ in psi} \quad \ldots (3a)$$

for slabs with shear reinforcement

where

4b is the circumference of the loaded area.

and ϕ_o - ratio of ultimate shear capacity to ultimate flexural capacity computed without regard to shear.

The formula implies that the shear reinforcement becomes effective only when its contribution exceeds a value equal to 0.05 U_{cyl}. This is proved otherwise in the slabs tested in the present series.

In 1954 Keefe[6] investigated the effectiveness of shear reinforcement. Two pairs of octagonally shaped slabs were tested and he concluded that the provision of shear reinforcement increased the shear capacity by about 40%.

Whitney[7], on the basis of a re-evaluation of previously reported results, presented an ultimate strength theory in 1957. Assuming shear strength to be primarily a function of ultimate resisting moment of the slab per unit width, (m), inside the 'pyramid of rupture' he proposed,

$$q = 100 + 0.75\ \frac{m}{d_1^2} \cdot \sqrt{d_1/l_s} \text{ in psi} \quad \ldots\ldots\ldots (4)$$

where q is computed at a distance of $d_1/2$ from the perimeter of loaded area and l_s the shear span, which he suggests as the distance from the edge of the column to the line of contraflexure.

In 1959 Base[8] carried out tests on a series of small square slabs, some with shear reinforcement. The shear reinforcement was comprised of vertical stirrups and bent up bars. Since the yield point of the reinforcing steel is not stated in Base's paper it was not possible to utilise the results for the present investigation. According to Base, vertical stirrups were more advantageous than bent up bars.

In the same year Rosenthal[9] reported the results of tests on eleven simply supported circular reinforced concrete slabs. These tests included three specimens loaded eccentrically through column stubs. His conclusion that the eccentricity of the applied load did not have any influence on the punching strength was not justified, in view of the fact that the eccentricity of the loads in the test specimens was far too small to arrive at the above result.

In 1966 Yitzaki[10] carried out a series of tests on circular slabs with bent up bars as shear reinforcement. He concluded that the punching resistance depends on the strength of main steel as in the case of flexural strength. Comparing the flexural strength and punching strength the aim was to obtain a balanced reinforcement.

Based on his experiments he proposed,

$$Q_{punching} = 8d_1^2(1 - r_{st}.f_{y/2\ U_{cyl}})(149.3 + .164\ r_{st}.f_y)(1 + .5b/d_1) \quad \ldots\ldots\ldots\ldots (5)$$

Equating the punching strength to flexural strength

$$Q_{flex} = 8d_1^2(1 - r_{st}.f_y/2\ U_{cyl}).r_{st}.f_y \quad \ldots\ldots (5a)$$

and, balanced reinforcement was given as,

$$r_{st}.f_y = \frac{149.3(1 + .5b/d_1)}{1 - .164(1 + .5b/d_1)} \quad \ldots\ldots\ldots\ldots (5b)$$

Accordingly slabs with less reinforcement than the balanced one for a specific b/d ratio will fail in flexure, whilst slabs with more reinforcement than the balanced one will fail in punching. Use of diagonal reinforcement was recommended as shear reinforcement to prevent punching failures. In obtaining the required diagonal reinforcement the resistance to punching of the concrete was disregarded and was designed to carry the entire load. The above proposal would result in a conservative design and hence not economical.

The various formulae given by the above authors are based on assumed critical sections and co-efficients which fit particular test results. They take little or no account of the actual behaviour of slabs. For example, they ignore the variation in stresses between the head and tail ends of shear cracks.

Even if this basic lack of logic were accepted the formulae would still be of little use as the range of circumstances over which satisfactory predictions of strength are given by any one formula is extremely limited. This early work has thus only one real use now, and that is the considerable total number of test results produced.

2.3 Elastic theories.

DI STASIO AND VAN BUREN.

Di Stasio and Van Buren[11] recommended a working stress method of analysis for the strength of slab-column connections under eccentric loading. In consideration of punching shear it was proposed to limit the maximum vertical shear stress to .0625 U_{cyl} on a critical section adjacent to the column periphery. For stresses from shear and moment, the diagonal tension recommendations of 1956 A.C.I. Building Code[23] are followed. The critical section is assumed to be located at a distance d_1 outside the column periphery, and the maximum vertical shear stresses are limited to 0.03 U_{cyl}.

The assumed vertical shear stress distribution is shown in Fig (1) and the maximum vertical shear stress q is calculated from,

$$q = \frac{d}{\frac{7}{8} d_1} \cdot \left[\frac{Q}{A_C} + \frac{(Q.EC - m_{AB} - m_{CD})}{J_C} \right] \cdot \frac{1}{1 + (m_p - 1) r_{st}} \quad \ldots (6)$$

where $A_C = 2d(x + y)$

$$J_C = \frac{dx^3}{6} + \frac{xd^3}{6} + \frac{ydx^2}{2}$$

m_p = the modular ratio; x and y as defined in Fig.(1).

m_{AB}, m_{CD} = flexural moments acting on faces AB and CD of critical section.

Since the moment resisted by sides AB and CD is a predetermined quantity the above implies that the shear stress is produced only when Q.EC exceeds $(m_{AB} + m_{CD})$. Calculating the vertical shear stress as a function of this difference was found not to be in accord with the behaviour of the specimens tested later by Hanson and Hanson[21].

BERESFORD.

In 1967 Beresford[12] reported the results of six slabs with edge columns subjected to combined load. He tested and reviewed the existing methods (i.e.) Di Stasio, Van Buren and Anderson (see section 2.4). He concluded that "the method proposed by Di Stasio - Van Buren predicted safe results for the slabs tested. In this method, as in the ultimate design approach proposed by Anderson it appears that the contribution to the strength by transverse reinforcement is not taken into account. The results indicate that this factor has a marked influence on the ultimate capacity". The transverse reinforcement is the steel passing through the column parallel to the free edge.

LONG AND BOND.

A theoretical method of analysis based on elastic thin plate theory was presented to the I.C.E. by Long and Bond[13] in May 1967. An octahedral stress criterion of failure was used in the analysis. It was assumed that the shear stress distribution on a vertical plane is constant between the neutral axis and the reinforcement. This is unrealistic in view of the fact that, in the presence of shear cracks the tensile zone will not be capable of supporting such a large part of shear. The proposed analysis assumes elastic behaviour throughout and is applicable only to internal columns with concentric loads, and is hence restricted in scope.

2.4 Inclined Compression Theories:

The preceeding methods have all been phrased in terms of essentially nominal shear stresses. Those reviewed in this section attempt a more realistic approach in which shear is taken to be supported by inclination of thrust in the compressive zone.

SWEDISH THEORY (KTH STOCKHOLM).

A valuable study of shear failures of slabs was presented by Kinunnen and Nylander[14] in 1960. This was the first real attempt to establish a theoretical method of analysis. A number of circular slabs 1840 mm in diameter and 150 mm thick with central columns were tested.

Based on their observations of the behaviour of slabs during testing, they arrived at an idealised model as shown in Fig. (2). The outer portions of the slab, bounded by the shear crack and by radial cracks were supposed to be carried by the conical shell that develops from the column to the bottom of shear crack.

The conical shell was assumed to have the shape indicated in the figure and its thickness was assumed to vary in such a way that the compressive stresses at the intersection with the column and at the root of the shear crack were approximately equal.

Further it was assumed that the slab sectors outside the shear crack rotated round the root of the shear crack and the slab portion inside the shear crack did not undergo any deformation in a radial vertical plane.

The various forces on a sector, (i.e.) the oblique compression force $T_o.\Delta\phi$ in the compressed conical shell, the tangential forces $C_T.\Delta\phi$ in the concrete, the tangential forces $R_1.\Delta\phi$ in the reinforcement at rightangles to the radial cracks and the radial forces $R_2.\Delta\phi$ in the reinforcement cutting across the shear crack, follow from the angle of rotation ψ. Based on their observation of tests the criterion of failure was expressed as follows: "failure occurs when the concrete strain in the tangential direction, 'e_{ct}', at the bottom surface of the slab reaches a characteristic value". Expressions for e_{ct} in agreement with test results were given in terms of B/d.

By applying the above failure criterion and conditions of equilibrium and compatability a method was outlined to predict Punching

loads by a trial and error process.

The method is very cumbersome to use. The contribution of the dowel force (which is quite considerable in two-way reinforced slabs) to the carrying capacity of the slab is ignored and hence the proposed solution is too conservative and not satisfactory.

In 1963 Kinnunen[15] extended the above theory of Kinnunen and Nylander[14], based on the same conical concept but including dowel and membrane effects to estimate the punching loads of two-way reinforced slabs. However the method was not made simpler in any respect and the same cumbersome trial and error process was used.

In 1963 Andersson[16] carried out a series of tests on slabs (28 no), to study the effects produced by the type and amount of shear reinforcement on the ultimate load and the deformations at failure. A simplified approach based on the conical concept of Kinnunen and Nylander was given. The idealised model adopted for the analysis is shown in Fig. (3). The case where failure was initiated by a flat crack underneath and outside was dealt with in the analysis. (This will hardly be the case if the shear reinforcement is not large enough, in which case the shear crack cuts the shear reinforcement).

The outer slab portion was assumed to be bounded by a tangential flexural crack and two radial cracks and carried by the compression zone which is supported on the column. The centre of rotation of the sector element at failure was assumed to be located at the point of intersection on the extension of the generatrix of the column and a horizontal plane passing through the root of the tangential flexural crack. A criterion that "failure occurs when the compressive strain at the stage of plastification is reached in a tangential direction of the concrete up to a certain definite distance from the centre of the slab" was adopted. A trial and error process to calculate punching loads from conditions of equilibrium is outlined.

Since the critical shear is assumed to fall outside the shear reinforcement, (presumably due to the large area of shear reinforcement) it would imply that the only contribution of shear reinforcement is that, a part of it acts as flexural reinforcement and thereby increases the flexural reinforcement above the column. The observation that, the vertical component of the resultant of the forces in the shear reinforcement at the yield point stress was 50 to 60% of the ultimate load

led to a design recommendation that to be on the safe side 70% of the ultimate load has to be carried by shear reinforcement which seems to have no general justification.

In a later investigation Anderson[17] tested a series of 3 slabs with edge columns subjected to normal moments. He proposed a formula for calculating the nominal shear stress at the ultimate load stage at the column-slab interface. The proportion of the bending moment passing through the inside column face to that resisted by torsional moments on the column sides was determined from the number of reinforcing bars which pass through the column on the sides in question. The torsional component was considered to be resisted by a shear stress distribution based on complete plasticity of the rectangular sections at the column sides. The resultant of the downward acting shear stress on these sections was added to the end reactions of the slab, determined in the normal manner, and this enhanced force acts upon the column-slab interface.

A nominal shear stress was given by:

$$q = \frac{Q}{d_1^2} \left[\frac{1 + K.EC/2(b_y - d_1/3)}{b_x/d_1 + b_y/d_1(1+b_y/6EC) + /2} \right] \text{ in } {}^{kgm}/_{cm}{}^2. \quad .(7)$$

where K is the proportion of bending moment resisted by torsional stresses, taken as 0.4 and the other symbols are as defined in the general notation.

He concluded that the tests indicate that shear stresses at edge columns could be permitted to be as high as those at internal ones if the edge columns were designed for a moment, 20% greater than the calculated moment.

ANIS

The latest work on this type of approach to the ultimate strength of column heads without shear reinforcement was done by Anis[18] at Imperial College. Employing the conical shell concept, originally adopted by Kinnunen and Nylander[14] a theory was developed, based on simplified assumptions to calculate the ultimate strength of column heads for combined loads and differing column locations. Like Kinnunen and Nylander he assumed that each slab sector outside the shear crack, bounded by two radial cracks and the circumference of the slab, was to be regarded as a rigid body. Under the load action this rigid element was assumed to rotate about the neutral axis at the column face which

was assumed to be located at the root of the shear crack. Unlike Kinnunen and Nylander and later Kinnunen[15], according to whom failure occurred when the strain in the concrete, in the tangential direction reached a limiting value, Anis according to his observations, claimed failure occurs when the concrete strain in the radial direction reaches a limiting value. However in the majority of the tests conducted by the author, neither the tangential nor the radial strains were large enough to cause failure, though in general the tangential strains were much higher than the radial ones.

Based on the above failure criterion and on an idealised model as shown in Fig. (4), Anis set up seven equations based on the following assumptions.

1. Plane sections not crossed by the shear crack remain plane after deformation, and hence the value of extreme fibre can be calculated from the expression $f = \frac{Q}{A} \pm \frac{Q \cdot EC}{I} \cdot \frac{d_1}{2}$.
2. A simplified bi-linear stress-strain diagram for concrete under bi-axial state of stress is used.
3. All steel remains elastic up to failure.
4. The angle of inclination of the shear crack is 45° to the horizontal plane. (Although in other parts crack lengths are calculated inconsistent with this.)
5. The shear cracking load V_{cr} = 0.6 times the ultimate load.

The proposed equations based on compatability and equilibrium conditions are as follows:

$$\Delta c = \int_{x=o}^{x=c} e_c^{\,r}\, x\, dx \quad \ldots\ldots\ldots\ldots\ldots\ldots (8)$$

$$c/r = \frac{d_1}{r} \cdot \frac{1}{\tan B^{*}} \cdot (1 - i - n/2) \quad \ldots\ldots\ldots\ldots (9)$$

$$2n\, r/c = \frac{\Delta c}{e_o^{*} c} \left[2m^{*}p' \,(1+r/c)\left(\frac{1-n}{n}\right) + 2m^{*}p\left(\frac{1-n}{n}\right) \cdot \log \frac{1+\frac{a}{r}}{1+c/r} - \bar{n} \log\left(1+\frac{a}{r}\right) \right] \quad \ldots\ldots\ldots\ldots (10)$$

$$\tan B^{*} = \frac{d_1}{a} \cdot \frac{1}{n} \left[n.(1-n/2) + \frac{\bar{n}}{2} \cdot \frac{c}{re_o^{*}} \log(1+a/r)(1-\bar{n}/3) \right] \quad . . (11)$$

$$r+c-d_1/2 = \frac{V_{cr}}{2\pi d_1 . q_{cr}} \quad . . . . . (12)$$

or

$$r+c-d/2 = \frac{V_{cr} + \sqrt{V_{cr}^{2} + 44 d_1 \, q_{cr} . \, V_r \, . \, EC}}{12.56 \, d_1 \, . \, q_{cr}} \quad . . . . . (13)$$

$$V = 2\pi r \; nd \, f_o^{*} \, . \, \tan B^{*} \quad . . . . . (14)$$

where

Δc = the total deformation of concrete in radial direction along the horizontal projection of shear crack.

e_c^{r} = compressive strain of concrete measured in the radial direction.

e_o^{r} = strain limit in concrete under bi-axial compressive stress.

c = length of the horizontal projection of shear crack.

n = neutral axis factor in the radial direction in a slab failing in shear.

$\bar{n}$ = neutral axis factor in the tangential direction.

B^{*} = inclination of the thrust line in the radial direction.

q_{cr} = shear cracking stress.

and f_o^{*} = cubic strength of concrete under combined bi-axial compression.

With the above equations in hand, a method of successive approximation as given below was adopted to solve the equations and to arrive at the ultimate load. (See p.67-68 Anis[18].)

<u>Step 1</u> Substituting equation (9) into equation (8) $\frac{\Delta c}{e_o^{*} c}$ is expressed in terms of tan B^{*}, i and n.

For given values of i, families of curves can be plotted (Fig.27[18]) giving n V_s $\frac{\Delta c}{e_o^{*} c}$ relationships for various values of tan B^{*}.

Step 2 Choose a value of i and assume values for n and B^*, then Fig. 27[18] will give the corresponding value of $\frac{\Delta c}{e_o{}^*c}$.

Step 3 With this value of $\frac{\Delta c}{e_o{}^*c}$, and the assumed value of n determine tan B^* from equation (11).

Step 4 If tan B^* so obtained does not agree with the assumed value in Step 2, then assume a different value of tan B^* and repeat steps (2) to (4) until values agree.

Step 5 Substitute equation (9) into equation (10) so that $\frac{\Delta c}{e_o{}^*c}$ is expressed in terms of n, i and B^*.

Step 6 Use the values of i, n and tan B^* in Steps (2) to (4) in equation (10) after substitution as described in Step (5), and determine the corresponding $\frac{\Delta c}{e_o{}^*c}$ value. If this does not agree with the value obtained in Step (2) assume a different value of n and repeat steps (2) to (6) until the values agree.

Step 7 Substitute equation (14) in equation (12) with V_{cr} = .6V, then c will be expressed in terms of tan B^* and n.

Step 8 Use the values of n and tan B^* that satisfy steps (2) to (7) and equation (12) to obtain a value for i. If this value does not agree with that assumed in Step (2), assume a different value of i and repeat steps (2) to (8) until they agree, consequently all unknowns can be determined.

If the slab is under eccentric load then the procedure is similar to the above but equation (13) is to be used instead of equation (12).

This method has been further extended to edge and corner columns. It can be seen from the above how cumbersome and time consuming the whole process is. After all this, the accuracy so obtained is no better than that of simpler methods and hence the theory is considered not suitable for practical use.

2.5 Interaction Theories:

The methods reviewed here are more empirical than the inclined compression theories of Section 2.4. Their authors have

made rational studies of the factors influencing punching strength, but express their proposals in terms of relatively simple equations based on interactions between shear and flexure.

MOE.

In 1961 Moe[19] reported an investigation of the shearing strengths of slabs and footings. This included 43 slabs which he tested and a statistical study of 140 footings and 120 slabs. All the slabs tested by Moe were 6' square and 6" thick. The principal variables were the concentration of tensile reinforcement in narrow bands across the column, some special type of shear reinforcement, column sizes, holes near the columns and eccentricity of the applied load.

A linear interaction formula was proposed to express the relation between the flexural and punching strengths of slabs as:

$$\frac{Q}{Q_o} + k_1 \cdot \frac{Q}{Q_{flex}} = (1 - C.b/_{d_1}) \quad \ldots\ldots\ldots\ldots (15)$$

where Q_o, the fictitious shear strength = $A.4bd.\sqrt{U_{cyl}}$

Q_{flex} - the flexural capacity of the slab with no regard to eccentricity.

When rewritten equation (15) gives,

$$q = \frac{Q}{4b\ d_1} = \left[A \times (1 - Cb/_{d_1}) - B\ \phi_o\right] \sqrt{U_{cyl}} \quad \ldots\ldots (16)$$

where $B = k_1 A$ and

$\phi_o = Q/_{Q_{flex}}$

The constants A, B and C were determined empirically on the basis of a statistical study of results from tests on 106 footings and 37 slabs. The equation so arrived at was also modified to include effects of shear reinforcement and transfer of bending moments. The shear reinforcement was assumed to be fully effective in transmitting shear force and its effect directly additive to the shear resistance of the concrete.

The expressions are as follows:

$$q = \frac{Q}{4bd_1\sqrt{U_{cyl}}} = \frac{15(1-0.075b/d_1) + A_{sq}f_{yq}\sin\theta/4bd_1\sqrt{U_{cyl}}}{1 + 21\,b.d_1\sqrt{U_{cyl}}/Q_{flex}}$$

(in psi) . . . . . (17)

and $Q_{eccentric} = \dfrac{Q_{concentric}}{1 + EC/b}$ . . . . . (17a)

Though the proposed expressions generally give satisfactory predictions of ultimate strengths of centrally loaded junctions, when applied to eccentrically loaded junctions they are unsatisfactory.

STAMENKOVIĆ

In 1970 Stamenković [20] conducted a series of tests to study the effect of vertical (concentric), horizontal and combined vertical and horizontal (eccentric) loading, applied to column stubs for differing locations of columns. On the basis of his investigation (52 slabs, 3 ft. square and 3 inches thick) and existing data he concluded as far as concentrically loaded junctions are concerned, the ultimate strength can be calculated by modifying Moe's formula. He proposed (Imperial units)

$$Q = k\left[4bd_1\sqrt{U_{cyl}} \cdot \frac{15(1-.075\,b/d_1)}{1 + 21bd_1\sqrt{U_{cyl}}/Q_{flex}}\right] \quad . . . . (18)$$

with $k = .9$ for internal columns

$= .9\,\dfrac{(3b + 4d)}{(4b + 8d)}$ for edge columns and

$= .9\,\dfrac{(2b + 2d)}{(4b + 8d)}$ for corner columns.

It is to be noted that although Moe assumed the critical section to be at the column face, the above formulae give a proportionate reduction based on the perimeters d_1 out from the column face, for edge and corner columns.

The ultimate strength at the column head under horizontal loading only (pure moment), was given as a combination of bending resistance developed at the interfaces normal to the moment plane.

Depending on the number of column faces normal to the moment plane which provide bending resistance he divided the slabs into two categories (viz.).

(1) Internal columns and edge columns with tangential moments where there are two faces resisting bending directly and

(2) Edge columns with normal moments and corner columns, where there is only a single face offering resistance to bending directly (see Fig. 5).

For the purpose of calculating the internal forces balancing the external moment, he assumes the model shown in Fig. 6, for category 1 (applicable to internal columns and edge columns with tangential moment).

The compressive forces are assumed to act with a lever arm $d/_2$. The increment in steel forces FS_2 and FS_1 across the column face is assumed to be dependent on the bond stress. He arrives at the expression for bending resistance as,

$$\text{bending resistance} = M_{concrete} + M_{steel} + M_{shear}$$

$$= k_c' \cdot U_w \cdot b_1 \cdot (d/_2)^2 + 0.13\, U_w \Sigma O\, b_2 \cdot a_s + k_s'\, U_w b_1 \cdot b_2 d_1 \quad \ldots\ldots\ldots\ldots (19)$$

where k_c' and k_s' are constants

b_1 side length of the column normal to the moment plane

b_2 side length of the column parallel to the moment plane.

and ΣO the sum of the perimeters of top or bottom bars which ever is smaller.

For the bending resistance provided by a single column face, as in category (2) the ultimate strength design formula given by A.C.I. was adopted.

$$\text{Bending resistance} = 0.9\, A_s\, f_y \cdot d_1\, (1 - .59\, pf_{y/U_{cyl}}) \quad \ldots (20)$$

where A_s is the area of tensile steel passing through the column face normal to the moment plane.

$$P = \frac{A_s}{b_1 d_1} \quad \text{and } U_{cyl} = .85\ U_w$$

Torsional resistance at the column head was expressed by:

$$M_{tu} = \frac{n \cdot k' \cdot A_t \cdot f_y}{b_2 d} \int g \cdot dA$$

where n = the number of interfaces at which torsional resistance is developed.

k' coefficient of friction.

A_t area of reinforcement passing through torsional faces.

g the radius from the centroid of intersection to an area dA. In obtaining the value of the integral it is assumed that at failure the shear stress is uniform.

From this,

$$\text{Torsional resistance } M_{tu} = \frac{n \cdot k' A_t\ f_y}{b_2 d} \cdot d^2\ (b_2 - d/_3) \cdot \quad (21)$$

Subjected to the limitation that the nominal shear stress $\frac{k'\ A_t f_y}{b_2 d} < 1/_3\ U_w$

A combination of equations (19) and (21) was shown to give the internal forces for category (1) and a combination of equations (20) and (21) was shown to give the internal forces balancing external moments in the case of category (2).

For column heads subjected to eccentric or combined loads interaction curves were proposed. Interaction curves were given in terms of $Q/_{Q_u}$ and $M/_{M_u}$ where Q and M are the observed failure load and moment, Q_u is the failure load due to concentric load Q only and M_u the ultimate moment for horizontal forces only. The proposed interaction relations were,

$$\frac{Q}{Q_u} + M/_{M_u} = 1 \quad \ldots\ldots\ldots\ldots\ldots\ldots\ldots \quad (22)$$

in the case of internal columns and edge columns with tangential moments

and $\left(\frac{Q}{Q_u}\right)^2 + \left(\frac{M}{M_u}\right)^2 = 1$ . . . . . (23)

in the case of edge columns with normal moments and corner columns. Some of the interaction curves as given in his thesis are given in Figs. 7a and 7b.

HANSON AND HANSON.

N.W. Hanson and H.W. Hanson[21] reviewed recent methods in the light of their own experiments and with special reference to Moe's work. They arr ived at the conclusion that the method of ultimate strength design recommended by A.C.I.- A.S.C.E. 326[24] would give a better prediction of ultimate strength than any other method if the moment reduction factor K was changed from 0.2 (original recommendation) to 0.4.

Their experimental investigation consisted of 17 slabs subjected to combined loading. Out of the 17 slabs tested, all except one, represented column slab connection of an interior panel, while one specimen represented an edge column connection. Eight of the slabs had holes adjacent to the column and three slabs were tested under reversal of loading.

2.6 Design Specifications.

British Code of Practice C.P.114[22].

The working load shearing stresses in slabs are calculated at a distance from the column equal to half the overall depth and the permissible stresses are as follows:

$$\text{for } U_w \leq 3000 \text{ psi, q permissible} = U_{w/30}$$

$$\text{and for } U_w > 3000 \text{ psi, q permissible} = U_{w/50} + 40 \quad \ldots (24)$$

$$\text{but q permissible} \not> 130 \text{ psi}$$

It should be noted that neither the effect of eccentric load nor the differing locations of columns is taken into consideration here.

A.C.I.318-63[23]

The critical section in this Code, is taken at distance equal to half the effective depth from the column face and the nominal ultimate shear stress is calculated from

$$q = \frac{Q}{b_{crit} \cdot d_1} \not> 4\phi \sqrt{U_{cyl}} \text{ (in psi)} \quad \ldots\ldots (25)$$

where ϕ is the capacity reduction factor.

For slabs greater than 10" thick, shear reinforcement can be used, in which case the shear reinforcement's contribution is added to the concrete term. The permissible shear stress in this case is increased, but may not exceed $6\ \phi \sqrt{U_{cyl}}$.

Here again the effect of eccentricity is not dealt with. But in the code commentary[24], the transfer of moment between the column and slab is covered. It is required that the stresses on the critical periphery surrounding the column, which involve shear, torsion and bending moments be investigated by a rational analysis. For this purpose a width of the slab at right-angles to the direction of moment is considered effective, which extends not more than 1.5 d_1 each side of the column. The critical periphery is considered as extending $d_{1/2}$ on each side of the column in the direction of the moment.

The latest recommendations for revisions[25] include the effect of combined load in greater detail. When unbalanced gravity loads, wind, earthquake or other lateral forces cause transfer of moment between slab and column a fraction of the moment is assumed to be resisted by uneven shear.

Shear stresses are taken as varying linearly about the centroid of the critical section and must not exceed $4\sqrt{U_{cyl}}$ in psi. The maximum shear stress can be calculated from:

$$q = Q/A_c \pm \frac{k\,M}{J_c} \cdot y \quad \ldots\ldots\ldots\ldots\ldots\ldots (26)$$

where $$k = 1 - \frac{1}{1 + \frac{2}{3}\sqrt{\frac{c_1 + d}{c_2 + d_1}}}$$

$c_2 + d_1$ is the width of the face of the critical section resisting moment

$c_1 + d_1$ is the width of face at right-angles to $(c_2 + d_1)$

and $A_c = 2d_1 (c_1 + c_2 + 2d_1)$

$$J_c = \frac{d_1 (c_1 + d_1)^3}{6} + \frac{(c_2 + d_1)d_1^3}{6} + \frac{d_1(c_2 + d_1)(c_1 + d_1)^2}{2}$$

for an interior column.

Similar equations based on a critical section $d_{1/2}$ out from the column face are to be used for columns located at edges or corners of slabs.

Requirements regarding detailing of shear reinforcement are also outlined consistent with those for beams. When there is shear reinforcement the allowable stresses are to be increased by 50%, but the shear reinforcement is allowed to work at only half its yield stress.

Separate recommendations are made for designs using "shear heads" made up of rolled steel sections, but these are not included in this thesis. The recommendations are a considerable improvement on the existing specification.

Australian Code of Practice AS.CA2 1963[26]

The working load shearing stresses are calculated at a vertical section located at a distance of 0.7 d_1 out from the column face from the formula,

$$q = \frac{Q}{b_{crit} d_1} \not> (0.02\ U_{cyl} + 20) \text{ psi or } 90 \text{ psi}$$

whichever is less . . . . . (27)

b_{crit} is the perimeter at the critical section.

For slabs more than 8" thick shear reinforcement can be used, in which case the critical section for shear is taken as the vertical section located at the centre line of the lower anchorage ring of the shear cage. Details of a shear cage with minimum dimensional requirements and types of construction are also given (see Fig. 8a). Further it is specified that the cross-sectional area of web reinforcement in the shear cage shall not be less than 0.8 % of an area which is the product of the perimeter of the lower anchorage ring of the shear cage and $\frac{3}{4}$ in.

plus the overall vertical depth of the shear cage. The shear cage is to occupy the whole depth of space between the lowest layer of bottom reinforcement and the lowest layer of top reinforcement.

The fact that the diameter of web reinforcement is not to be less than $\frac{1}{2}$ in. would generally result in slabs very much over-reinforced in shear.

Here again neither the effect of eccentric load nor differing locations of columns is taken into consideration.

Swedish Code[27]:

In this Code the column load is to be determined according to the elastic theory or if the deformation conditions used for the determination of moments give a column load more than 10% greater than its elastic value then the larger value is to be used.

A nominal shear stress is calculated using

$$q_{\text{nominal}} = \frac{Q}{d^2(B/d + 1)} \quad \text{for } B/d \leq 3.5 \quad \ldots\ldots\ldots (28)$$

$$\text{and} \qquad = \frac{Q}{d^2(0.5B/d + 2.75)} \quad \text{for } 3.5 < B/d < 6. \quad . \; (29)$$

the value of Q nominal is compared with q, obtained from the formula $q_1 = q_o \frac{1.5}{10 + c/2d}$ (the values of q_o are given in a tabular form for various concrete strengths). Rules for calculating the value of c ($\frac{1}{2}$c being the distance from the centre of the column to the point of contraflexure for radial moment) in conjunction with the moment design are given separately.

a) If $q_{\text{nominal}} \leq 0.65q_1$ no further check is required

b) If $0.65\, q_1 < q_{\text{nominal}} \leq q_1$ no shear reinforcement is required, and

c) If $q_1 < q_{\text{nominal}} \leq 1.5\, q_1$ shear reinforcement is to be provided.

The shear reinforcement which can be used for slabs under (c) are divided into two types. The first type are those made of loops so arranged that they make no contribution to the flexural reinforcement

over the column and the second type is of bent down flexural bars. In regard to placing the shear reinforcement, it is to satisfy the requirements of Fig. 8b. The loops are to be placed within a band of breadth $\sim$ 1.5 d around the column. The distance between two loops is not to exceed .75 d and is to be suitably anchored around the flexural reinforcement in the top of the slab. In the case of the bent down bars, an equal number of bars of shear reinforcement is to be provided in both reinforcement directions. When the shear reinforcement is bent down in two layers, each layer is to contain approximately the same number of bars. Further the sum of the vertical components of the forces in the shear reinforcement is to be at least 75% of the column load.

In the case of an eccentric load causing moment at the column, the worst quarter is to be designed taking the slab as encastre at the column. The negative steel required for this is to be provided for all segments of the slab.

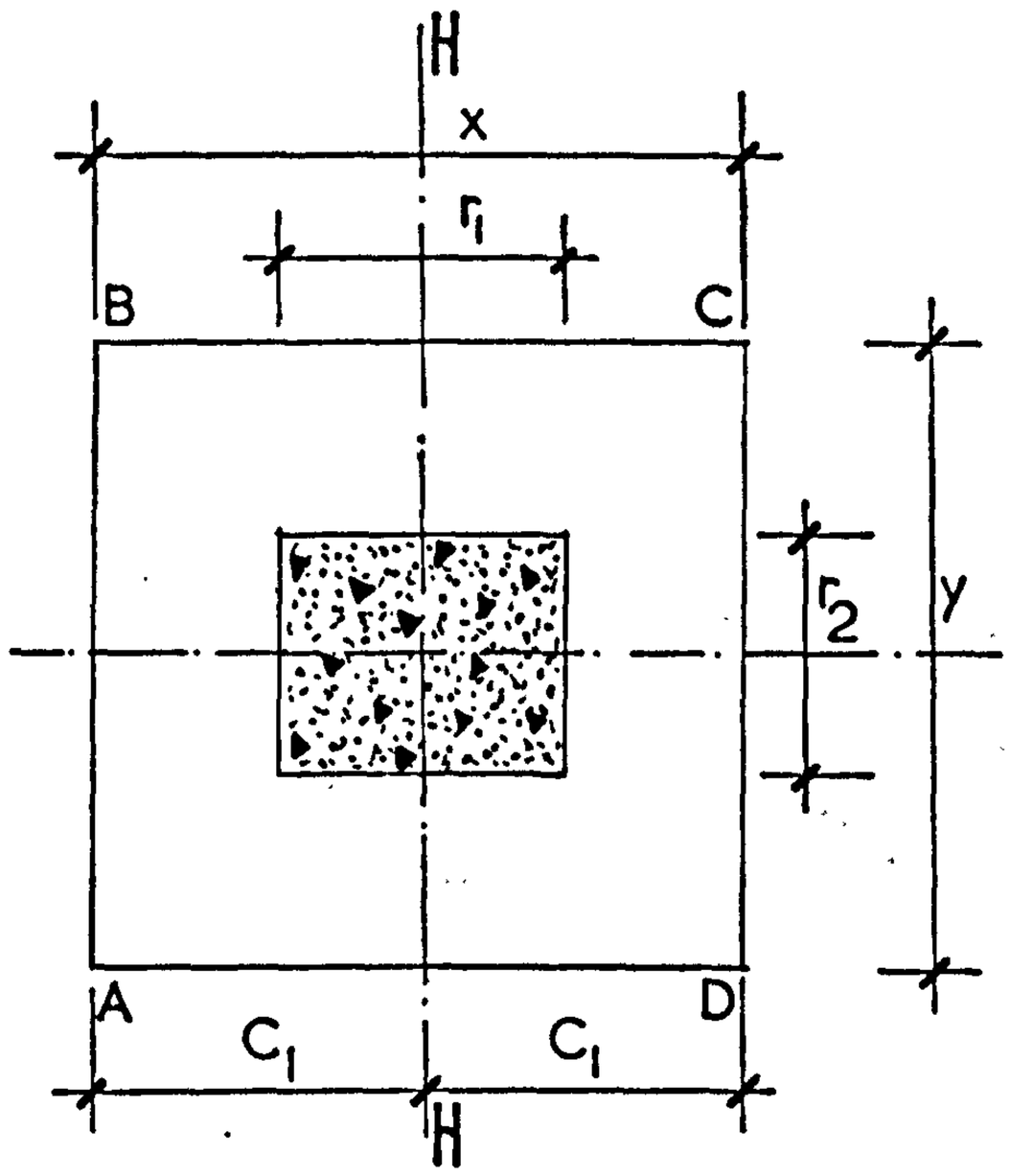

CRITICAL SECTION.

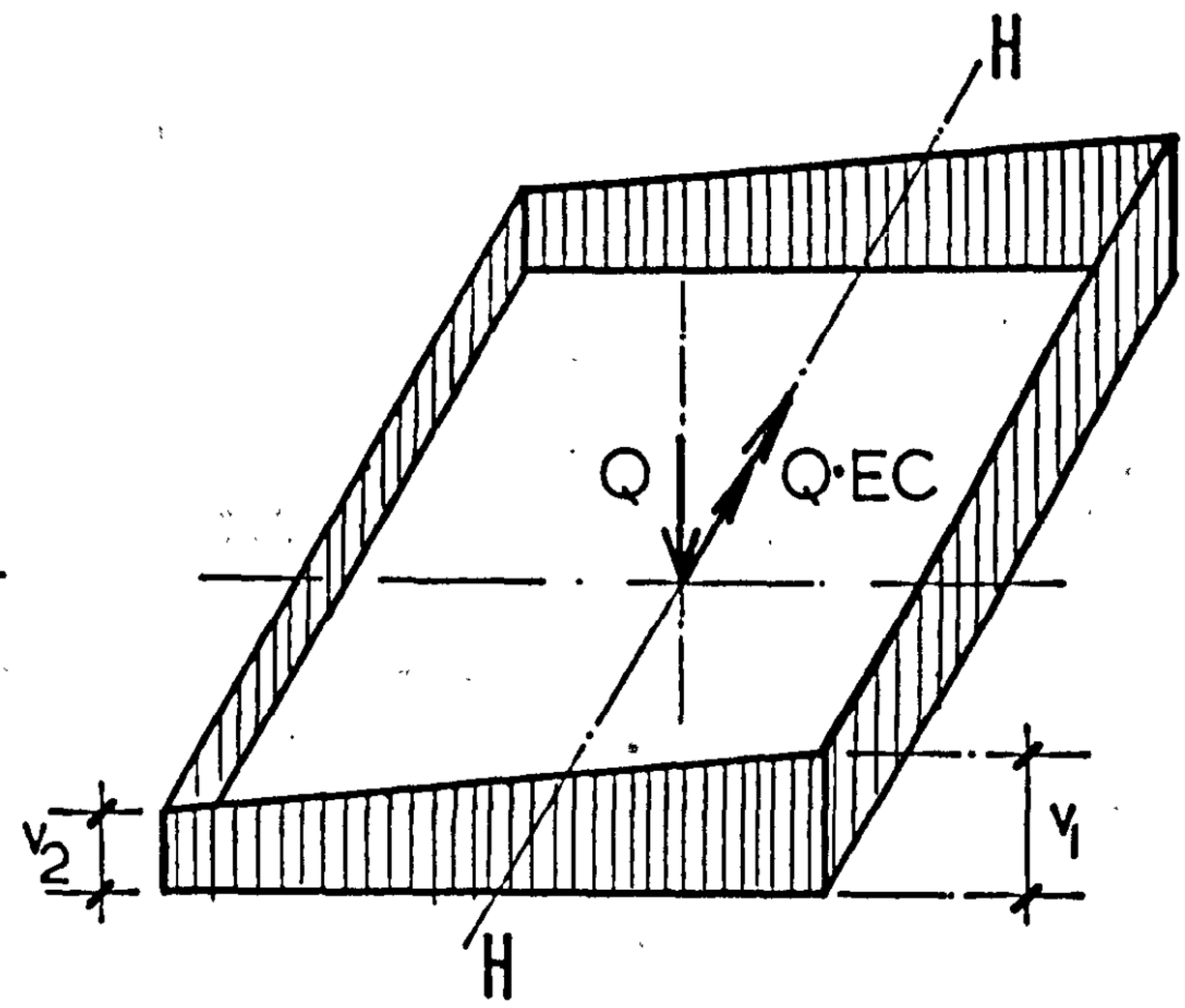

VERTICAL SHEAR STRESS AT CRITICAL SECTION.

INTERNAL COLUMNS.

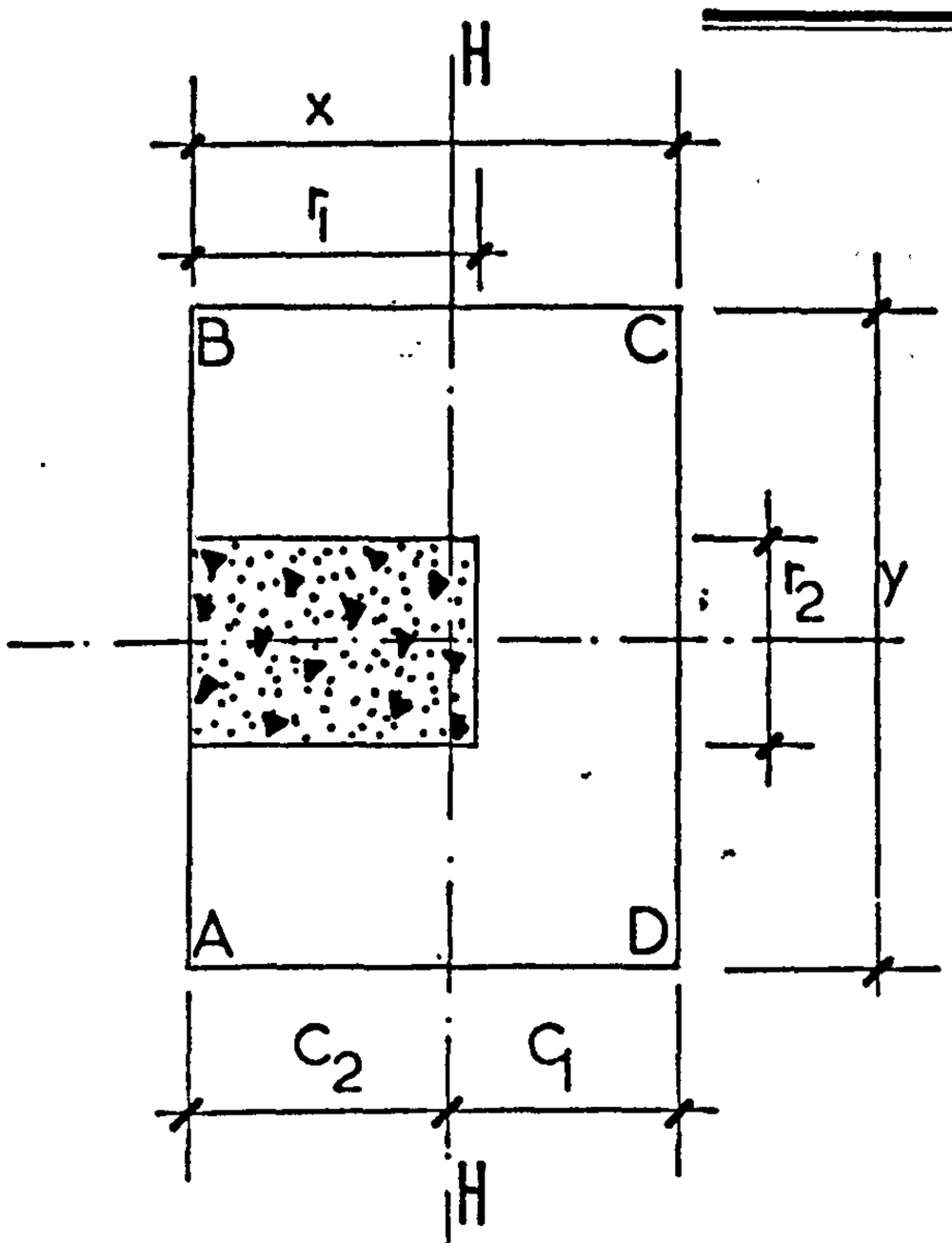

CRITICAL SECTION.

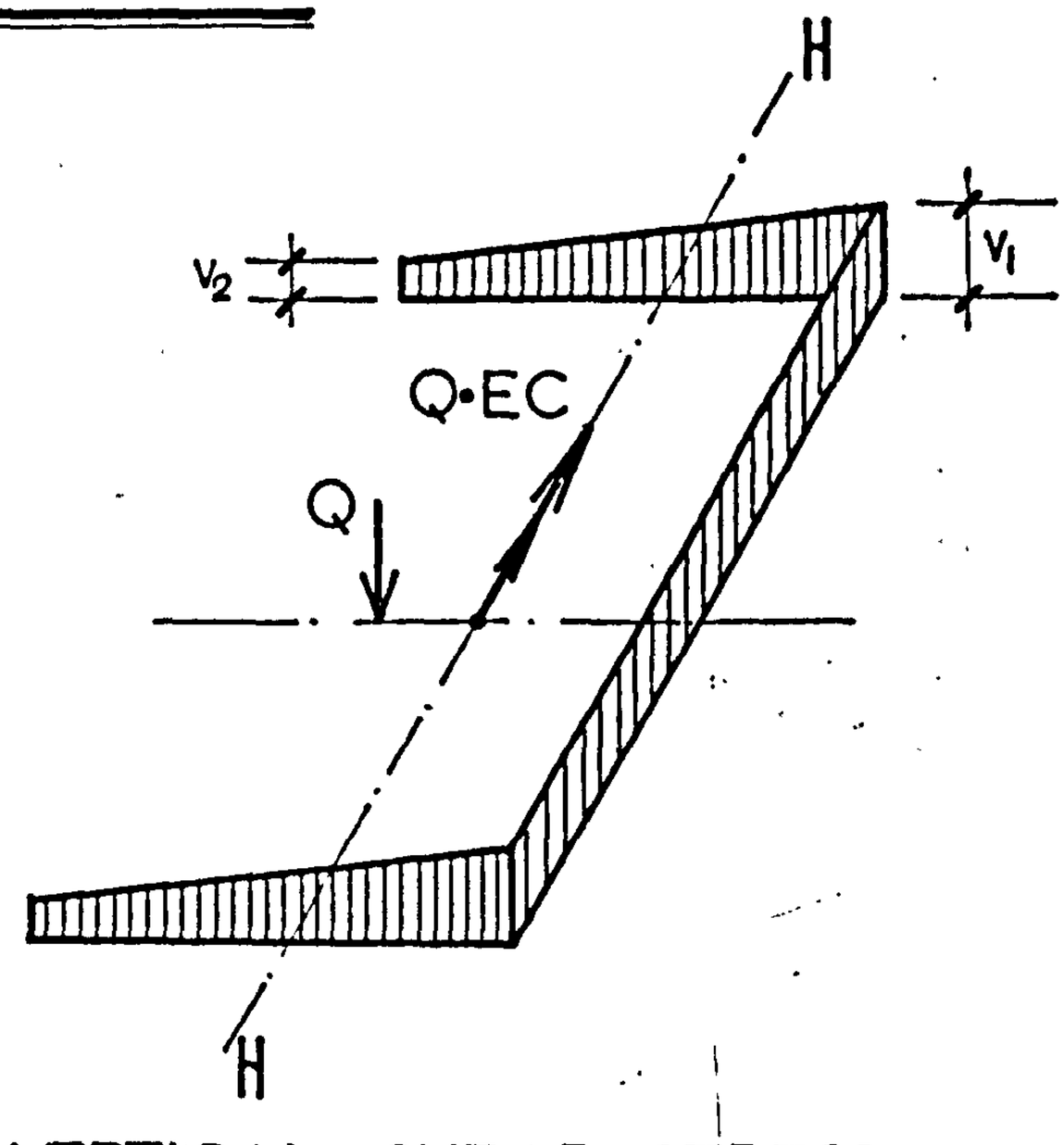

VERTICAL SHEAR STRESS AT CRITICAL SECTION.

EXTERNAL COLUMNS.

Fig.1. DISTASTIO'S ASSUMED SHEAR STRESS DISTRIBUTION.

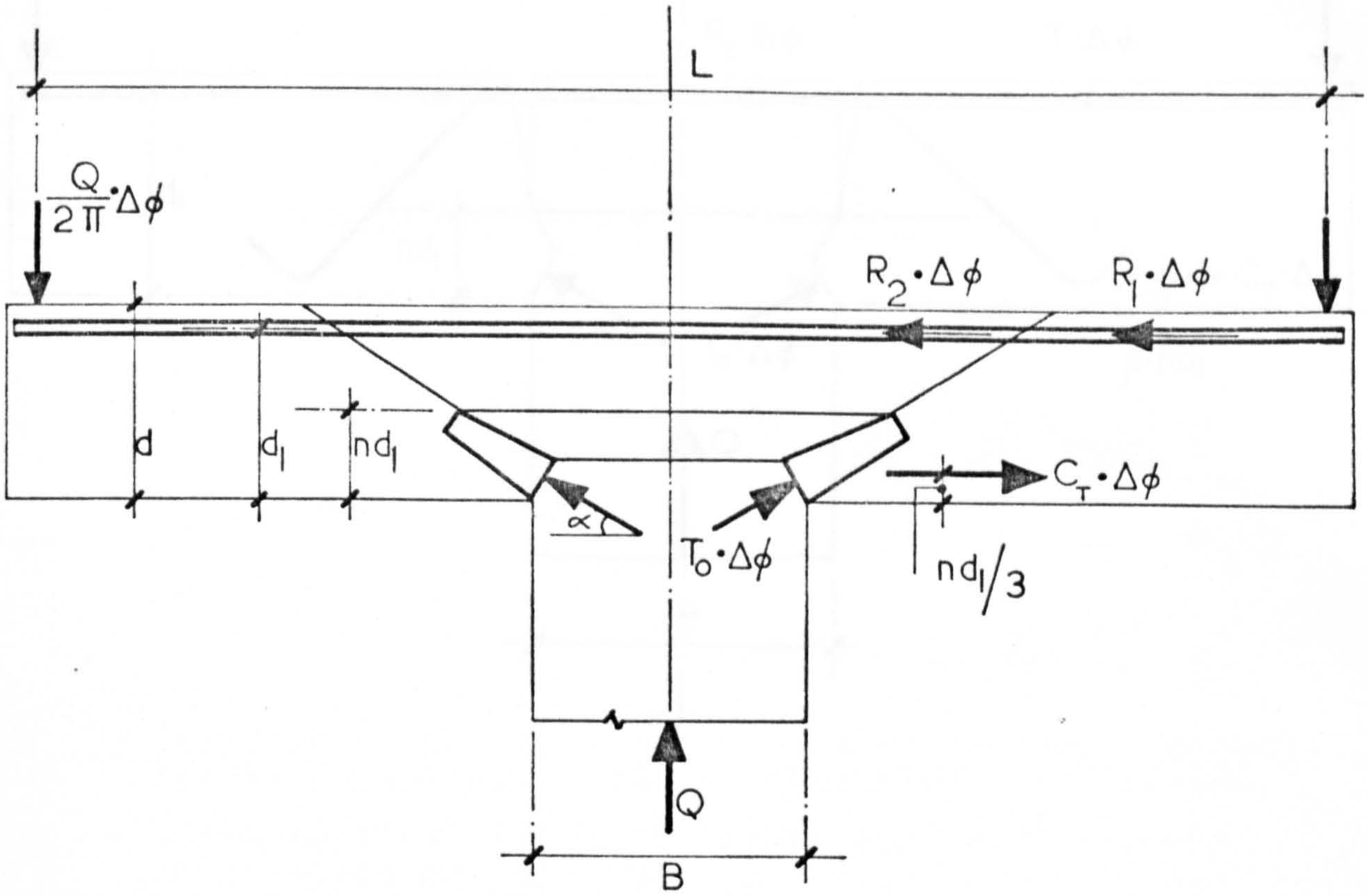

R_1 = Resultant of tangential forces in the reinforcement at right angles to radial cracks over the column.

R_2 = Resultant of radial forces in the reinforcement cutting across the shear crack.

T_o = Oblique compression force in the imaginary conical shell.

$\Delta\phi$ = Angle of an elemental sector of the slab over a column.

α = Inclination of T_o to the horizontal plane.

Fig.2. IDEALISED MODEL — KINNUNEN & NYLANDER.

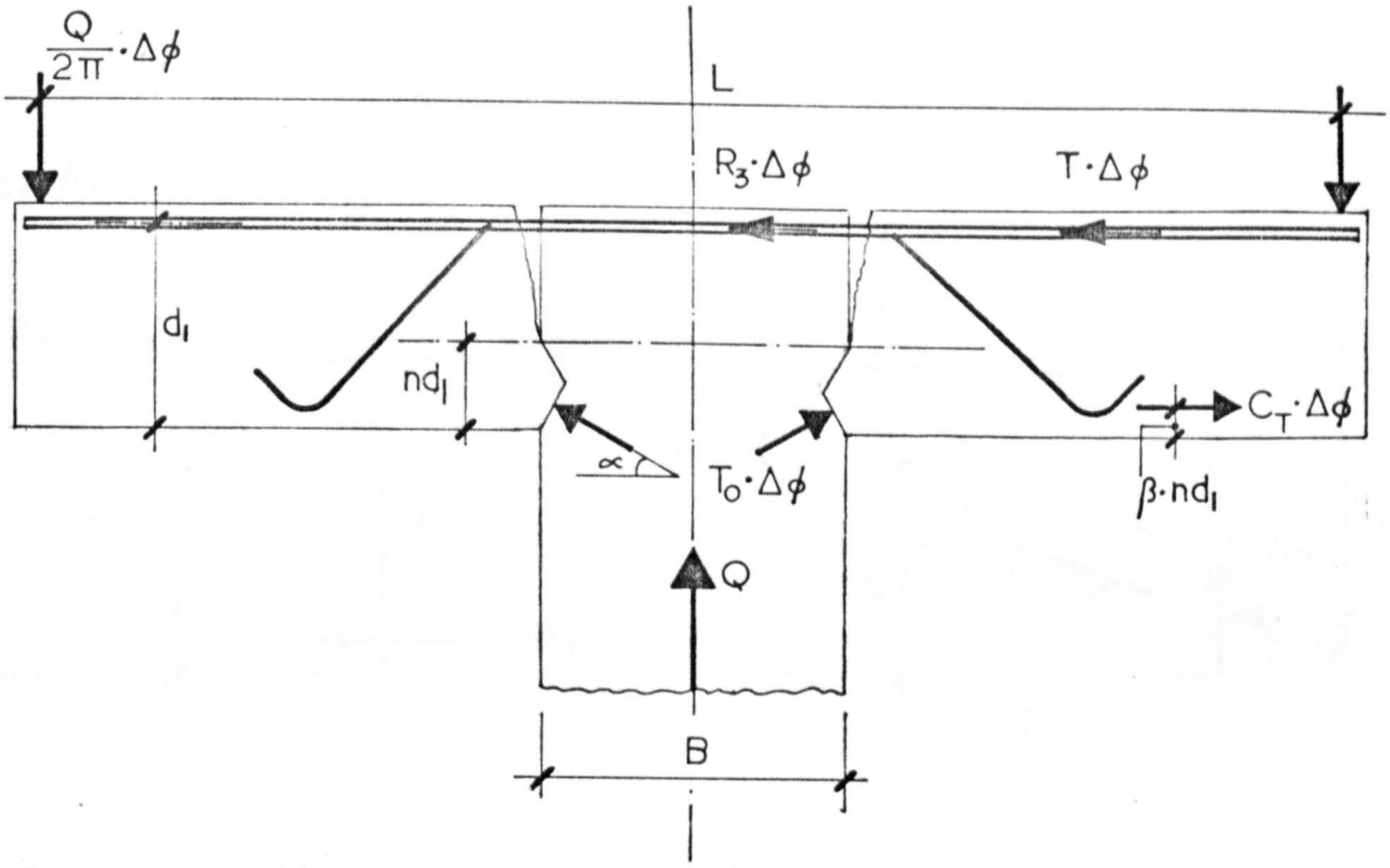

T_o = Oblique compressive forces in the compression zone.

$\Delta\phi$ = Angle of elemental sector considered.

R_3 = Radial resultant of the forces in the shear reinforcement.

α = Angle between the horizontal plane and T_o.

$\beta.nd_1$ = Distance from the bottom surface of the slab to the force C_T.

Fig. 3. IDEALISED MODEL - ANDERSON.

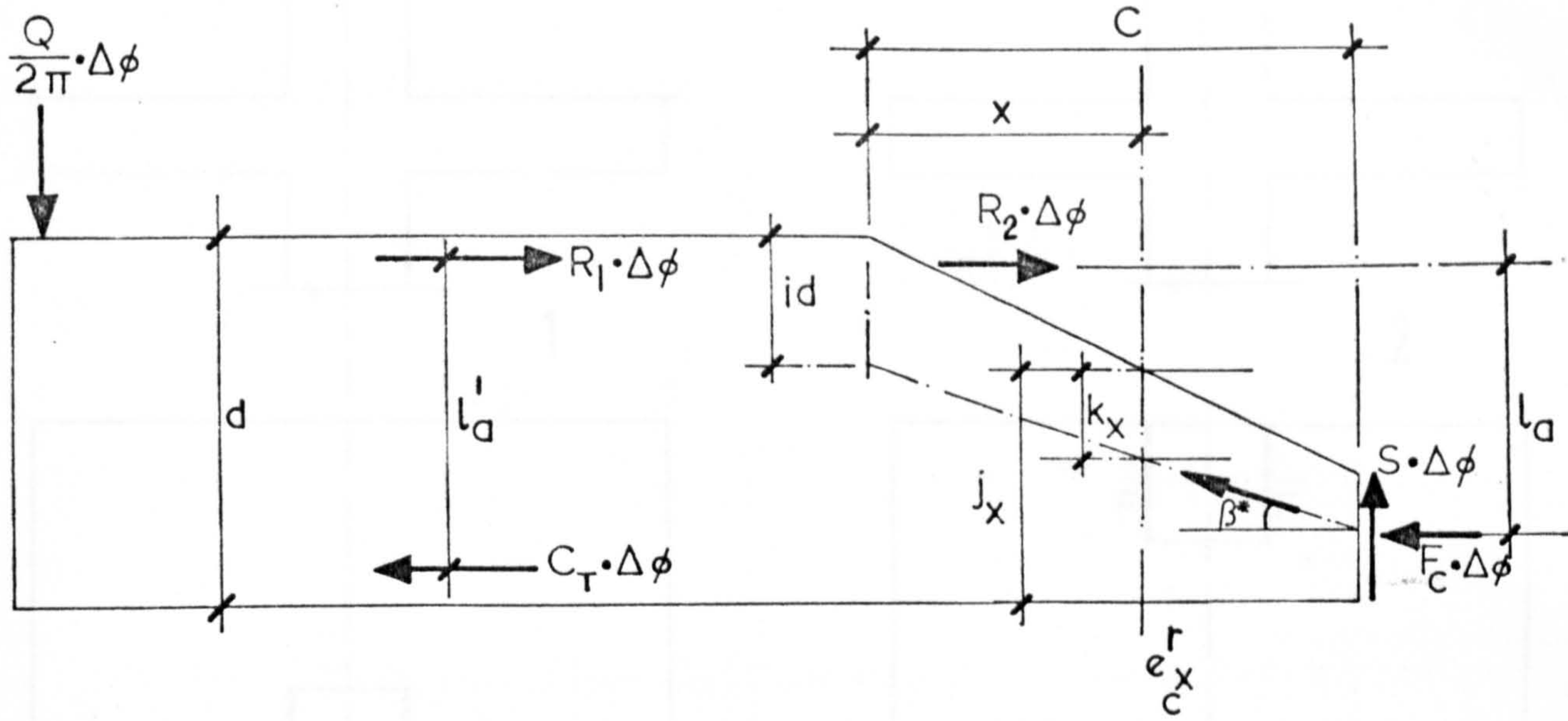

R_1 = Resultant of tangential forces in the reinforcement at right angles to radial cracks over the column.

R_2 = Resultant of radial forces in the reinforcement cutting across the shear crack.

S = Resultant of the shear forces in the compressive area of concrete.

F_c = Resultant of the radial compressive forces of the concrete.

o = Angle of elemental sector considered.

id = Distance from tensile reinforcement to the position of thrust line in the section located at the end of the shear crack.

j_x = Distance from the extreme compressive fibre to the shear crack.

l_a = Lever arm in the radial direction.

l'_a = Lever arm in the tangential direction.

Fig.4. FORCES AND THRUST LINE IN THE ASSUMED MODEL ACCORDING TO ANIS.

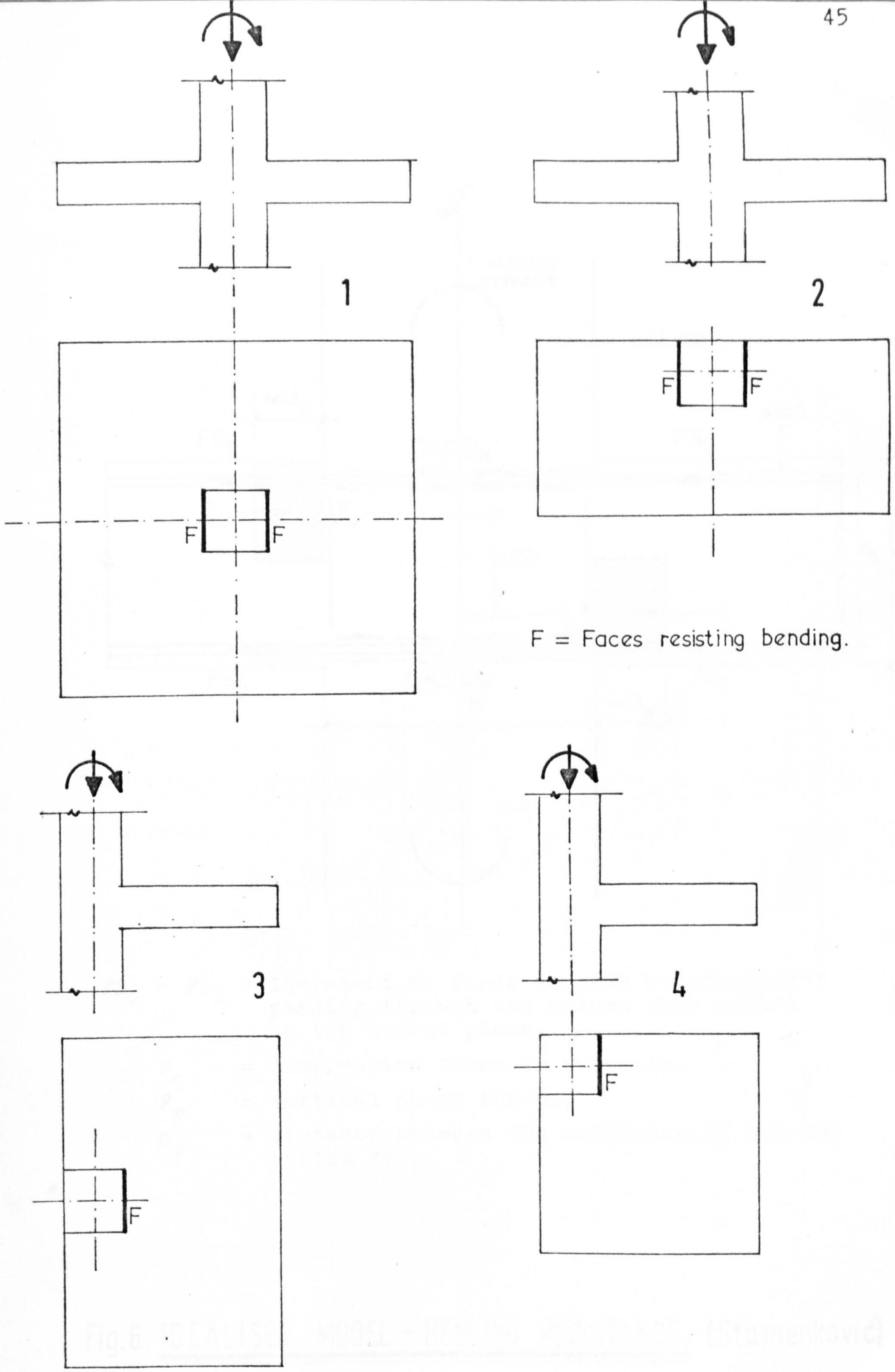

1,2 - CATEGORY. 1. INTERNAL & EDGE COLUMNS WITH TANGENTIAL MOMENT.

3,4 - CATEGORY. 2. EDGE COLUMN WITH MOMENT ⊥r TO FREE EDGE & CORNER COLUMN.

Fig.5.

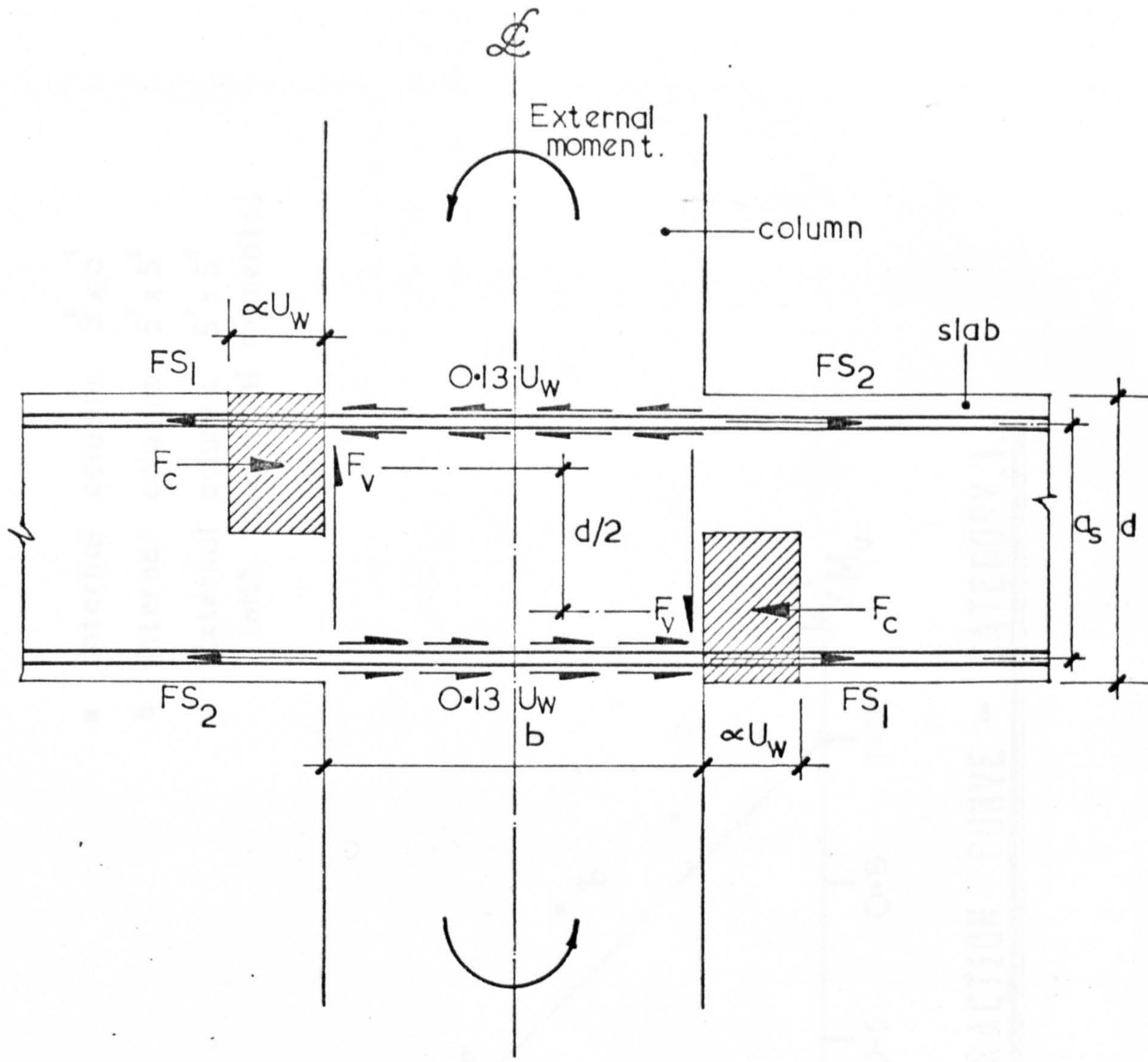

$FS_2 - FS_1$ = Increment of force in slab reinforcement passing through the column side normal to the moment plane.

F_c = Compressive force in concrete.

F_v = Vertical shear forces.

a_s = Distance between the centroids of top and bottom bars.

Fig.6. IDEALISED MODEL - BENDING RESISTANCE. (Stamenković)

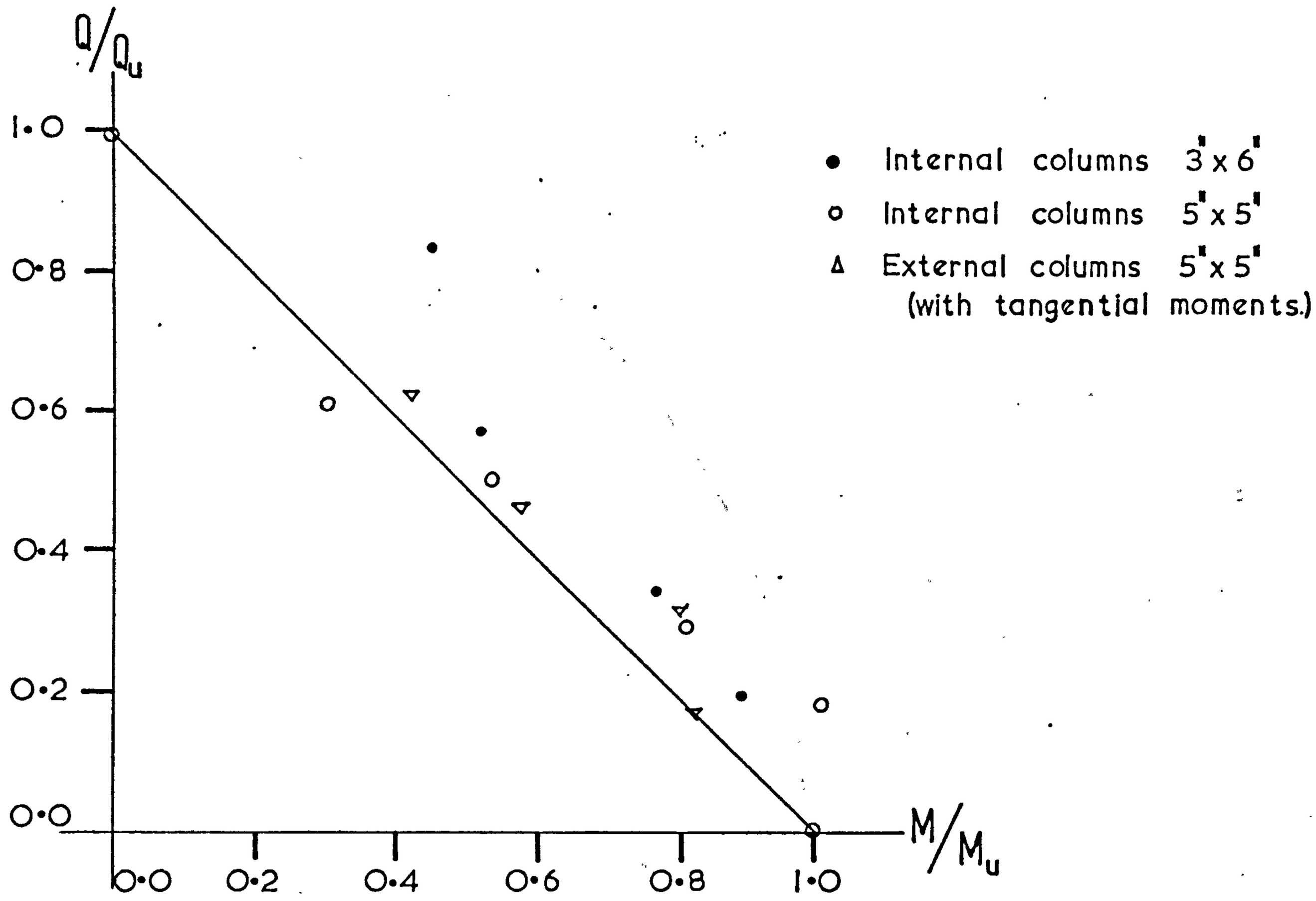

Fig.7a. INTERACTION CURVE - CATEGORY.1.

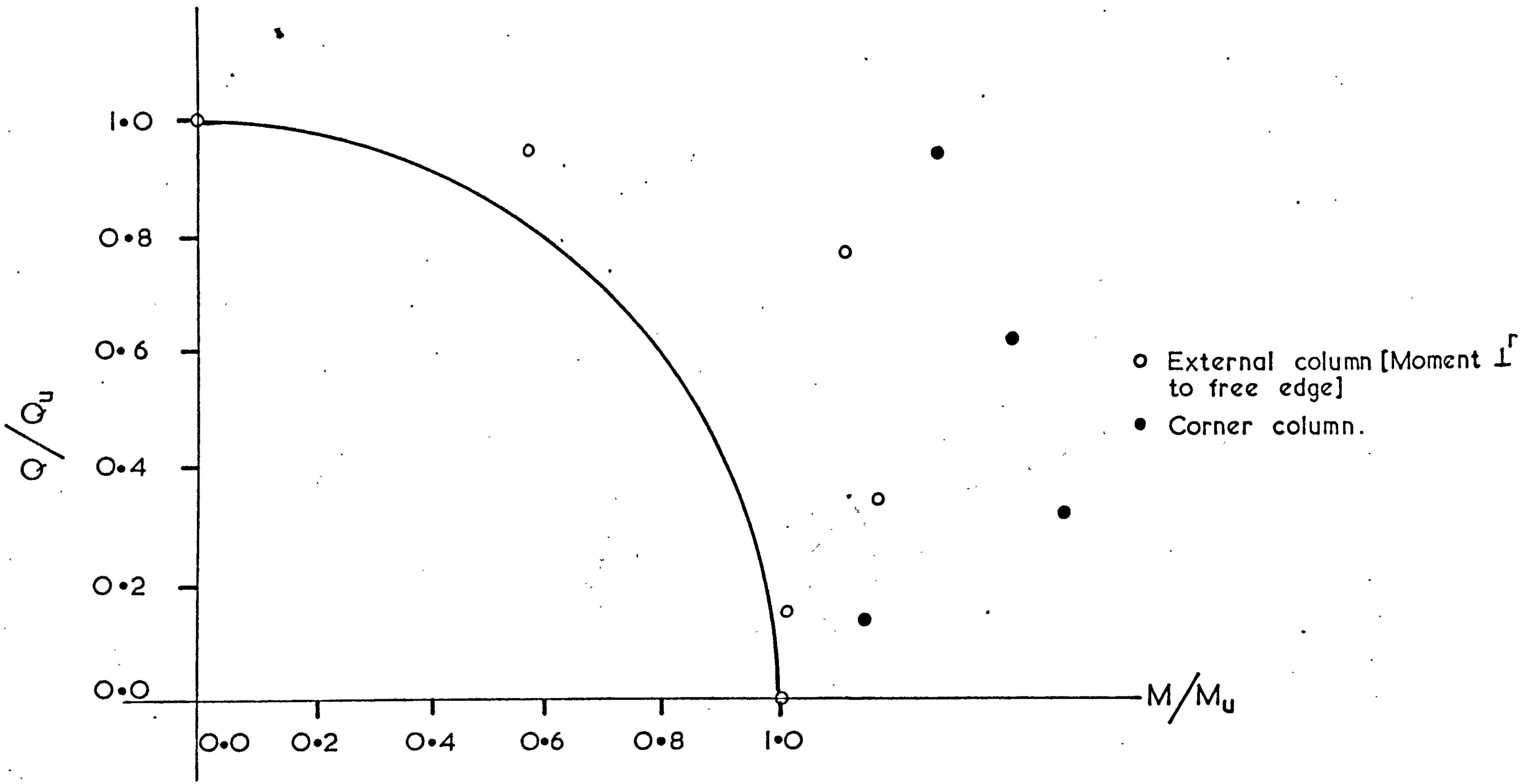

Fig.7b. INTERACTION CURVE – CATEGORY. 2.

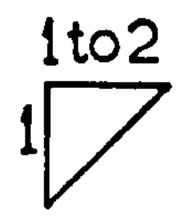

7

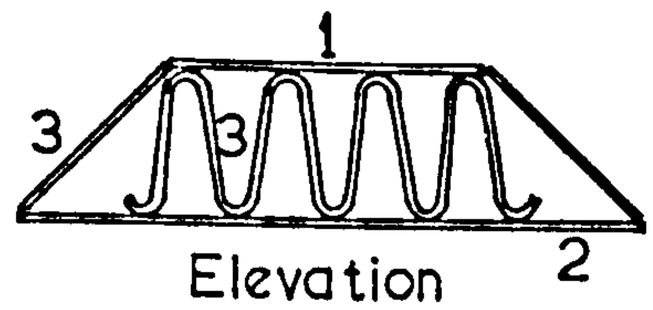

Elevation

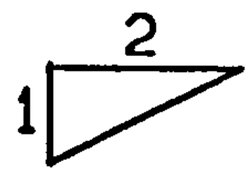

8

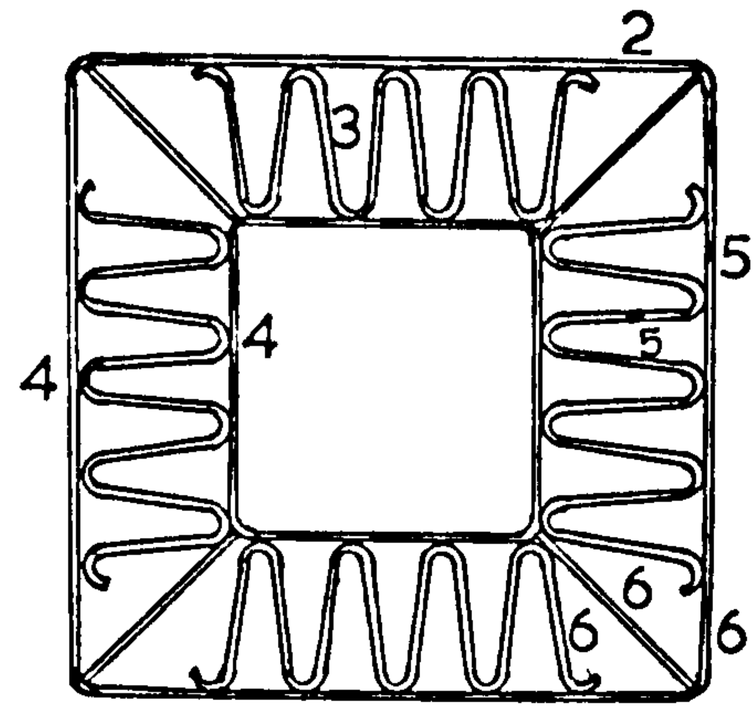

Square or Rectangular Column.
PLAN

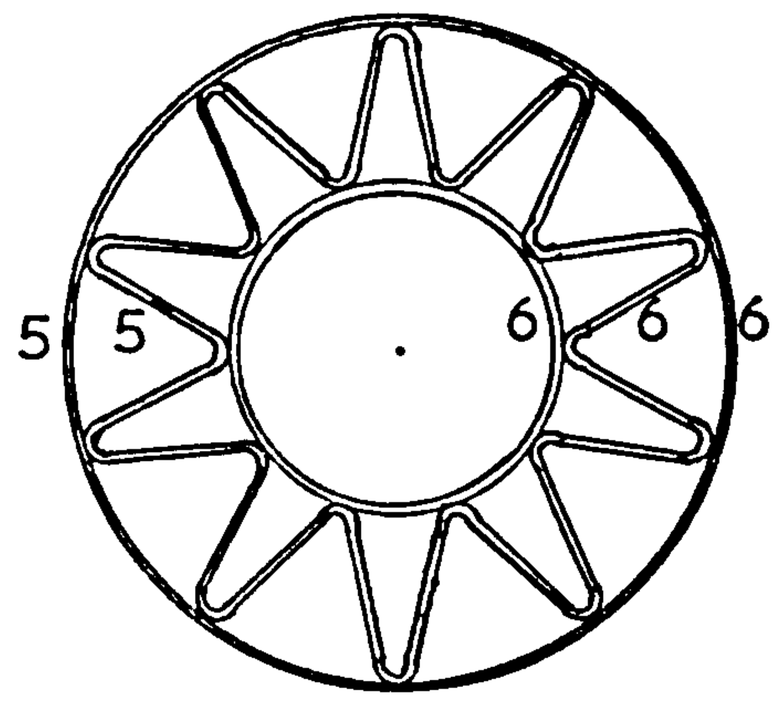

Circular Column.
PLAN

1 = Upper anchorage ring.

2 = Lower anchorage ring.

3 = Web reinforcement. Slope to be between 1:1 & 1:2 (Detail 7, vertical:horizontal) in a section normal to the anchorage ring.

4 = Diameter of bends in web reinforcement to be not less than Five bar diameters. Sideways inclination of the straight sections to be not more than 1:2 in horizontal projection. (Detail 8).

5 = Joints in reinforcement to be full butt welds.

6 = All bars to be not less than ½" diameter.

7 = Web reinforcement slope.

8 = Sideways inclination of straight sections.

Fig. 8a. SHEAR CAGE DETAILS – AUSTRALIAN CODE.

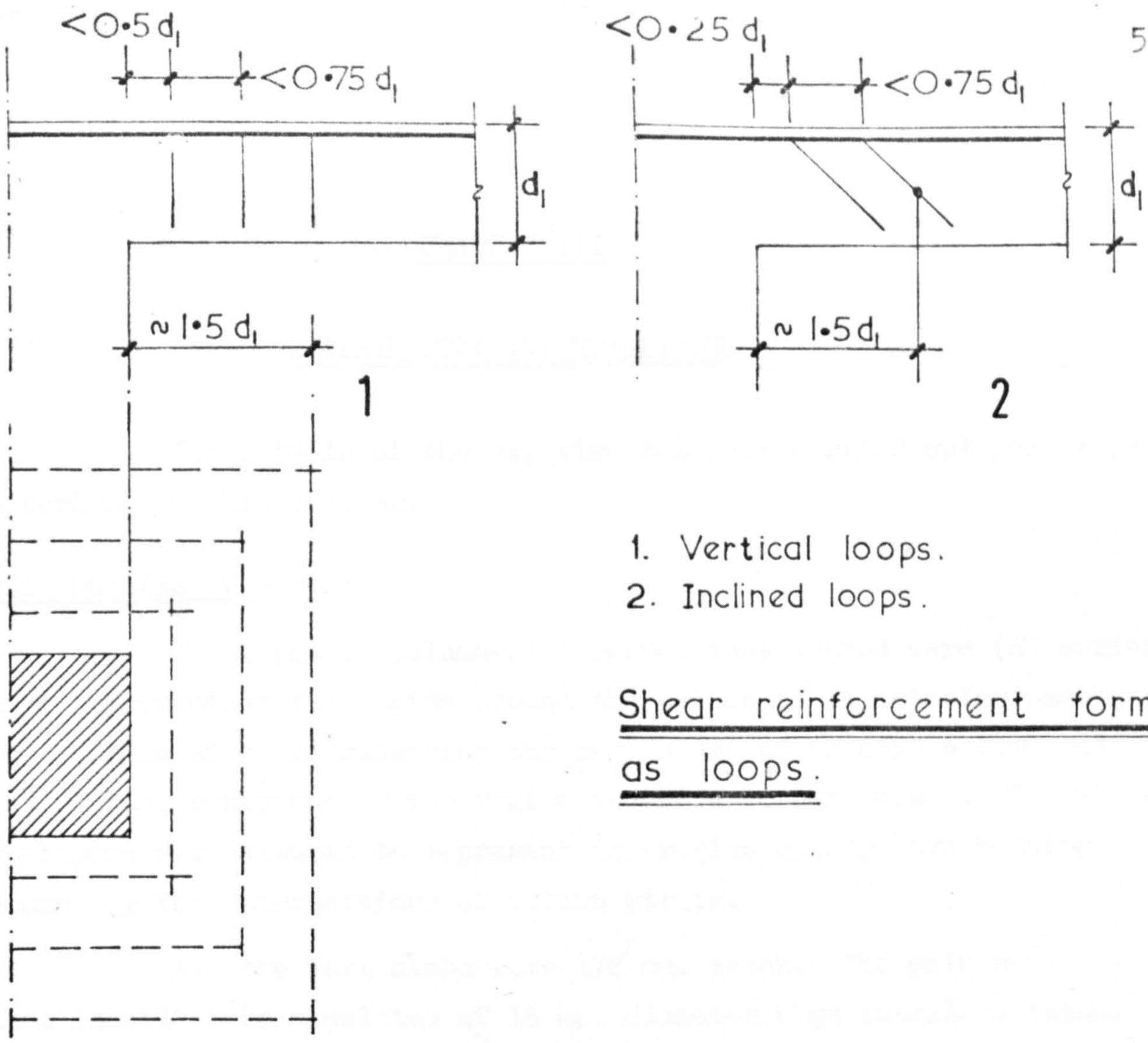

1. Vertical loops.
2. Inclined loops.

Shear reinforcement formed as loops.

Reinforcement bent down

1] One layer.
2] Two layers.
3] Reinforcement placed round a rectangular column.

Fig. 8b. DETAILS OF SHEAR REINFORCEMENT – SWEDISH CODE.

CHAPTER III

EXPERIMENTAL INVESTIGATION.

The details of the experimental work carried out are briefly described in this chapter.

3.1 Outline of Tests:

The types of column-slab connections tested were (a) series L ~ representing the region around the column of an interior panel, (b) series ES ~ representing the region around an edge column and (c) a slab representing the region around a corner column. The above specimens were assumed to represent the region of negative bending moment or the intersections of column strips.

All the test slabs were 178 mm. thick. The main reinforcement in all slabs consisted of 16 mm. diameter high tensile deformed bars in two perpendicular directions, top and bottom, at 127 mm. centres, with a clear cover of 19 mm. at both faces.

Column stubs were 305 mm. square and provided with 8 numbers of 25.4 mm. diameter high tensile deformed bars. This heavy reinforcement was provided in the columns so that any failure in the column was avoided before that in the slab. Eccentric loads were applied to the column-slab connection by means of the cantilever portion on the column stub.

3.1.1 Series L:

All slabs under this series were 2.285 metre square. The overall dimensions of the specimens and arrangement of main reinforcement are shown in Fig. 9. Concrete cube strengths varied from 32.8 N/mm^2 to 45.8 N/mm^2. The main variables were the eccentricity of the applied load and the amount of shear reinforcement provided. Eleven slabs were tested under this series.

3.1.2 Series ES:

Seven slabs were tested under this series and were 2.285 metre x 1.295 metre. They were simply supported along three sides (two short sides and a long one) and the fourth one containing

the column was free. Concrete cube strengths varied from 33.8 N/mm^2 to 51.3 N/mm^2.

The main variables as in Series L, were the eccentricity of the applied load and the amount of shear reinforcement. For details of specimen and the arrangement of reinforcement see Fig. 10.

3.1.3 Corner Column.

The slab for this case was 1.295 metre square and was simply supported along two adjacent sides and the other two sides containing the column were free.

3.2 Materials used.

3.2.1 Concrete.

Ready mix concrete with a minimum strength of 30 N/mm^2 at 28 days and a nominal slump of approximately 50 mm. was used for all slabs. The mix was supplied by Ready Mixed Concrete (London) Ltd. The following were the details of ready mix used:

Ordinary Portland cement	1.0
Sand	2.1
10 mm. aggregate	0.8
19 mm. aggregate	2.8
water cement ratio	variable according to workability, to obtain a slump of $\pm$ 50 mm.

The aggregate was ordinary land gravel.

In order to assess the degree of control obtained for the concrete two numbers, 152 mm. cubes, 152 x 305 mm. cylinders and 152 x 228 mm. (split) cylinders were taken for each slab. Table No.III-1 gives the details of control tests.

TABLE III - 1

Details of Concrete Control Specimens. (Each average of two tests.)

Slab No.	Cube Strength (152mm.) U_w in N/mm^2	Cylinder Strength (152 x 305 mm.) U_{cyl} in N/mm^2	Split Cylinder Strength (152 x 228 mm.) U_t in N/mm^2
L1	32.8	26.6	2.70
L2	34.2	33.4	3.10
L3	33.1	27.7	2.66
L4	45.8	37.8	3.45
L5	35.0	-	2.98
L6	42.1	35.1	3.07
L7	44.4	33.0	2.97
L8	31.2	24.8	2.46
L9	41.4	30.4	2.78
L10	41.8	34.6	2.47
L11	43.5	38.5	3.51
ES1	33.8	-	2.70
ES2	32.8	30.4	2.70
ES3	51.3	40.0	3.10
ES4	50.0	41.6	3.31
ES5	37.6	32.1	2.63
ES6	40.4	26.5	2.23
ES7	45.8	35.5	3.38
CS	38.5	34.1	2.55

3.2.2. Reinforcing Steel:

The details of reinforcement bars used as main steel, column steel and shear reinforcement are listed in Table III-2. Typical stress-strain diagrams are shown in Fig. 11.

A special type of shear reinforcement called 'Hats' were used in these tests. Fig. 12 shows details of the Hats. Increases in the area of shear reinforcement were achieved by keeping the number of "shear arms" constant and increasing the diameter of bar used. The shear arms were welded to spacer rings to give the required inclination.

TABLE III - 2

Details of Reinforcement bars.

Use of steel	Bar diameter in mm.	Type of bar	Yield or 0.2% proof stress in N/mm^2	Ultimate strength in N/mm^2.
Main steel	16.0	High tensile*	398	685
Column steel	25.4	High tensile*	433	685
Shear Reinforcement	12.7	Mild steel	355	508
Shear Reinforcement	9.5	Mild steel	309	474
Shear Reinforcement	8.0	Mild steel	355	508
Shear Reinforcement	6.35	Mild steel	238	356

* Trade name 'Welbond'.

In all slabs with shear reinforcement excepting L10 the inclination of the shear arms was 45°. In slab L10 it was 30° to the plane of the slab.

Adequate anchorage of shear reinforcement was obtained by allowing the main bars to pass through the shear reinforcement. (See Fig. 12.)

3.3 Fabrication and Curing:

The slabs were cast in form work made of 19 mm. thick plywood. The column steel was first lowered into position and the shear reinforcement dropped in position next. The main bars were then threaded through the shear and column reinforcements and tied in position. Steel chairs were used to achieve the required distance between the top and bottom mats. They were placed away from the column to eliminate their effect on the shear strength of the slab/column connection.

The slabs were cast in two stages. Firstly the slab and the bottom stub and secondly the projecting column stub on the following day. This was necessary to prevent any concrete bulging or flowing out and increasing the slab depth at the junction. Control specimens were taken to estimate the strength of concrete in compression and tension.

The slab and control specimens were covered with wet hessian cloth and polythene sheeting. Forms were struck along with control specimen after a week and stored under laboratory conditions until testing.

3.4 Testing:

All slabs tested were mounted vertically and bolted to the supporting frame by means of 13 mm. bolts. Hard rubber pads were glued to the supporting frame in continuous strips in order to provide an even support.

The vertical setup was to facilitate observation of the development of cracks on both sides, the deflection etc. The self weight being negligible compared to the applied load the set-up was satisfactory.

Details of the test rig are shown in Fig. 13b while Fig. 13a shows the general experimental set-up. The load was applied to the specimens by means of a 200 ton capacity Tangy hydraulic jack. The oil pressure was fed through an Amsler cabinet. Load increments were applied to the specimens at intervals of 20 minutes (approx.) and in approximately ten stages to failure.

3.5 Details of Measurements:

3.5.1 Deflection:

Deflections were measured by means of dial gauges mounted from steel fixtures on the test frame. Locations of the gauge points for internal and external panels are shown in Fig. 14.

3.5.2 Strains:

The tensile strains of the flexural and shear reinforcement as well as compressive strains of concrete were measured by means of electrical resistance gauges at points of special interest. The gauge lengths used were 10 mm. and 30 mm. on steel and concrete respectively. The gauges were fixed on the opposite ends of a diameter (top and bottom) in the case of bars adjacent to the column and on the shear arms on the side of eccentricity to obtain the average value of strain. This was necessary because the bars were subjected to considerable bending in these cases. Additional strain readings for the concrete were made using 'Demec' gauges.

3.5.3 Cracks and Ultimate Load.

Cracks were marked at each loading stage and the ultimate load was recorded.

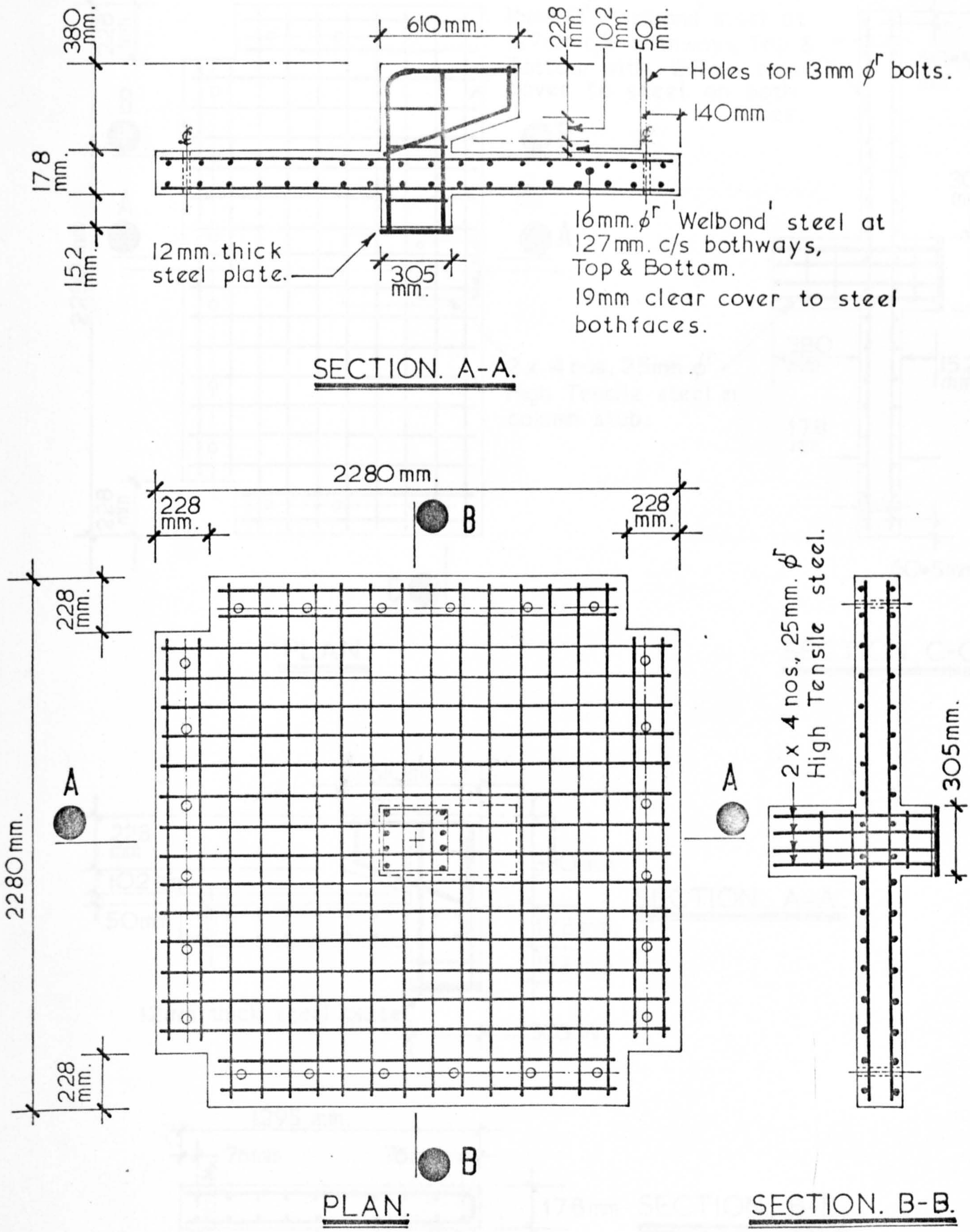

Fig. 9. REINFORCEMENT DETAILS FOR SERIES - L. INTERNAL SLABS.

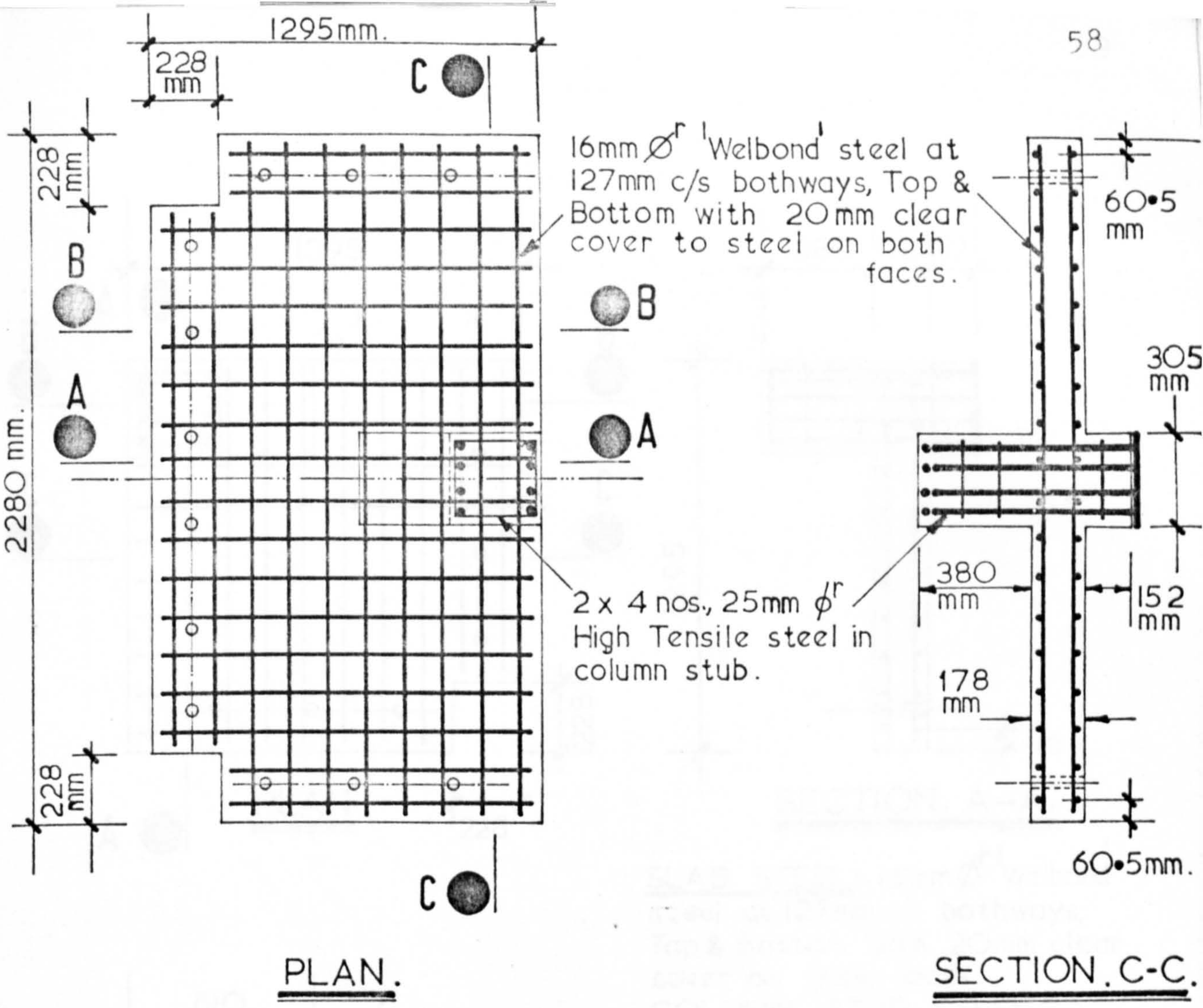

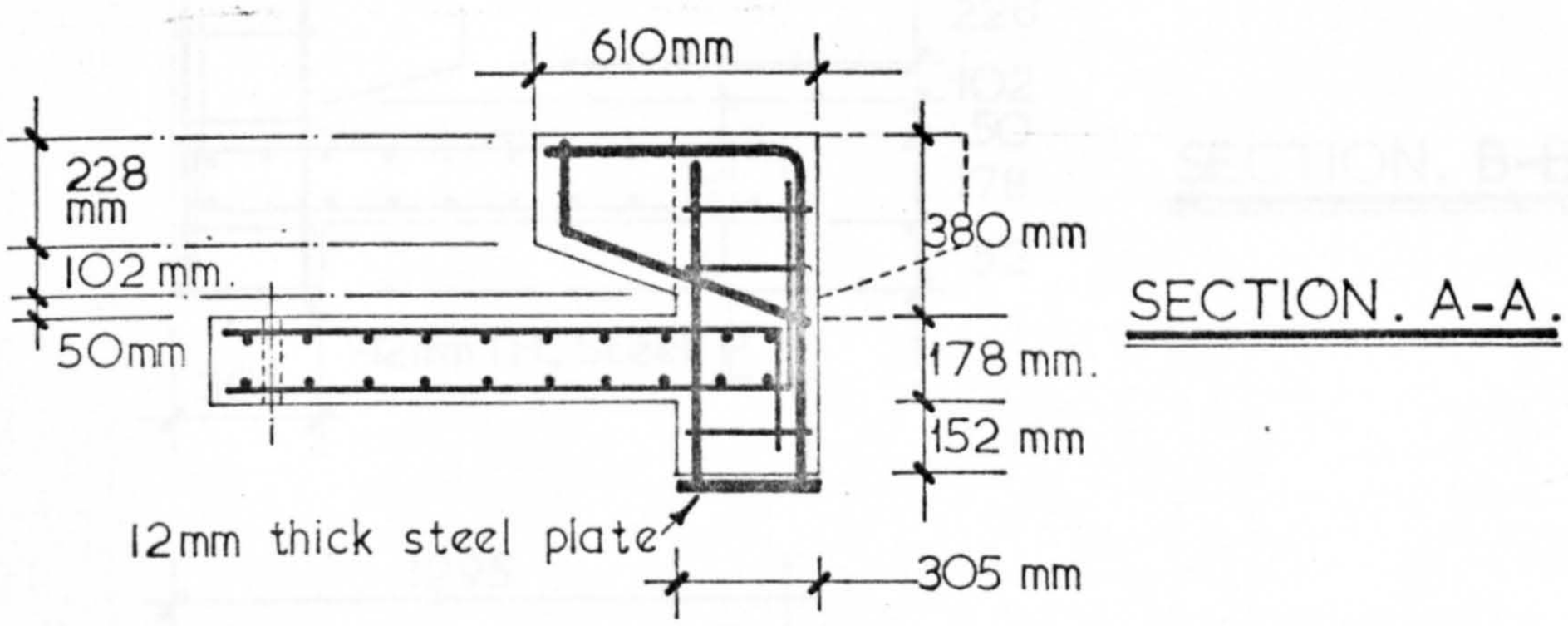

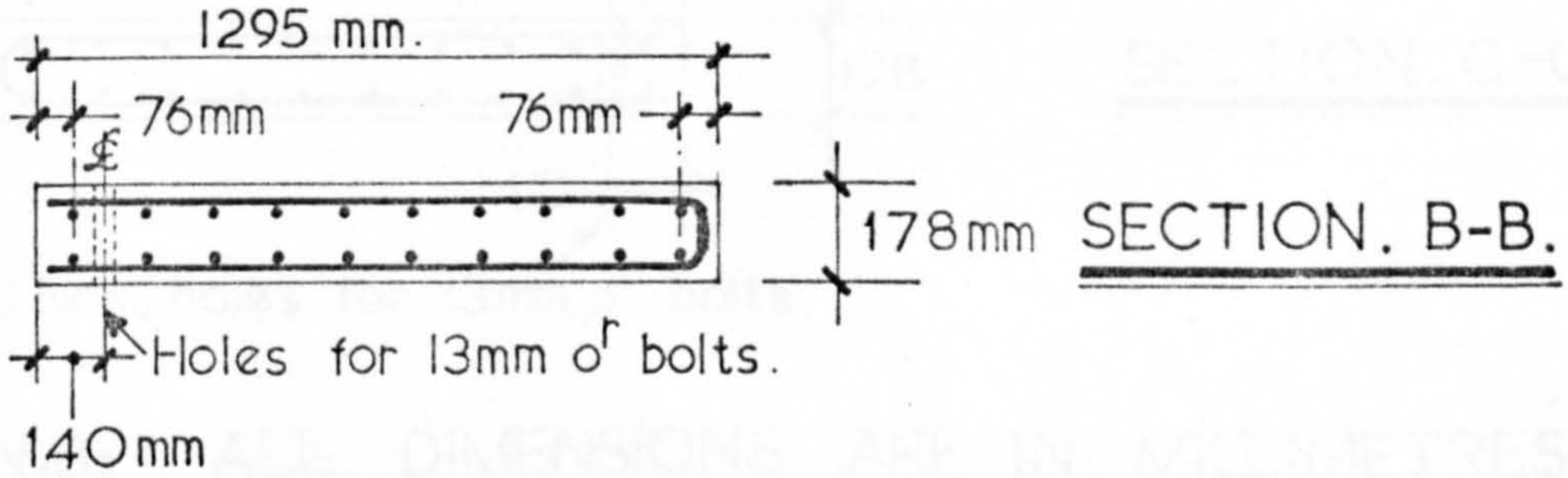

Fig. 10. REINFORCEMENT DETAILS FOR SERIES – ES. EXTERNAL SLABS.

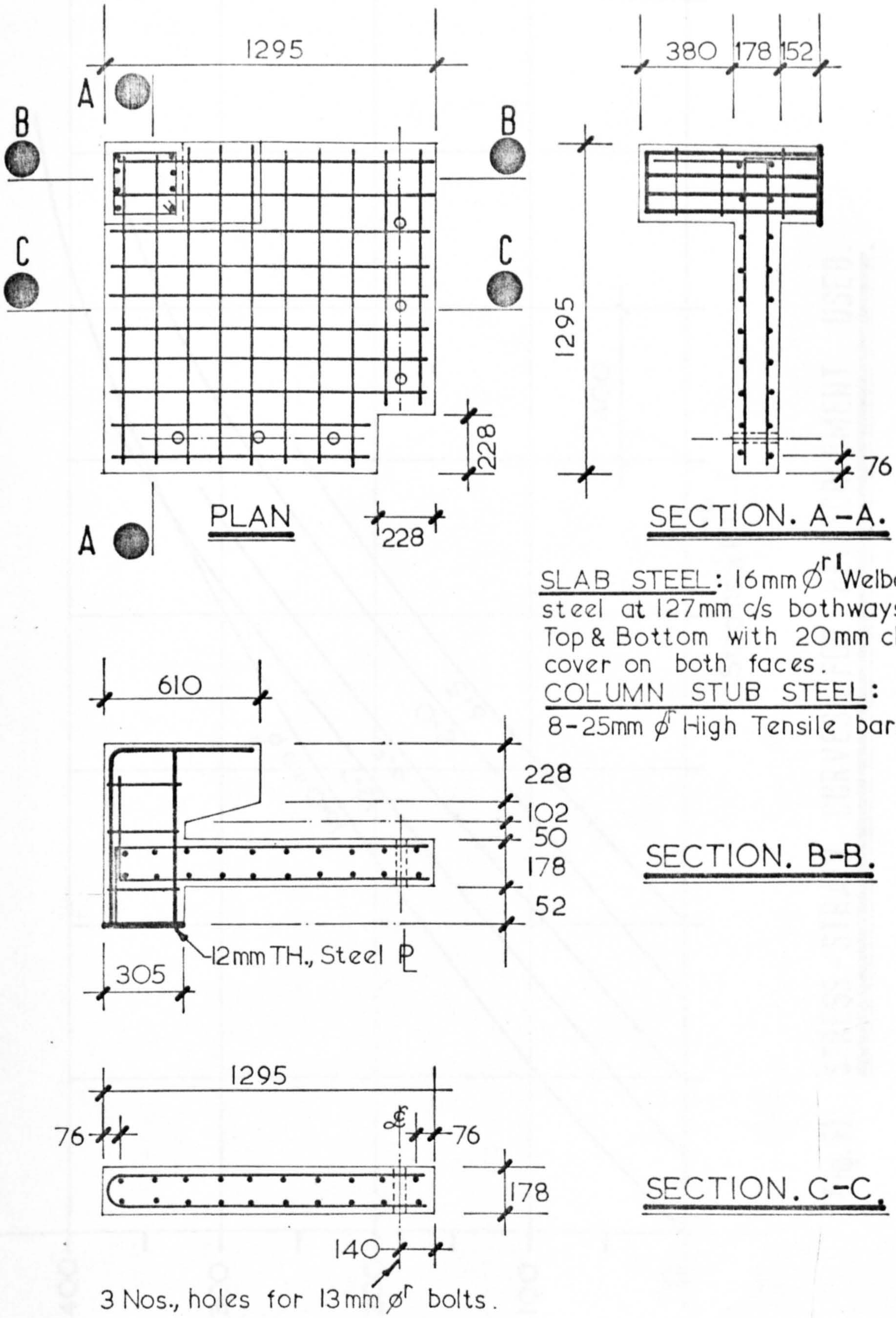

N.B: ALL DIMENSIONS ARE IN MILLIMETRES.

Fig.10a. REINFORCEMENT DETAILS FOR SLAB-CS.

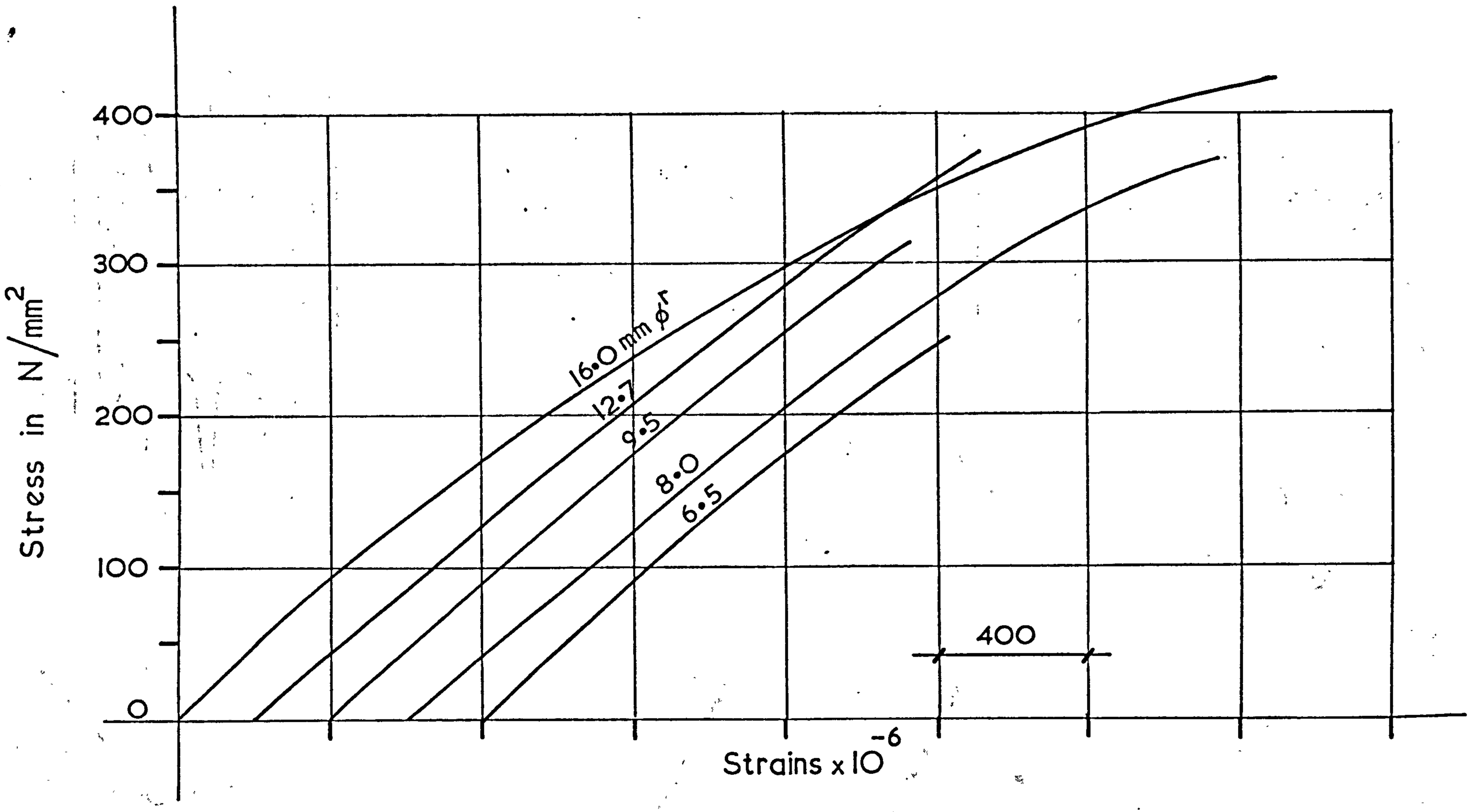

Fig. 11. STRESS-STRAIN CURVES FOR REINFORCEMENT USED.

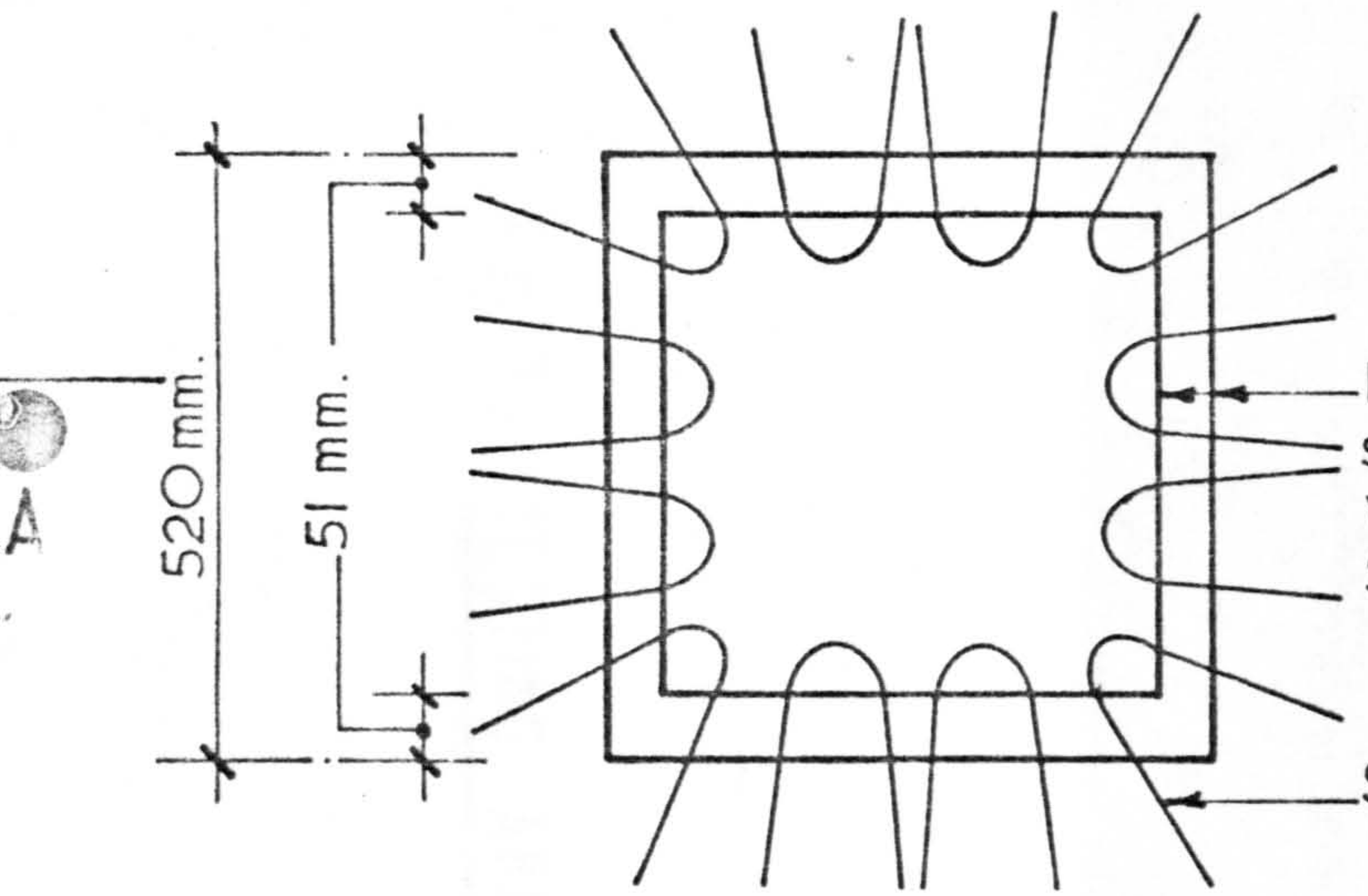

PLAN. SERIES-L.

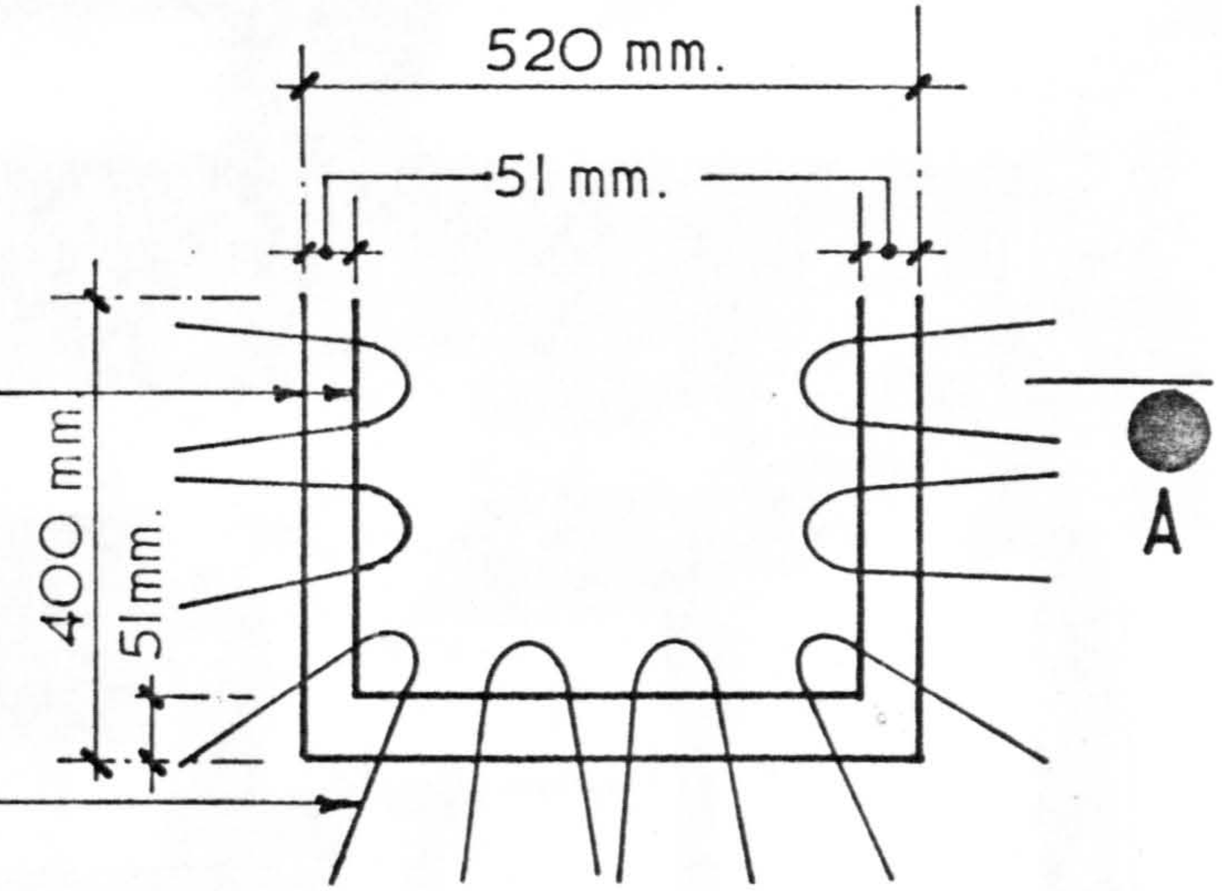

PLAN. SERIES.-ES.

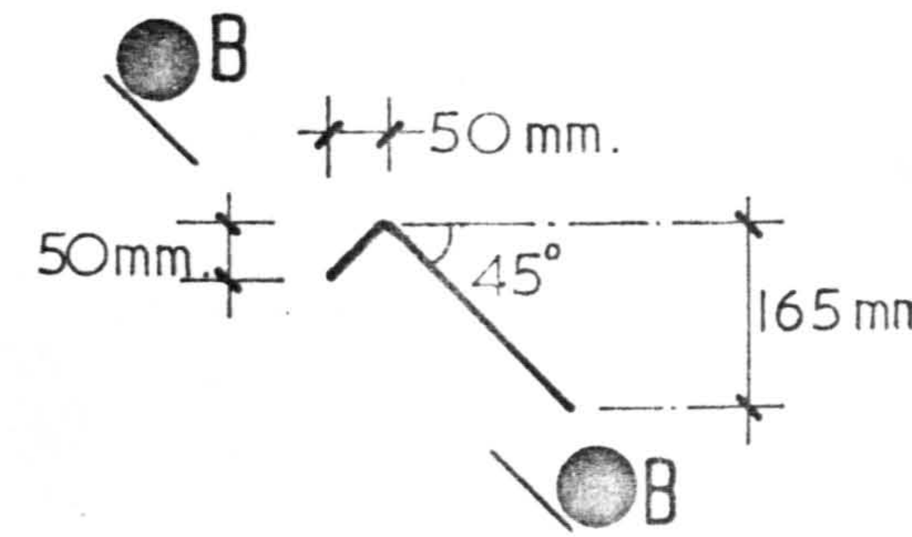

SHEARARM DETAILS

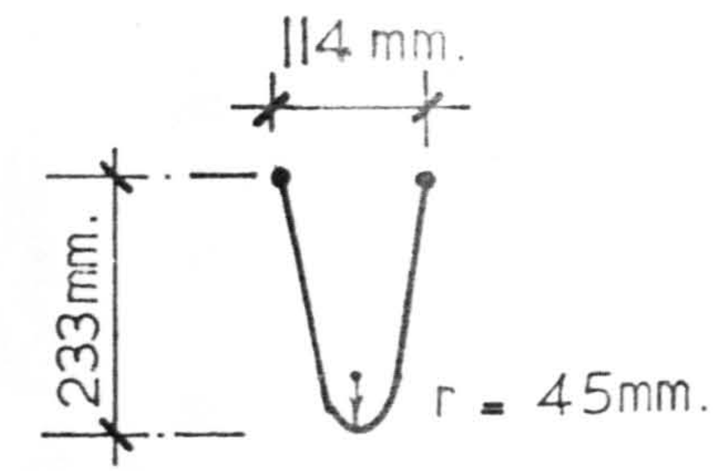

SECTION. B-B.

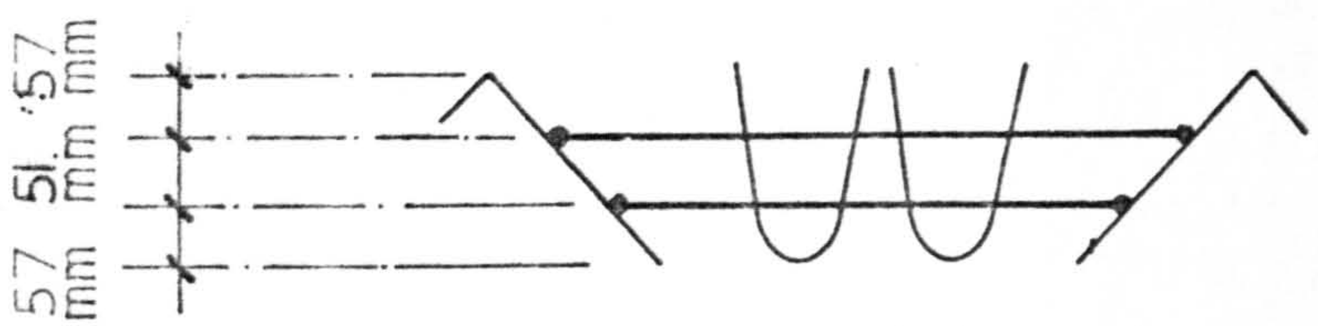

SECTION. A-A.

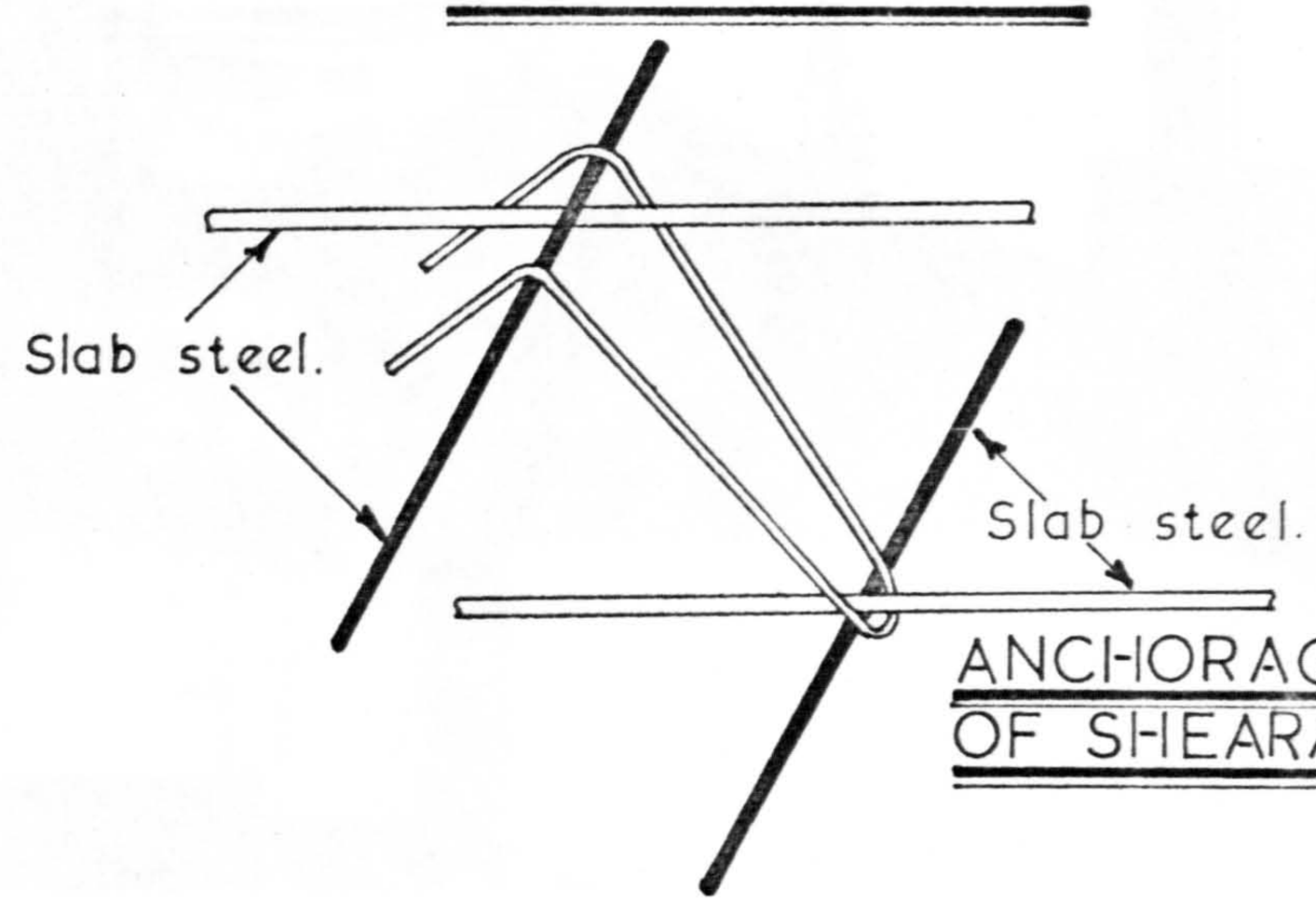

ANCHORAGE DETAILS OF SHEARARM.

Fig. 12. DETAILS OF SHEARHATS.

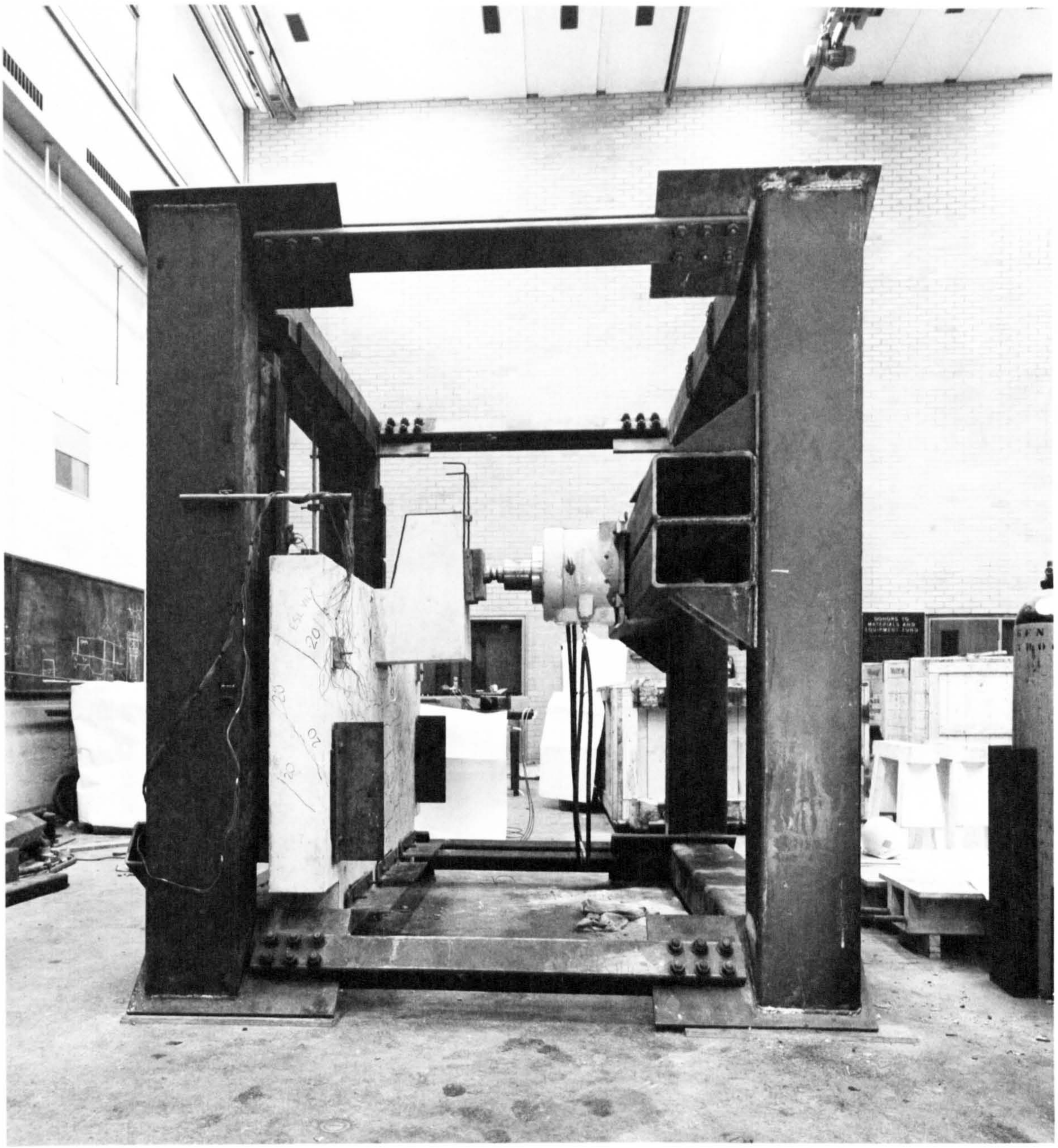

Fig.13a. TESTING ARRANGEMENT.

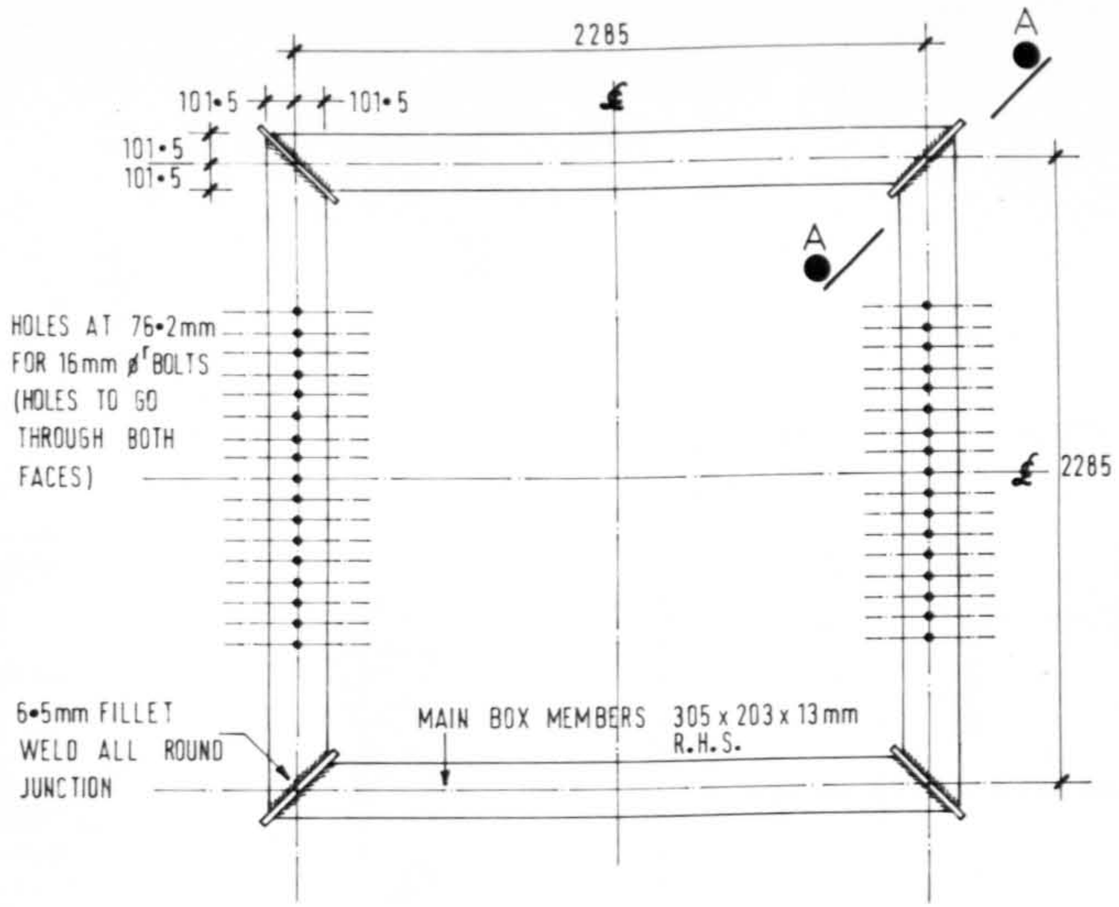

ELEVATION OF END FRAME.1

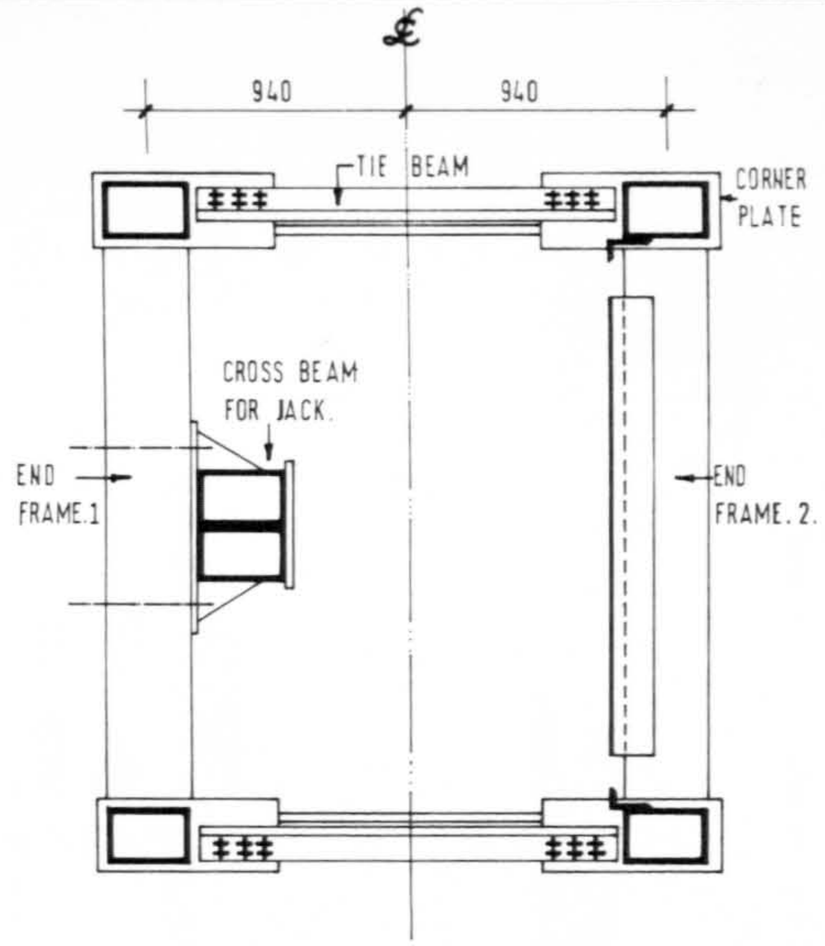

LONGITUDINAL SECTION OF FRAME

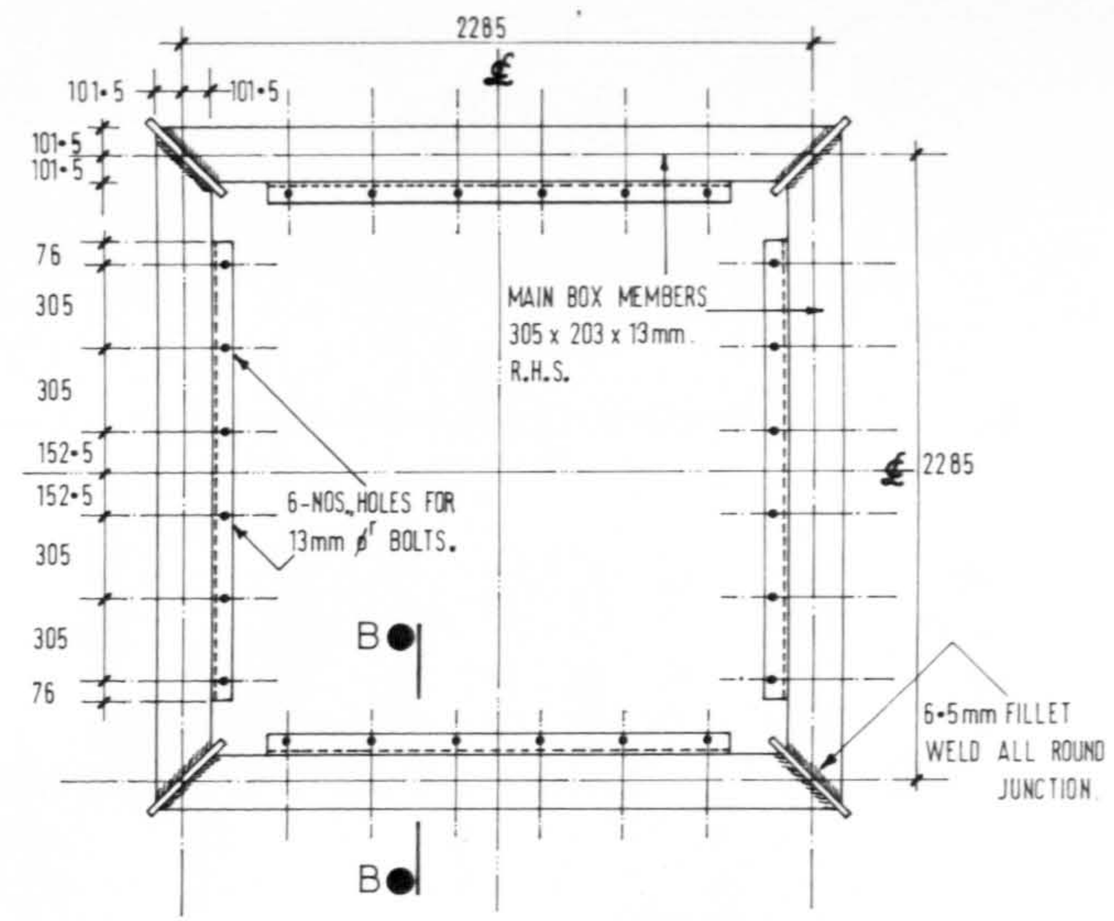

ELEVATION OF END FRAME.2

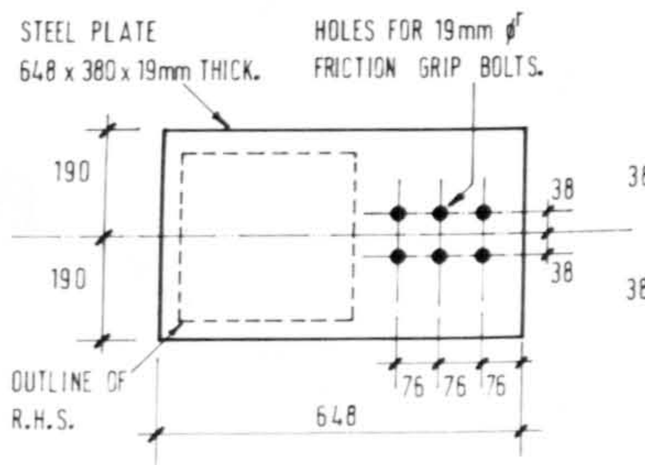

SECTION. 'A-A'.
DETAIL OF CORNER PLATE.

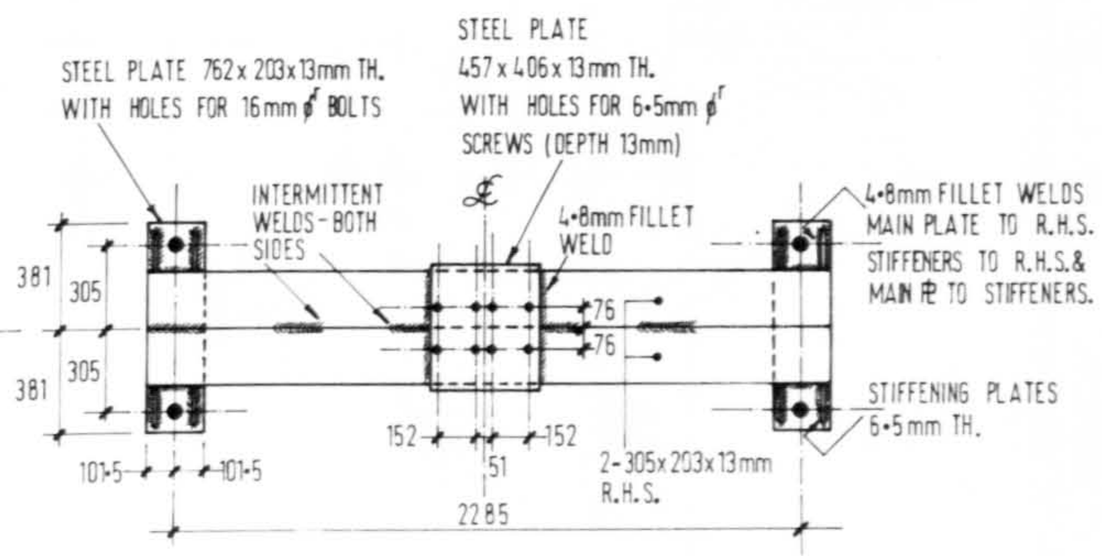

DETAILS OF CROSS BEAM.

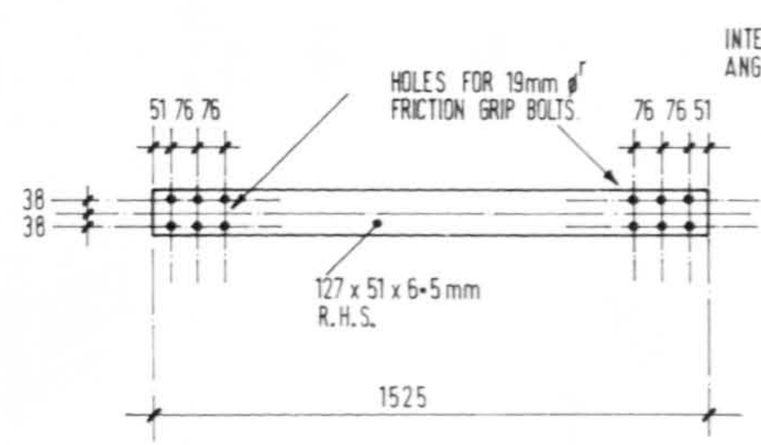

DETAILS OF TIE BEAMS.

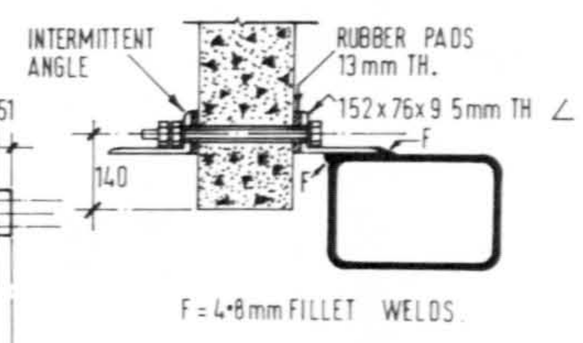

SECTION. 'B-B'.
(SHOWING ALSO SLAB SUPPORT DETAIL)

NOTE: ALL DIMENSIONS ARE IN MILLIMETRES

TEST FRAME DETAILS

FIG. 13b.

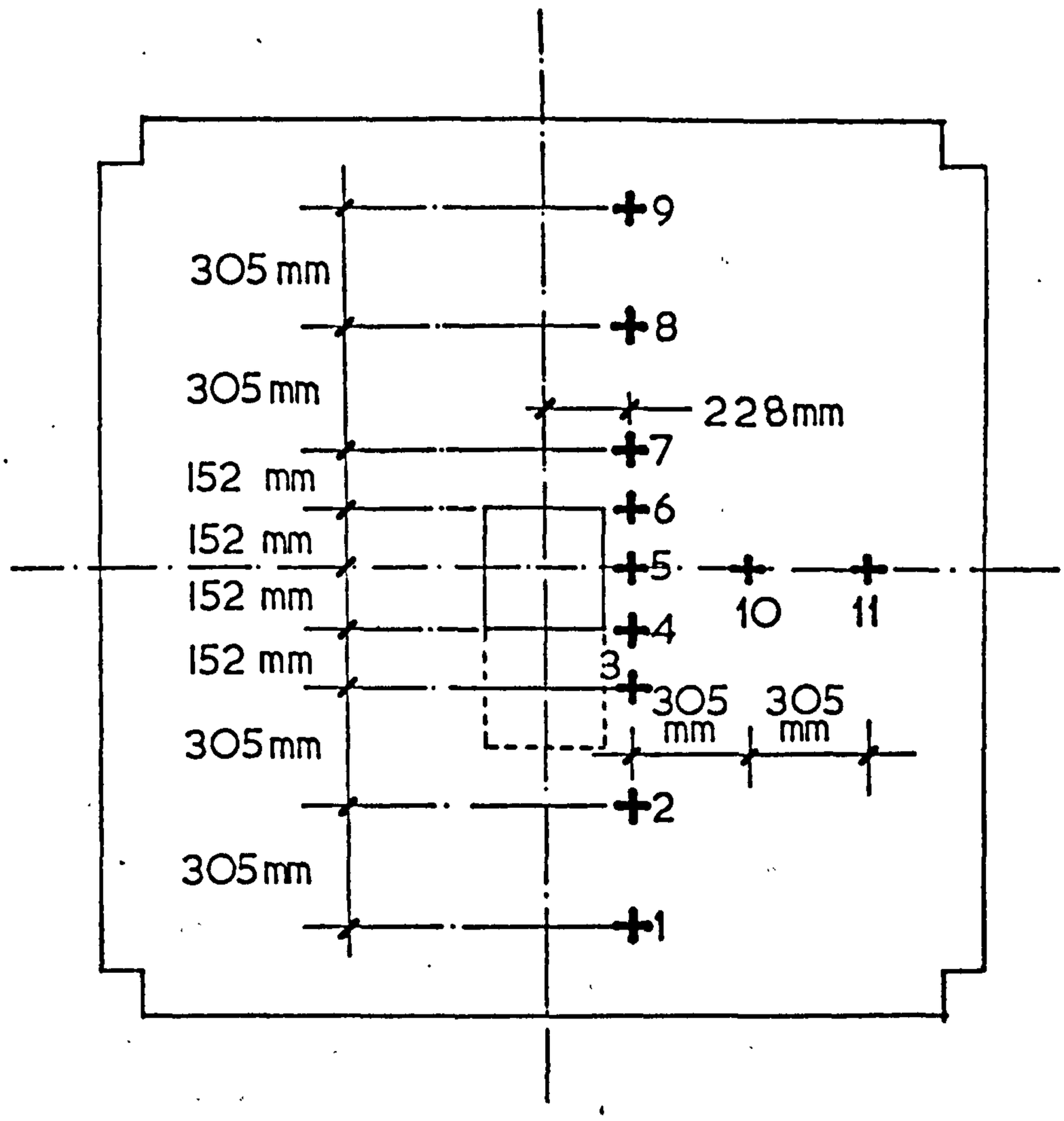

INTERNAL SLABS. SERIES -L.

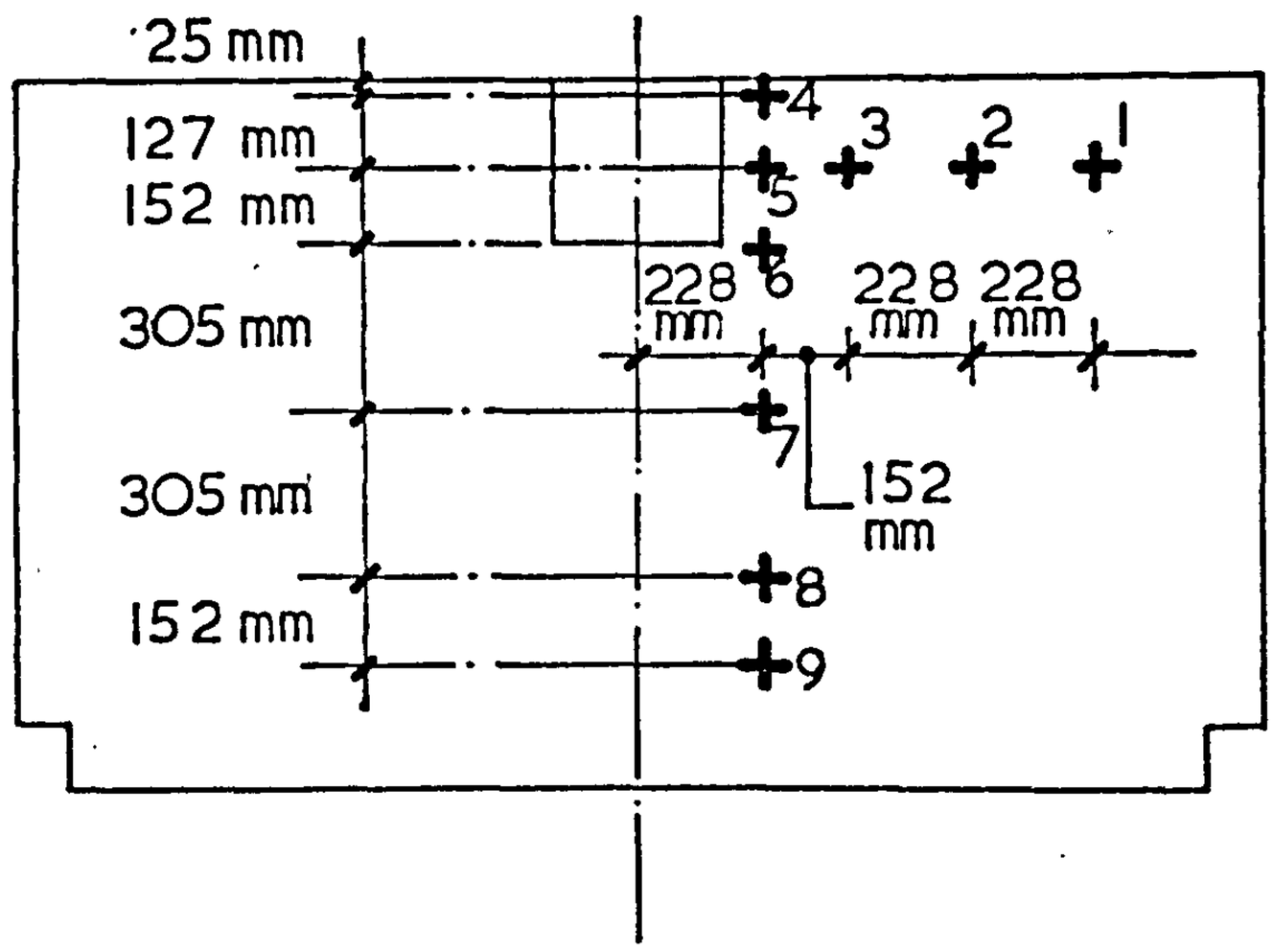

EDGE SLABS. SERIES - ES.

Fig.14. LOCATION OF DIAL GAUGES.

CHAPTER IV

PRESENTATION OF TEST RESULTS.

4.1. Introduction.

The behaviour of both internal and external column connections tested by the author are discussed here, in relation to their deflected profiles, strains, crack patterns and ultimate loads.

The slabs were tested to furnish information on the behaviour of slabs subjected to combined loading. Hence all the other variables, such as the dimensions of the slab, column dimensions and percentage of main steel were kept constant. The provision of main steel was such as to ensure shear failure of slabs in the absence of shear reinforcement. Though it was intended to maintain the concrete strength uniform, the use of ready mix rendered it a variable.

The effectiveness of the shear hats provided as shear reinforcement was of particular interest in the tests. The area was increased from none, to increasing values. The gradual increase of punching load, with increasing shear reinforcement was observed. As a means of increasing the load-carrying capacity further a second layer of shear reinforcement further out from the column face was also tried. The details of shear reinforcement for the various slabs are given in Table IV-1.

4.2. Deflection.

The deflection of each slab was measured by means of dial gauges to an accuracy of 0.025 mm (0.001"). Fig 14 shows the locations of dial gauges.

4.2.1. Series L.

Fig. 15a shows the deflected profiles of slabs L_7 and L_9, subjected to concentric load and without shear reinforcement. The deflected profiles of the otherwise similar slabs L_1, L_4, L_3 and L_5 with different amounts of shear reinforcement (diameter of shear arms being 0, 6.5, 9.5 and 13 mm respectively) are shown in Fig. 15b.

TABLE IV.1. DETAILS OF SHEAR REINFORCEMENT.

SLAB NO.	TYPE OF REINFORCEMENT.	DETAILS OF SHEAR ARMS			A_{sq} in sq.mm.	f_{yq} in $N/_{mm}^2$
		ϕ_v mm.	No.	θ in degrees.		
L2	Shear hat	9.5	24	45	1710	309
L3	Shear hat	9.5	24	45	1710	309
L4	Shear hat	6.5	24	45	775	238
L5	Shear hat	13.0	24	45	3040	355
L6	Shear hat	8.0	24	45	1190	355
L8	Shear hat +	13.0	24	45	3040	355
	Bent up bars.	16.0	8	45	1013	398
L10	Shear hat	8.0	24	45	1190	355
L11	Shear hat +	13.0	24	45	3040	355
	Vertical stirrups	6.5	28	90	905	238
ES3	Shear hat	6.5	16	45	517	238
ES4	Shear hat	9.5	16	45	1140	309
ES6	Shear hat	6.5	16	45	517	238
ES7	Shear hat	6.5	16	45	517	238

The deformation at failure increased with the amount of shear reinforcement. The deflection curve in the portion of the slab outside the column stub was practically rectilinear, with no violent discontinuities. Further it can be seen that the slab rotated about the column faces.

The above was also observed in slabs L_2, L_8 and L_{11} which failed in flexure. Fig. 15c shows the deflected profiles while Fig. 16 shows the load V_s maximum deflection curves (at point 4 - for location see Fig. 14), for the same slabs.

4.2.2. Series ES.

Deflection of these slabs were measured parallel to (adjacent to the column) and perpendicular to the free edge as shown in Fig. 14. Deflection profiles, parallel to and perpendicular to the free edge of slabs ES_1 to ES_4 are shown in Figs. 17 and 18.

There was an increase in ultimate deformation with an increased amount of shear reinforcement, as in the case of internal columns. No appreciable difference in deformation between slabs with outward eccentricity and inward eccentricity was noticed. Fig. 19 shows the load deflection curves for slabs ES_1 to ES_5.

4.3. Strain in shear reinforcement.

4.3.1. Series L.

The strains in the shear arms are very much dependent on the amount of shear reinforcement provided, which in turn governs the position of the shear crack causing failure. If the area of shear reinforcement provided is more than that needed to carry the shear, then the shear crack causing failure falls outside the shear reinforcement, and the reinforcement does not yield. A typical example of this, is slab L_5 shown in Fig. 20. In slabs L_4 (ϕ_v = 6.5 mm, EC = 305 mm), L_6 (ϕ_v = 8.0 mm, EC - 152.5 mm) and L_{10} (ϕ_v = 8.0 mm, EC = 152.5 mm) where the shear failure crack cut across the shear reinforcement, the strains in the arms (adjacent to the column face, nearer to the eccentric load) were high, with the reinforcement yielding. Figs. 21 to 23 show the load V_s strain in shear reinforcement for these slabs.

The strain readings taken indicate that shear reinforcement works effectively and that the shear reinforcement crossed by the

critical cracks, reaches yield. The straining of the shear reinforcement appears to be continuous under increasing load, and does not show any sharp discontinuity. The shear reinforcement is subjected to considerable bending in addition to axial forces, indicating that the opening of the shear crack is not perpendicular to the crack plane, but more nearly perpendicular to the plane of the slab. When the column load is eccentric, the shear cracks extend round only part of the column (or perimeter outside this) and it is only in this part of the slab that the shear reinforcement works effectively.

Slabs L_8 and L_{11}, which were provided with a second layer of shear reinforcement (bent up bars in the case of slab L_8 and a row of stirrups in the case of slab L_{11}), in addition to a single shear hat, with 13 mm diameter shear arms, the failure occurred so far out from the column as to miss even the outer reinforcement. Fig. 24 shows the measured strains in the stirrups against load.

In the shear hats used, the shear arms were bent round the main steel (main steel passing through shear arms) and this resulted in excellent anchorage. The concrete adjacent to the shear arms was intact at failure as can be seen from Fig. 26.

The load carried by the shear hats with different areas of shear arms were calculated approximately from the strain readings. Fig. 29 shows the applied load V_s shear carried by the shear hats. It can be seen that there is an increase in shear carried with an increased amount of shear reinforcement.

4.3.2. Series ES.

The same type of shear hat was used for external columns, as for the internal columns, with a slight modification to suit the location of the column. The relation between the observed values of strains in the shear arms and loads for slabs ES_3, (ϕ_v = 6.5 mm, EC = 228.5 mm), ES_4 (ϕ_v = 9.5 mm, EC - 228.5 mm), ES_6 (ϕ_v = 6.5 mm, EC = 0) and ES_7 (ϕ_v = 6.5 mm, EC = - 228.5 mm) are shown in Figs. 30, 31, 32 and 33. The strain readings indicate that the shear reinforcement works effectively and that the reinforcement crossed by the critical crack reaches yield near failure.

4.4. Strain in the main steel.

Strain measurements were taken in order to assess the

extent of yielding of main steel. In the majority of the slabs, yielding occurred in the reinforcement, adjacent to the column, on the side towards the eccentric load. The relationship between the observed values of strains and the loads are given in Figs. 35a to 35e for slabs L_1, L_3, L_4, L_5 and L_6, while Figs. 36a to d, correspond to series ES for slabs ES_1, ES_2, ES_3 and ES_4.

It can be seen that in the case of edge column connections (Series ES), the strains in the gauges adjacent to the column and parallel to the free edge were considerably higher than those perpendicular to the free edge, reaching yield values. Strains parallel to the free edge seem to gradually reduce towards the parallel edge further away from the column.

4.5. Concrete strains on the surface of the slab.

4.5.1. Series L.

Strains were measured at points of interest in both radial and tangential (perpendicular to, and parallel to a particular column face) directions with electrical resistance strain gauges and in some cases with 'Demec' points.

The tangential and radial strains measured in the case of slabs L_7 and L_9 with concentric load were as shown in Fig. 37. The radial strains diminished rather steeply with increasing distance from the column. The variation in tangential strains across the slab was much more gradual. It could be said that tangential strain is inversely proportional to the distance from the column with a maximum value at the column face.

The tangential strains as well as the radial ones were fairly high on the side of the eccentric load (area closest to the most heavily loaded edge of the column), but not large enough to create failure by crushing in any of the slabs. The absence of any crushing can be seen from Fig. 27 which shows a typical junction of the column and slab after failure, and also from Figs. 38a to e which indicate the load V_s strain in concrete for some of the slabs tested.

4.5.2. Series ES.

The measured strains for slabs ES_1, ES_3 and ES_5 are shown in Figs. 39a to c as functions of column loads. The radial strains near the inner faces of the columns were rather small, being compressions

initially, but becoming tensile at failure. Radial strains at the other two faces were large, and the tangential ones small, indicating the tendency to span one way. However, this cannot be generalised, for the eccentricities used in the tests were rather small. The strains measured suggest the presence of torsion adjacent to the column faces, perpendicular to the free edge (see Fig. 39b), but this may just as well be due to the inclined components of strains parallel to the free edge.

4.5.3. Corner column CS.

Measured strains against load are shown in Fig. 40. Since some of the gauges failed to function, it was not possible to study the distribution of strains around the column. However Fig. 40 gives an approximate idea about the distribution around the column.

4.6. Crack Patterns.

4.6.1. Series L.

In all slabs the first crack to appear was a flexural crack adjacent to the column face or faces. This was followed by radial cracks which extended from the column face, and spread towards the supports with increments of load. This was accompanied by tangential cracking which generally formed in two or three loops round the whole of the column, for concentric loads and part of the column for combined loads. In the case of combined loads, such tangential cracks appeared only on the side of the eccentric load and the radial cracks were more pronounced on this side.

Cracked surfaces of some of the slabs are shown in Figs. 41 to 43. The bottom surfaces of slabs L_9 and L_1 which had no shear reinforcement and were subjected to loads with 0 and 305 mm eccentricities respectively are shown in Fig. 41. Fig. 42 shows the bottom surfaces of slabs L_3 and L_4 with different amounts of shear reinforcement, but the same eccentricity (EC = 305 mm) while Fig. 43 shows the bottom surface of slab L_{11} which failed in flexure.

An effort to measure the crack widths was made using a graduated telescope. The main interest would have been in the widest crack, but as this was at the column face, it was not possible to measure its width with the available equipment. Hence the idea of measuring crack widths was abandoned.

In slabs L_3 and L_4, 25 mm diameter holes were left in the slab at about 305 mm from column face, to detect the formation of shear cracks. Cracks were detected at 60% of the ultimate load. After failure the critical crack was observed to have a flat slope of approximately 1 in 2 (1 vertical to 2 horizontal). Fig. 28 shows a typical flat crack in one of the slabs after failure.

In slab L_7 instead of an observation hole, a set of PML 30 strain gauges were used. The strain gauges were cast in the concrete vertically, tied to the main steel. It was anticipated that the formation of the shear crack would be indicated by a sudden increase in strain reading. However the fact that the gauges had sensitive length of only 30 mm, (depth of slabs being 178 mm) required prior guessing of the location of the shear crack for the gauge to be cut by the crack and the readings obtained were of little use.

Similar gauges were used by Anis[18] in some of his slabs during the same time, without much success and hence further use of the gauges was abandoned.

In all the slabs the shear crack was not visible on the compression face until at failure. The failure was gradual with reinforcement tearing the cover away from the end of the critical shear crack. Fig. 25 reveals this tearing clearly.

4.6.2. Series ES.

The cracks on the underside (loading from top) of the slab were predominantly radial in the inner segment, whilst in the other two segments their inclination to the free edge varied from 45 to 30 degrees, indicating the presence of torsion. As far as the underside of the slab was concerned, all slabs had the same crack pattern. The cracks on the other side were tangential and approximately at rightangles to the ones observed on the underside. The distance from the free edge up to which the cracks spread seemed to be governed by the eccentricity of the applied load. The edges perpendicular to the free edge had torsional cracks as can be seen from Fig. 49. The cracks that occurred at the tops and undersides of slabs ES_6, ES_3 and ES_7 are shown in Figs. 45 and 47 while Fig. 46 shows the bottom surfaces of slabs ES_1, ES_2 and ES_5. Fig. 50, shows the shear cracks at the free edge of the slabs ES_1 to ES_5.

4.6.3. Corner column CS.

The cracked pattern that occurred on the corner column slab connection along with one of the free edges showing the cracking along that edge are shown in Fig. 48.

4.7. Ultimate Load.

The ultimate load was affected by the two variables studied, viz., eccentricity of the applied load and the amount of shear reinforcement. An increased amount of shear reinforcement increased the punching strength, the limit being the flexural strength of the slab. Comparison of ultimate loads of similar slabs with different amounts of shear reinforcement, L_1 and L_3 (EC = 305 mm, ϕ_v = 0 and 9.5 mm, Failure load = 0.399 and 0.499 mega newtons respectively for L_1 and L_3), show that an increase of 25% could be obtained by using a single shear hat. The same applies to external column connections, where comparison of slabs ES_2 and ES_4 (EC = 228.5 mm, ϕ_v = 0 and 9.5 mm, Failure load = 0.342 and 0.508 mega newtons respectively for slabs ES_2 and ES_4), shows an increase of 25% as well if the variation in concrete strengths is taken into account.

In internal column-slab connections, eccentricity decreased the carrying capacity of the slab, in agreement with the other research findings[19] as can be seen from the results given below.

SLAB DESCRIPTION		EC mm	Q_{TEST} M.N.
a. SLABS WITH NO SHEAR REINFORCEMENT			
	L_9	0	0.588
	L_1	305	0.399
b. SLABS WITH SAME AMOUNT OF SHEAR REINFORCEMENT			
	L_2	0	0.868
	L_3	305	0.499

In the case of external column-slab connections, the outward eccentricities decreased the load-carrying capacity, while the inward eccentricities seemed to increase the carrying capacity (eccentricities measured perpendicular to the free edge) as shown below.

SLAB DESCRIPTION.		EC mm	Q_{TEST} M.N.
a SLABS WITH NO SHEAR REINFORCEMENT			
	ES_2	+ 228.5	0.342
	ES_1	0	0.309
	ES_5	- 228.5	0.264
b SLABS WITH SAME AMOUNT OF SHEAR REINFORCEMENT			
	ES_3	+ 228.5	0.442
	ES_6	0	0.370

In slabs L_9 and L_{11}, the support condition was slightly changed; the slabs were supported on 8 ball bearings, instead of the usual system consisting of bolts and rubber pads (for details see Fig. 44). This was to check whether there is any marked difference in behaviour, if the slab was allowed to have differential deflection along its edges. Comparing the slabs L_7 and L_9 there was an increase in the maximum deflection and a slight drop in the test load. But slab L_9 had a weaker concrete compared to slab L_7 and hence it could be said that the original set-up and the new set-up are comparable.

The corner column CS was tested under concentric load. The slab set-up was not quite satisfactory (see Fig. 44), as the corner of the slab which was held down by steel box section, failed before the connection. It is felt that slabs with four corner columns (a table-like set-up) should be tested rather than an isolated corner column connection. However due to lack of time it was not possible to test any of these.

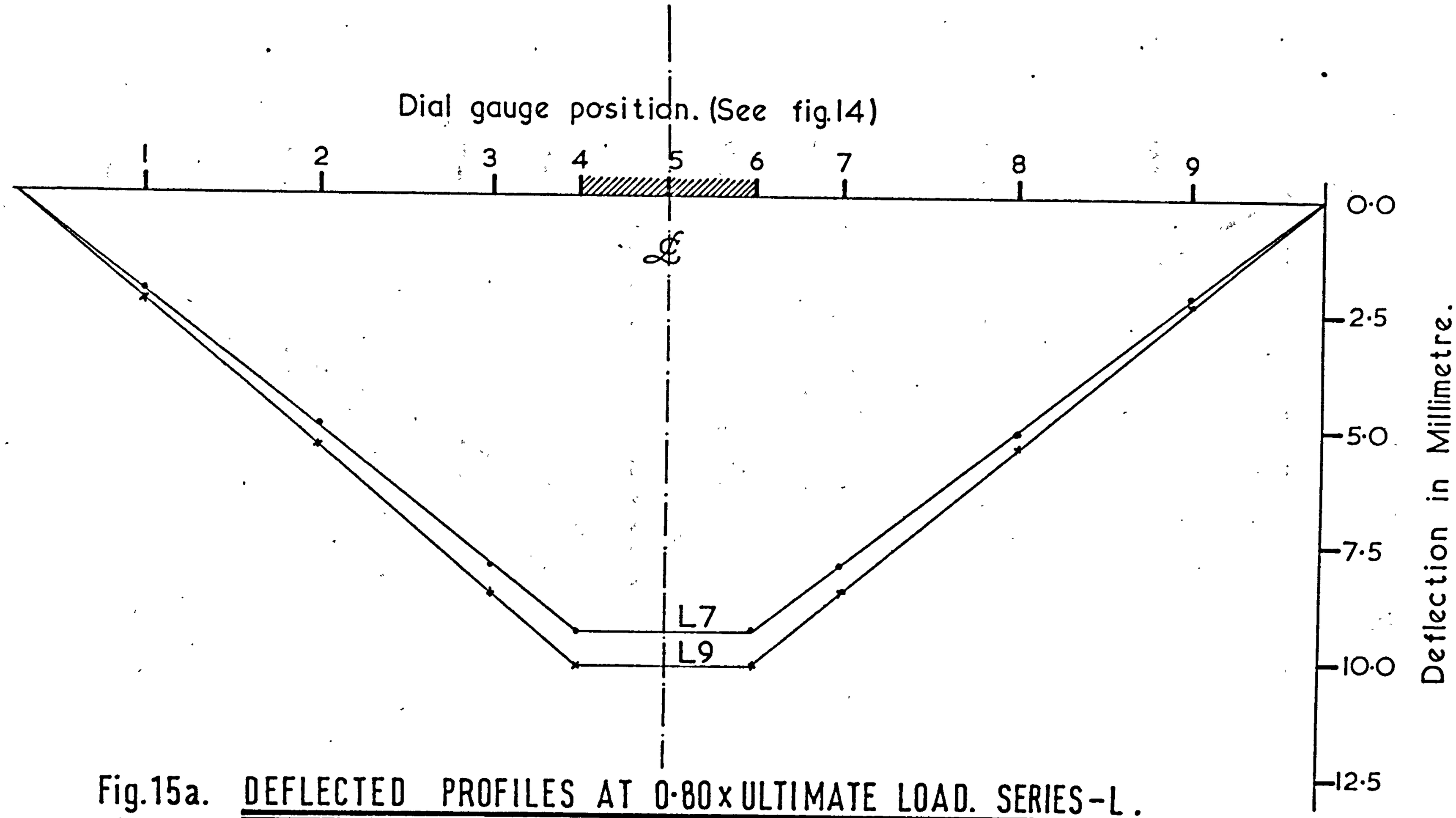

Fig.15a. DEFLECTED PROFILES AT 0·80 x ULTIMATE LOAD. SERIES-L.

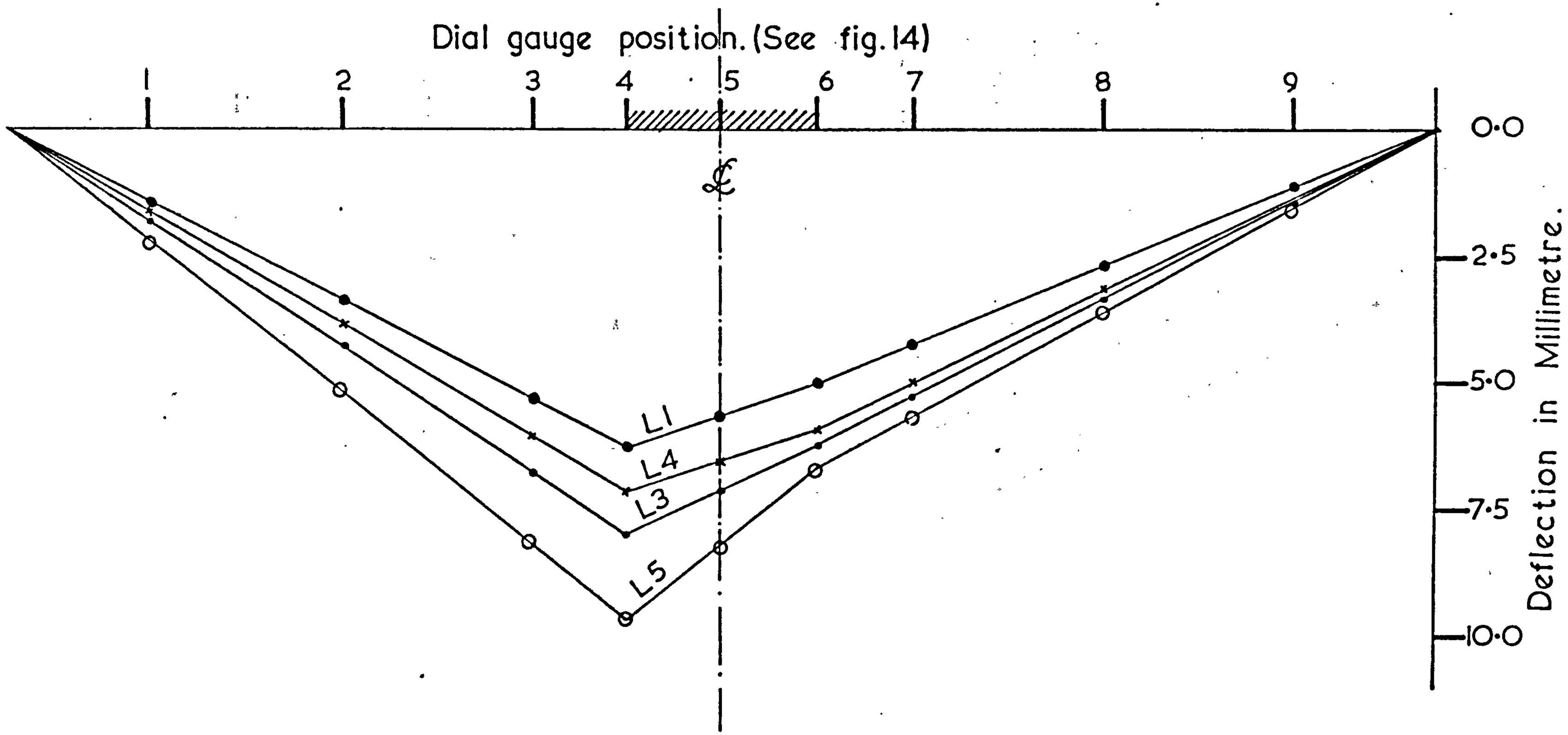

Fig.15 b. DEFLECTED PROFILES AT 0·80 x ULTIMATE LOAD. SERIES-L.

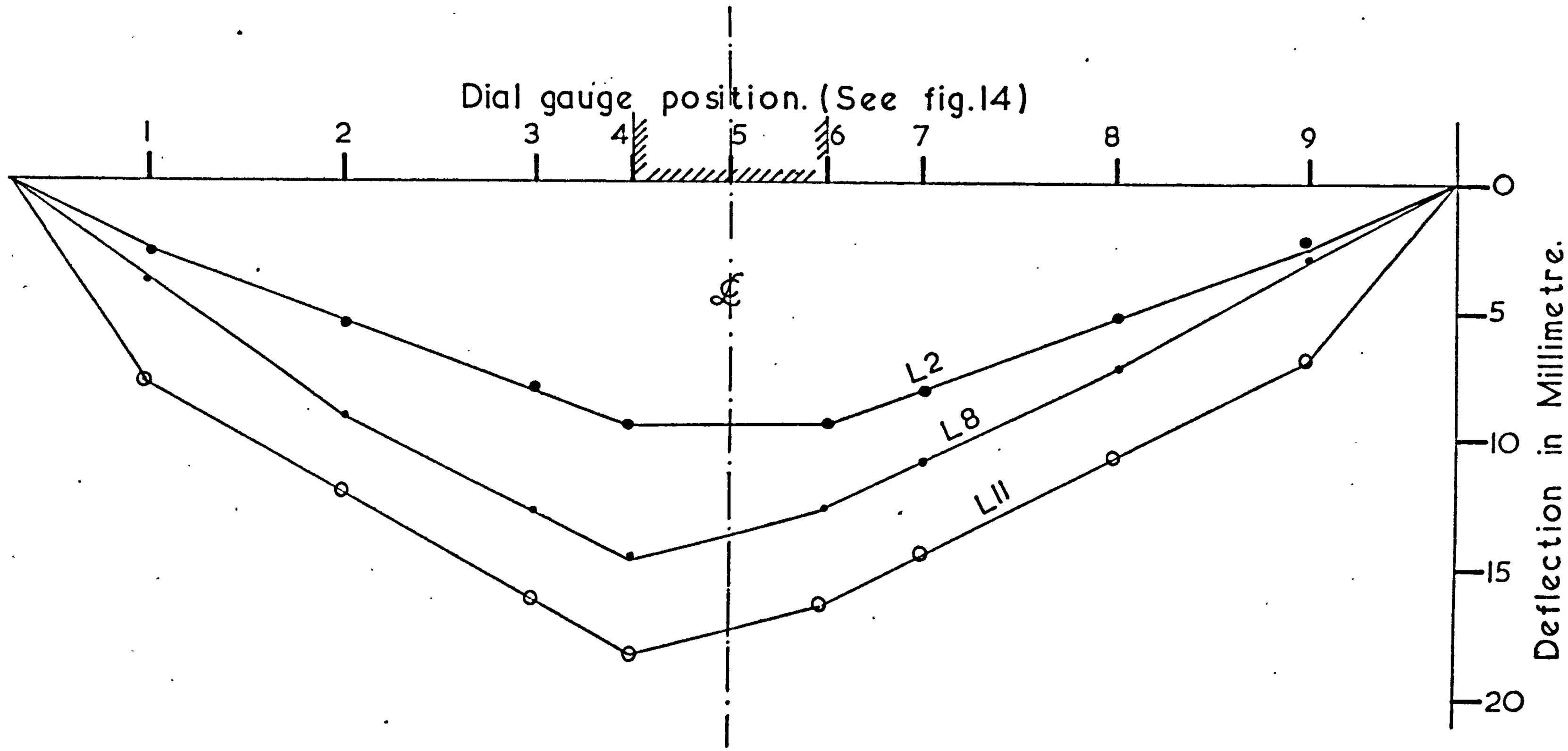

Fig. 15c. DEFLECTED PROFILES AT 0·85 x ULTIMATE LOAD. SERIES-L.

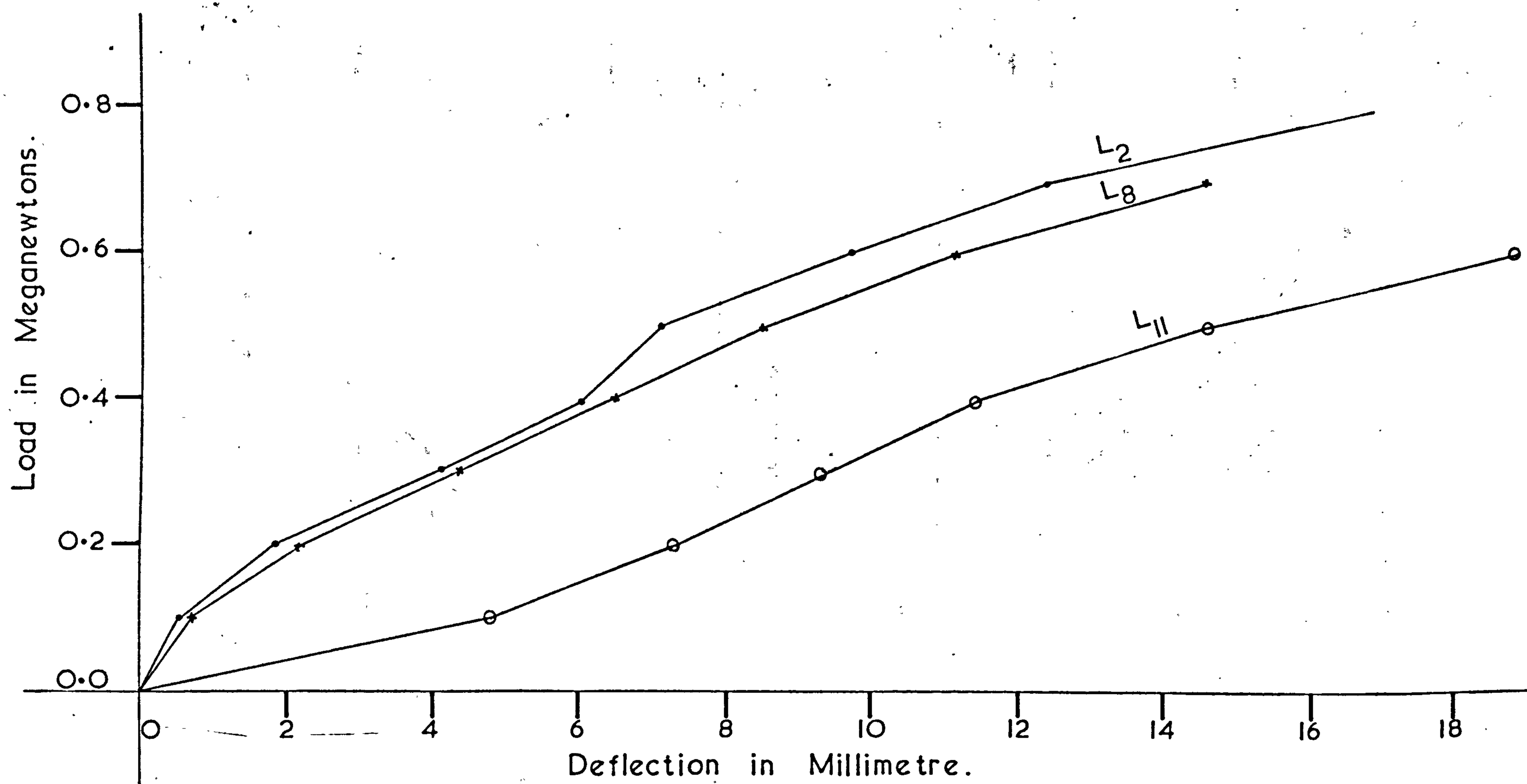

Fig.16. LOAD vs MAXIMUM DEFLECTION FOR INTERNAL SLABS.

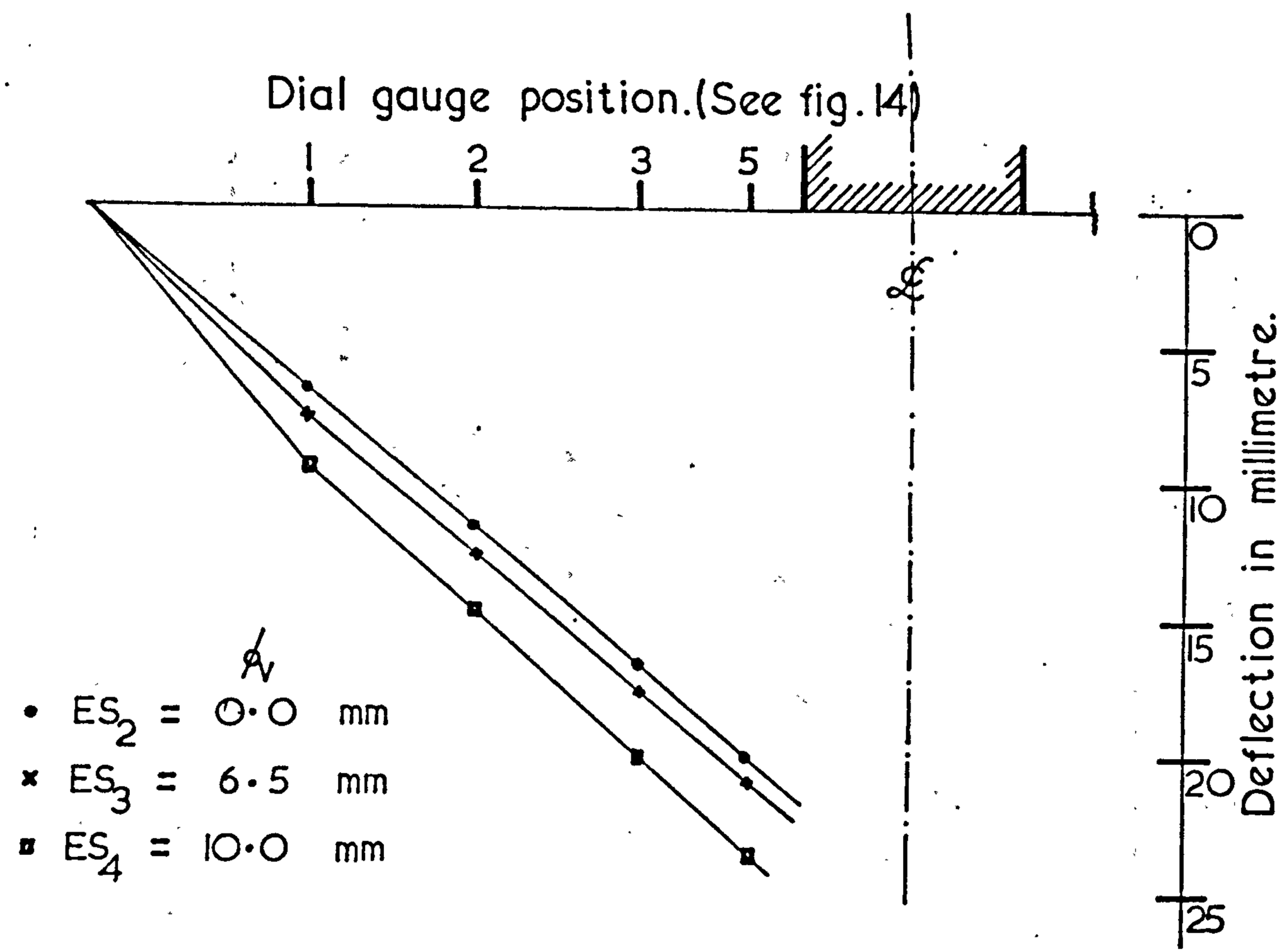

SLABS WITH DIFFERENT AMOUNTS OF SHEAR REINFORCEMENT.

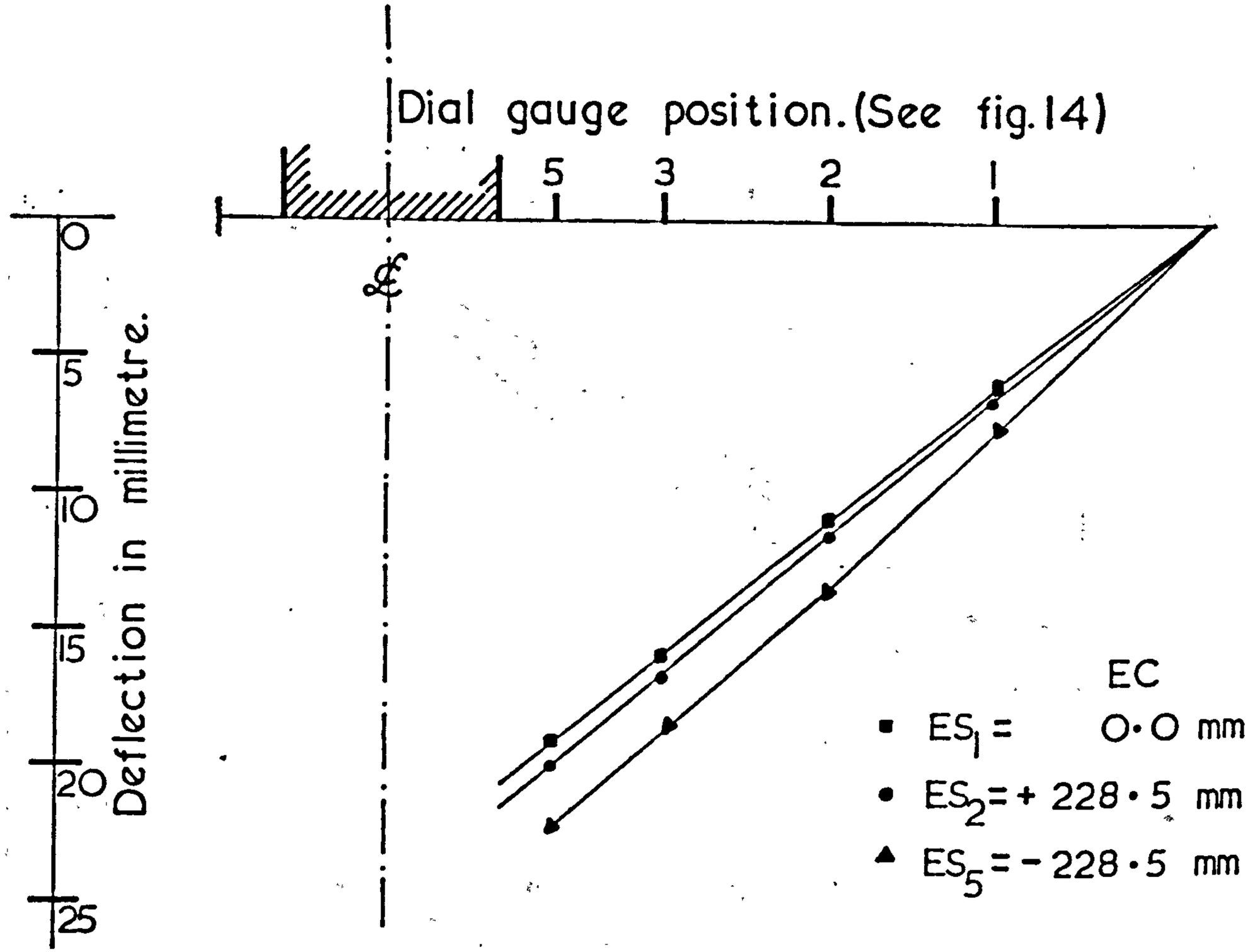

SLABS WITH DIFFERENT ECCENTRICITIES.

Fig. 17. DEFLECTED PROFILES - PARALLEL TO FREE EDGE. SERIES-ES.

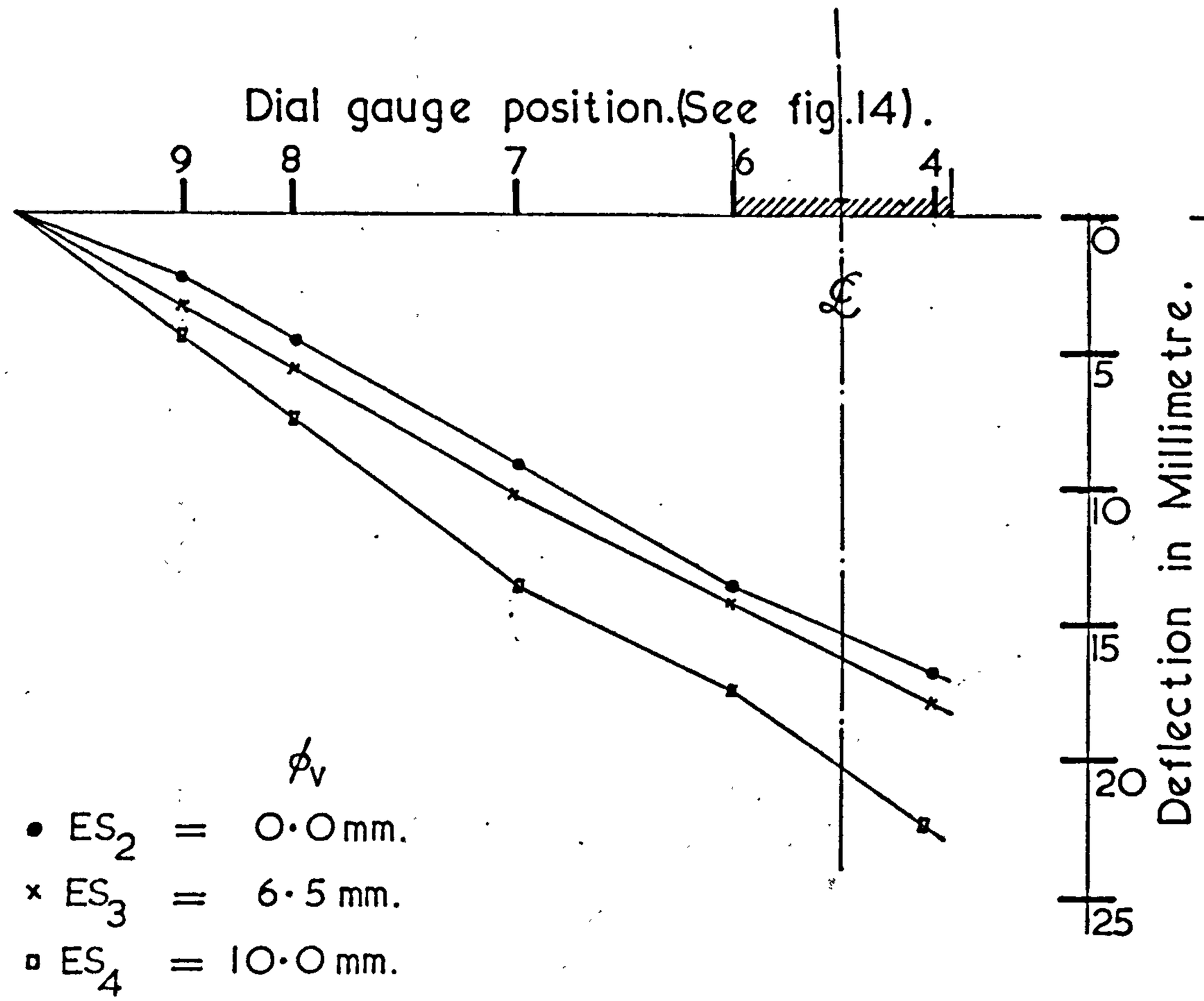

SLABS WITH DIFFERENT AMOUNTS OF SHEAR REINFORCEMENT.

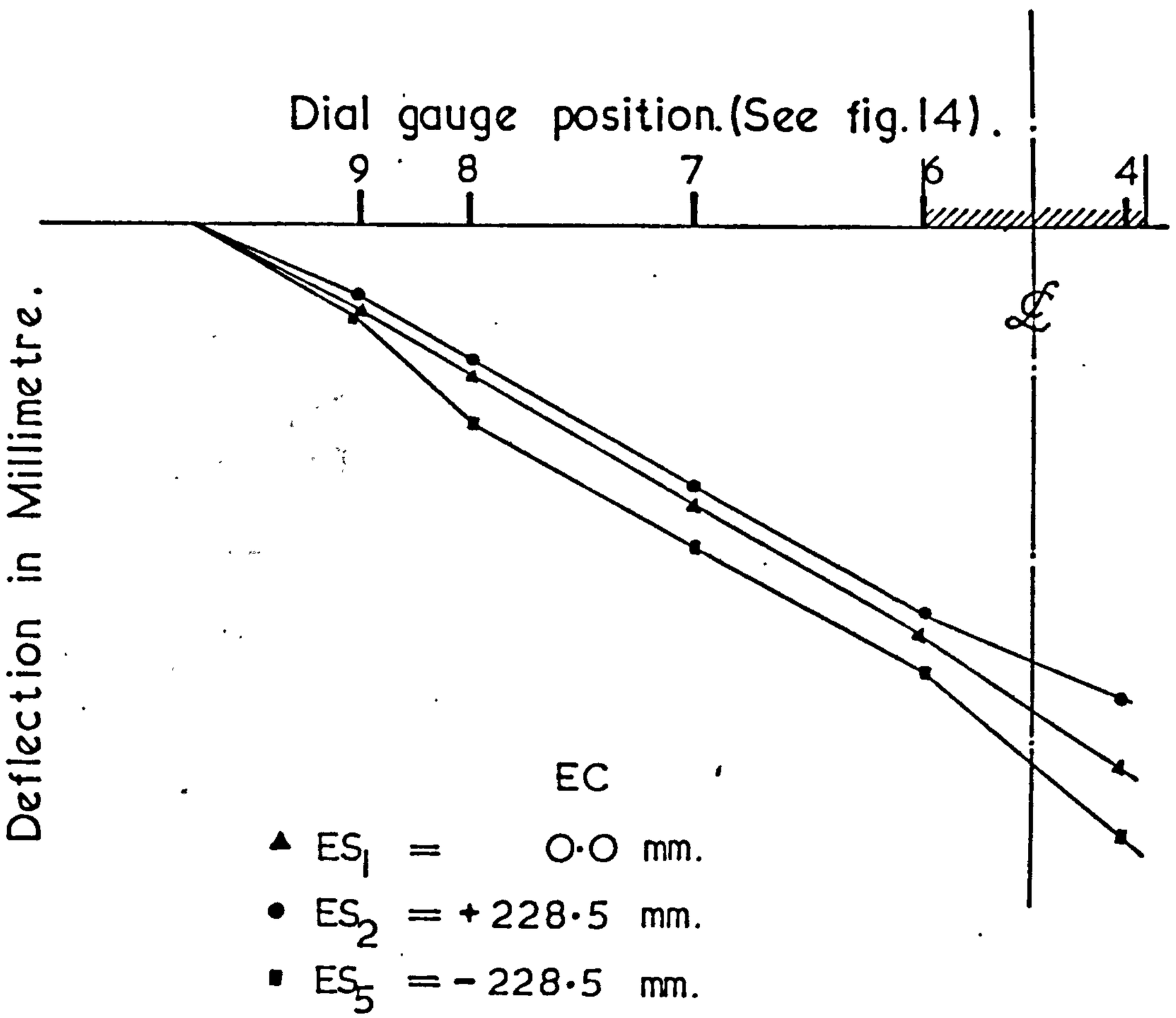

SLABS WITH DIFFERENT ECCENTRICITIES.

Fig.18. DEFLECTED PROFILES - PERPENDICULAR TO FREE EDGE. SERIES-ES.

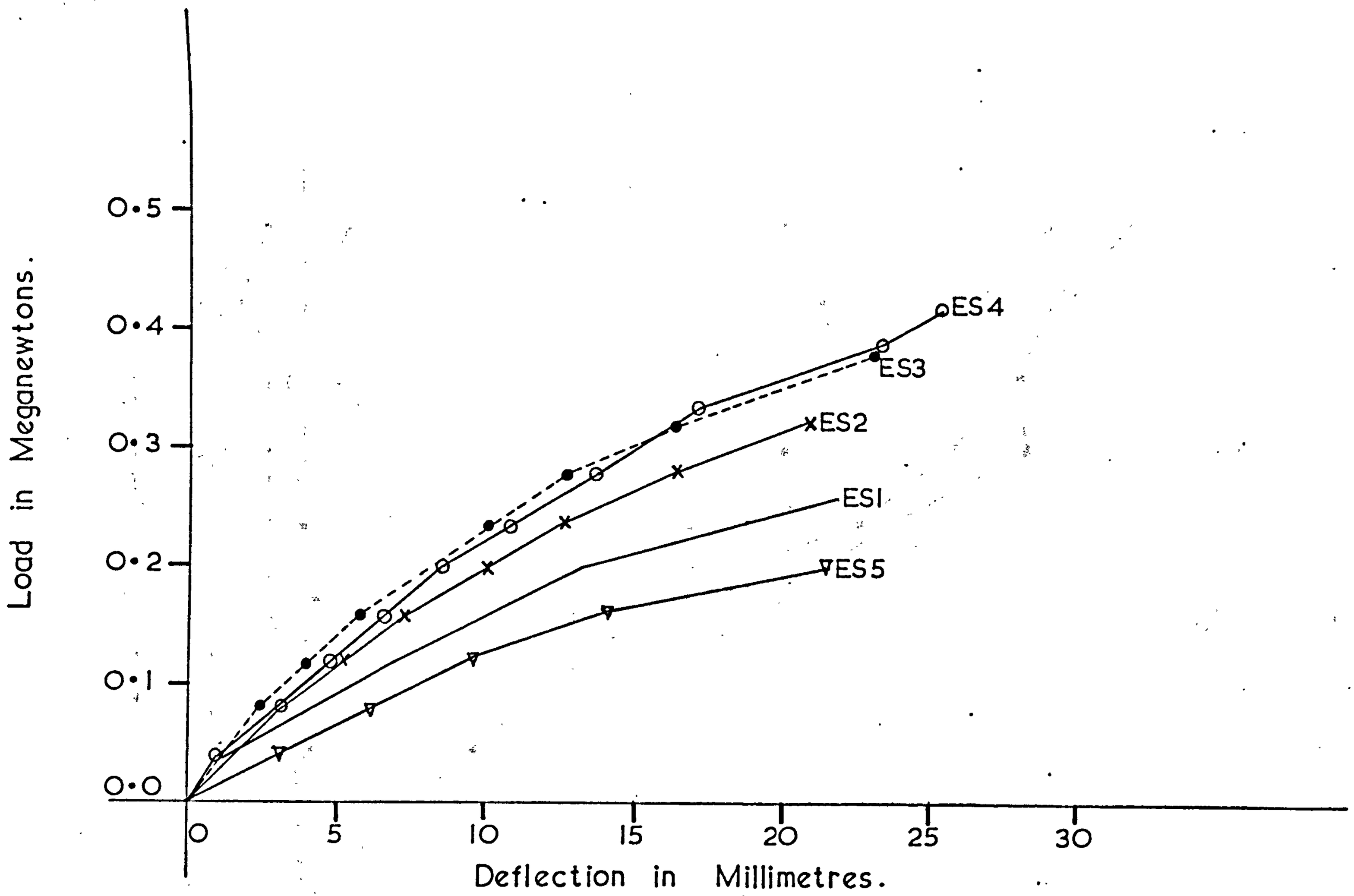

Fig.19. LOAD vs DEFLECTION CURVES. SERIES-ES.

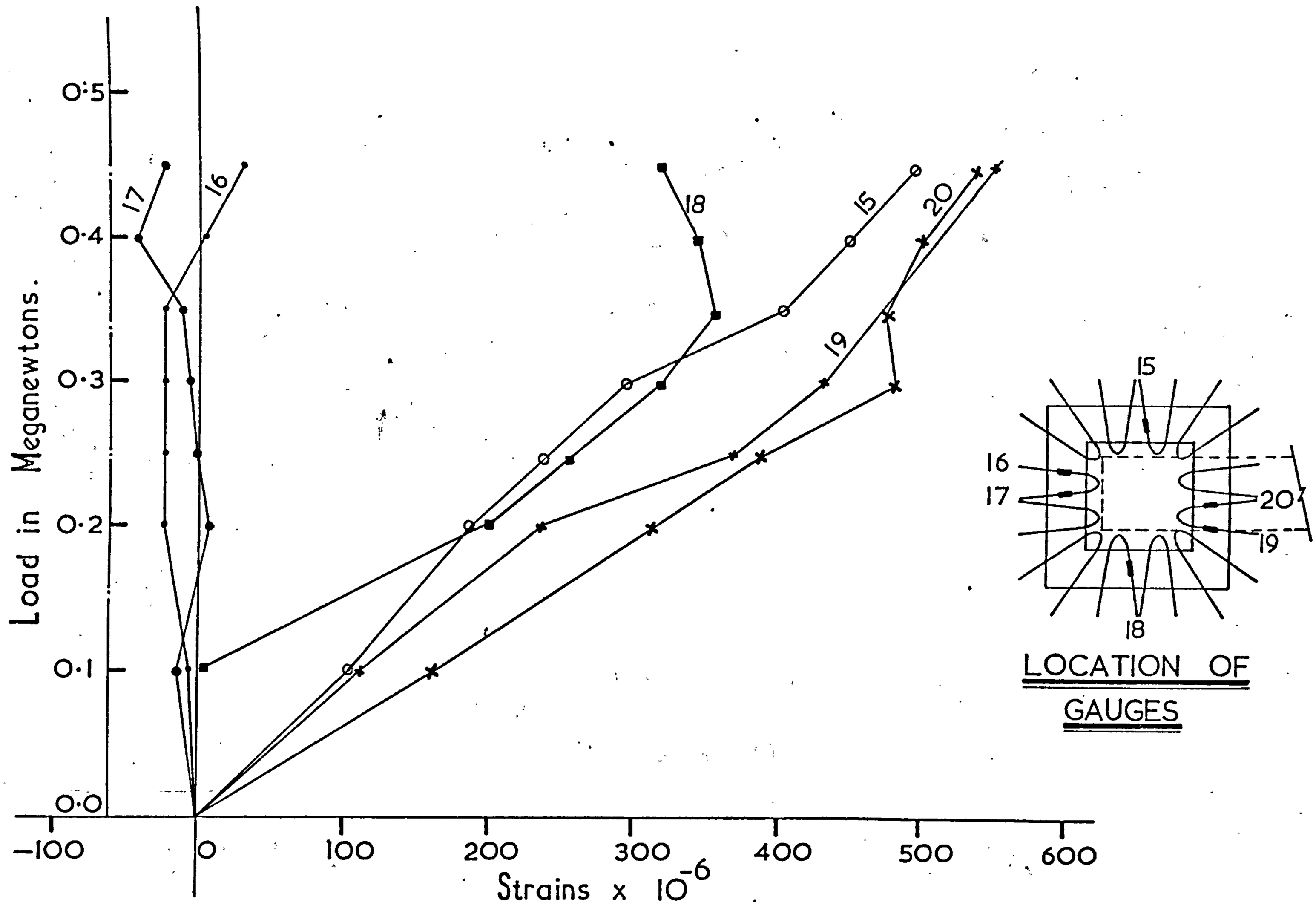

Fig. 20. LOAD vs STRAIN IN SHEAR REINFORCEMENT. SLAB-L5.

Text cut off in original

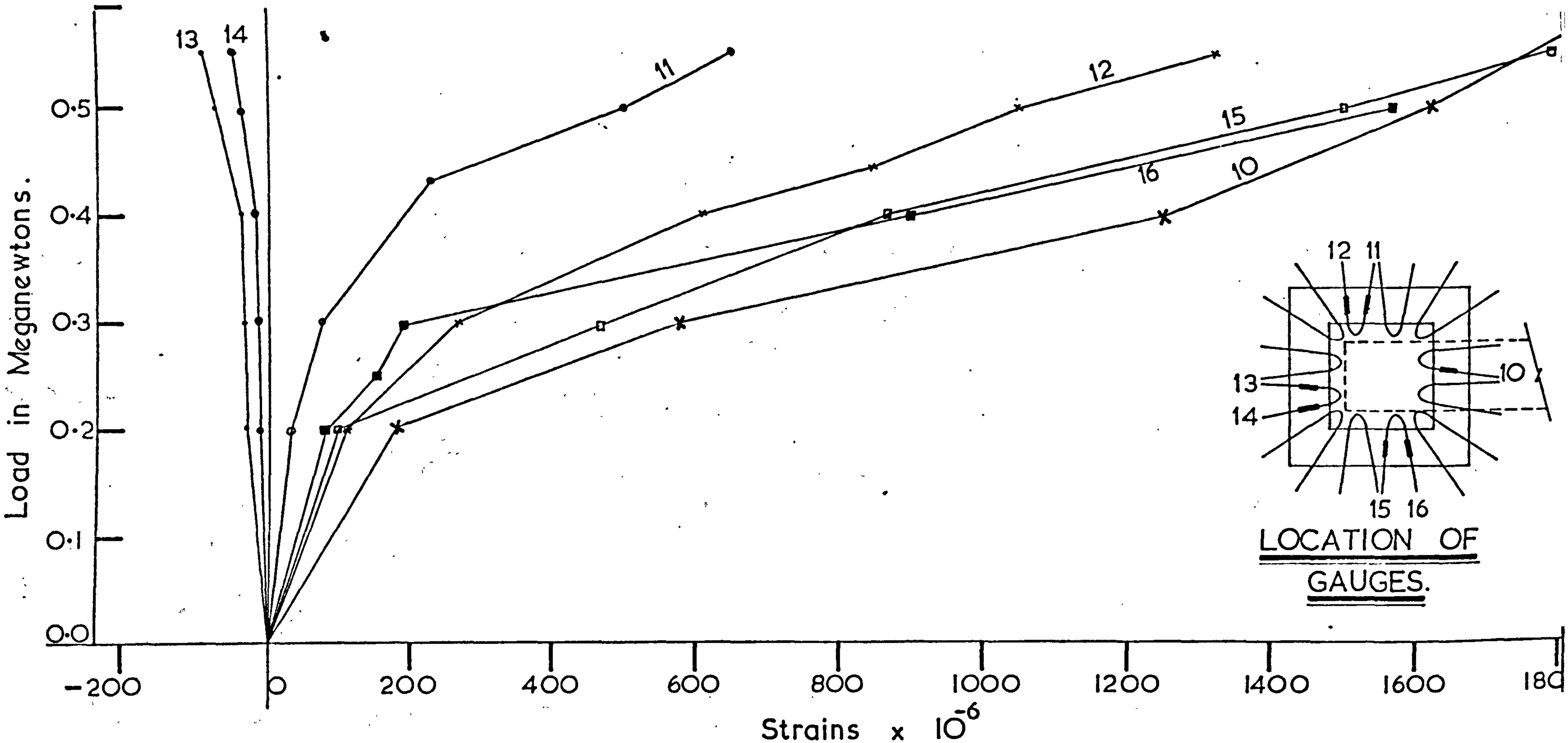

Fig. 21. LOAD vs STRAIN IN SHEAR REINFORCEMENT. SLAB-L4.

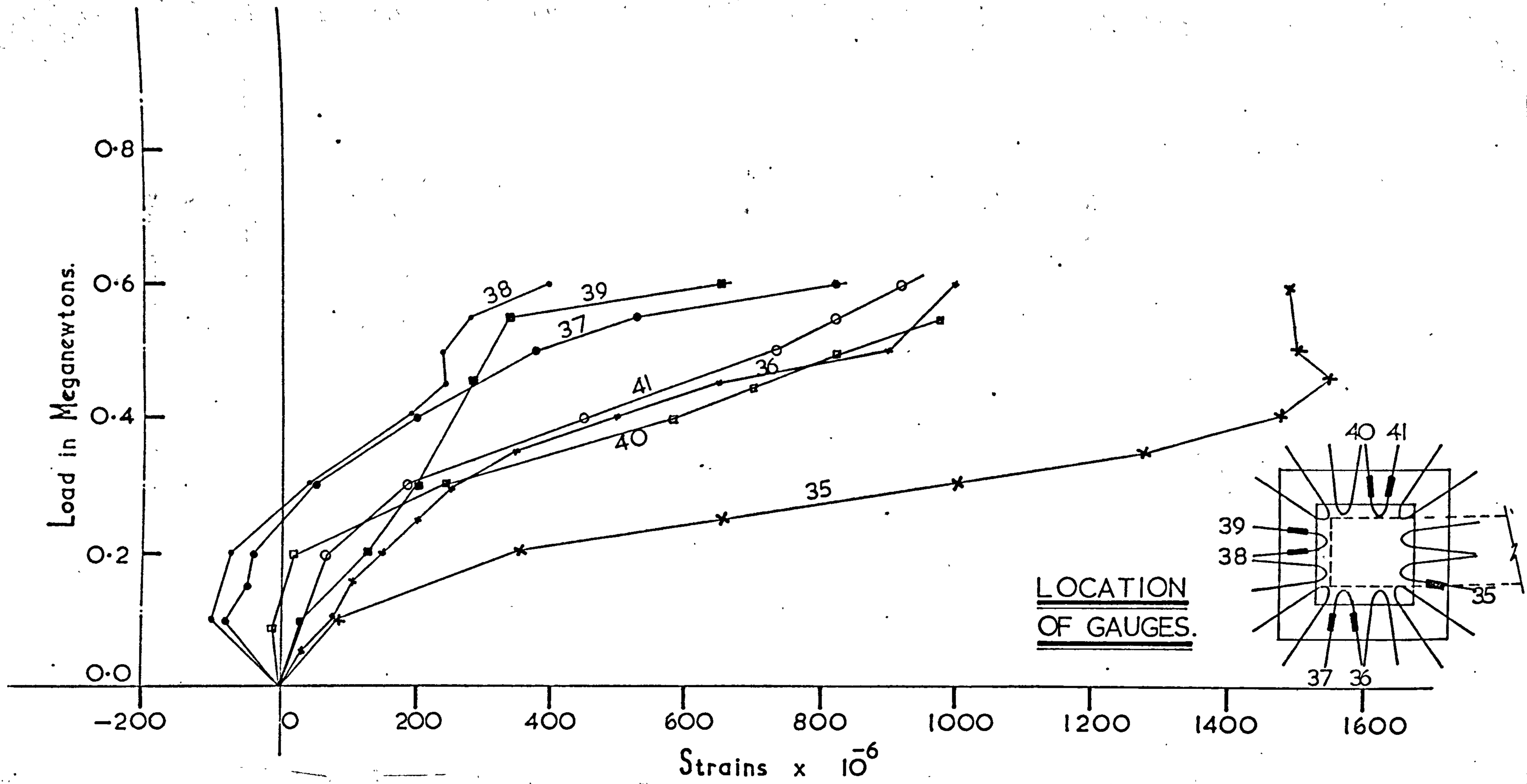

Fig. 22. LOAD vs STRAIN IN SHEAR REINFORCEMENT. SLAB-L6.

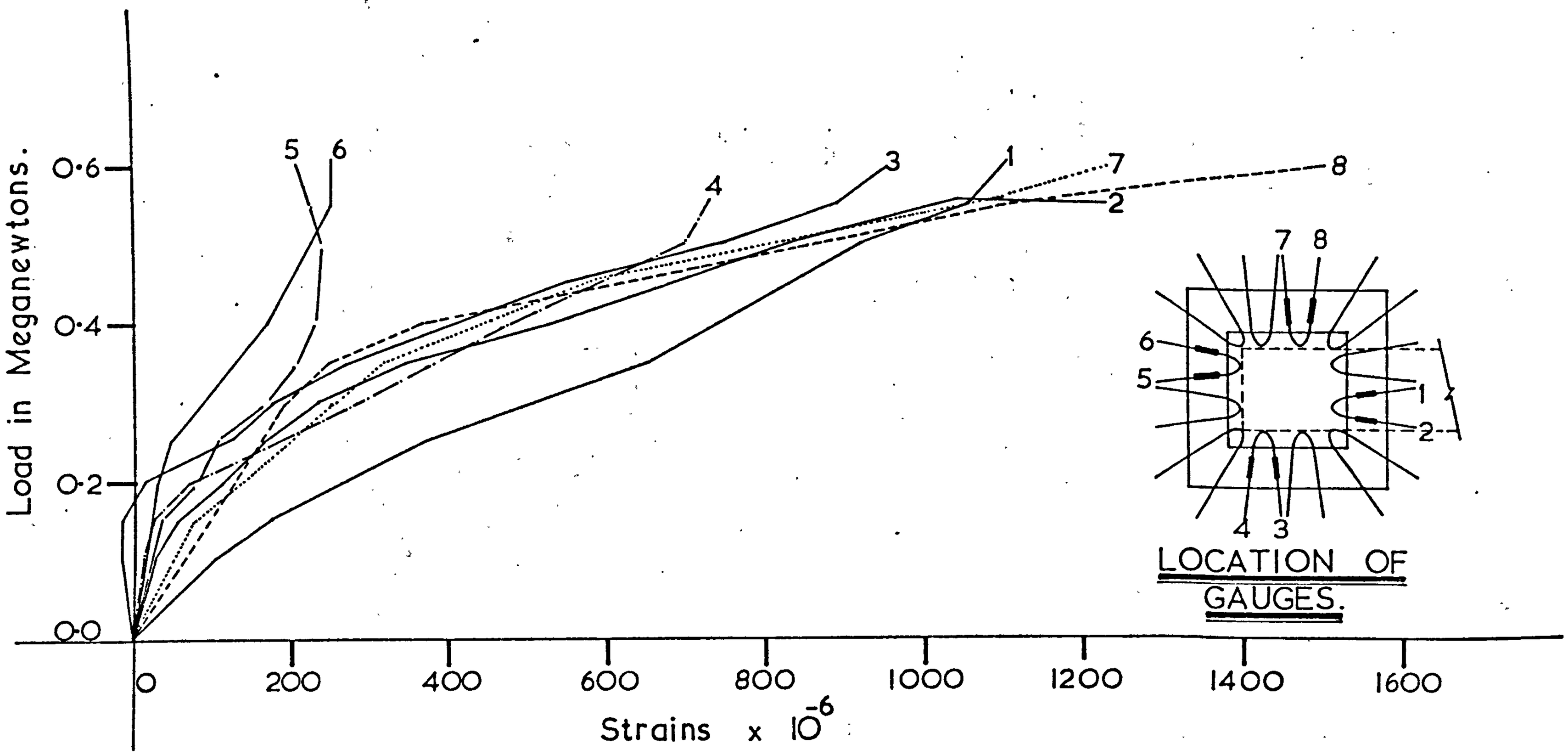

Fig. 23.—LOAD vs STRAIN IN SHEAR REINFORCEMENT. SLAB-L10.

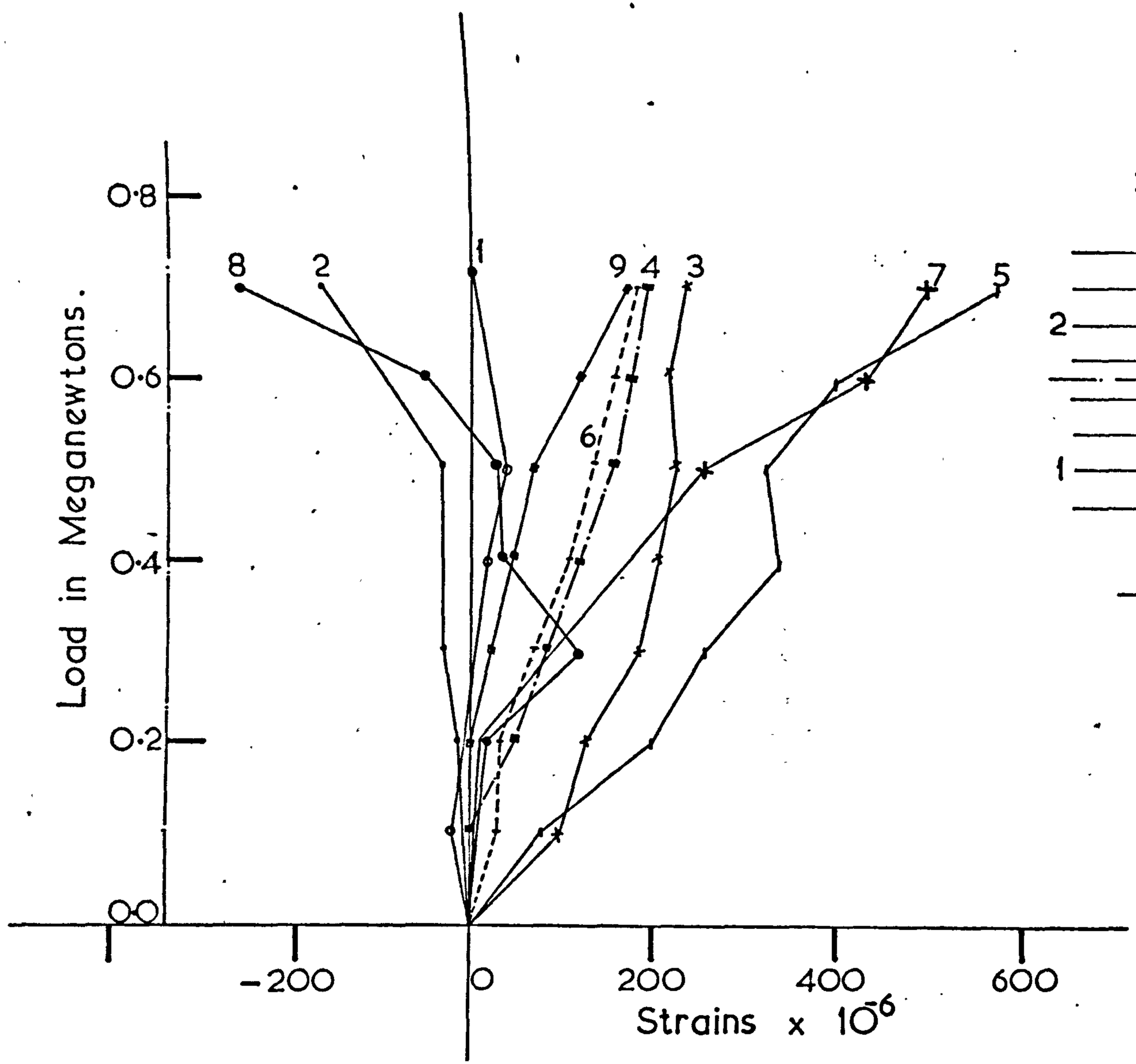

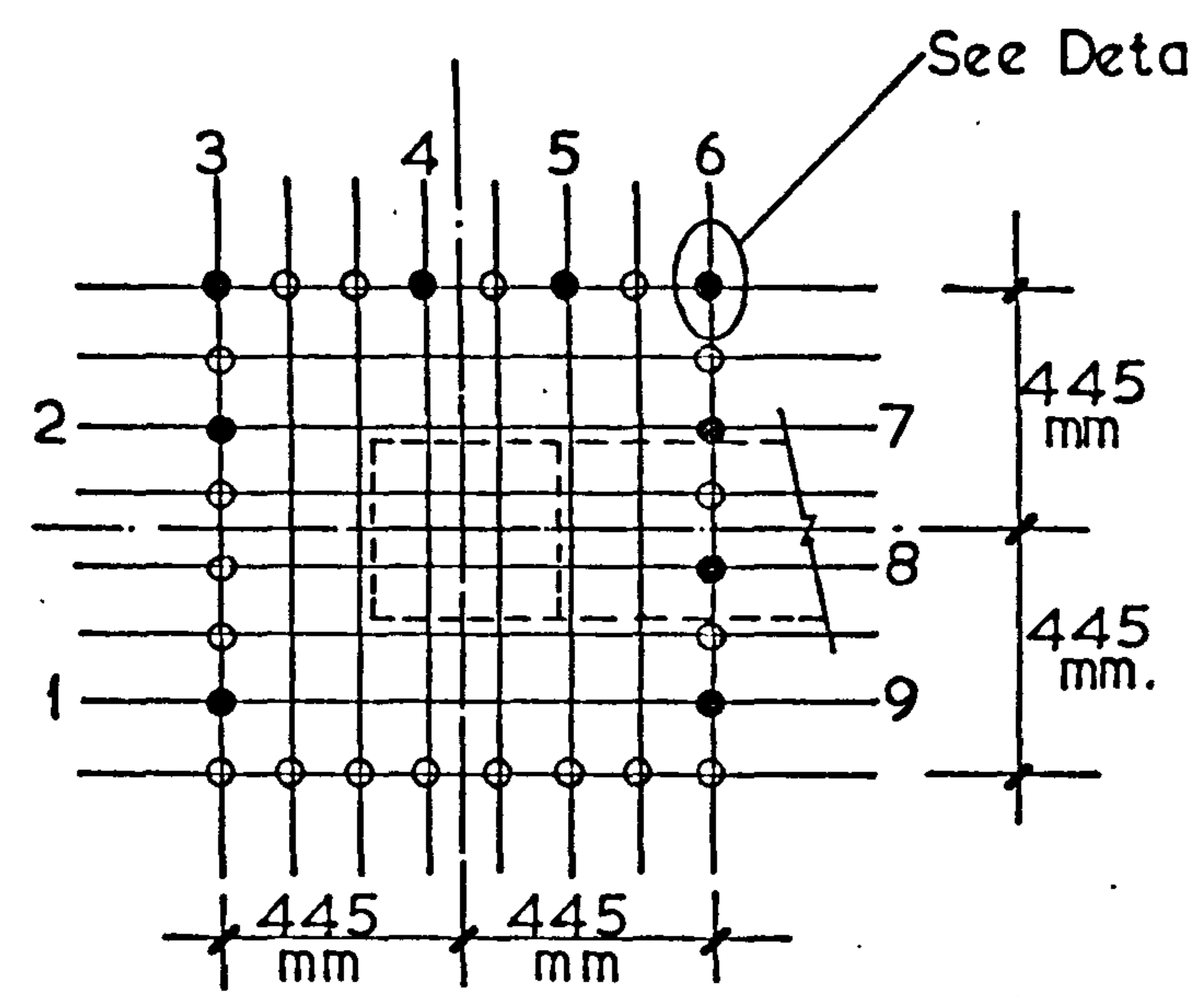

LOCATION OF GAUGES.

(Shear hat not shown for clarity)

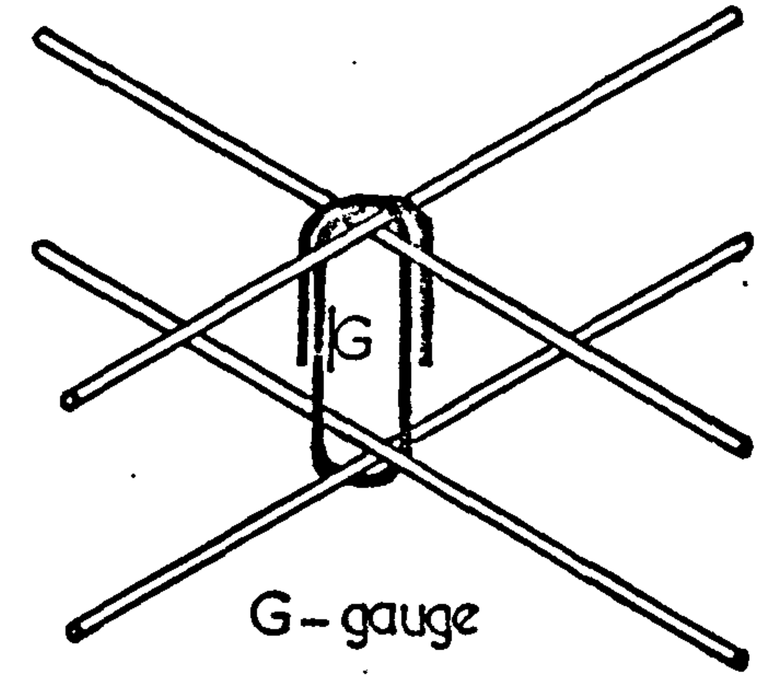

DETAIL. 'A'.

Fig. 24. LOAD vs STRAIN IN SHEAR REINFORCEMENT. SLAB-L11.

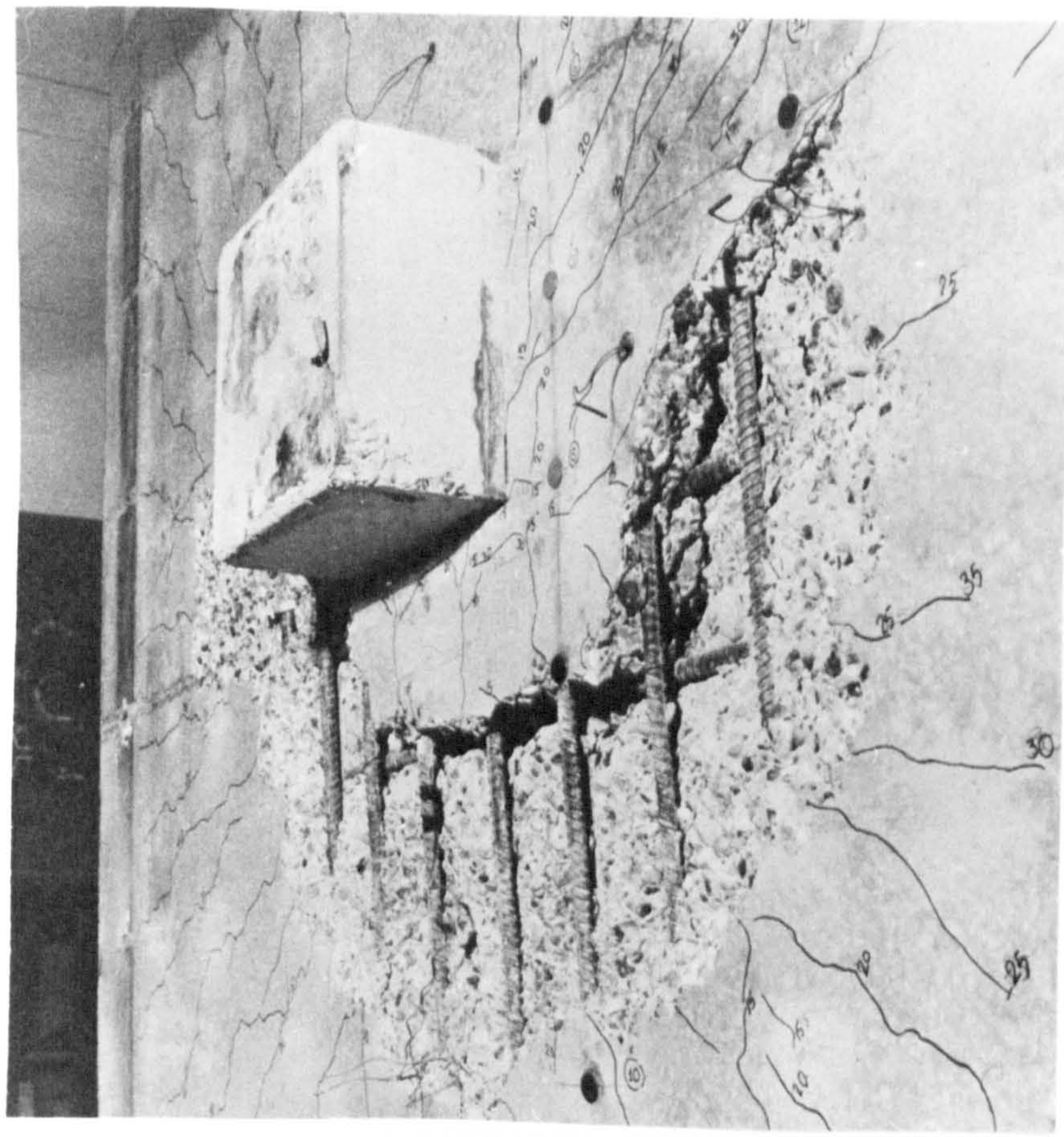

Fig. 25.

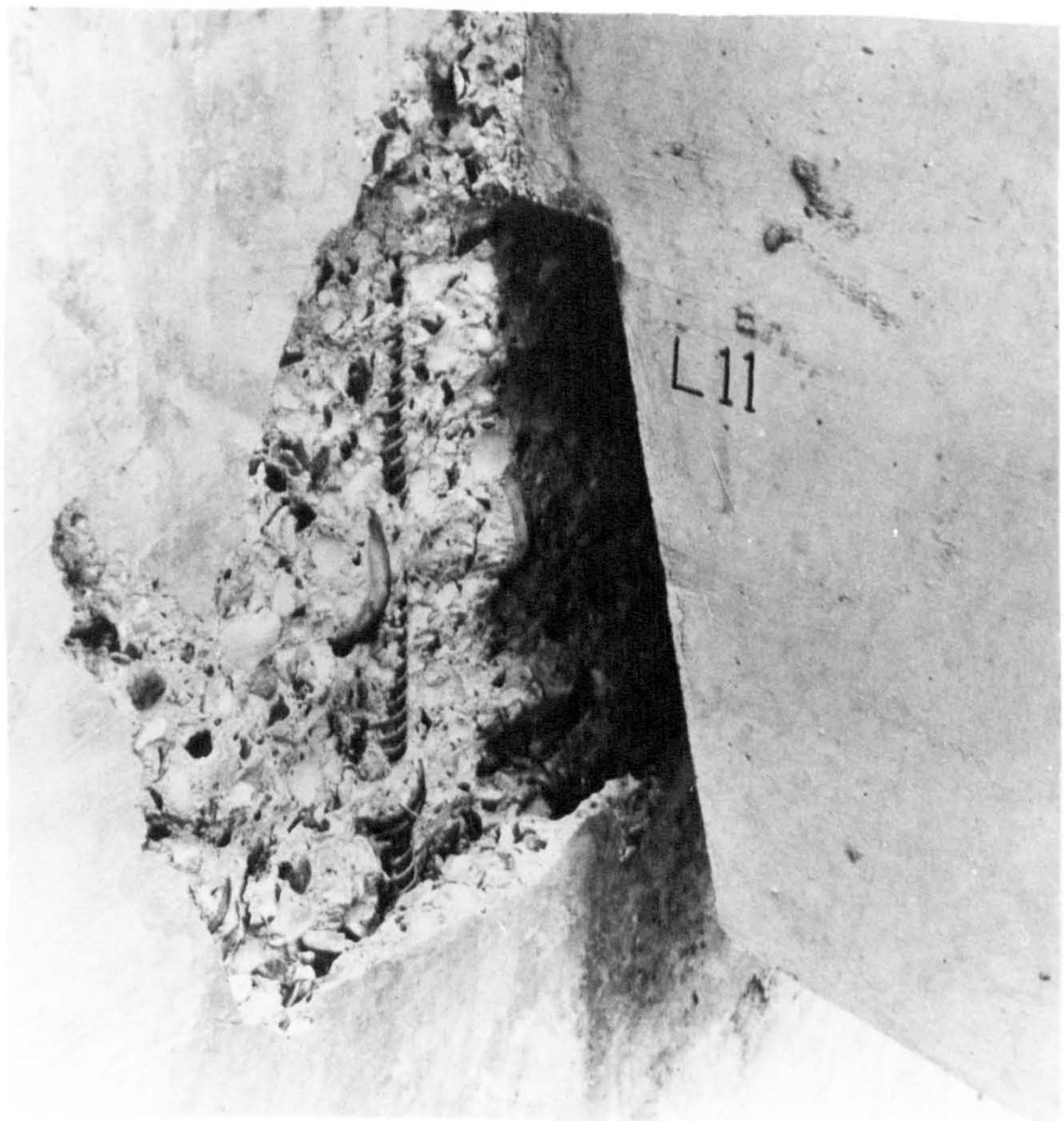

Fig. 26.

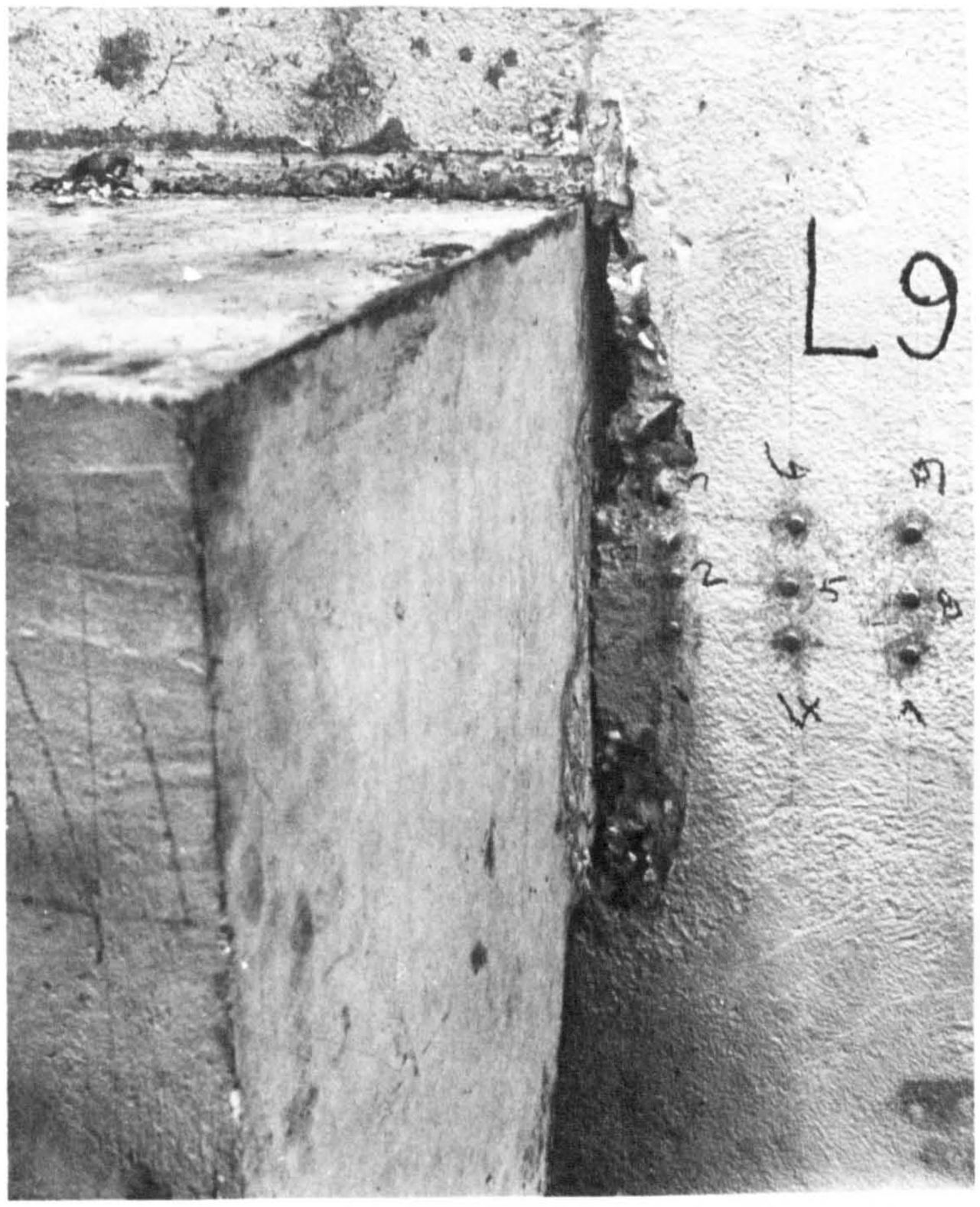

Fig. 27.

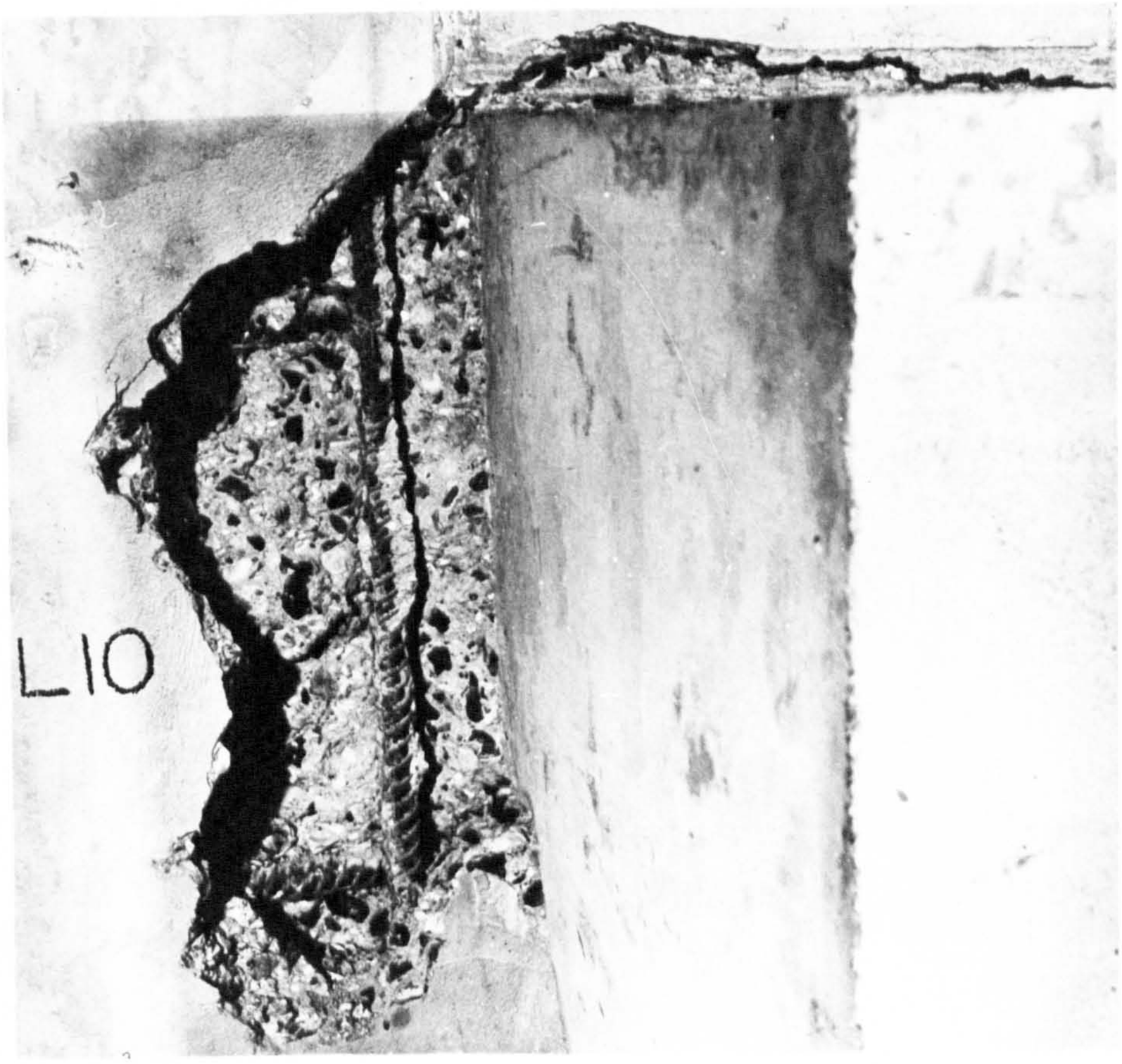

Fig. 28.

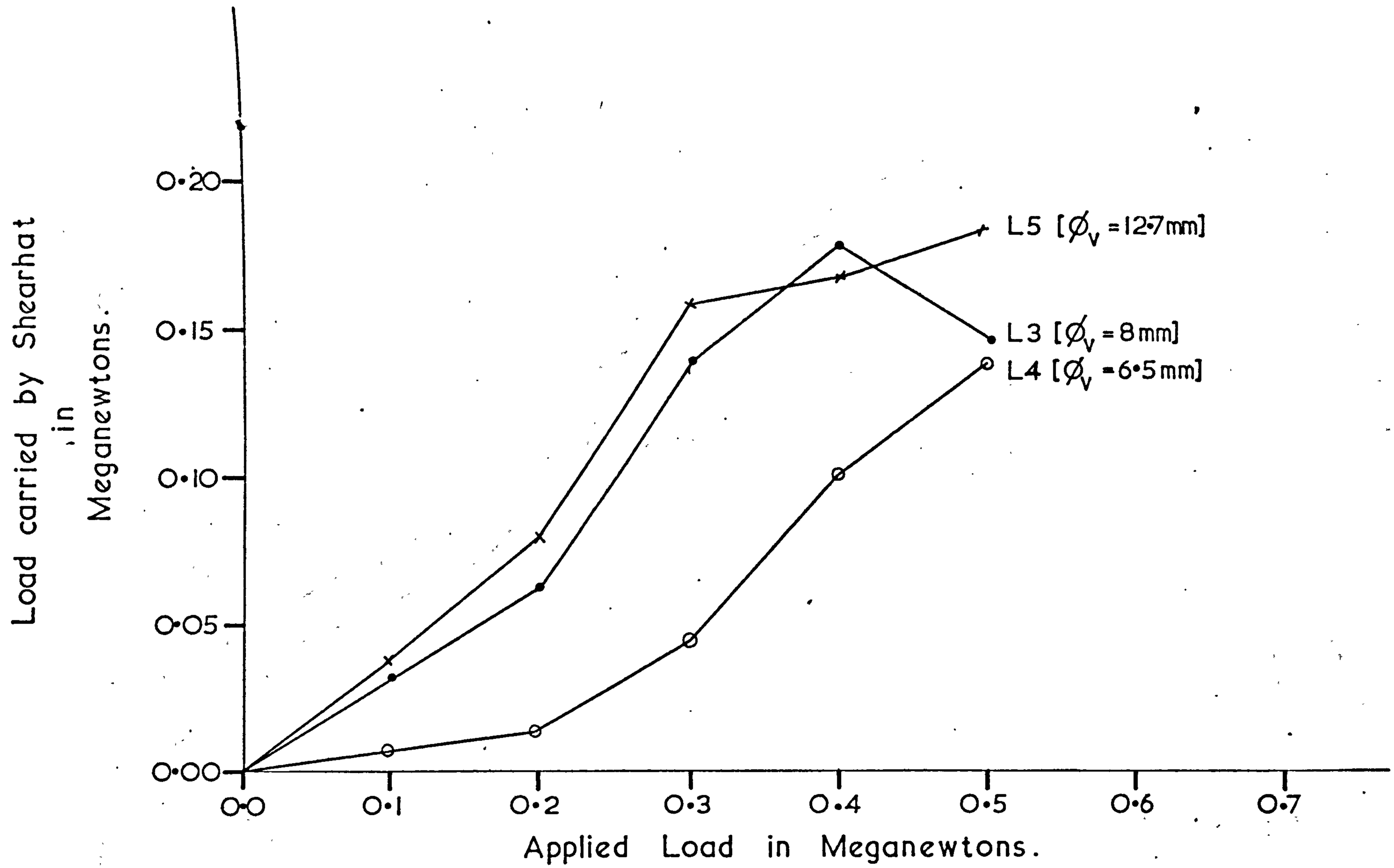

Fig. 29. APPLIED LOAD vs LOAD CARRIED BY SHEAR HAT. INTERNAL COLUMN CONNECTION.

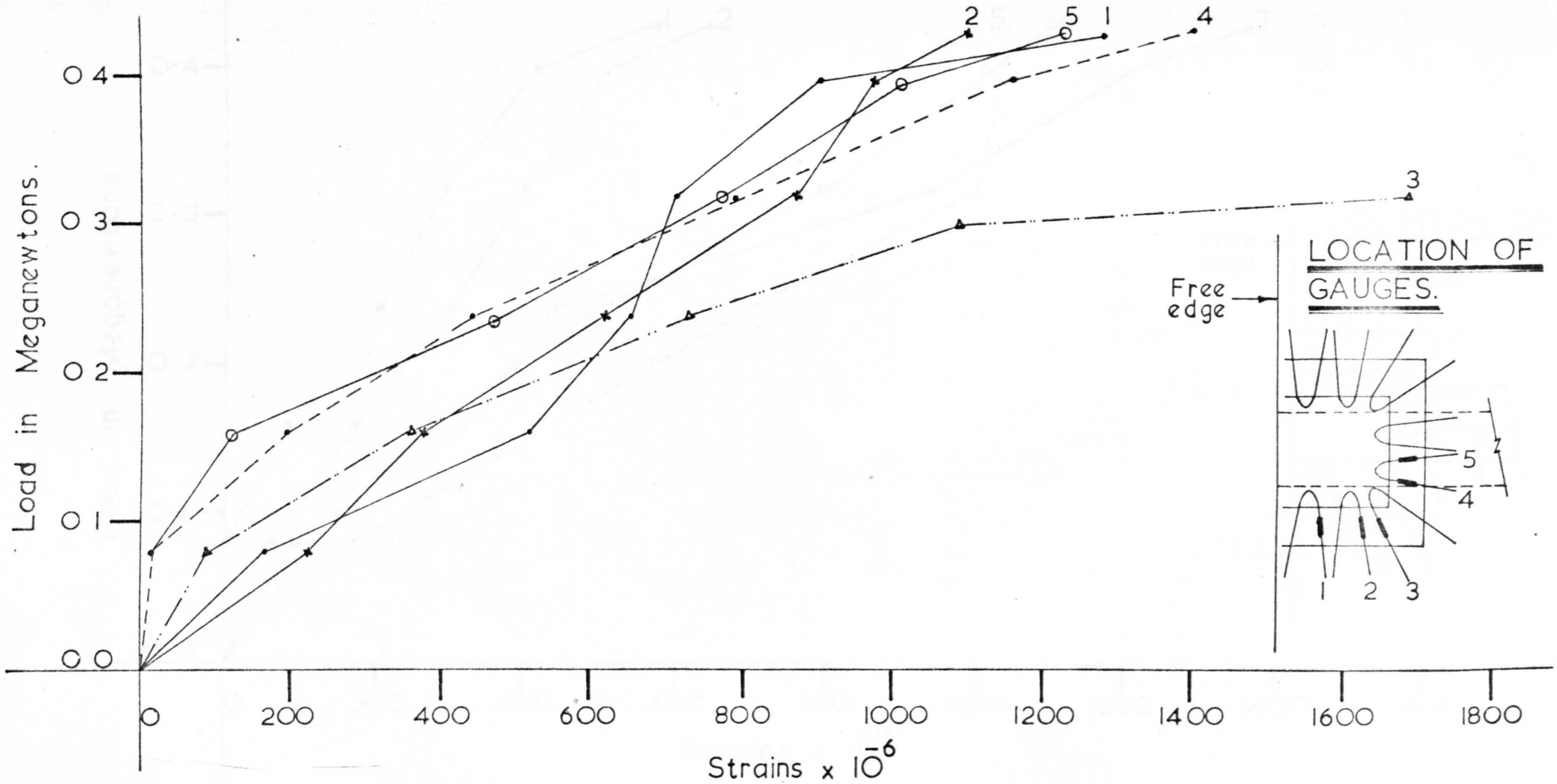

Fig. 30. LOAD vs STRAIN IN SHEAR REINFORCEMENT. SLAB – ES 3.

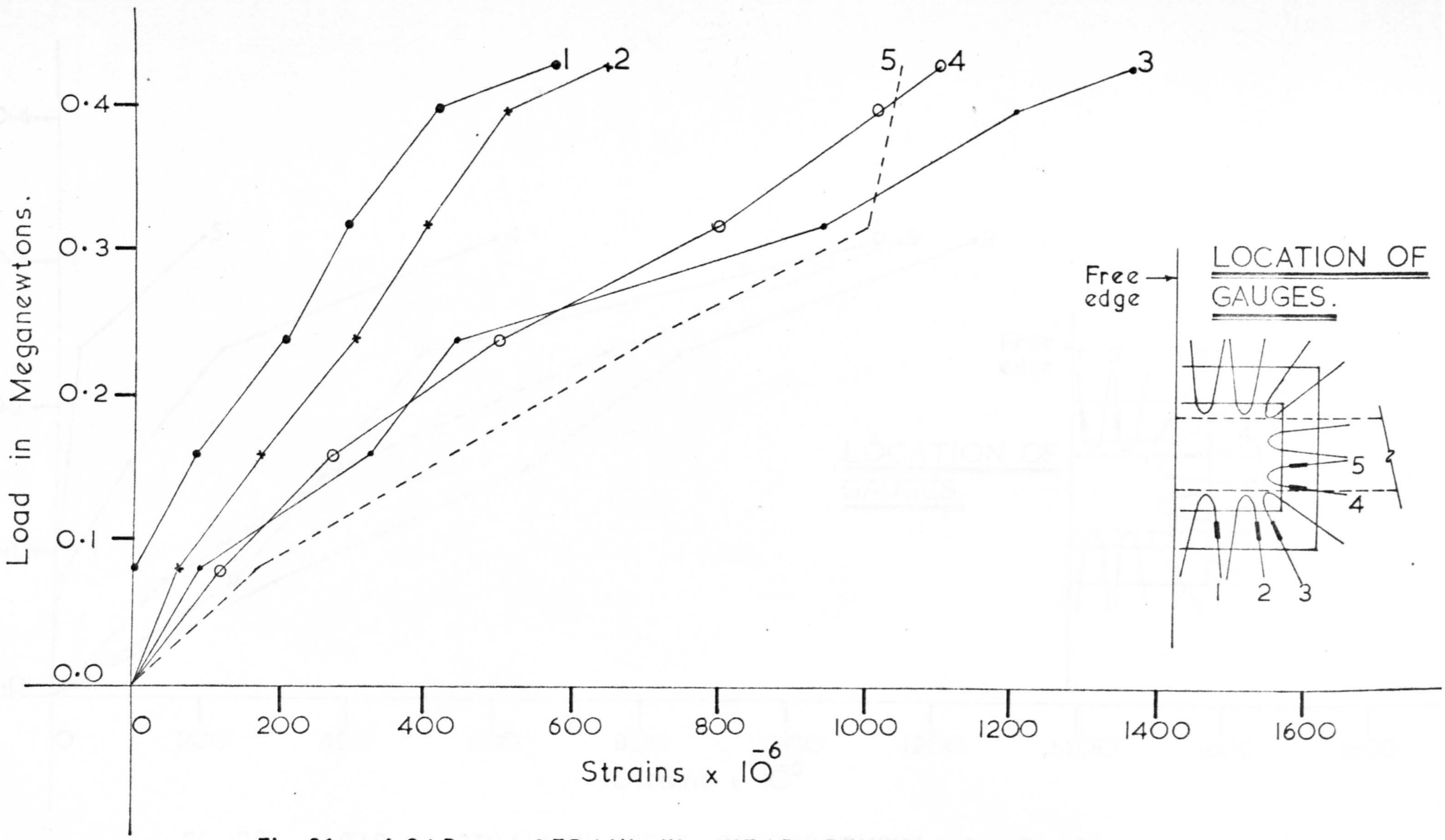

Fig. 31. LOAD vs STRAIN IN SHEAR REINFORCEMENT. SLAB - ES4.

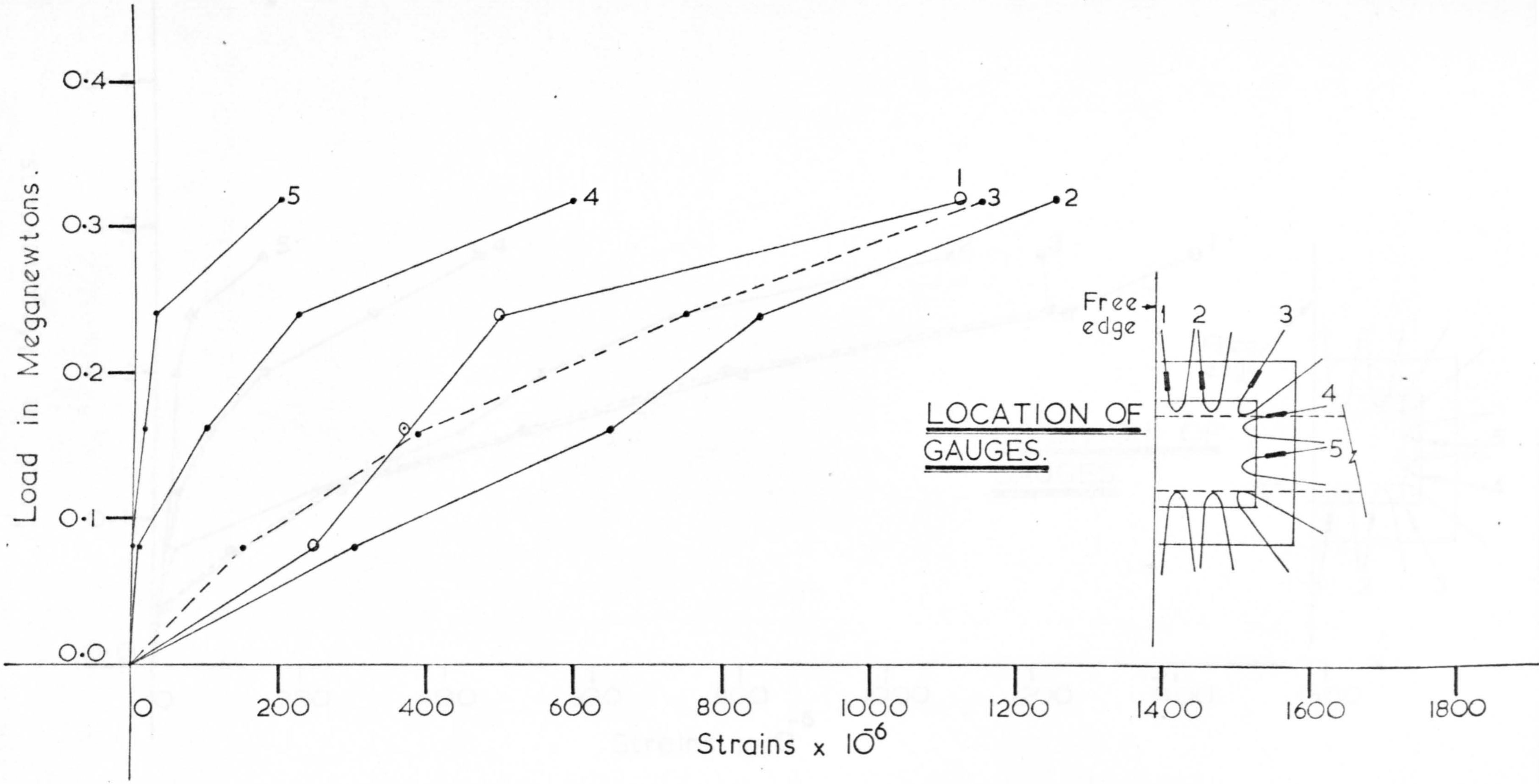

Fig. 32. LOAD vs STRAIN IN SHEAR REINFORCEMENT. SLAB – ES 6.

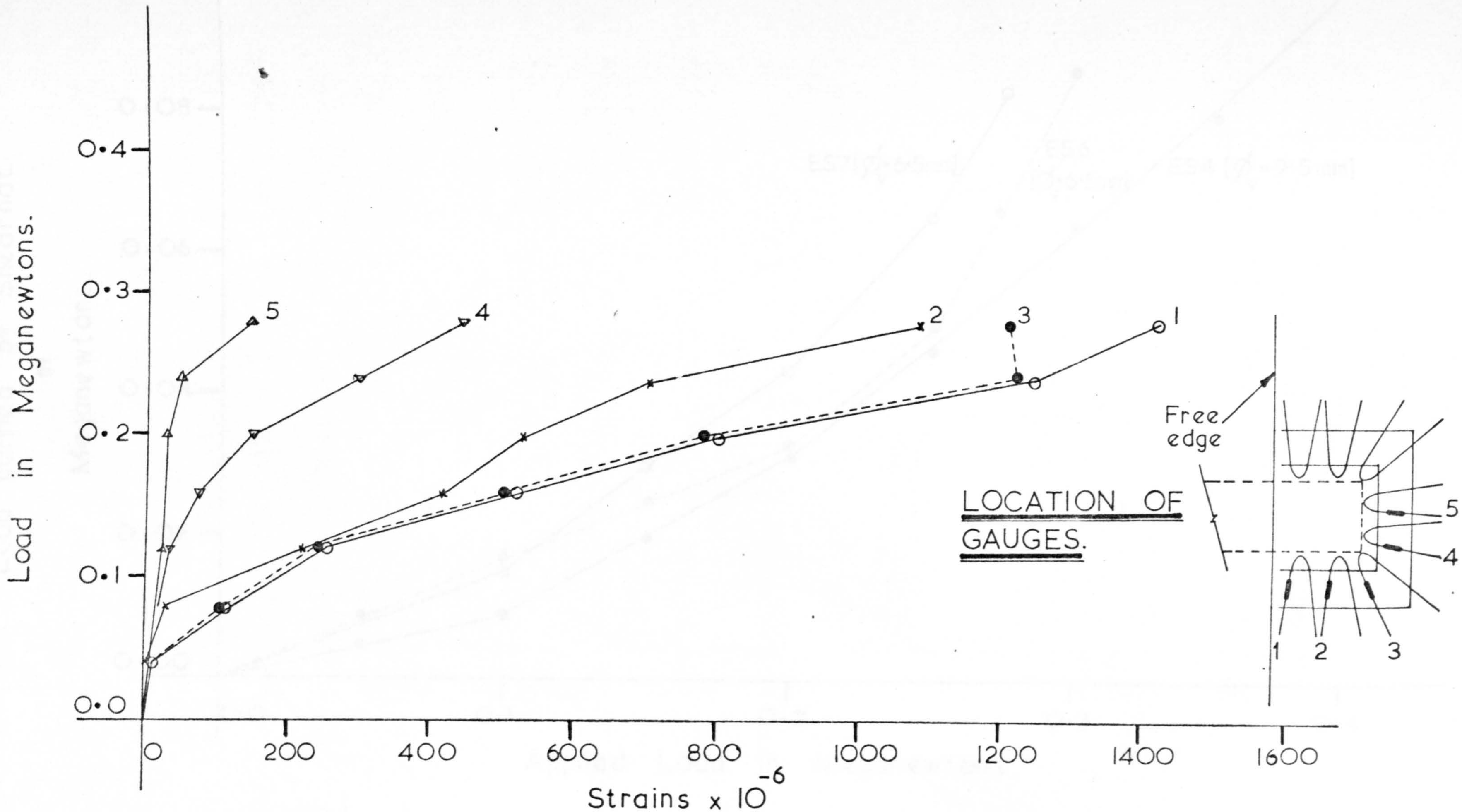

Fig.33. LOAD vs STRAIN IN SHEAR REINFORCEMENT. SLAB-ES 7.

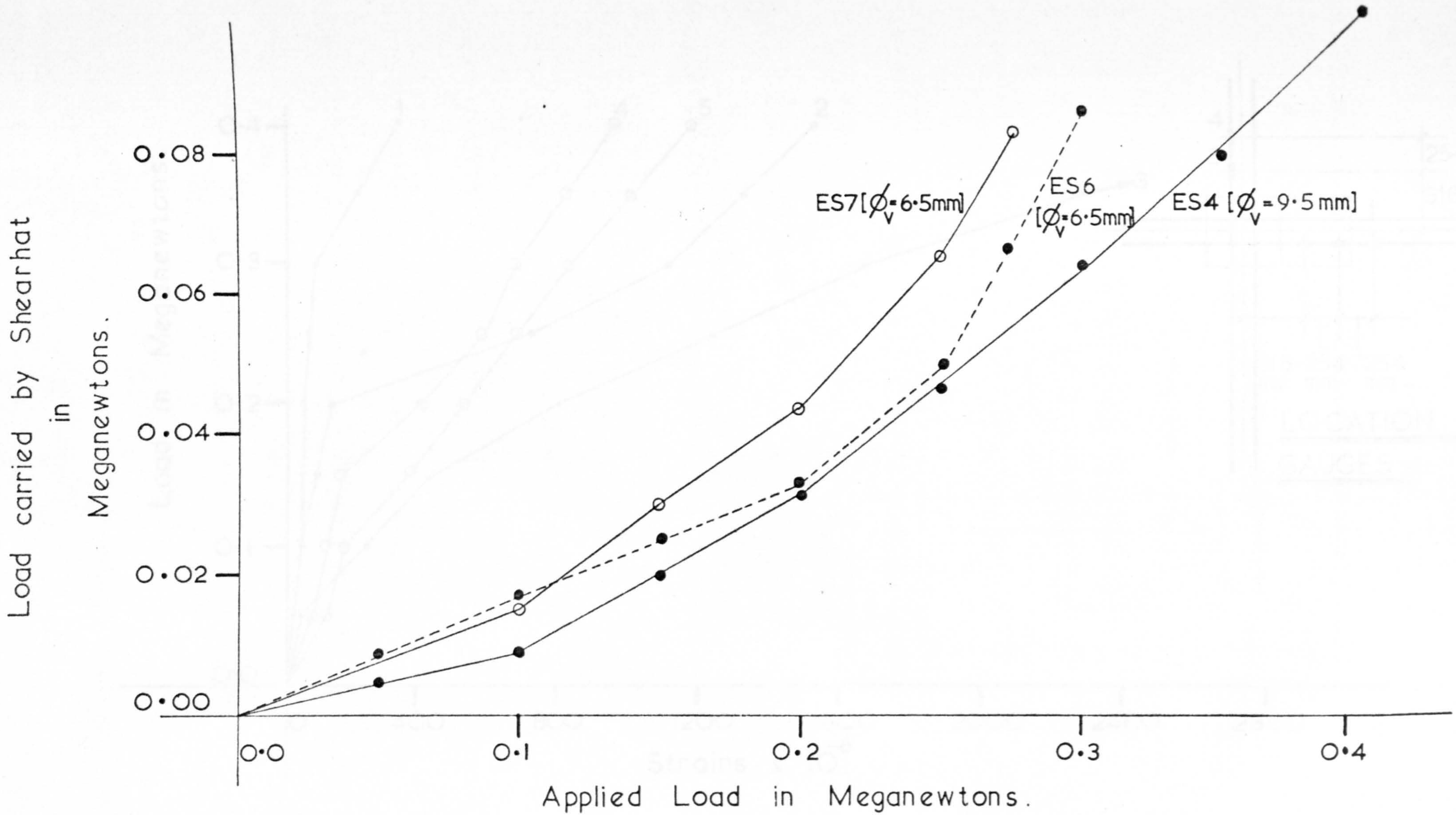

Fig. 34. APPLIED LOAD vs LOAD CARRIED BY SHEARHATS.

EXTERNAL COLUMN CONNECTION.

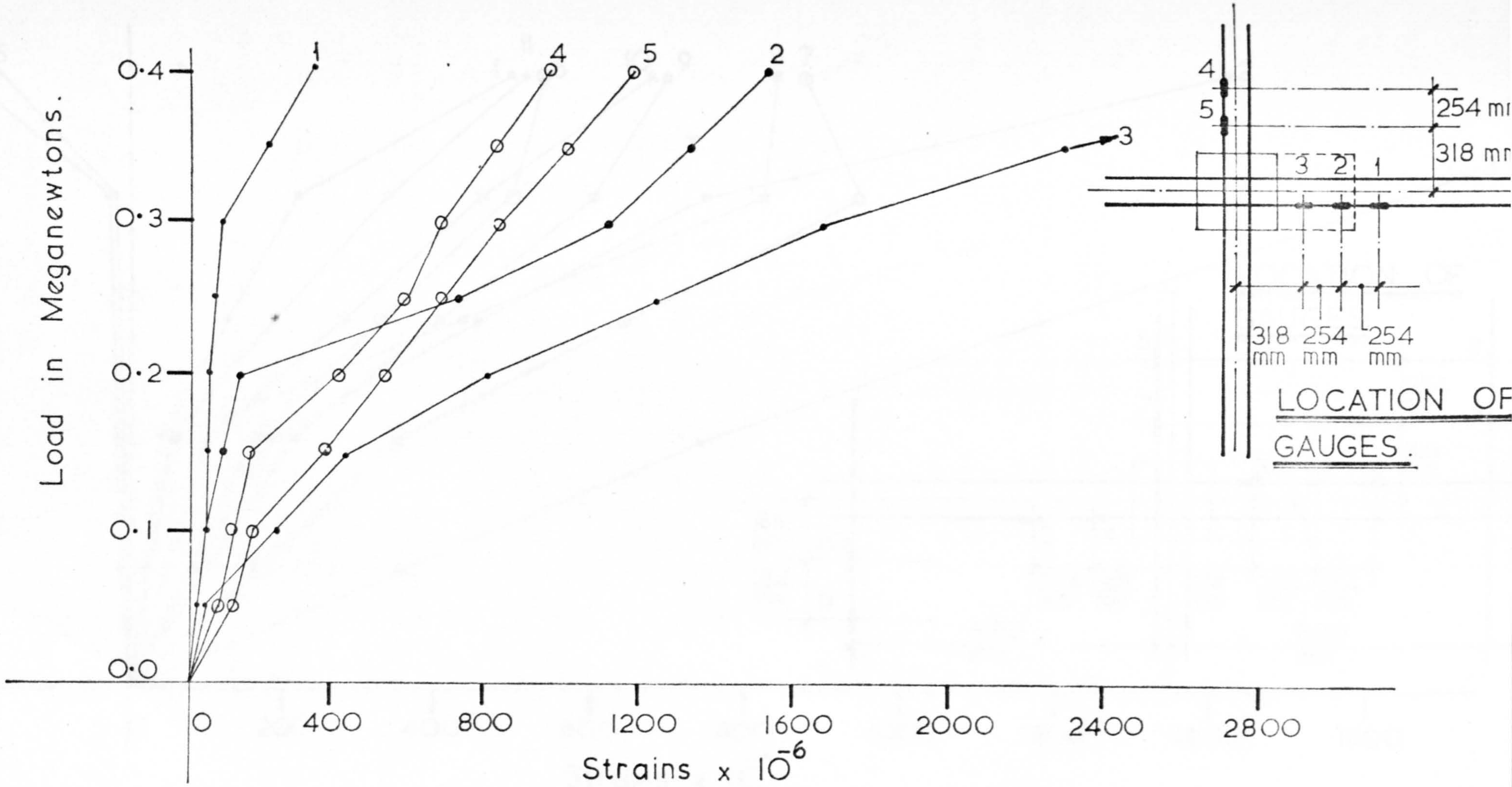

Fig. 35a. LOAD vs STRAIN IN MAIN REINFORCEMENT. SLAB-L1 (EC=305mm)

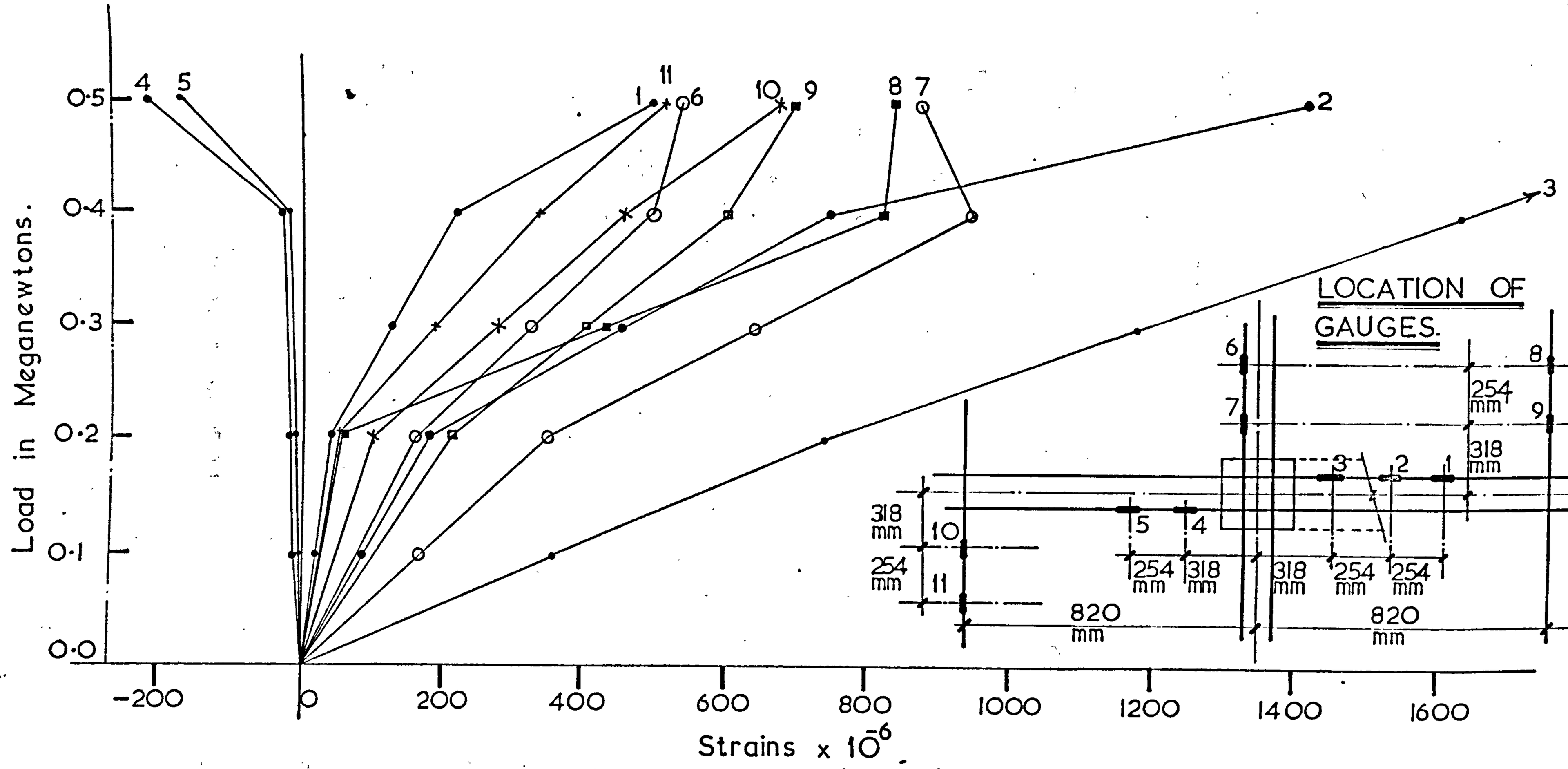

Fig. 35b. LOAD vs STRAIN IN MAIN REINFORCEMENT. SLAB-L3 (EC=305mm, S.S.H ϕ_v=9·5mm)

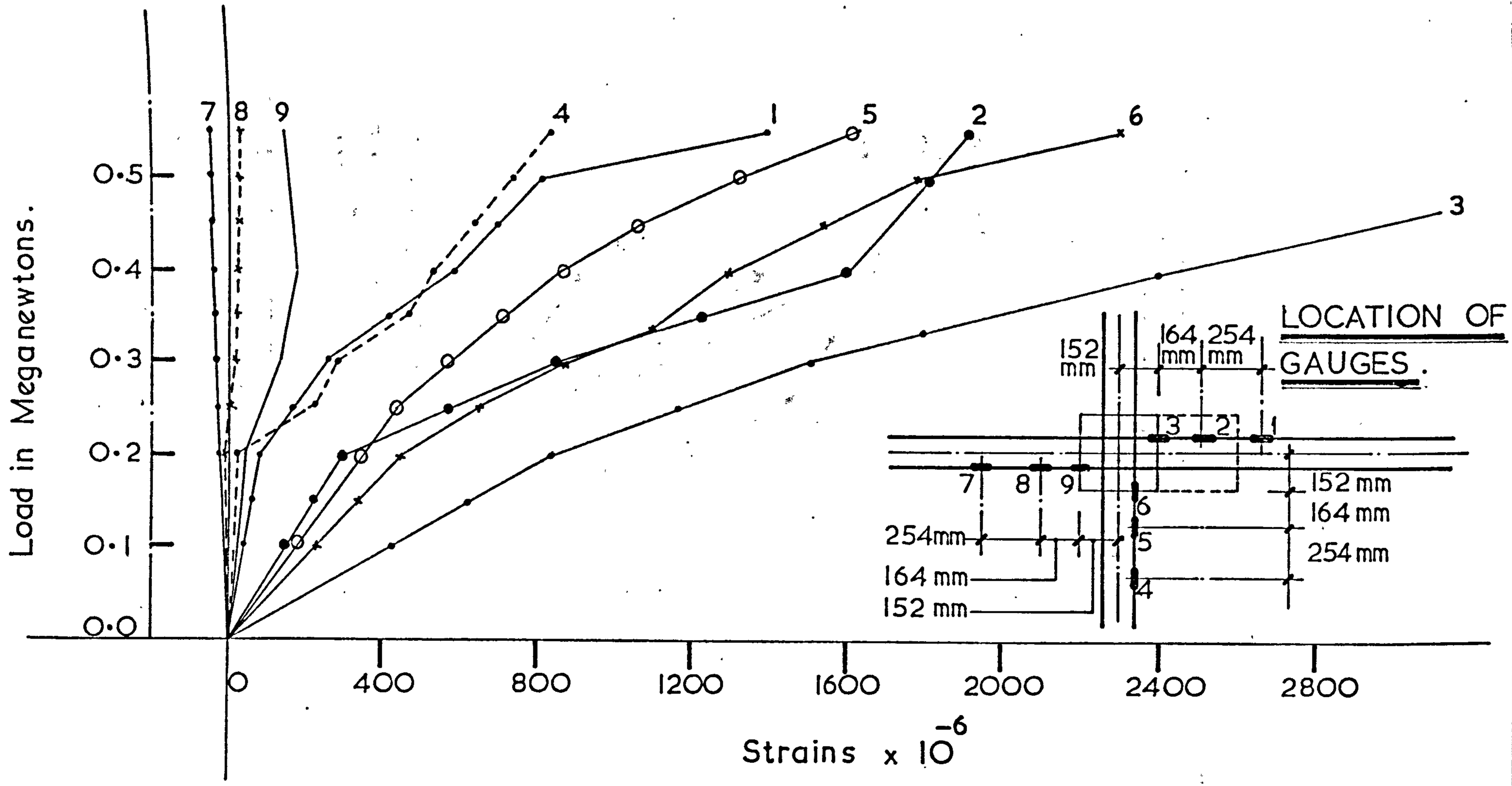

Fig. 35c. LOAD vs STRAIN IN MAIN REINFORCEMENT. SLAB-L4. (EC=305mm, S.S.H. ϕ_v=6·5mm)

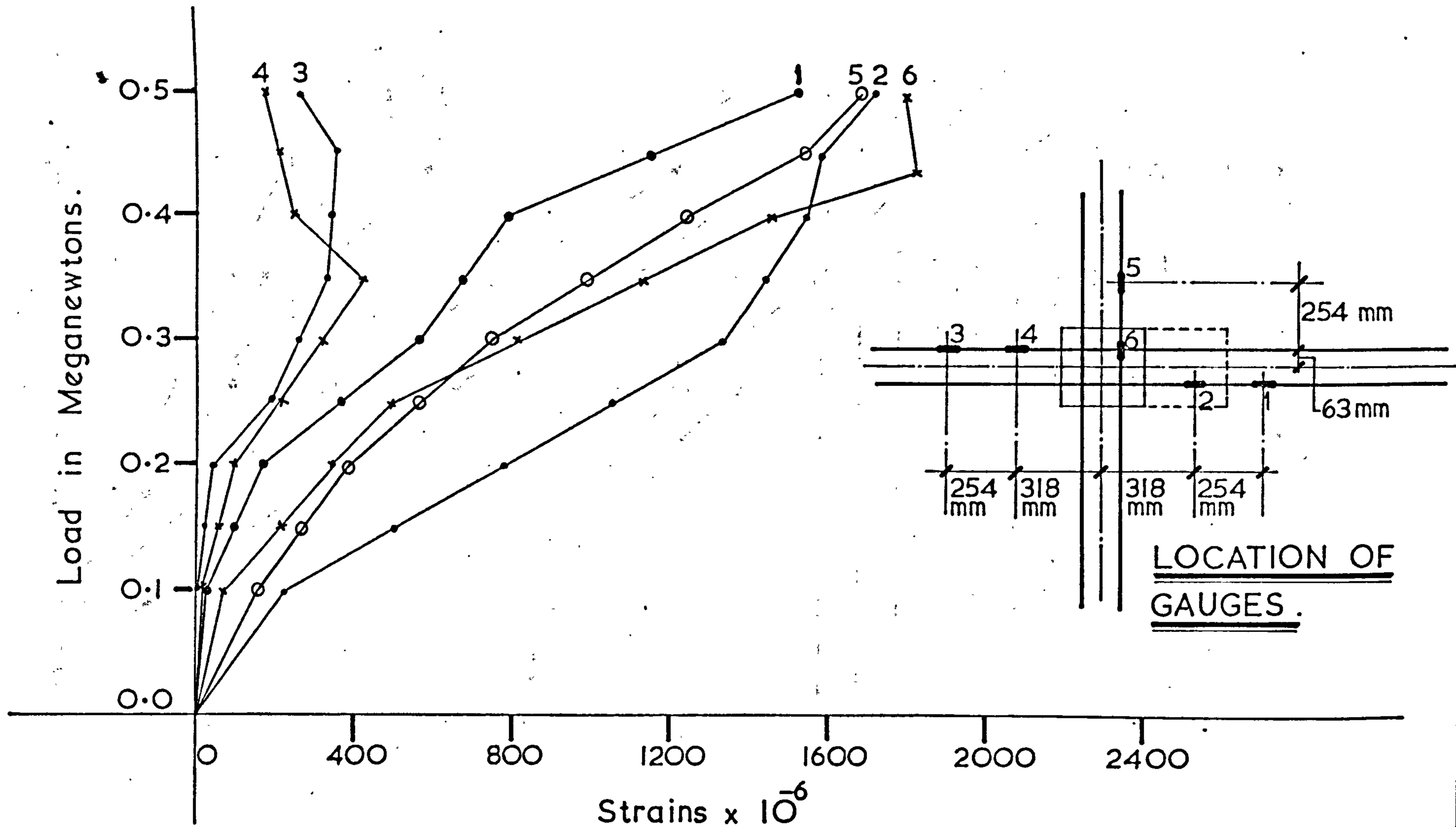

Fig. 35d. LOAD vs STRAIN IN MAIN REINFORCEMENT. SLAB-L5. (EC=305 mm, S.S.H. ϕ_v = 13 mm)

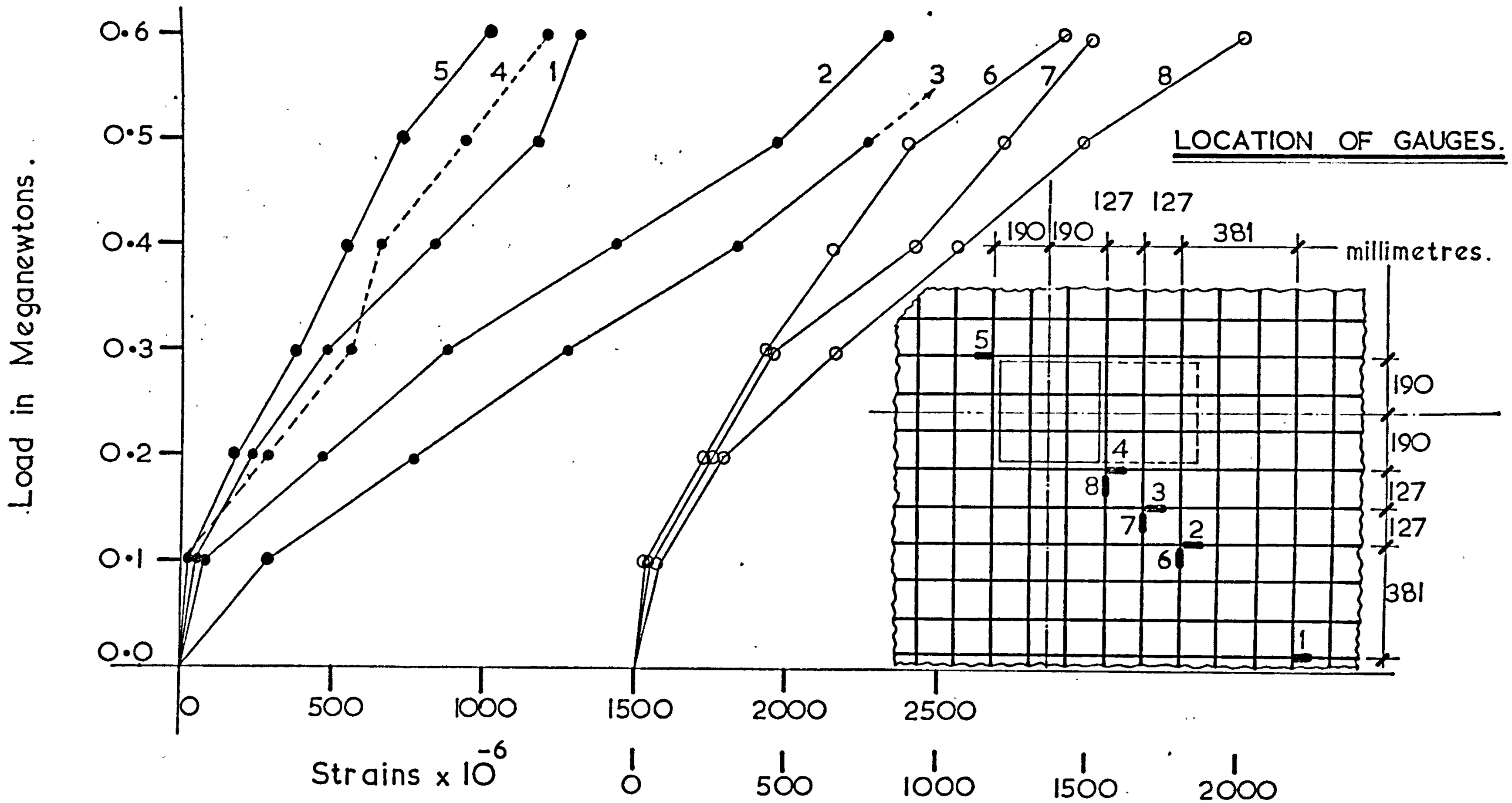

Fig.35e. LOAD vs STRAIN IN MAIN REINFORCEMENT. SLAB-L6. (EC=152·5mm, S.S.H. ϕ_v = 8mm)

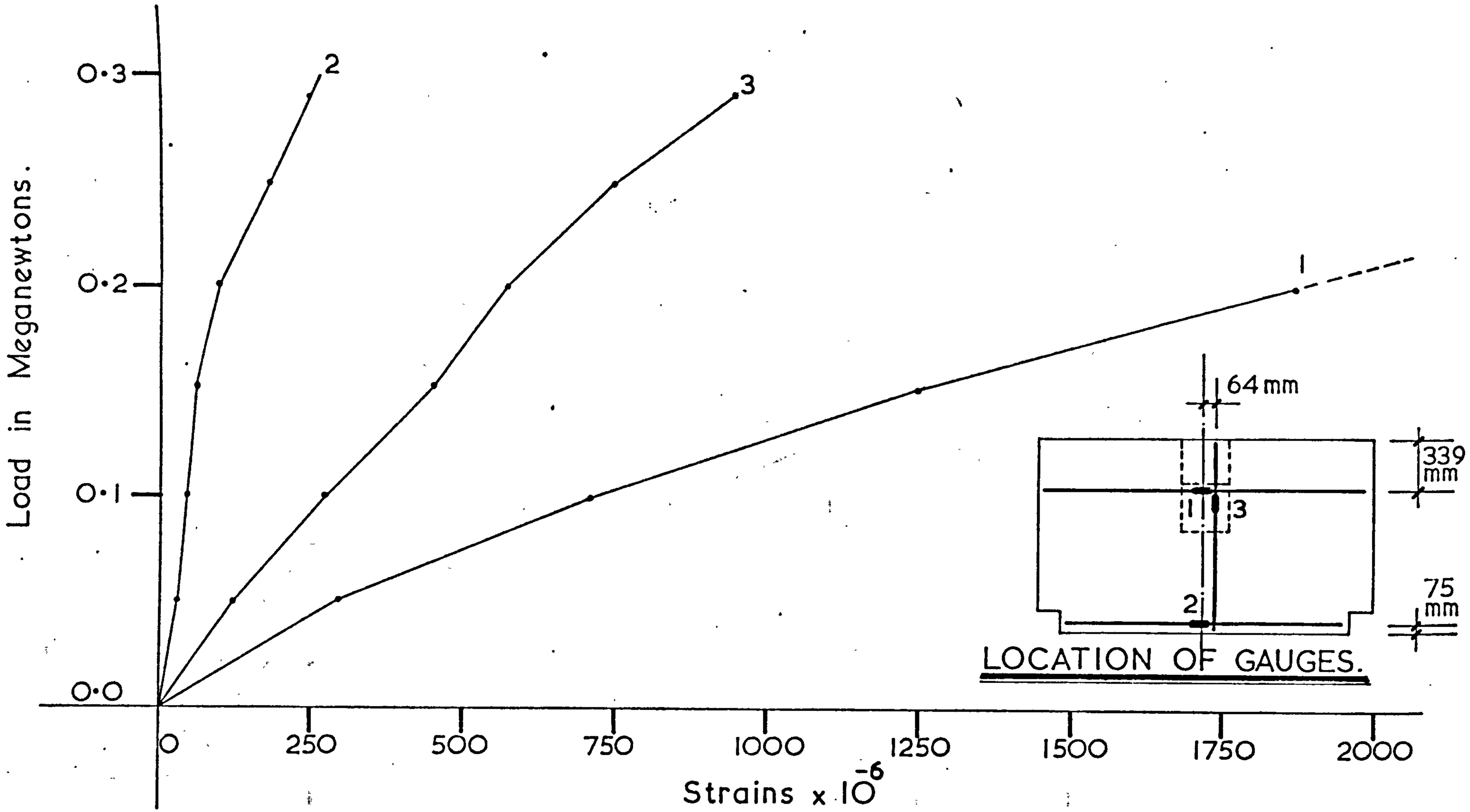

Fig.36a. LOAD vs STRAIN IN MAIN REINFORCEMENT. SLAB – ES1. (EC=0, ϕ_V=0)

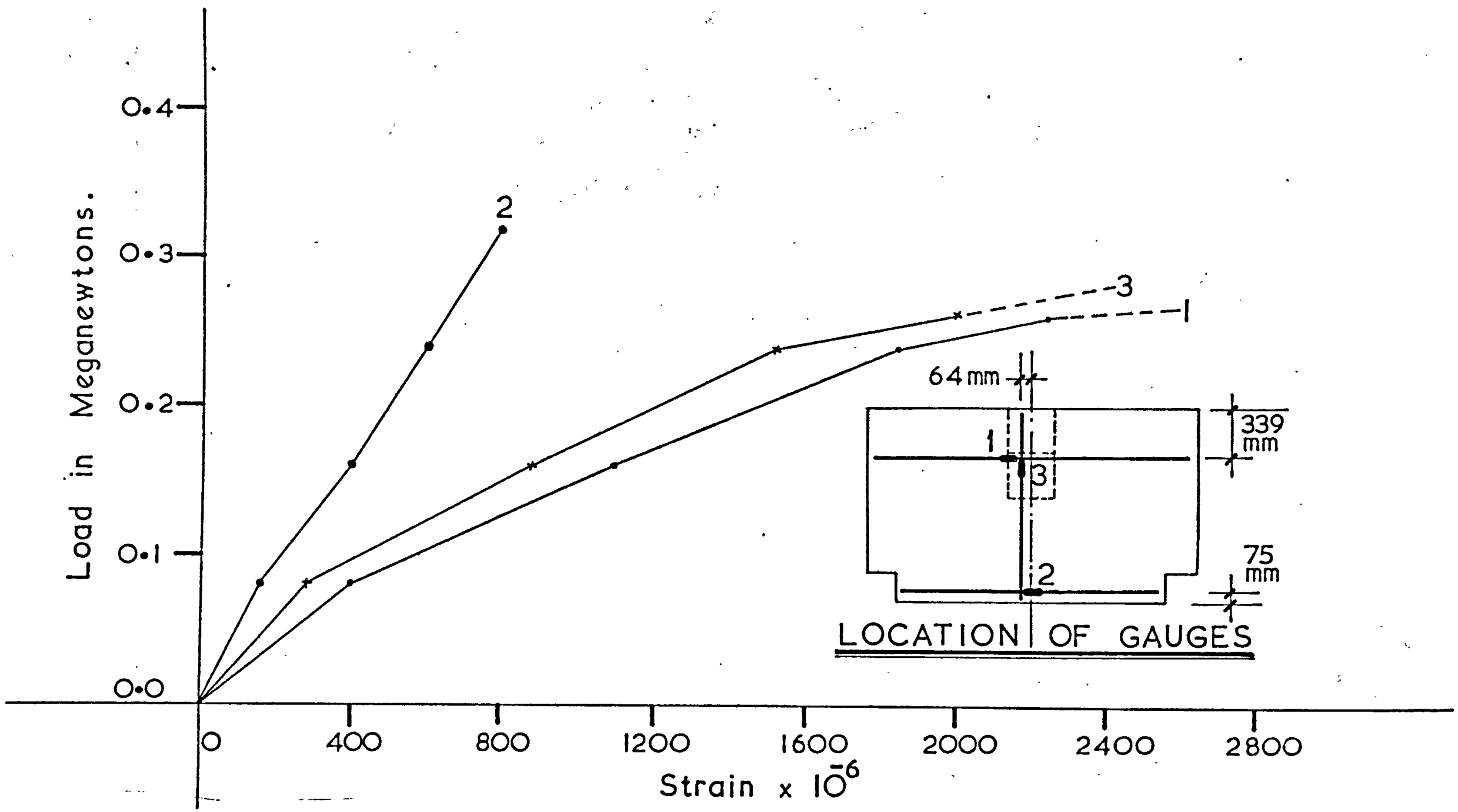

Fig. 36b. LOAD vs STRAIN IN MAIN REINFORCEMENT. SLAB - ES 2. (EC = +228·5 mm., ϕ_V = 0)

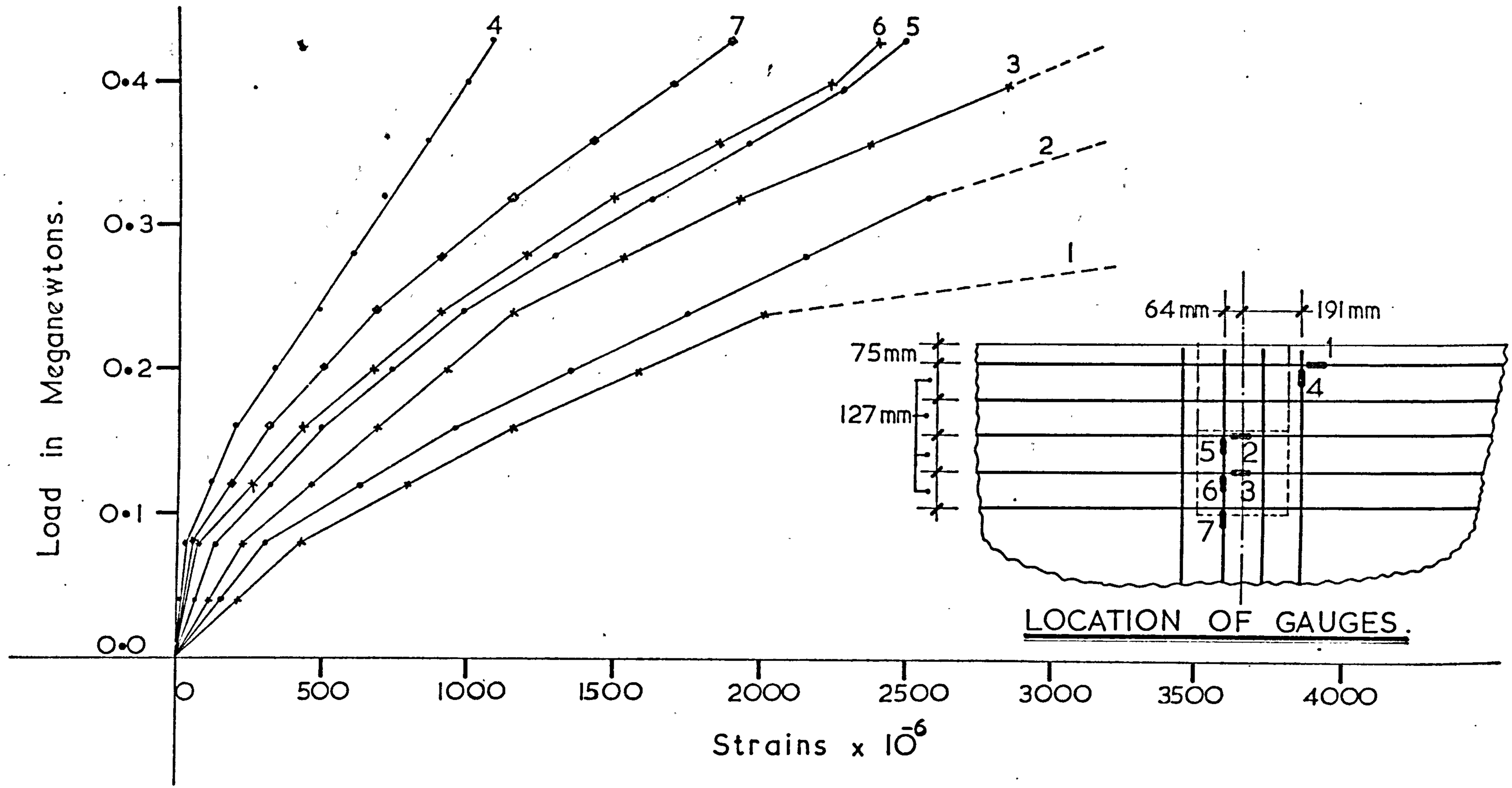

Fig. 36c. LOAD vs STRAIN IN MAIN REINFORCEMENT. SLAB – ES3. (EC=+228·5mm, S.S.H. ϕ_v=6·5mm.)

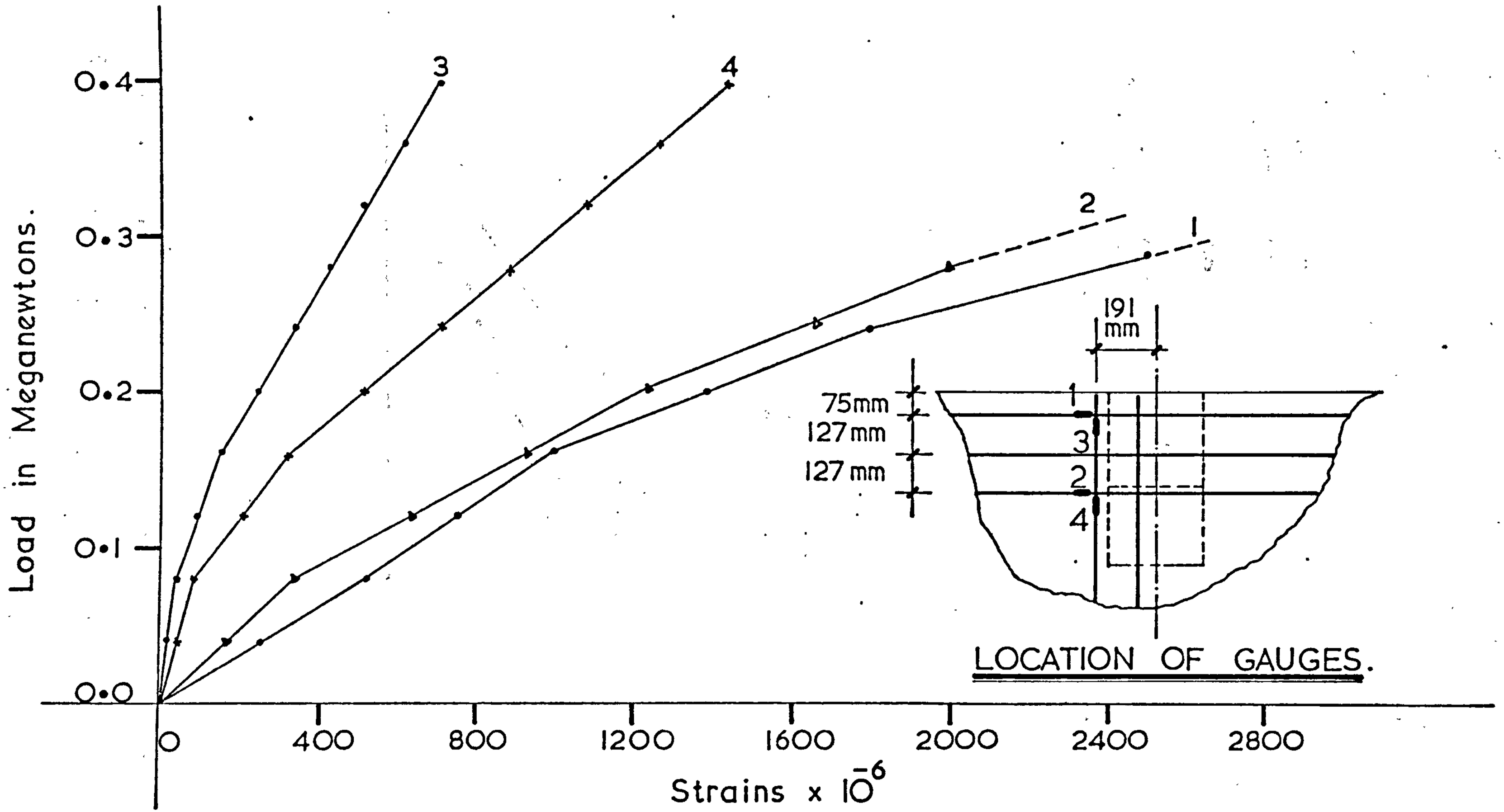

Fig.36d. LOAD vs STRAIN IN MAIN REINFORCEMENT. SLAB – ES4. (EC=+228·5mm, S.S.H. ϕ_v=9·5mm.)

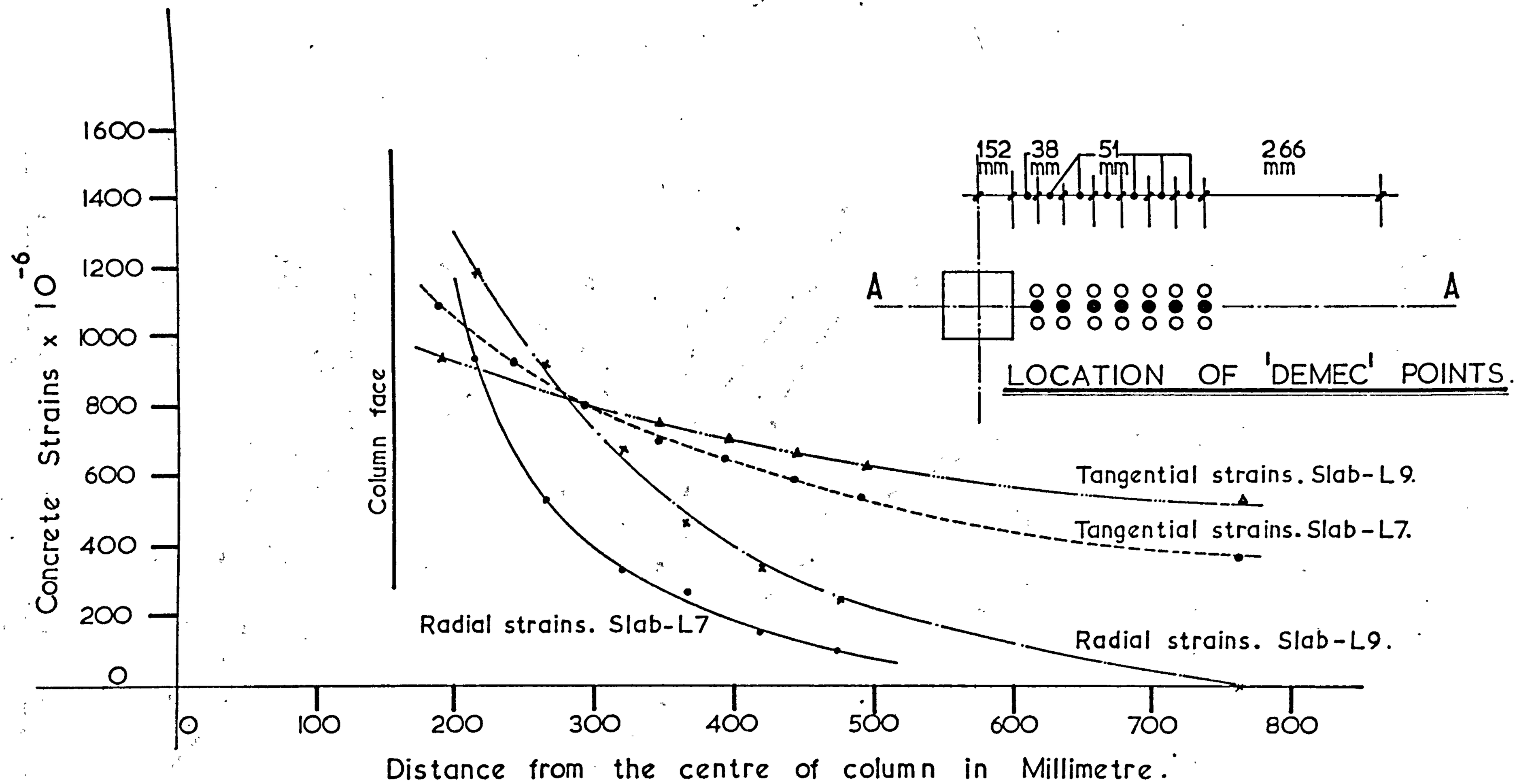

Fig. 37 . RADIAL & TANGENTIAL STRAINS ALONG A-A AT 0 85 x ULTIMATE LOAD.

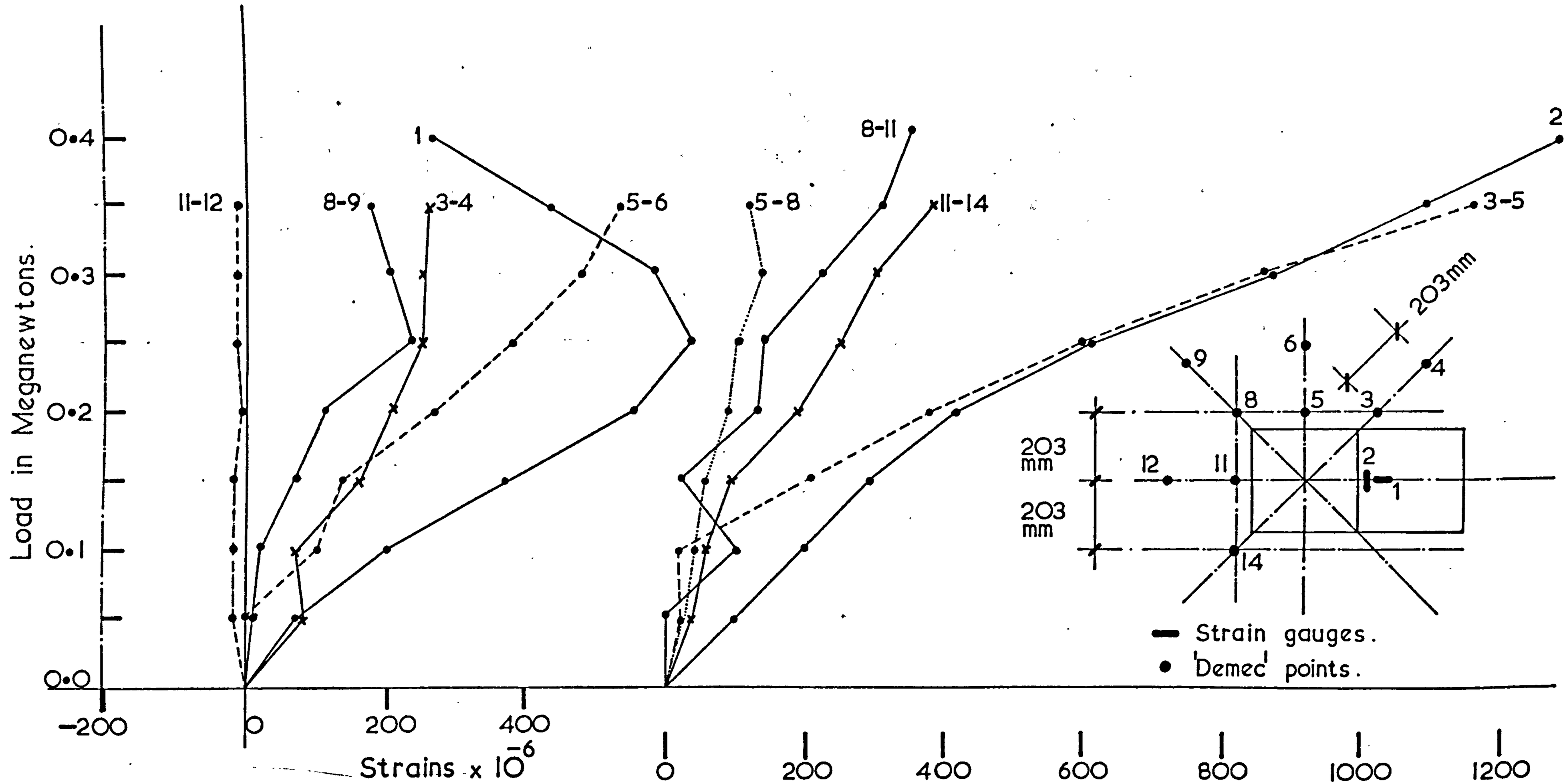

Fig.38a. LOAD vs STRAIN IN CONCRETE . SLAB-L1.

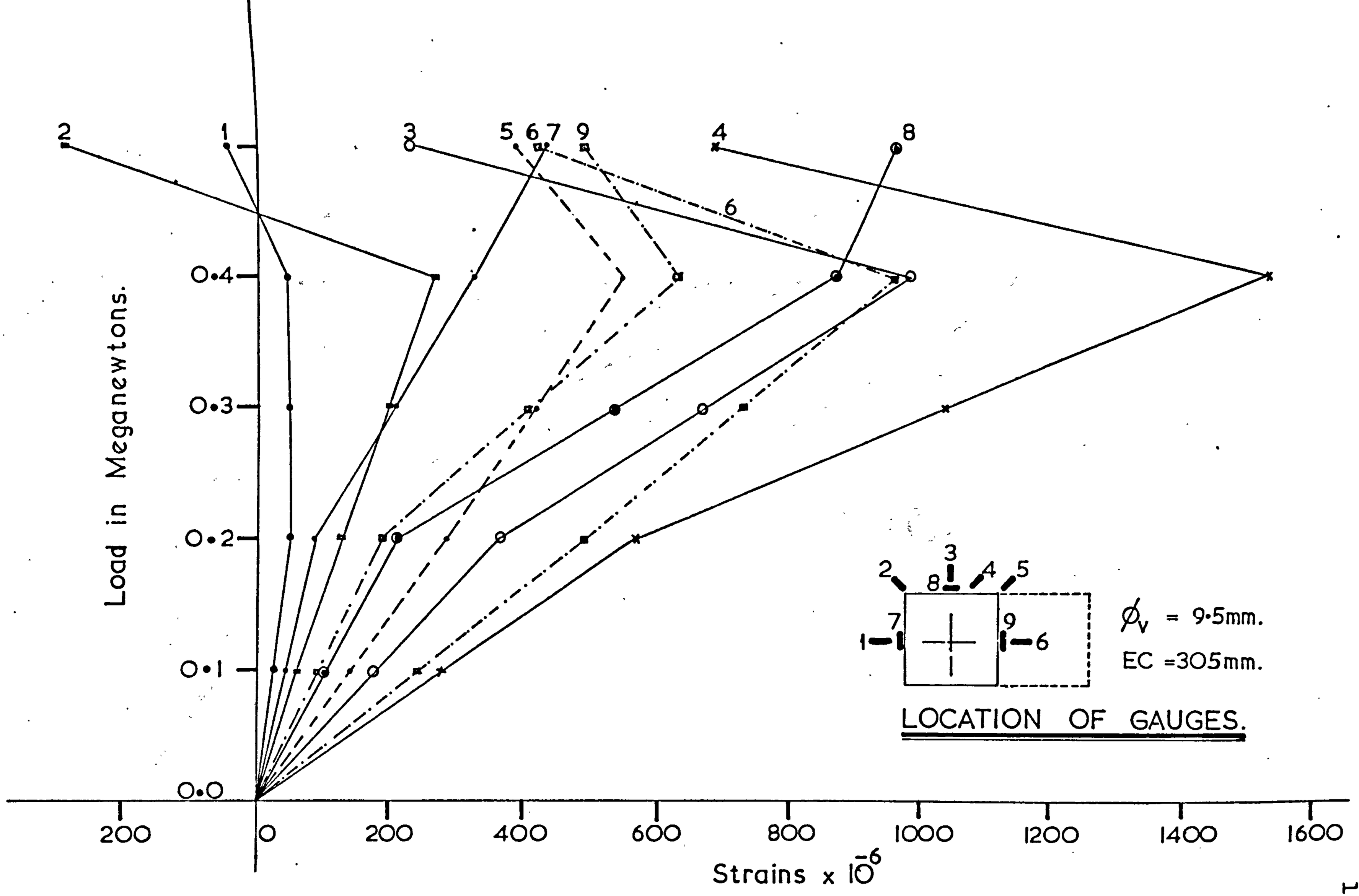

Fig.38b. LOAD vs STRAIN IN CONCRETE. SLAB-L3.

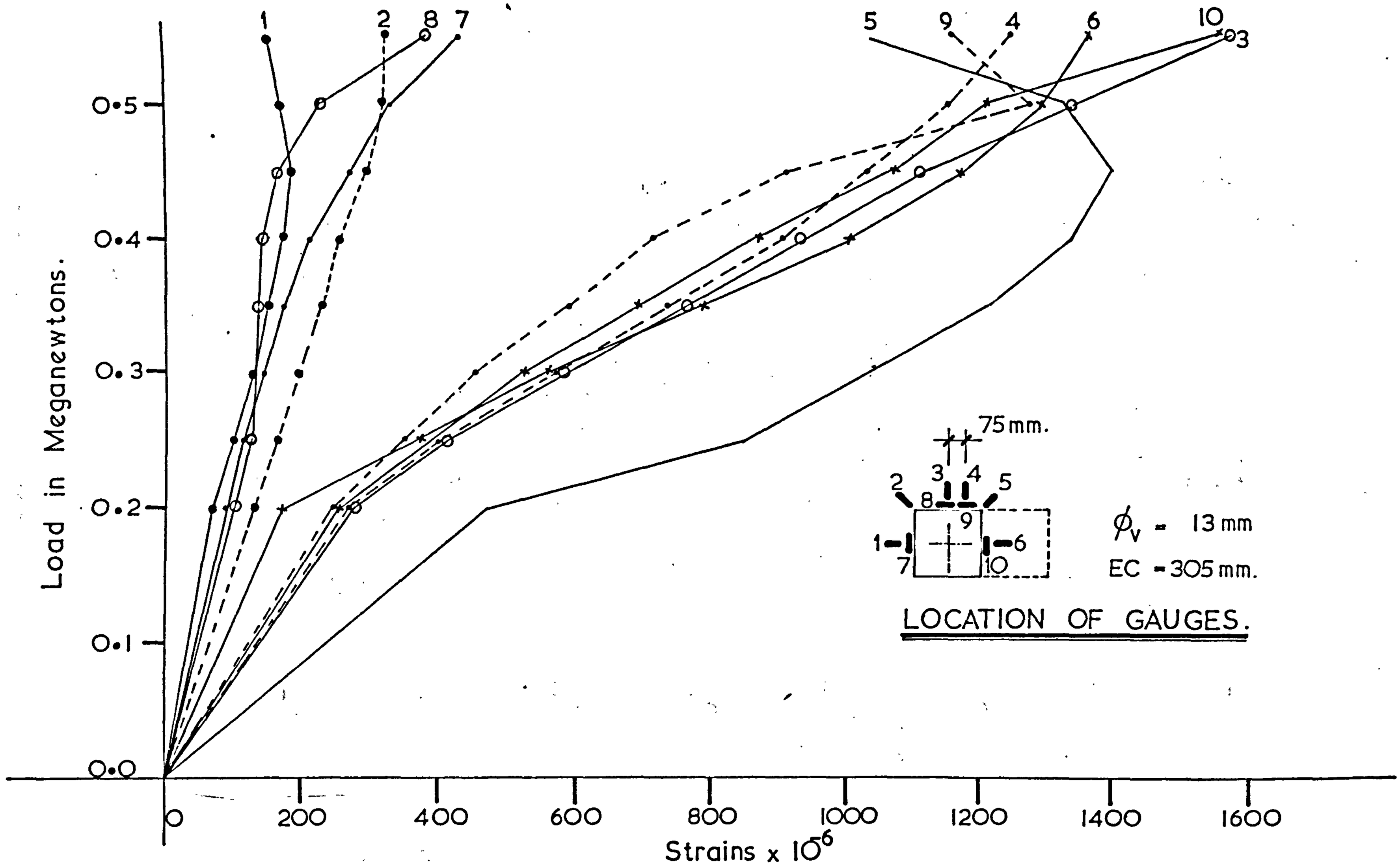

Fig.38c. LOAD vs STRAIN IN CONCRETE. SLAB-L4.

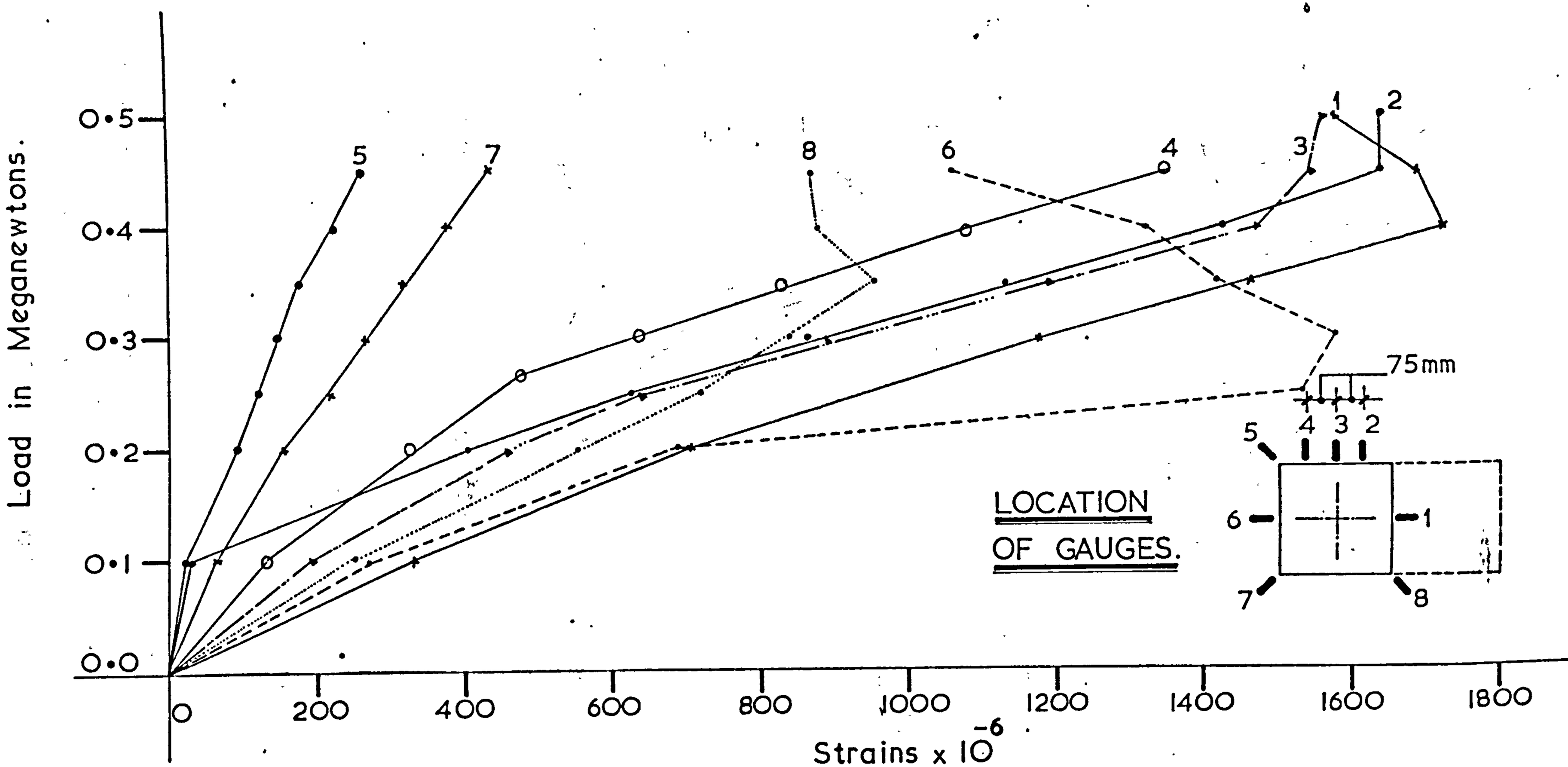

Fig. 38d. LOAD vs STRAIN IN CONCRETE. SLAB-L5.

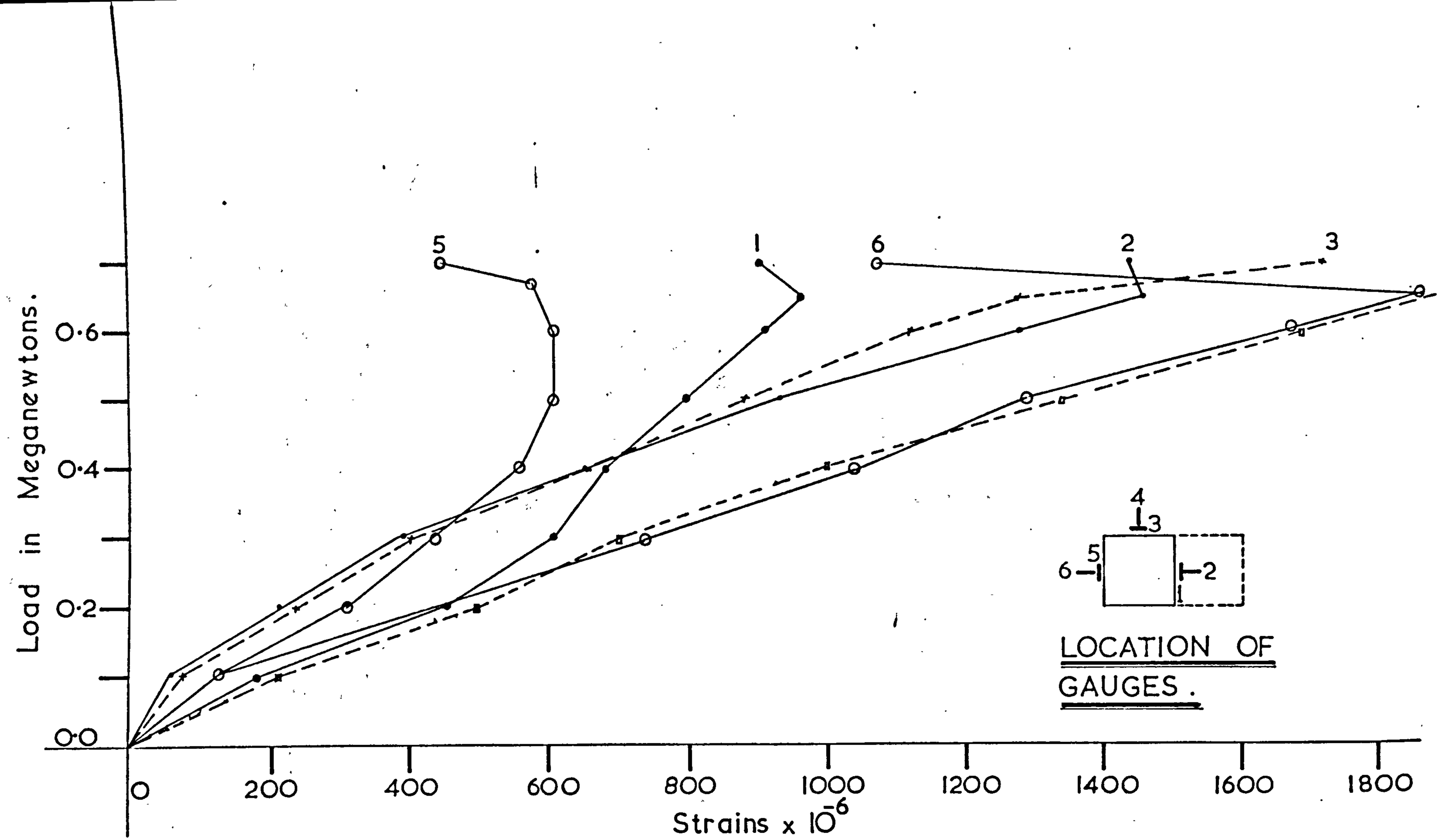

Fig.38e. LOAD vs STRAIN IN CONCRETE. SLAB -L11.

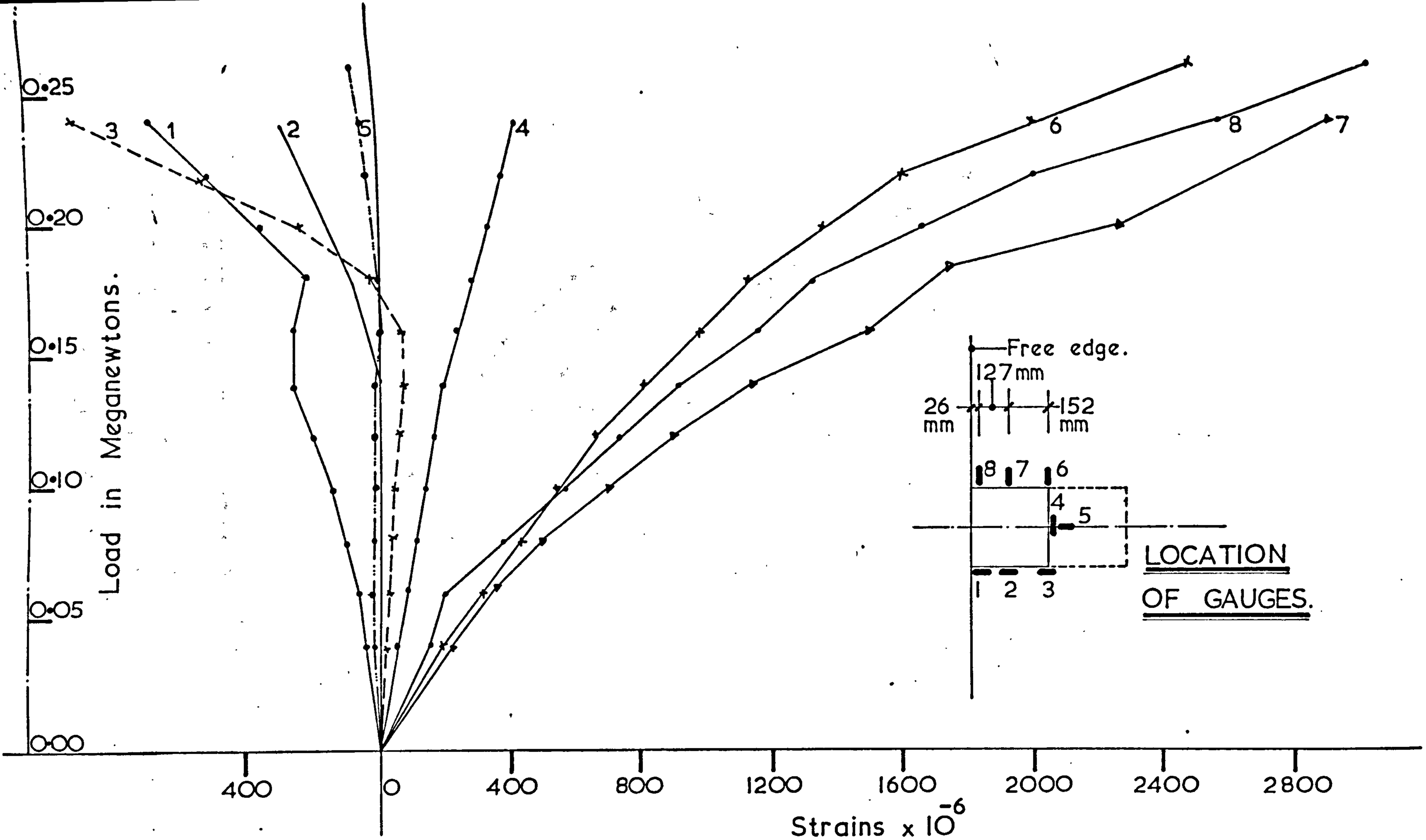

Fig. 39a. LOAD vs STRAIN IN CONCRETE. SLAB-ES1.

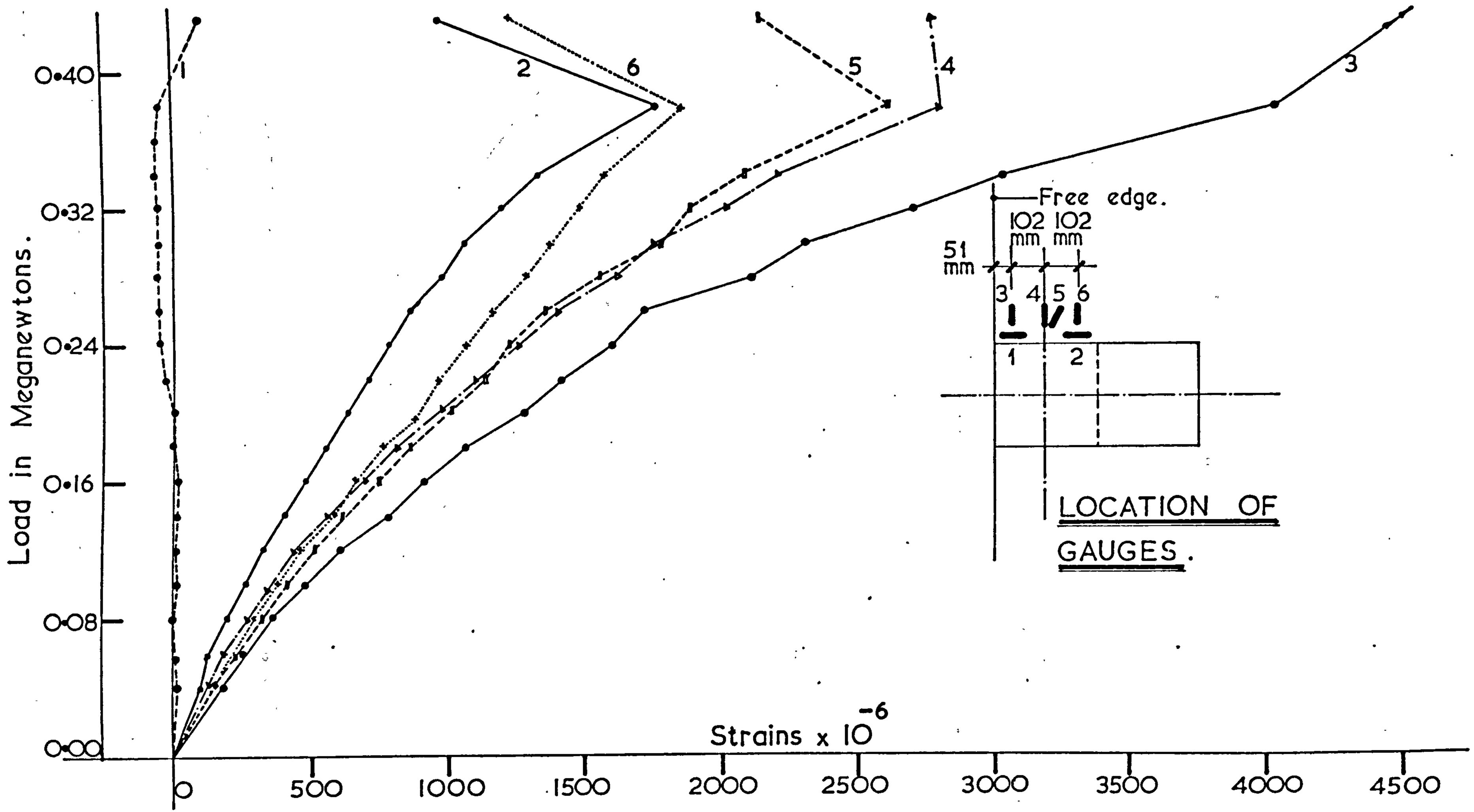

Fig.39b. LOAD vs STRAIN IN CONCRETE. SLAB - ES3.

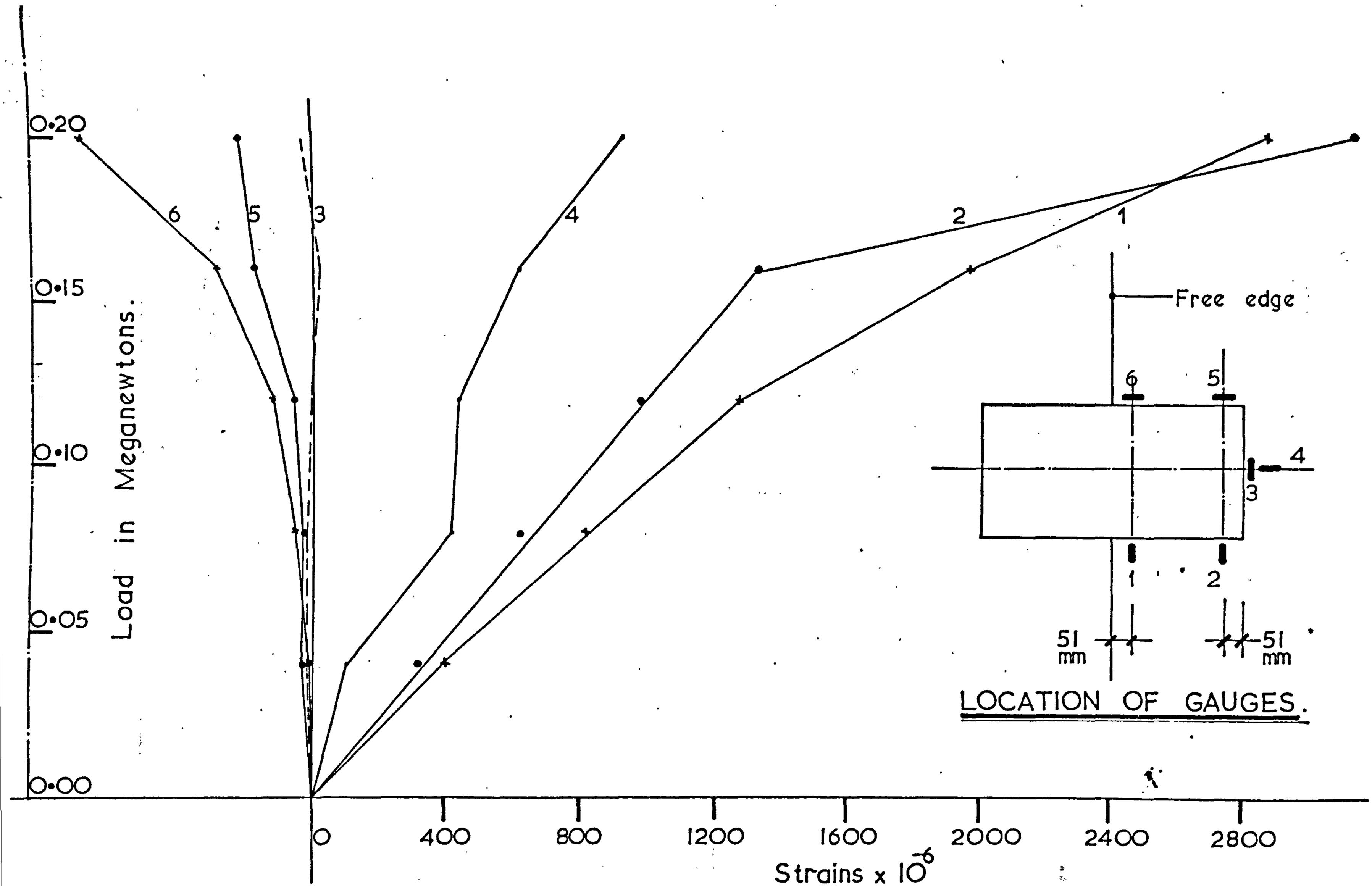

Fig. 39c. LOAD vs STRAIN IN CONCRETE. SLAB-ES5.

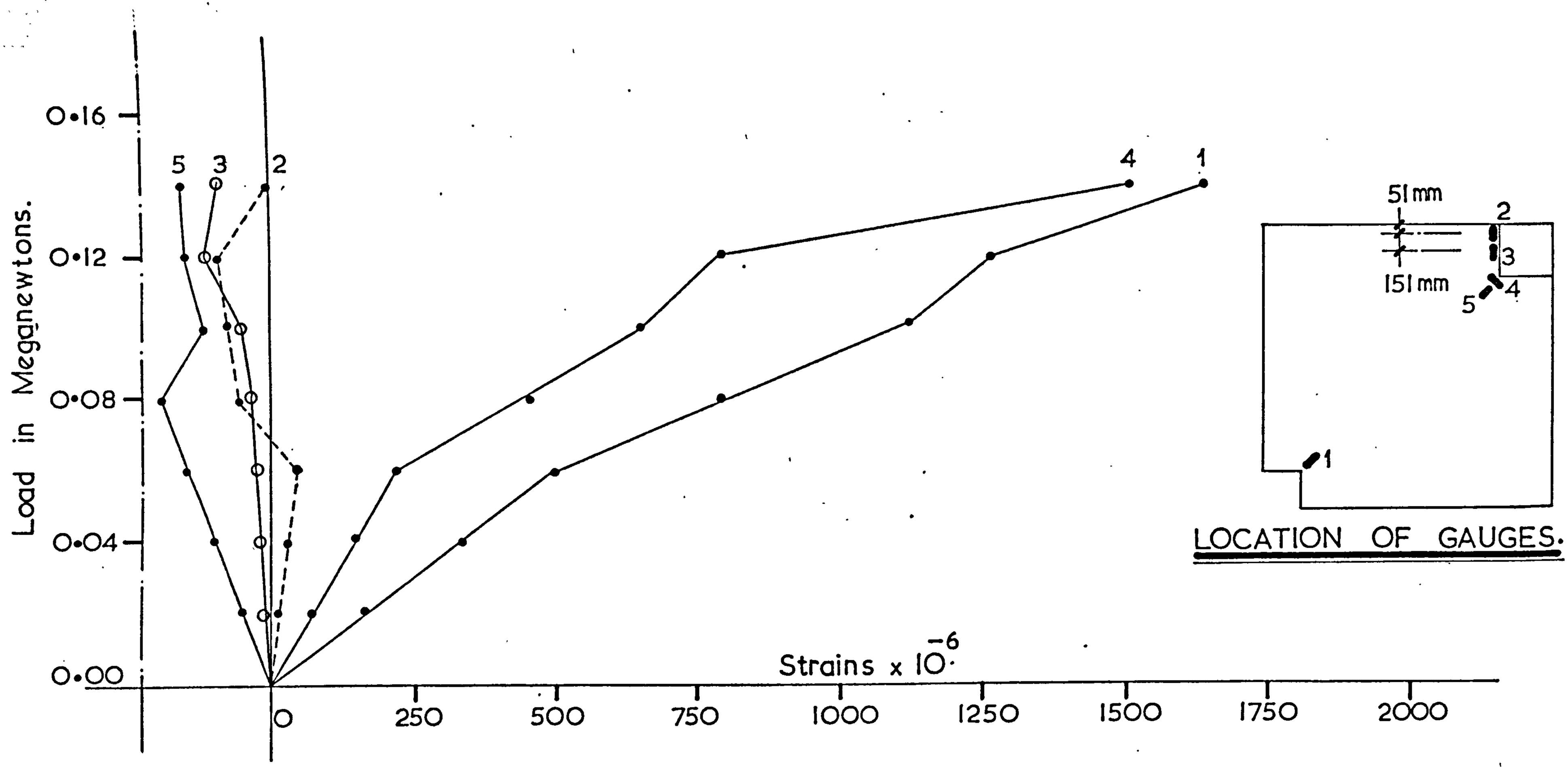

Fig. 40. LOAD vs STRAIN IN CONCRETE. SLAB-CS.

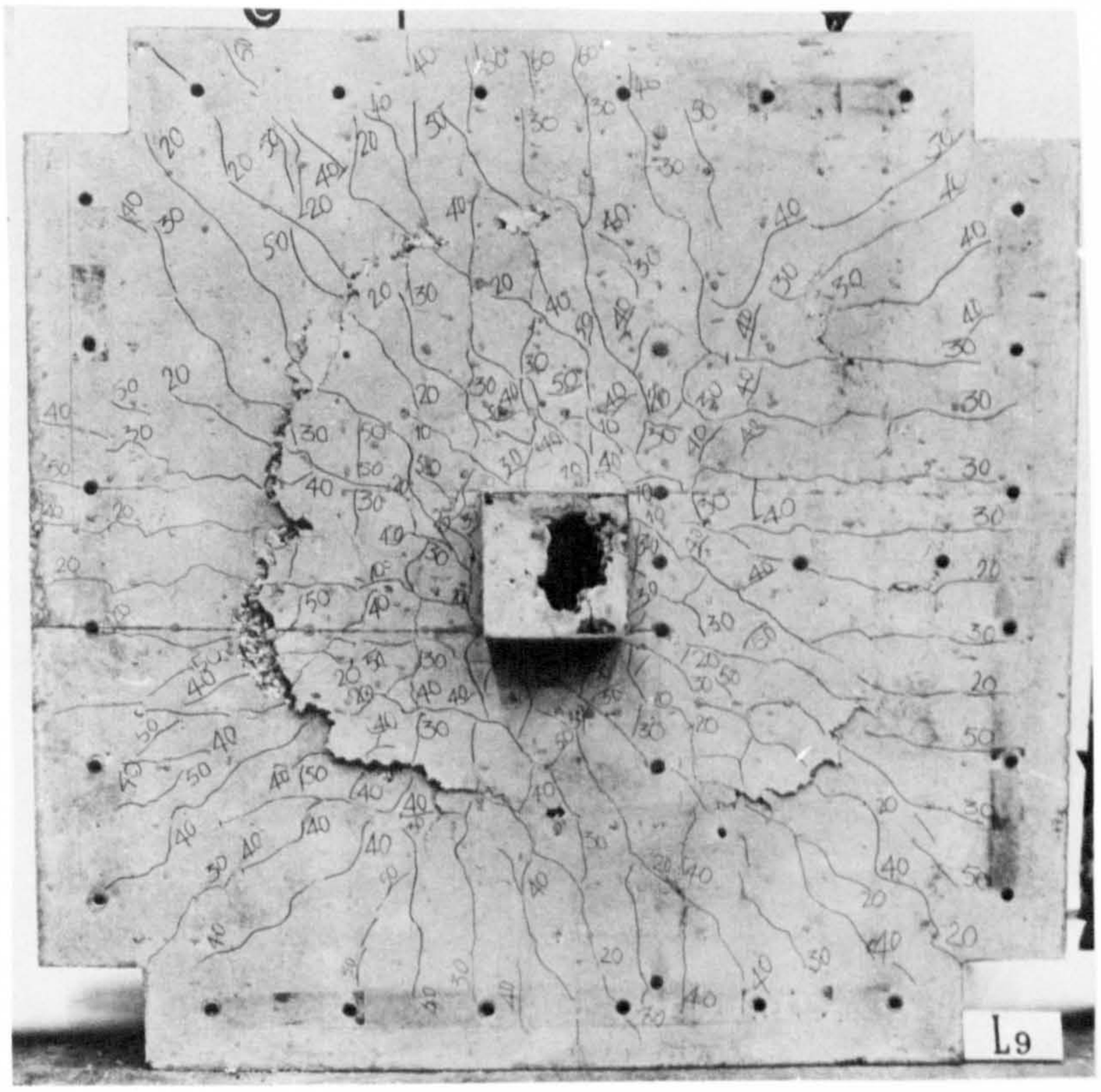

SLAB-L9. EC=0.

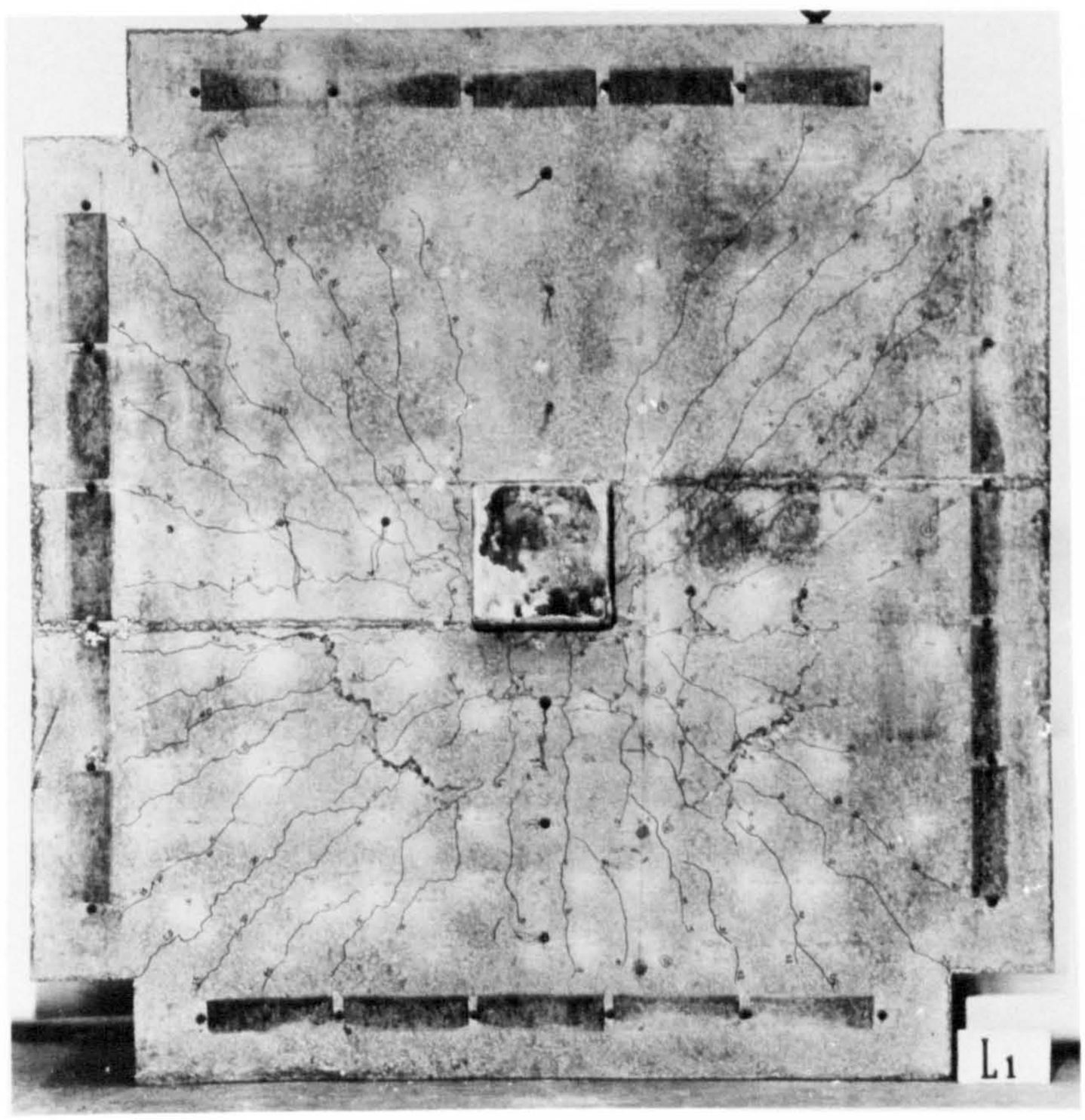

SLAB-L1. EC=305mm.

Fig. 41. BOTTOM SURFACES. SERIES-L.

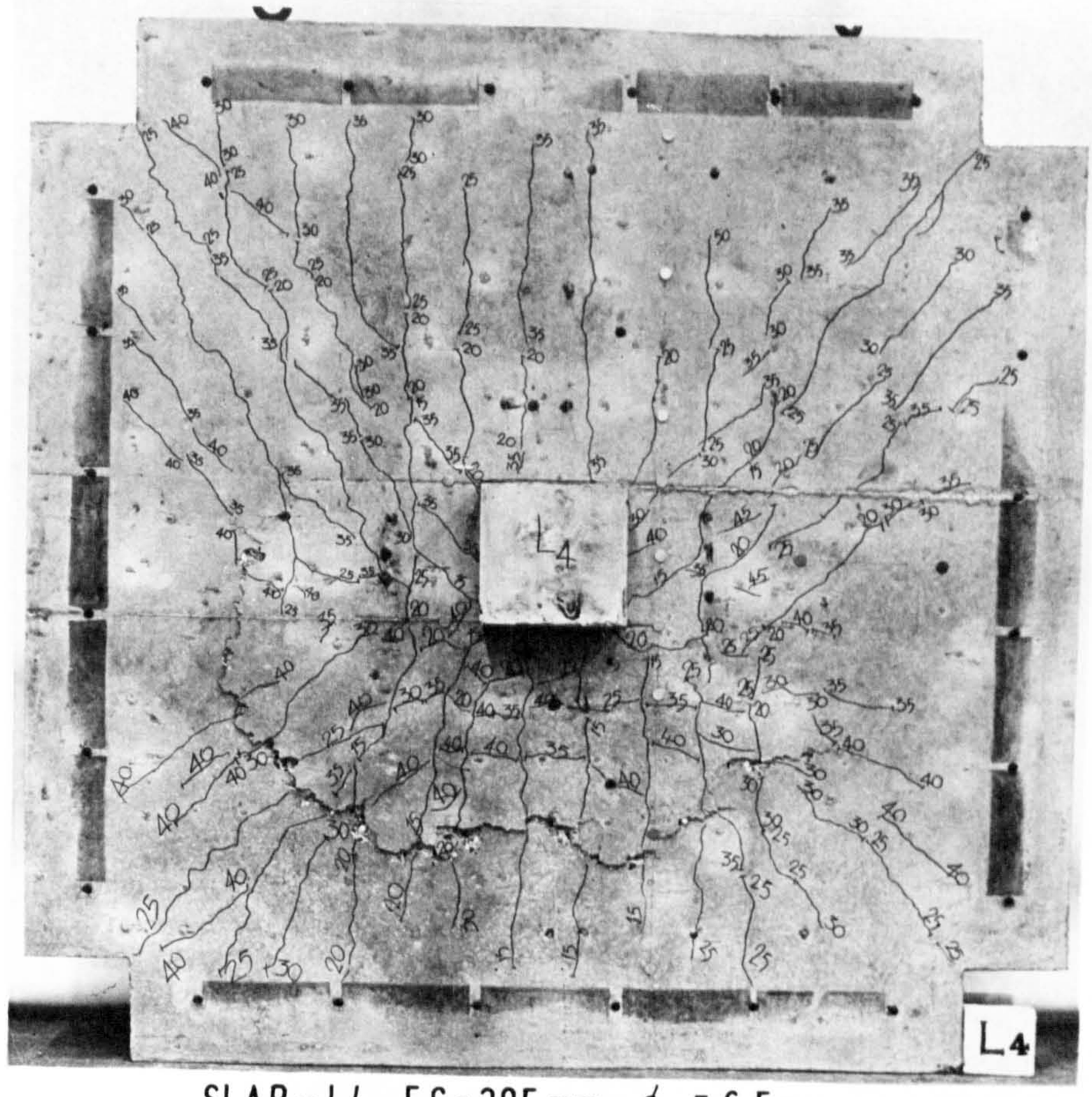

SLAB - L4. EC = 305 mm. ϕ_v = 6·5 mm.

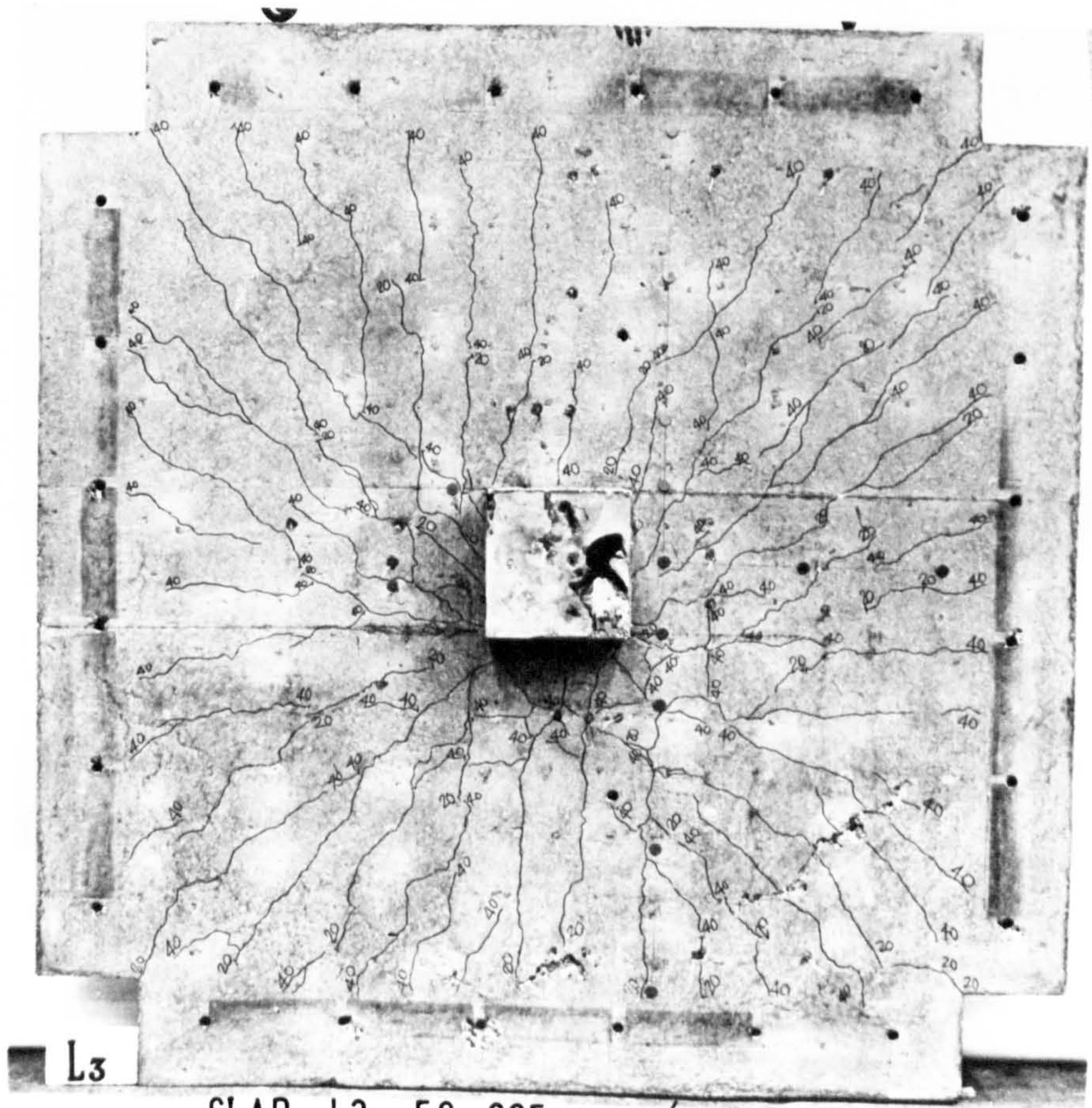

SLAB - L3. EC = 305 mm. ϕ_v = 9·5 mm.

Fig. 42. BOTTOM SURFACES. SERIES - L.

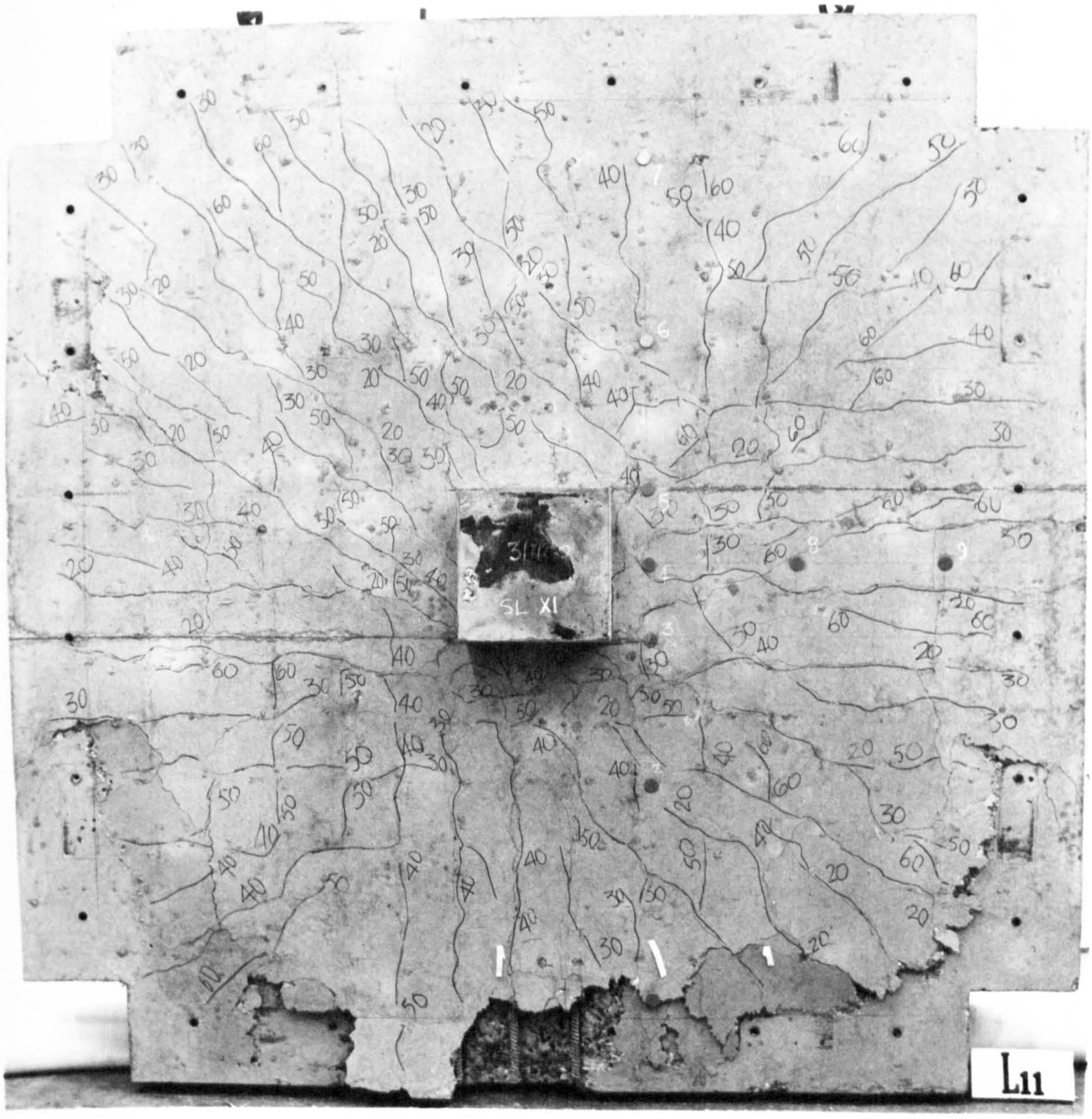

Fig. 43. BOTTOM SURFACE - SLAB L11.

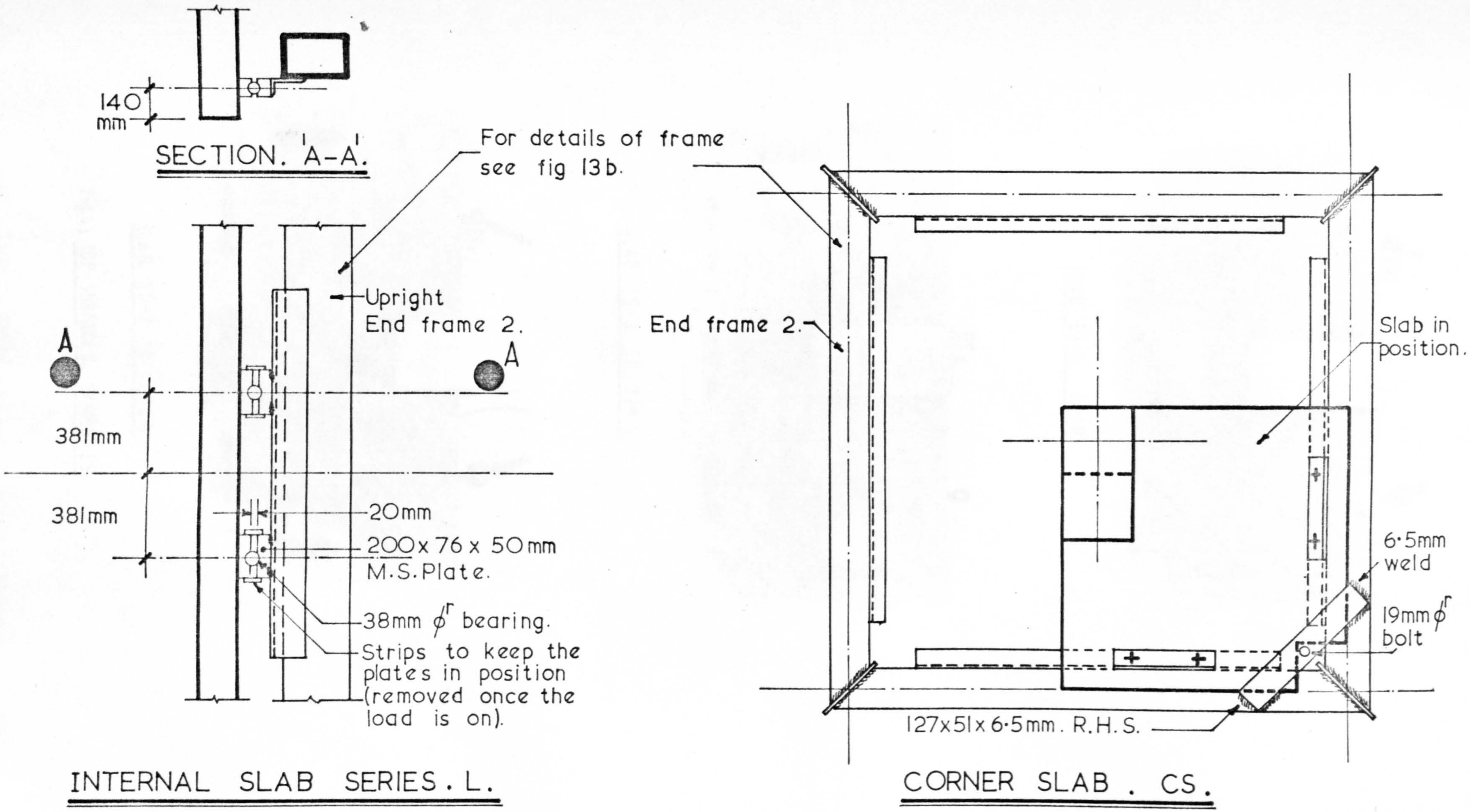

Fig. 44. SPECIAL SUPPORT DETAILS.

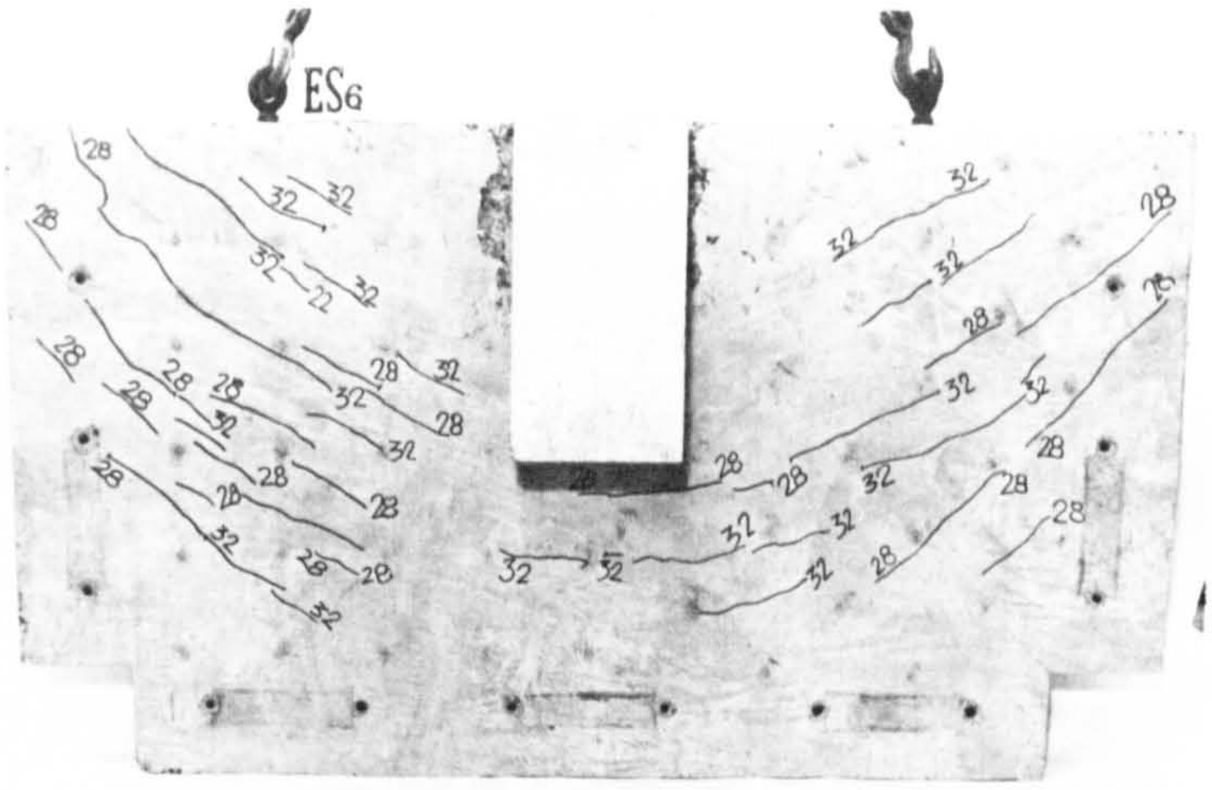

SLAB ES-6. EC=0.

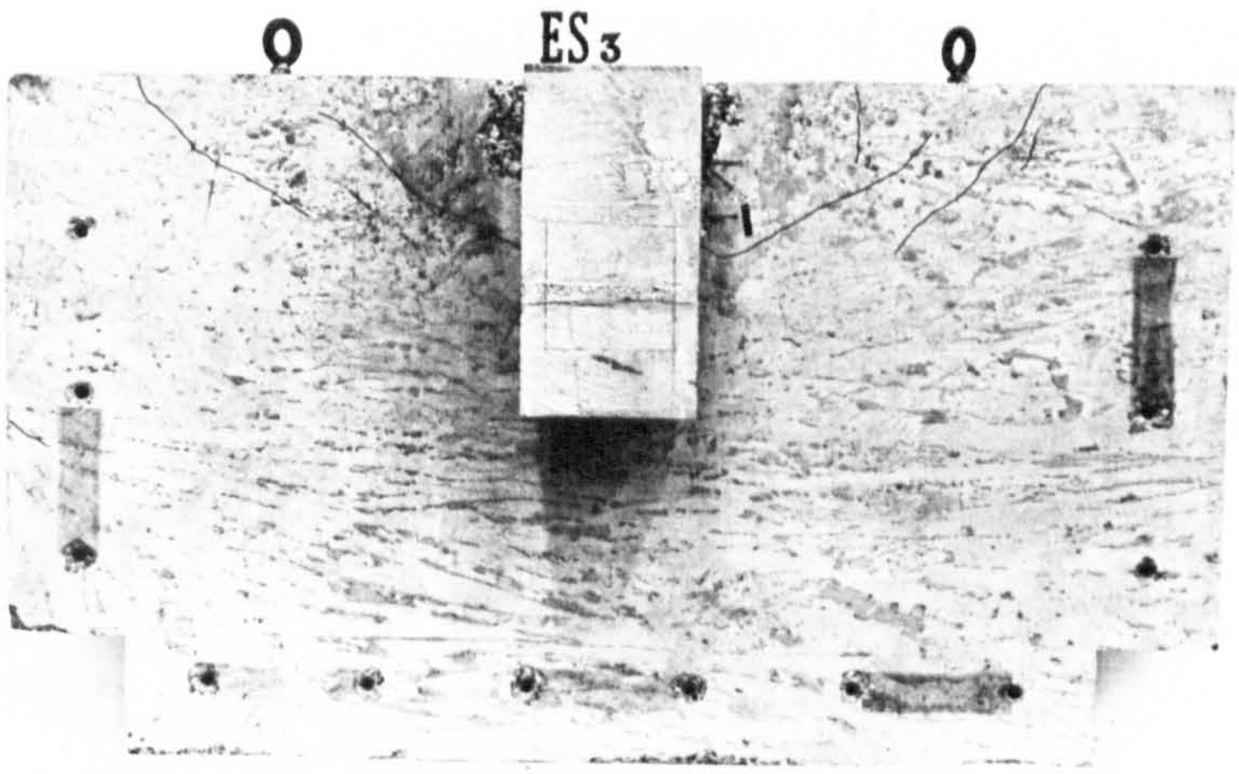

SLAB ES-3. EC=228·5.

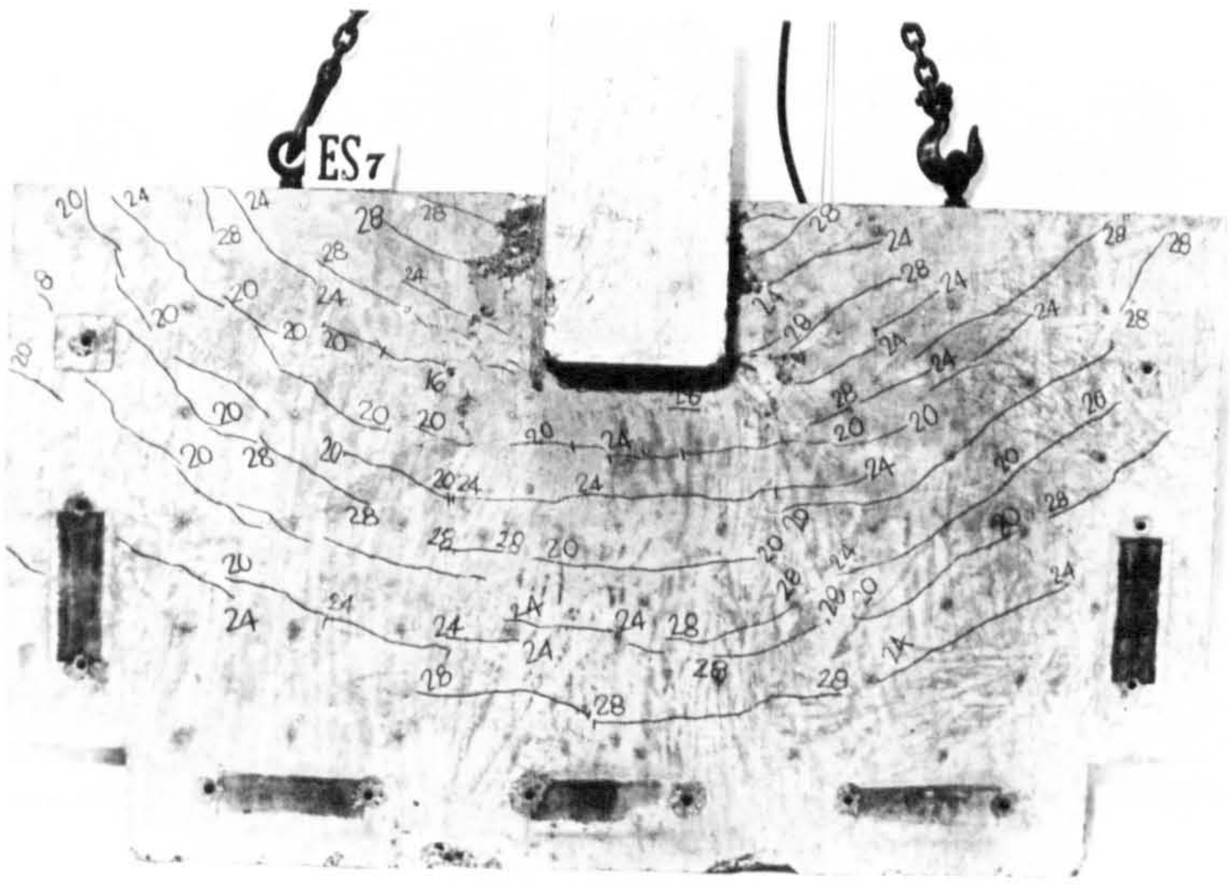

SLAB ES-7. EC=-228·5.

Fig.45 TOP SURFACES. SERIES-ES.

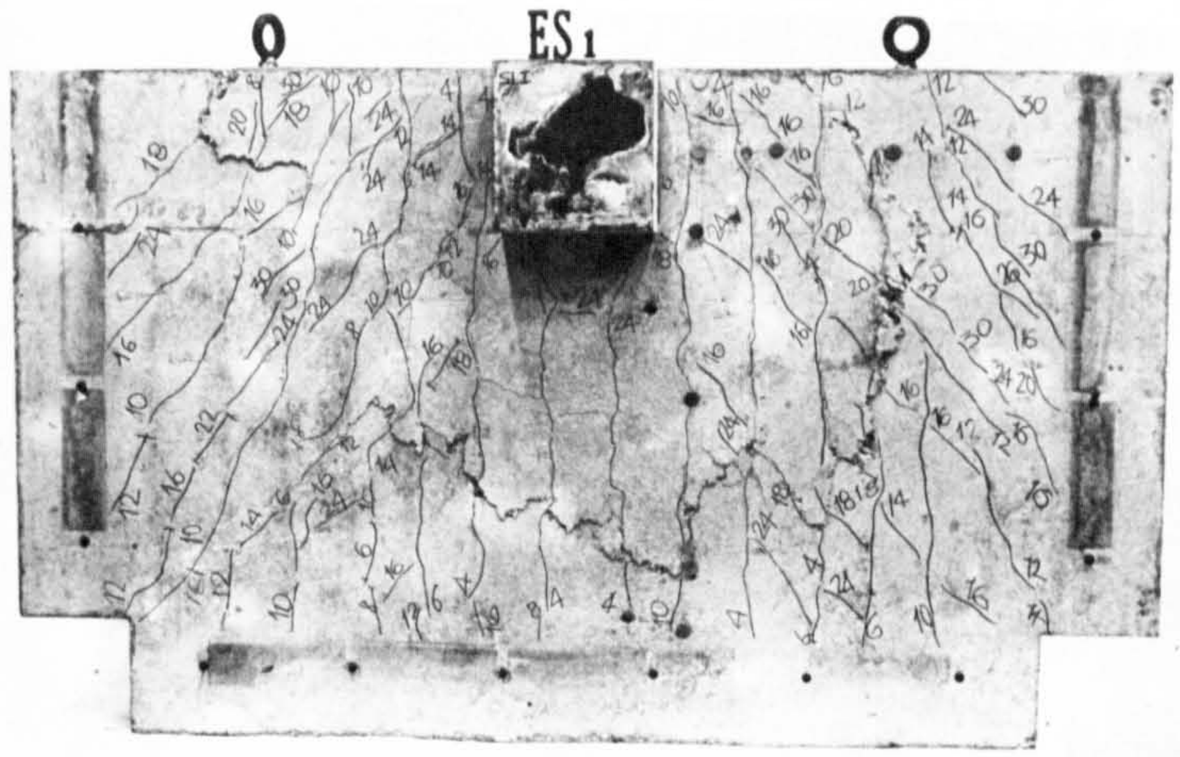

SLAB - ES.1. EC = 0.

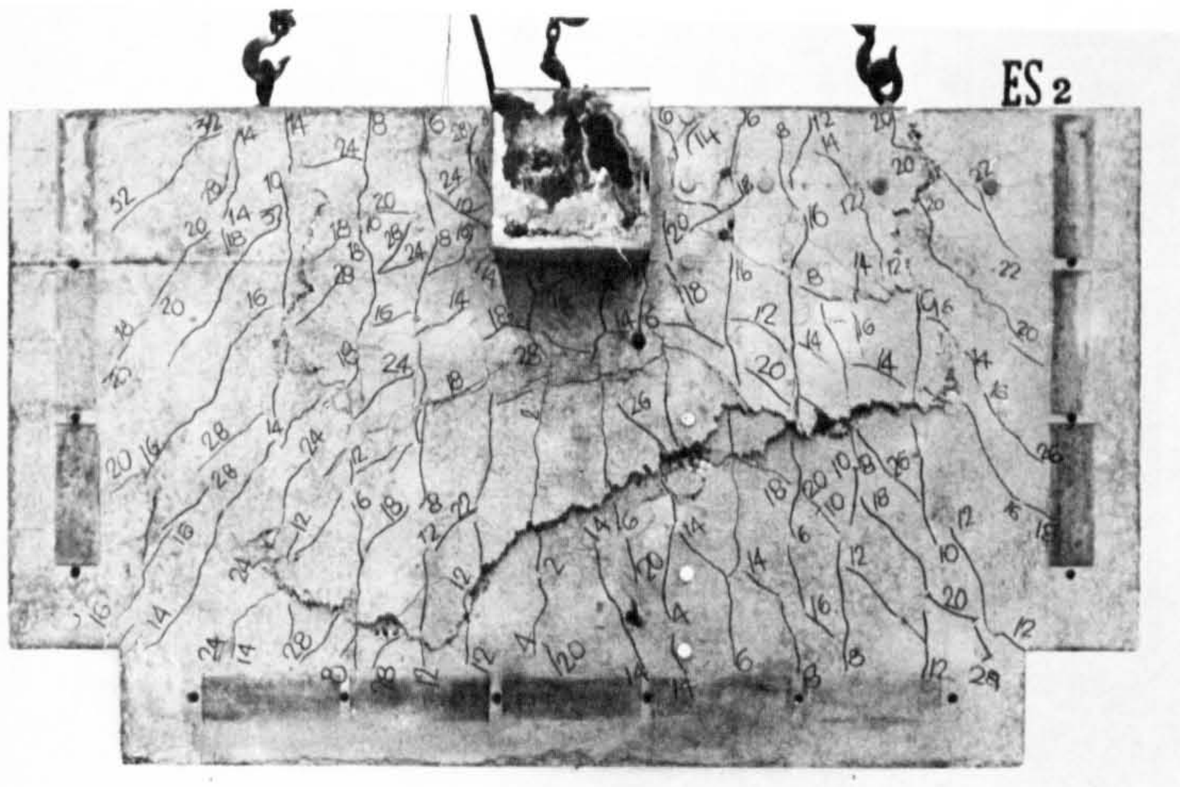

SLAB - ES.2. EC = +228·5mm.

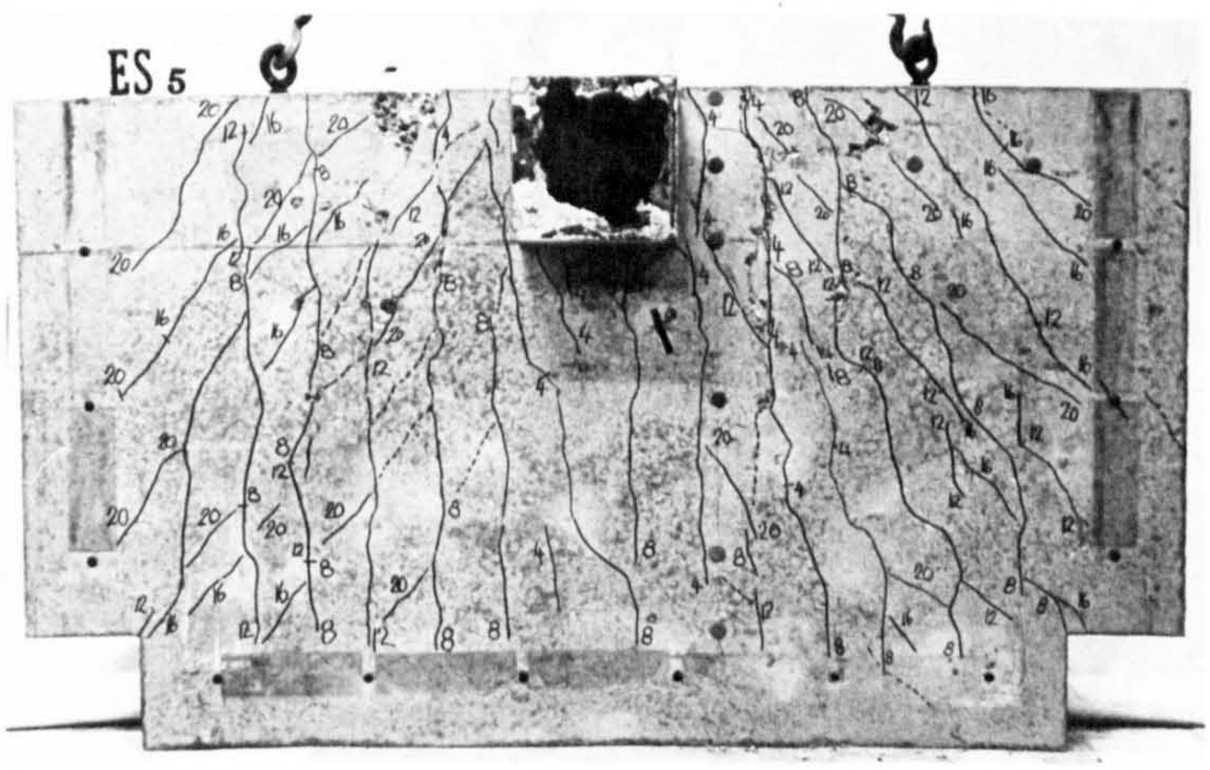

SLAB - ES.5. EC = -228·5mm.

Fig. 46. BOTTOM SURFACES. SERIES - ES.

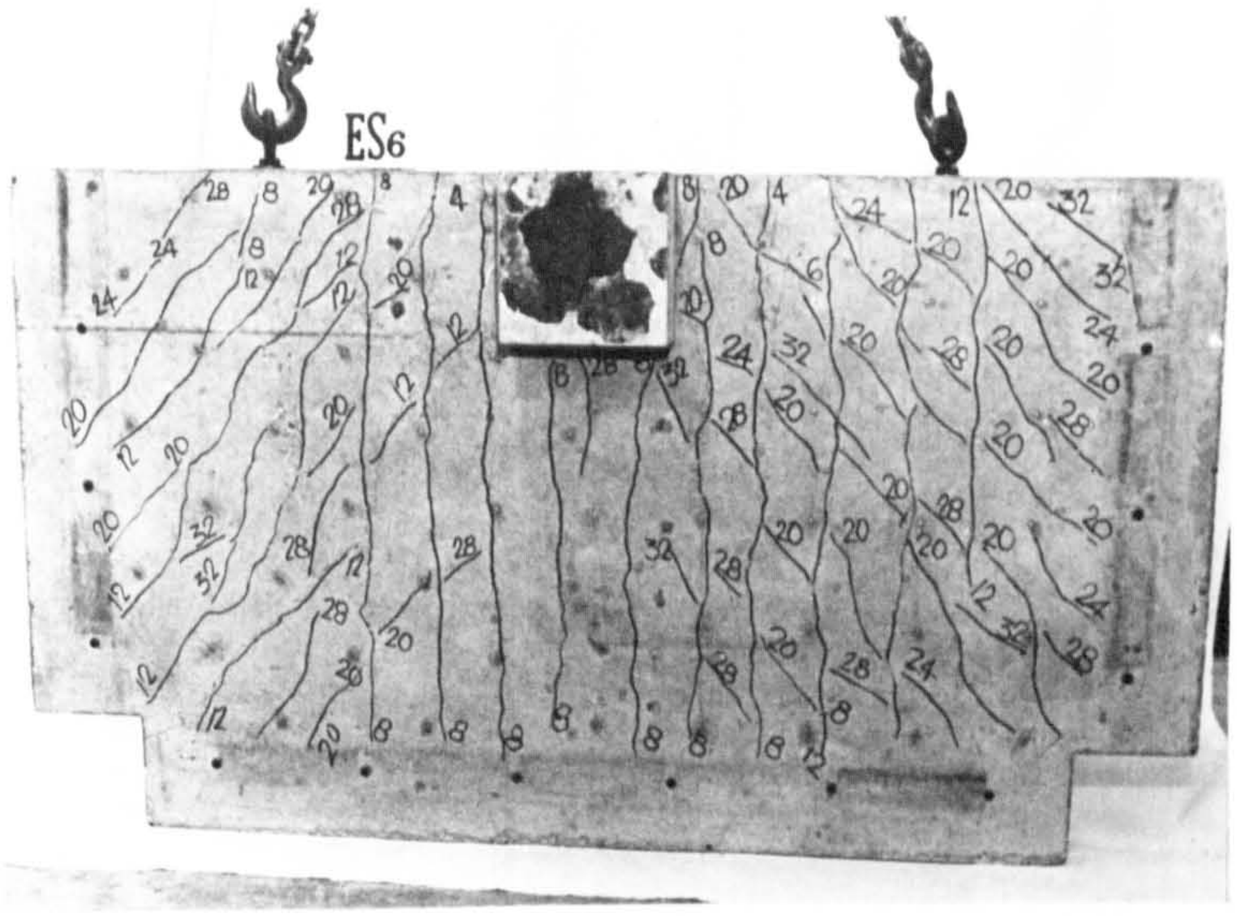

SLAB-ES.6. EC=0. ϕ_v=6·5mm.

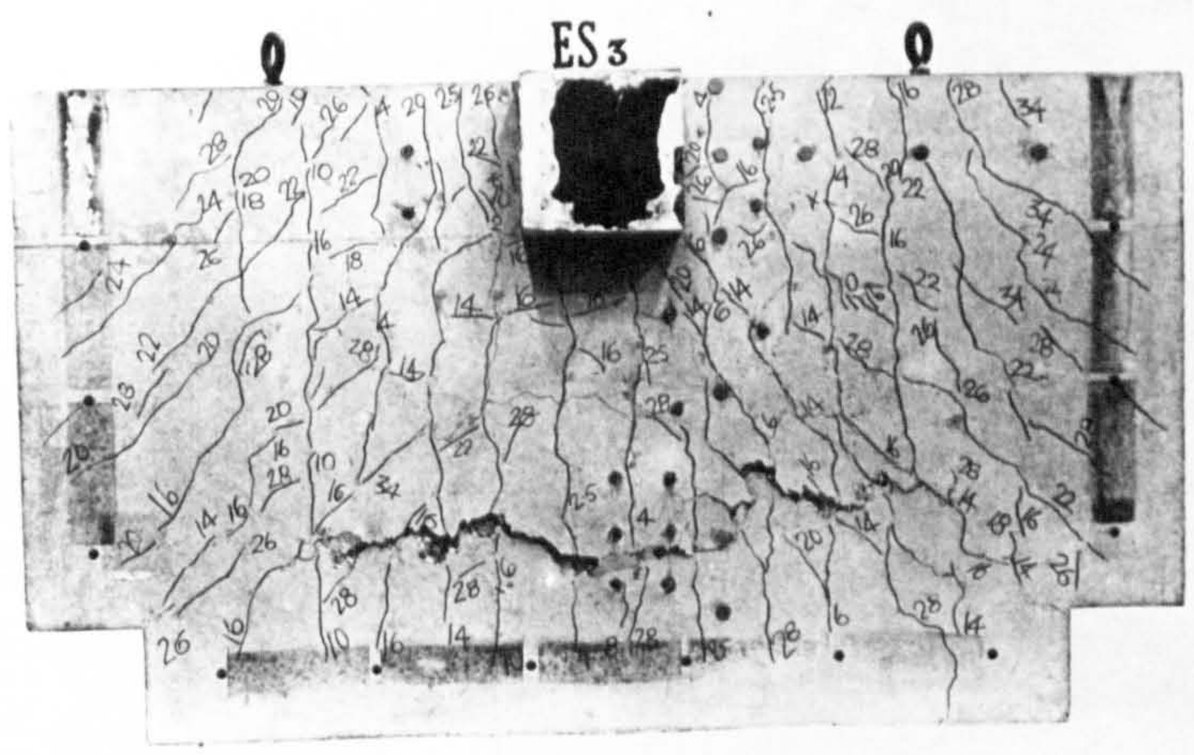

SLAB-ES.3. EC=228·5mm. ϕ_v=6·5mm.

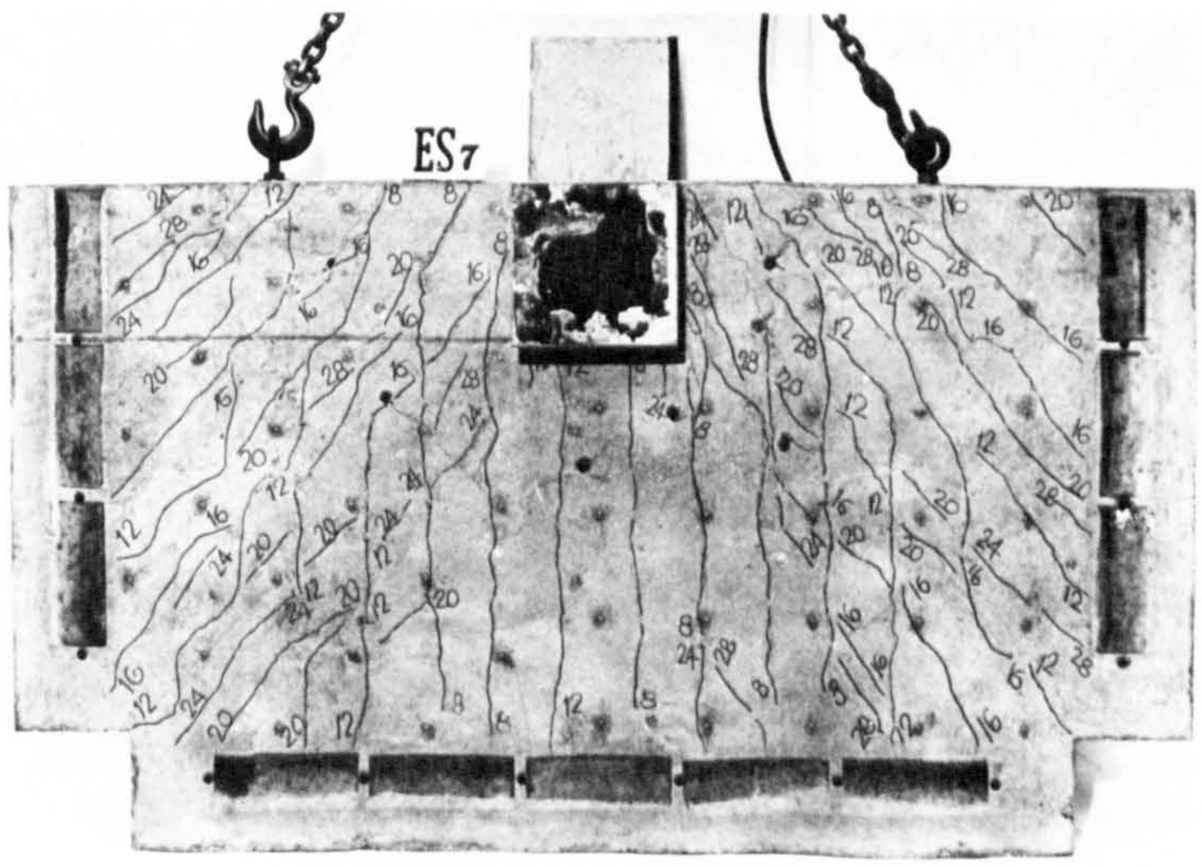

SLAB-ES.7. EC=-228·5mm. ϕ_v=6·5mm.

Fig. 47. BOTTOM SURFACES. SERIES-ES.

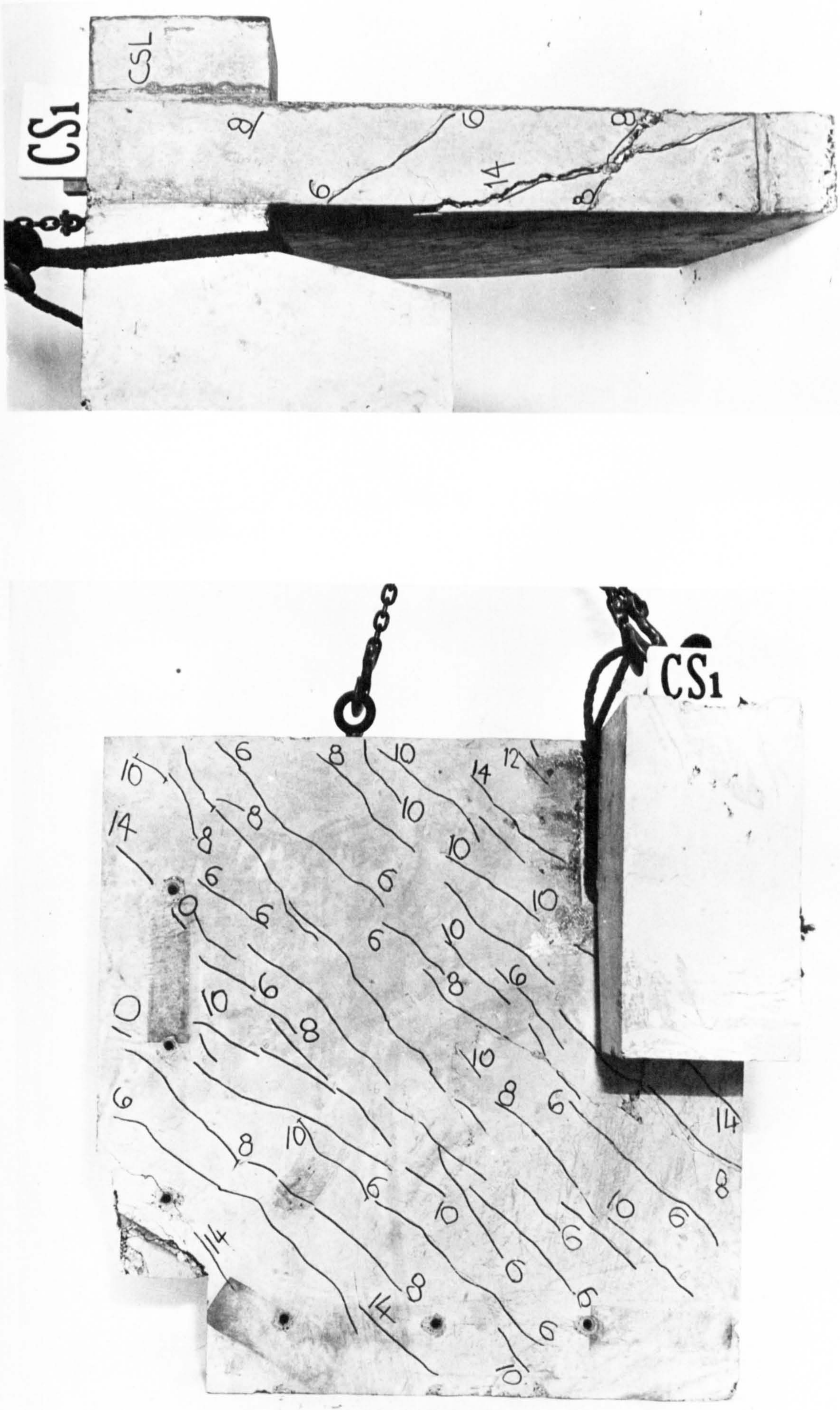

Fig. 48. CORNER SLAB AFTER FAILURE.

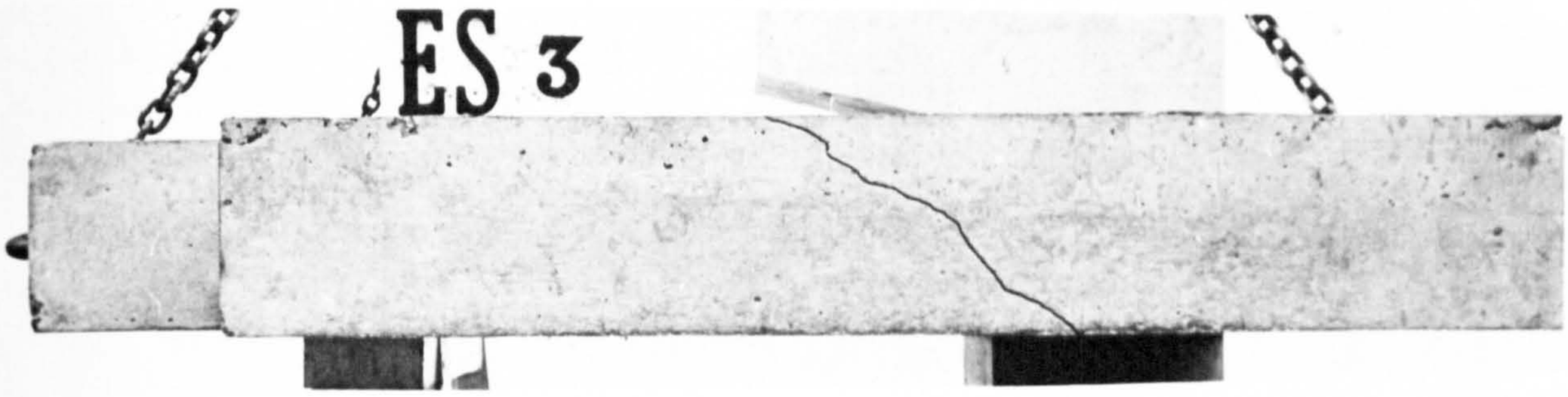

SLAB ES-3.

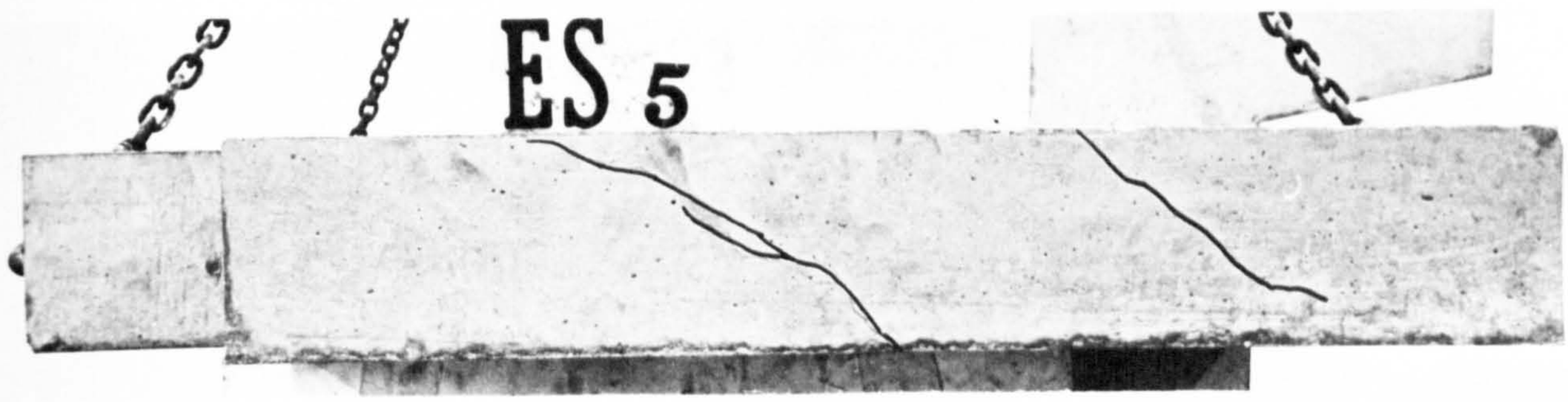

SLAB ES-5.

Fig.49 TORSIONAL CRACKS AT EDGES ⊥r TO FREE EDGES.

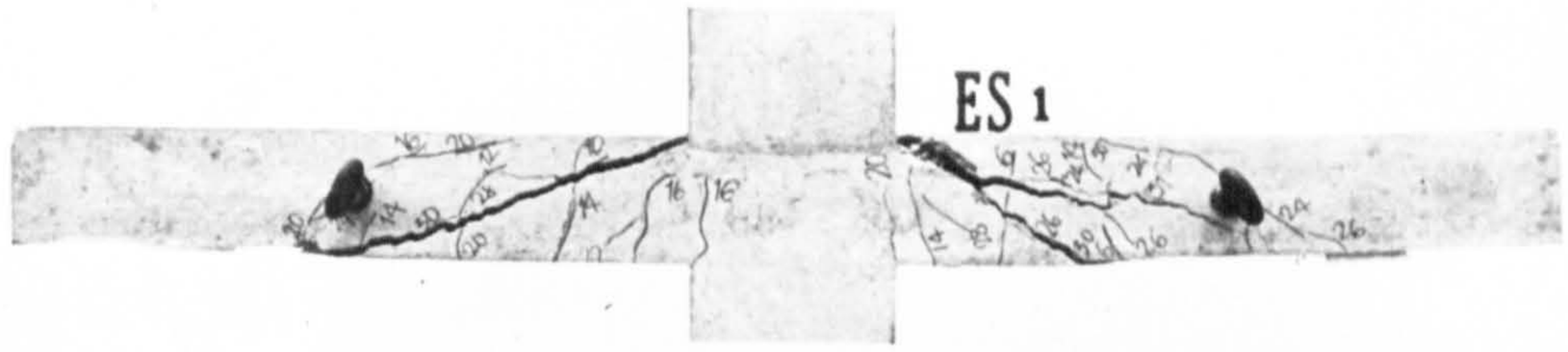

SLAB ES-1.

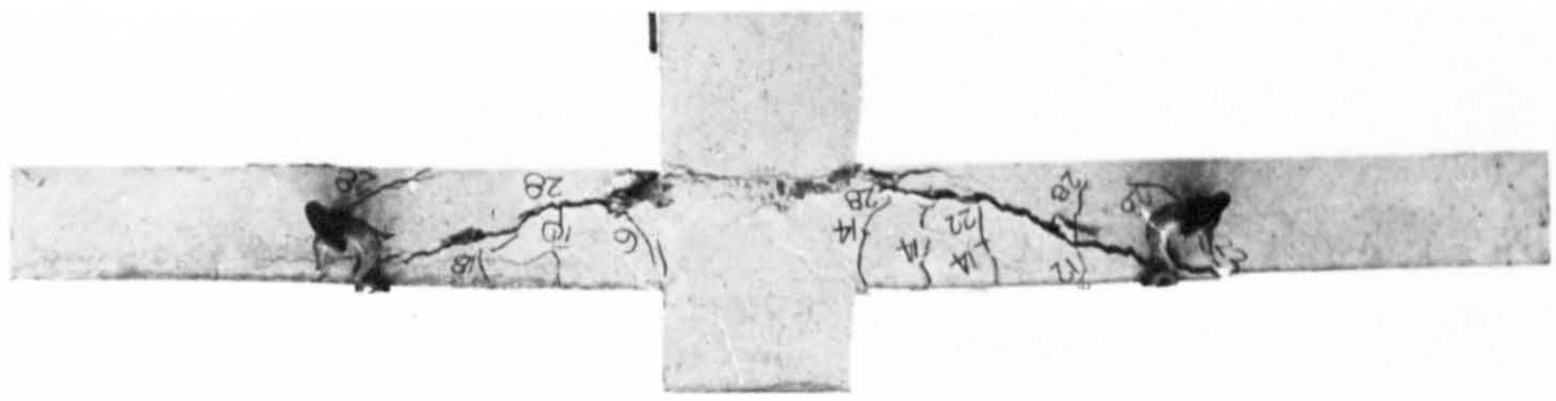

SLAB ES-2.

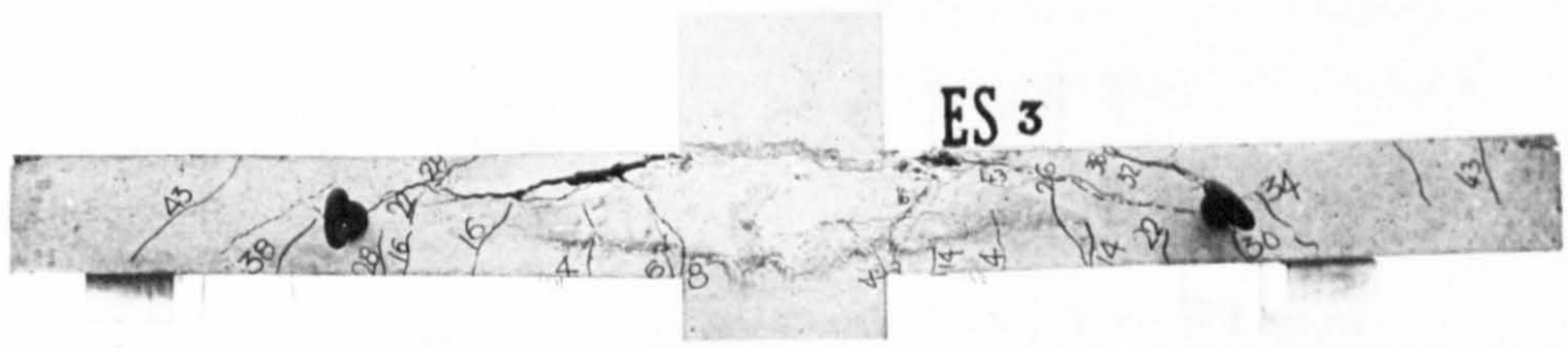

SLAB ES-3.

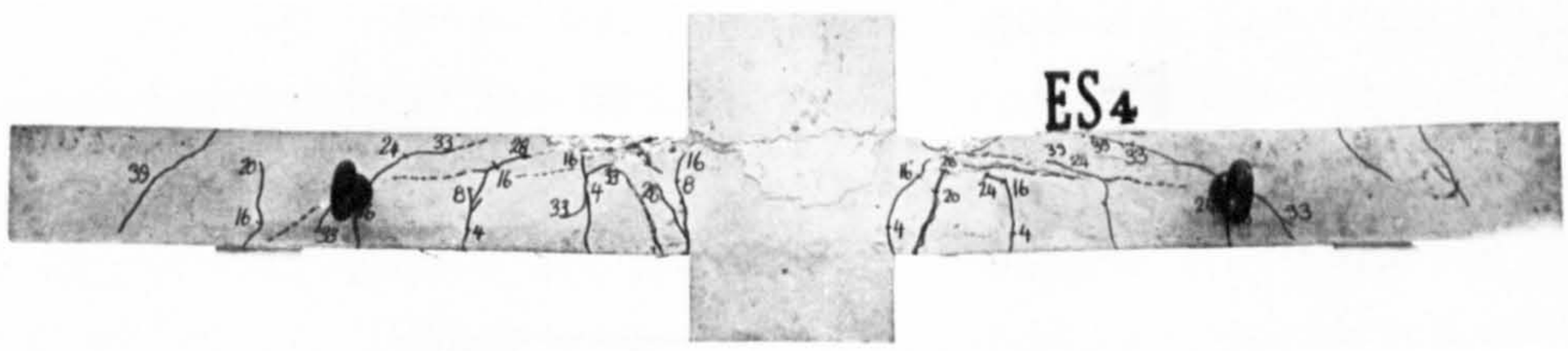

SLAB ES-4.

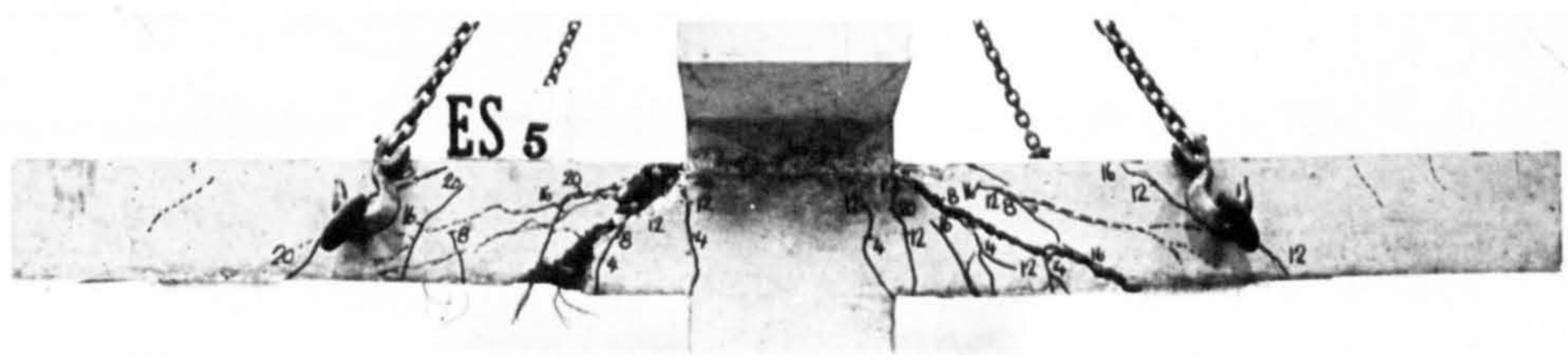

SLAB ES-5.

Fig.50 CRACK PATTERS AT FREE EDGES. SERIES-ES

CHAPTER V.

THEORY OF SHEAR FAILURE IN SLABS.

5.1 General behaviour of slabs.

In slabs with small amounts of flexural reinforcement, failure occurs when the yield stress is reached in sufficient of the flexural reinforcement and the slab fails in flexure. The ultimate strength can be computed using yield line theory.

If the slab is over-reinforced in flexure, failure may occur by crushing of concrete in the vicinity of the column head. This case and the first mentioned type of slabs are not common in flat plate construction and hence are not considered here.

The slabs tested by the author were representative of the normal slabs used in practice, unlike the ones described above. The behaviour of the slabs during testing can be described as follows. The inclined cracks usually started from flexural cracks, and there was a definite increase in load after the formation of these cracks. Failure seemed to occur due to a combination of "shearing and splitting" action in the compressive zones at the heads of the shear cracks.

The provision of a single layer of inclined shear reinforcement increases the rigidity of the connection in general. When the amount of shear reinforcement is small, the ultimate load is slightly increased and the failure crack cuts across the shear reinforcement (see Fig. 51). The deformation at failure and the ultimate load are increased by increasing the area of shear reinforcement provided, but only as long as this amount is smaller than a certain value. Further increases in shear reinforcement do not increase the ultimate load, as the failure crack falls outside the shear reinforcement. The limiting strength is that of the plain concrete outside the shear reinforcement, and the increase due to the reinforcement is limited to that obtained by increasing the critical perimeter.

Further increases of strength can be achieved by providing a second layer of shear reinforcement at a perimeter further out from column face. This might imply that by using one layer after another in succession, one could increase the punching strength indefinitely, but there is no point in increasing the punching resistance beyond the

flexural capacity. Fig. 51 shows the types of failures that can occur in general.

In all slabs tested, the failure crack had a slope of about 1 in 2 (1 vertical to 2 horizontal) within the depth between the top and bottom reinforcement. The above slope of shear crack was also observed by Richart and Kluge[62], Rosenthal[9] and Kinnunen[14] during their tests.

5.2 Vertical shear stresses in the compression zone.

In view of the relatively flat shear cracks at failure (see Fig. 28), the interlocking forces across the shear cracks must be negligible. Apart from the relatively unimportant amount of shear force carried by interlock across the cracks, all the shear force other than that carried by dowel action (see section 5.4) of the reinforcing bars, has to be carried by the compression zone at the head of the shear crack. (In the case of slabs with shear reinforcement part of the force is carried by the shear reinforcement).

These vertical stresses are uniform along the perimeter of a circular column, while this is not so in the case of a square column. The distribution across the depth is not uniform either, and can be taken as parabolic for all practical cases (see Fig. 52).

In the case of a square column while the moments are fairly uniformly distributed along the section adjacent to the column face, the shear forces are concentrated near the corner of the column. Fig. 53 shows the theoretical distribution of moments and shears around the column obtained by Moe[19] using a finite difference method for a square slab loaded through a square column. The analysis was based on the assumption that the flexural rigidity of the slab was constant throughout, all the points along the column face had equal deflection and the slab was fully fixed along the faces of the column while being simply supported along its edges.

Since some of the above assumptions are too rigid, and in the presence of cracks some redistribution occurs, the concentration can be taken as considerably reduced. Nevertheless some concentration of shear in the corners does exist as shown by Fig. 54.

5.3 Failure Criterion for concrete compression zone:

The compressive zone of a slab is subjected to longitudinal compressive forces in two directions and shear, while all the other forces are negligible. It follows that two principal stresses are compressive and the other tensile and consequently a two dimensional analysis is adequate.

In order to establish a satisfactory criterion, the existing failure hypotheses were studied. In recent years Brandzaeg[34], Reinus[35] and Baker[36,37] have succeeded in devising structural models of concrete to explain the mechanism of failure, while Bresler and Pister[38,39], McHenry and Karni[40] and Reeves[41] among others have tried empirical approaches to the problem.

Brandzaeg's model was based on a material composed of randomly oriented elements, which failed in shear, at a stress, which was governed by Coulombs internal friction law. Reinus[35] explained the breaking up of the crystalline structure of the concrete, considering the heterogeneous nature of concrete and an idealised model consisting of rods to represent the internal forces. The approach put forward by Baker[36,37] gives an interesting explanation of the internal structural behaviour, and could be a possible criterion. The pin jointed lattice model used is shown in Fig. 55. The weakness in tension of the mortar and its adhesion to stone are considered as the principal causes of failure. Accordingly, as the extensional strains increase, cracks form in the mortar pockets, and extend under further increase of load along the surfaces of cones, in which the mortar is restrained from extending by bond with the stiffer stones at the bases of the cones. Eventually, the cracks extend around the stone surfaces and failure takes place.

To adopt the above, suitable values of E_c, ν and the limiting extensional strain, which is used as a criterion of concrete failure, have to be assumed for a particular loading condition. The values of E_c, the Youngs Modulas for concrete and ν, the Poissons ratio are subject to variation depending on parameters such as grades of concrete, mortar, cement paste and σ_1, σ_2, σ_3 values (stresses in direction 1, 2, 3, see Fig. 55), and in the absence of a knowledge of the above, it is safer to use an empirical criterion based on test results. In order to establish a suitable criterion, the available experimental

data[38,40,41,42], where the concrete specimens were subjected to combined compressive and shear stresses, were studied. The combination of stresses was achieved by testing hollow cylinders under varying combinations of torsion and compression or tension and compression. Plotting dimensionless ratios of $q/U_w^{2/3}$ V_s f/U_w gives a graph as shown in Fig. 56 (see Ref.43). From the graph it can be seen that there is a wide scatter of results. But if one averages groups of results, the shear stress acting on the plane perpendicular to f at failure is a pretty constant value i.e., $0.45\ U_w^{2/3}$ for all practical purposes.

For a parabolic shear stress distribution across the depth, this gives an average shear stress of $0.3\ U_w^{2/3}$ (metric units) across the depth of the compression zone. Hence based on the above, the criterion of failure used is defined as follows:- 'Failure occurs when the shear stress reaches a limiting value of $0.3\ U_w^{2/3}$ across the critical section'.

5.4 Dowel Action.

When an inclined crack opens up, a relative moment takes place between the levels of the reinforcing bars on either side of the crack (see Fig. 57). This in turn, tends to split the concrete on one side of the crack. It is assumed that the dowel is supported by the concrete cover to the bars, which in turn is supported by vertical tension in the concrete below.

The maximum dowel force depends primarily on the split length of concrete, l_c (or primary bearing length of dowel), the strength of and stress distribution in the concrete along this length and the width of concrete involved at this level of the bar. The split length is affected by the stiffness of the dowel element, number of bars contributing (n), bond property of the bar and the stiffness of the surrounding mass. This would mean that the split length could be expressed as proportional to say $\sqrt[4]{\phi_M^4.n}/U_w^{1/3}$. In the case of slabs n is taken as unity because each bar acts independently.

The stiffness is taken to be dependent only on the bars and not on their cover, since very high local bond stresses are provided by any composite action as failure probably occurs as or after the bond breaks down. The beneficial influence of the improved bond qualities

of deformed bars is taken into account empirically below. The dowel effect is more marked in flat slabs than in beams because the ratio of the widths of the tensile and compression zones involved is much greater. However the other factors influencing dowel action being the same for beams as well as for slabs, beam type dowel tests[28,29,30,31] are used in deriving the following:

Dowel force $Q_d = L_c \cdot b_d \cdot U_t$ . . . . . (30)

where U_t = the tensile strength of concrete ($N/_{mm}2$) taken as $0.25\ U_w^{2/3}$ (see Fig.58)

$L_c = k.\ \phi_M \cdot n^{\frac{1}{4}} / U_w^{1/3}$

n = number of bars used.

b_d = effective width, dowel perimeter.

ϕ_M = diameter of bar used.

k is a factor which takes the bond property of the bar into account. Therefore,

$$Q_d = \frac{k.\phi_M.n^{\frac{1}{4}}}{U_w^{1/3}} \cdot b_d \cdot 0.25\ U_w^{2/3}$$

$$= K_d \cdot b_d \cdot \phi_M \cdot n^{\frac{1}{4}} \cdot U_w^{1/3} \quad . . . . . (31)$$

For the purpose of calculating the value of K_d for various types of steel bars the existing beam data as given by Roy[30], Baumann[28], Krefeld and Thurston[29] and Arroyo[31] was analysed (see Table V-1) and the values of K_d are approximated under three types of bars (i.e.) plain round, slightly deformed and highly deformed.

If the specific cross-sectional area of deformations, which is defined as the projected cross-sectional area of deformation at right-angles to the bar divided by the spacing of ribs, is greater than or equal to 0.2 times the diameter of the bar, the bar can be termed as highly deformed. Any type in between the above and the plain round bars can be classified as slightly deformed.

From table V-1, it could be seen that there is a wide scatter in the values of K_d obtained. The steel used by Arroyo (Swedish K_{60} steel) in his tests were highly deformed. Those used by Baumann (Tor steel), Krefeld and Thurston and part of tests by Roy (Helibond), had slightly deformed bars. The majority of the tests carried out by Roy had plain round bars. Values of K_d's obtained from Roy's tests using (Helibond) slightly deformed bars were considerably lower than the ones obtained from Baumann's and Krefeld and Thurston's beams, possibly due to the distance of the applied dowel load on the bar from the concrete. In view of this, it is felt that Roy's values for plain bars might also be on the low side. The only test result available on slabs was done by Anis[18] using plain round bars (mild steel) and the corresponding value of K_d is approximately 1.2. The ratio of the average value of K_d obtained by Baumann and Krefeld to the one obtained by Roy for slightly deformed bars is 1.3. Increasing Roy's value for plain round bars in the same ratio we get 1.1. Hence the formula for calculating the dowel force can be written as

$$Q_d = 1.1\, b_d \cdot \phi_M \cdot U_w^{1/3} \text{ for slabs with plain round bars.}$$

$$= 1.3\, b_d \cdot \phi_M \cdot U_w^{1/3} \text{ for slabs with slightly deformed bars.}$$

$$= 1.8\, b_d \cdot \phi_M \cdot U_w^{1/3} \text{ for slabs with highly deformed bars.}$$

The proposed formula predicts the dowel force as directly proportional to the diameter of the bar. The larger the diameter, the greater is the dowel force predicted, but one should realise that the use of large diameter bars can lead to a situation in which only part of the perimeter is stressed (s greater than s_{crit}), because of the relatively wide spacings of bars. Each bar acts independently to stress a given width of concrete, whereas in most beams several bars act together. If bars are very widely spaced it may be that only parts of perimeters of concrete (i.e. those close to the bar) are stressed. The critical spacing is probably dependent on the thickness of the concrete cover. If the spacing exceeds s_{crit}, only the perimeter over which dowel acts should be taken (i.e.) $n.s_{crit}$.

Where n is the number of bars involved. On available test evidence,

s_{crit} = approximately (ϕ_M + 8 . cover)

Figs. 59 and 60 show the type of specimens used by the various investigators. Brief summaries of the details of the tests can be obtained from Arroyo[31].

TABLE V - 1

Values of 'K_d' for highly deformed bars - Tests by Arroyo[31].

Beam No.	Cover c mm.	Depth d mm.	Concrete Strength U_w N/mm^2	Number of bars n	Diameter of bars ϕ_M mm.	Effective width b_d mm.	Dowel force Q_d Newtons	Dowel constant K_d in Eq.31
JD1.I	25	305	37.3	3	16	104.8	12500	1.72
II	25	305	37.3	3	16	104.8	13500	1.85
JD2.I	25	305	40.7	3	16	104.8	12500	1.67
II	25	305	40.7	3	16	104.8	12500	1.67
JD6.I	25	305	38.6	3	16	104.8	12750	1.71
II	25	305	38.6	3	16	104.8	18720	2.52
JD7.I	57	305	40.8	3	16	104.8	15450	2.04
II	57	305	40.8	3	16	104.8	20750	2.74
JD8.I	57	305	38.6	3	16	104.8	12950	1.74
II	57	305	38.6	3	16	104.8	7970	1.07

TABLE V - 1 (contd.)

Values of 'K_d' for slightly deformed bars.

Beam No.	Cover c mm.	Depth d mm.	Concrete Strength U_w N/mm^2	Number of bars n	Diameter of bars ϕ_M mm.	Effective width b_d mm.	Dowel force Q_d Newtons	Dowel constant K_d in Eq.31
TESTS BY BAUMANN[28]								
1	40	320	39.5	2	20	70	7000	1.25
2	40	320	35.0	2	20	70	9000	1.67
4	40	320	37.0	2	20	70	7000	1.28
6	40	320	40.0	2	16	118	11500	1.51
7	40	320	38.2	2	16	78	6000	1.21
8	41	320	31.2	2	16	78	6500	1.41
9	37	320	40.0	2	26	98	11500	1.12
10	40	320	38.2	2	26	58	7500	1.25
11	46	320	31.2	2	26	58	6500	1.16
12	40	400	38.8	2	20	160	17000	1.34
13	40	320	42.0	2	20	70	8500	1.48
14	40	320	36.5	2	20	70	9000	1.65
15	30	320	40.6	2	20	70	6000	1.06
17	40	320	40.7	2	20	70	7500	1.32
19	40	320	39.7	2	26	58	7500	1.24
20	40	320	39.5	2	20	70	12000	2.14
21	40	320	36.5	2	20	70	7000	1.28
25	43	320	40.5	1	16	84	11000	2.50
26	44	320	40.5	2	16	58	9000	2.40
27	40	400	37.2	4	20	120	14000	1.25
29	40	320	11.8	2	20	70	5500	1.46

TABLE V - 1 (contd.)

Values of 'K_d' for slightly deformed bars

Beam No.	Cover c mm.	Depth d mm	Concrete Strength U_w N/mm^2	Number of bars n	Diameter of bars ϕ_M mm.	Effective width b_d mm.	Dowel Force Q_d Newtons	Dowel Constant K_d in Eq. 31.
TESTS BY KREFELD AND THURSTON(29).								
DA 1	49	Varies	19.7	2	22	108	8940	1.17
DA 2	49		22.8	2	22	108	15950	1.99
DA 3	49		22.8	2	22	111	14050	1.70
DA 4	52		23.9	2	29	95	13180	1.43
DA 5	52		23.9	2	29	101	16080	1.63
DA 6	49		22.6	2	22	159	14500	1.23
DA 7	49		22.4	2	22	162	12280	1.03
DA 8	125		20.6	2	22	108	15610	2.01
DA 9	125		20.6	2	22	108	20100	2.61
TESTS BY ROY(30).								
BL1	19	133	33.6	2	13	51	2570	1.05
RBL1	19	133	44.8	2	13	51	2685	1.00
R'BL1	19	133	45.2	2	13	51	3280	1.21
BL2	19	133	33.6	2	13	51	2175	0.89
RBL2	19	133	44.8	2	13	51	2800	1.04
R'BL2	19	133	45.2	2	13	51	2885	1.07
BL3	19	133	33.6	2	13	51	2130	0.87
RBL3	19	133	44.8	2	13	51	3240	1.20
R'BL3	19	133	45.2	2	13	51	3370	1.25
BL4	19	133	33.6	2	13	51	2040	0.83
RBL4	19	133	44.8	2	13	51	3330	1.24
R'BL4	19	133	45.2	2	13	51	3330	1.23

TABLE V - 1 (contd.)

Values of 'K_d' for plain round bars - Tests by Roy[30]

Beam No.	Cover c mm.	Depth d mm.	Concrete strength U_w N/mm^2.	Number of bars n	Diameter of bars ϕ_M mm.	Effective width b_d mm.	Dowel force Q_d Newtons	Dowel Constant K_d in Eq. 31
AP1	19	133	33.2	2	6	63	2000	1.31
RAP1	19	133	33.2	2	6	63	2200	1.44
AP2	19	133	33.2	2	9	57	2620	1.15
RAP2	19	133	33.2	2	9	57	2665	1.30
AP3	19	133	33.2	2	16	44	2130	0.79
RAP3	19	133	33.2	2	16	44	2260	0.84
AC1	19	133	34.5	2	13	51	1975	0.80
RAC1	19	133	34.5	2	13	51	2220	0.90
AC2	25	127	34.5	2	13	51	2220	0.90
RAC2	25	127	34.5	2	13	51	2065	0.84
AC3	32	121	34.5	2	13	51	2220	0.90
RAC3	32	121	34.5	2	13	51	3330	1.35
AC4	44	108	34.5	2	13	51	2970	1.20
RAC4	44	108	34.5	2	13	51	2065	0.84
AC5	19	108	43.1	2	13	51	2175	0.82
RAC5	19	108	43.1	2	13	51	2110	0.79
AC6	32	108	43.1	2	13	51	2420	0.91
RAC6	32	108	43.1	2	13	51	2690	1.01
AC7	44	108	43.1	2	13	51	2242	0.84
RAC7	44	108	43.1	2	13	51	2310	0.87
AT1	19	133	24.2	2	13	51	2445	1.11
RAT1	19	133	32.7	2	13	51	3420	1.41
AT2	19	133	24.2	2	13	51	1780	0.81
RAT2	19	133	32.7	2	13	51	2220	0.91
AT3	19	133	24.2	2	13	51	2000	0.91
RAT3	19	133	32.7	2	13	51	2310	0.95

TABLE V - 1 (contd.)

Values of K_d for plain round bars - Tests by Roy (contd.)

Beam No.	Cover c mm.	Depth d mm.	Concrete Strength U_{w_2} N/mm^2	Number of bars n	Diameter of bars ϕ_M mm.	Effective width b_d mm.	Dowel force Q_d Newtons	Dowel constant K_d in Eq.31
AL1	19	133	26.1	2	13	51	1242	0.55
RAL1	19	133	29.9	2	13	51	1600	0.68
R'AL1	19	133	34.4	2	13	51	1575	0.64
AL2	19	133	26.1	2	13	51	1910	0.85
RAL2	19	133	29.9	2	13	51	888	0.38
R'AL2	19	133	34.4	2	13	51	1950	0.79
AL3	19	133	26.1	2	13	51	1530	0.68
RAL3	19	133	29.9	2	13	51	1552	0.66
R'AL3	19	133	34.4	2	13	51	1910	0.77
AL4	19	133	26.1	2	13	51	1640	0.73
RAL4	19	133	29.9	2	13	51	1464	0.62
R'AL4	19	133	34.4	2	13	51	1995	0.81
AS1	19	133	49.9	2	13	51	2350	0.84
RAS1	19	133	49.9	2	13	51	2040	0.73
AS2	19	133	36.9	2	13	51	2040	0.81
RAS2	19	133	36.9	2	13	51	1885	0.75
AS3	19	133	34.0	2	13	51	1730	0.70
RAS3	19	133	34.0	2	13	51	1685	0.69
AS4	19	133	22.0	2	13	51	1600	0.75
RAS4	19	133	22.0	2	13	51	1950	0.92

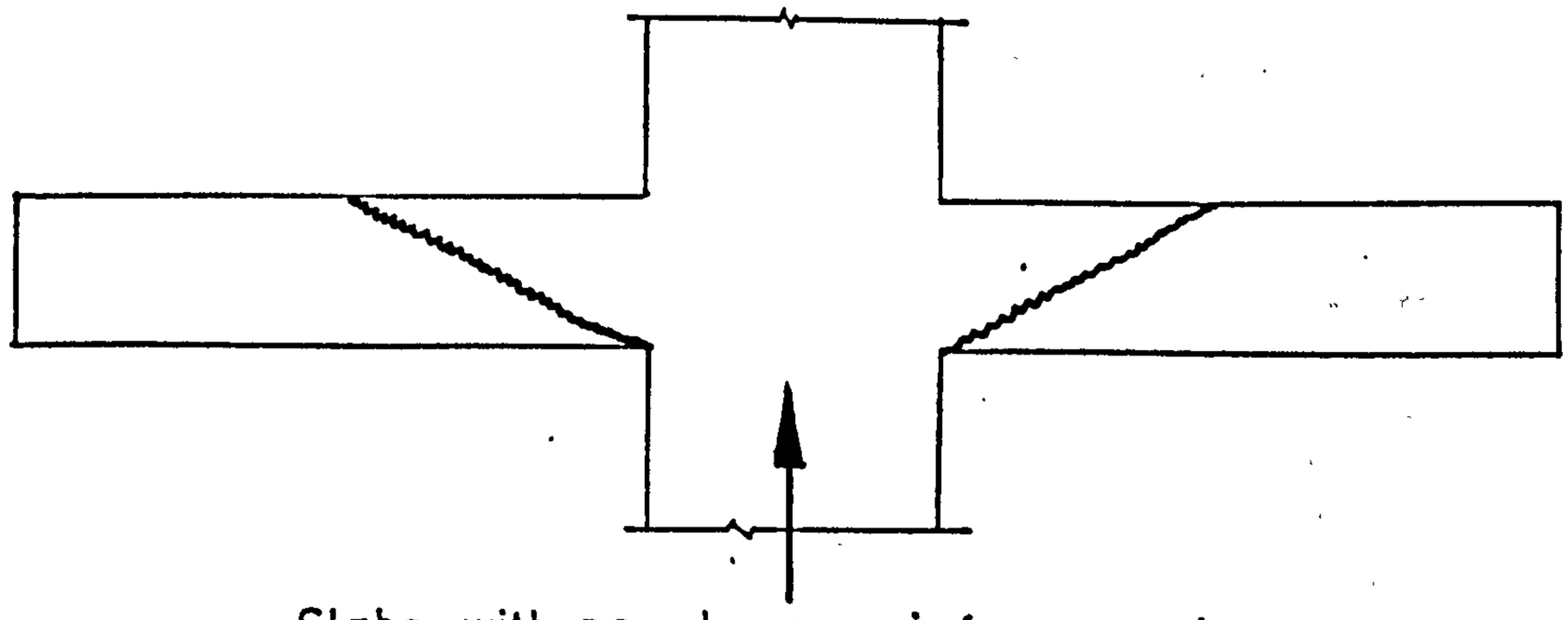

Slabs with no shear reinforcement.

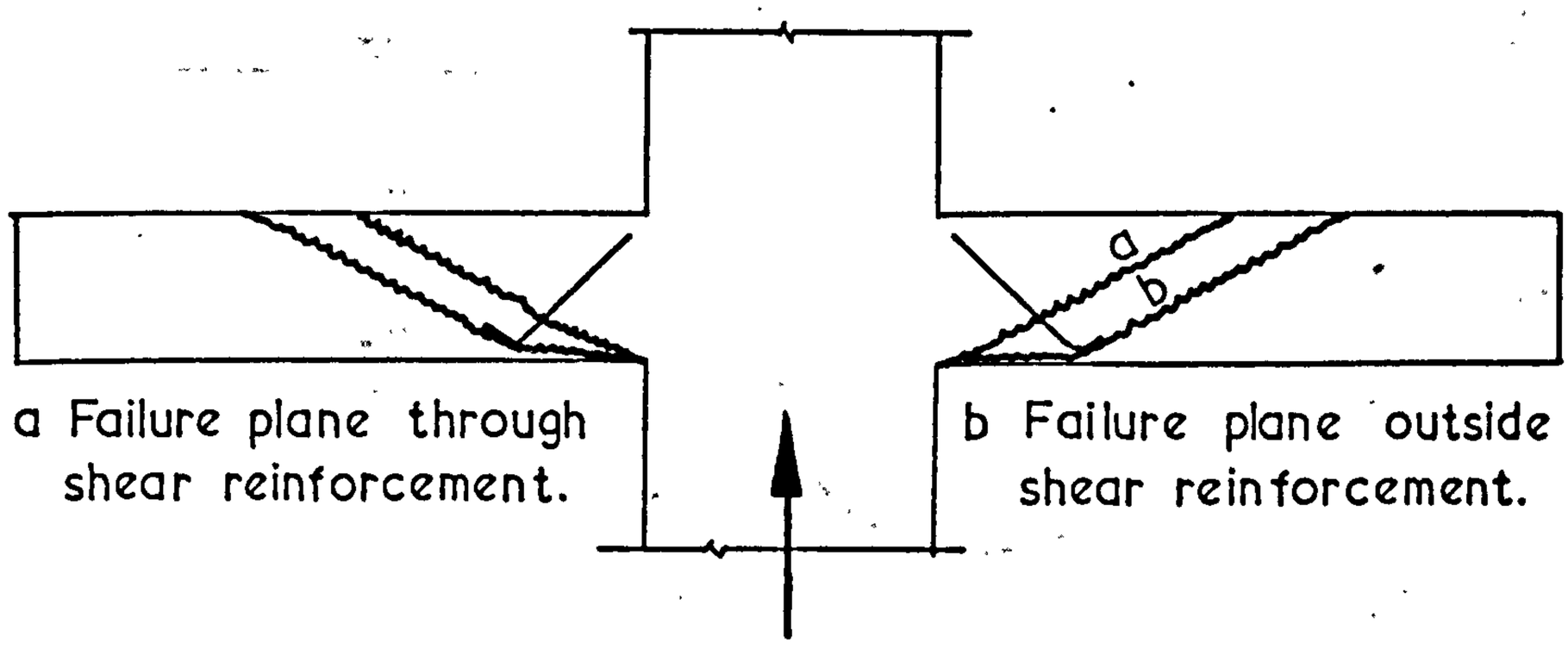

a Failure plane through shear reinforcement.

b Failure plane outside shear reinforcement.

Slabs with one layer of shear reinforcement.

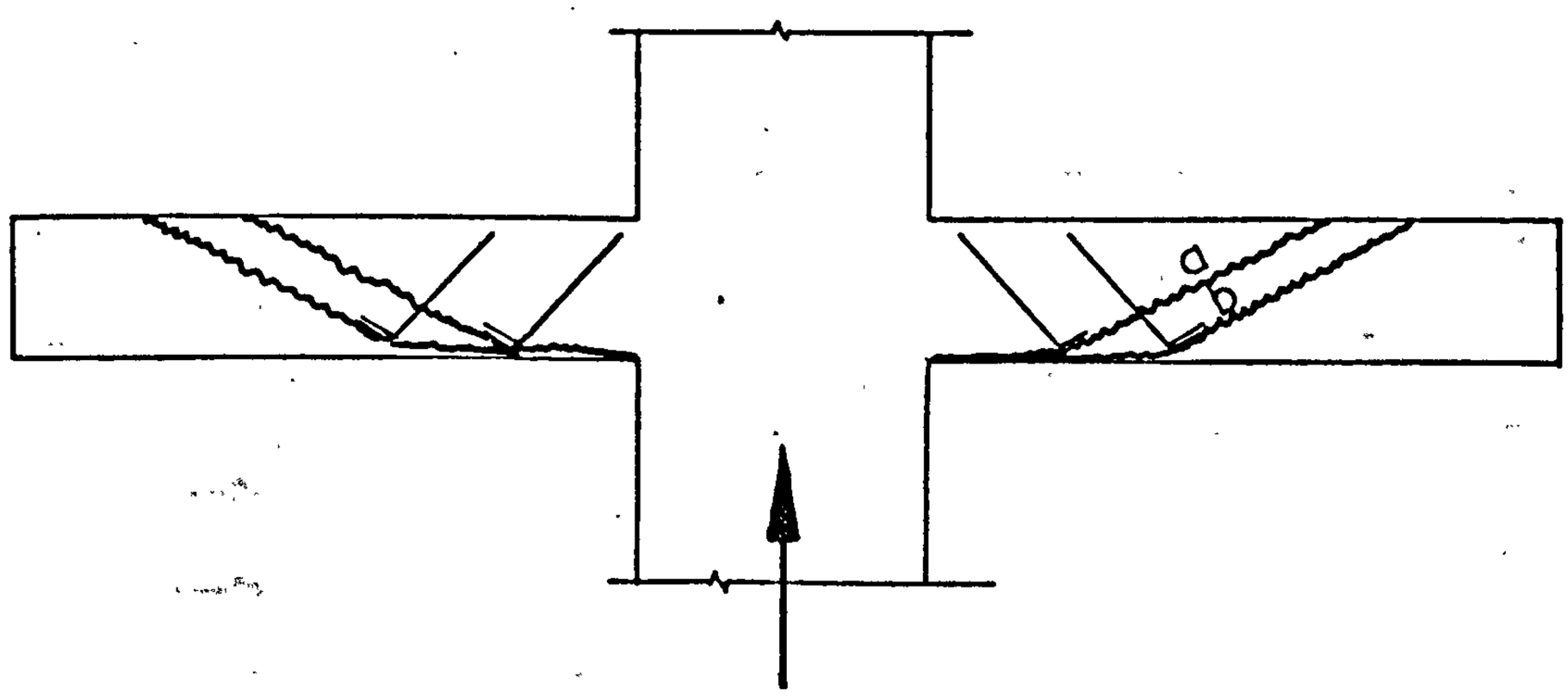

Slabs with two layers of shear reinforcement.

Fig. 51. GENERAL TYPES OF FAILURE THAT CAN OCCUR.

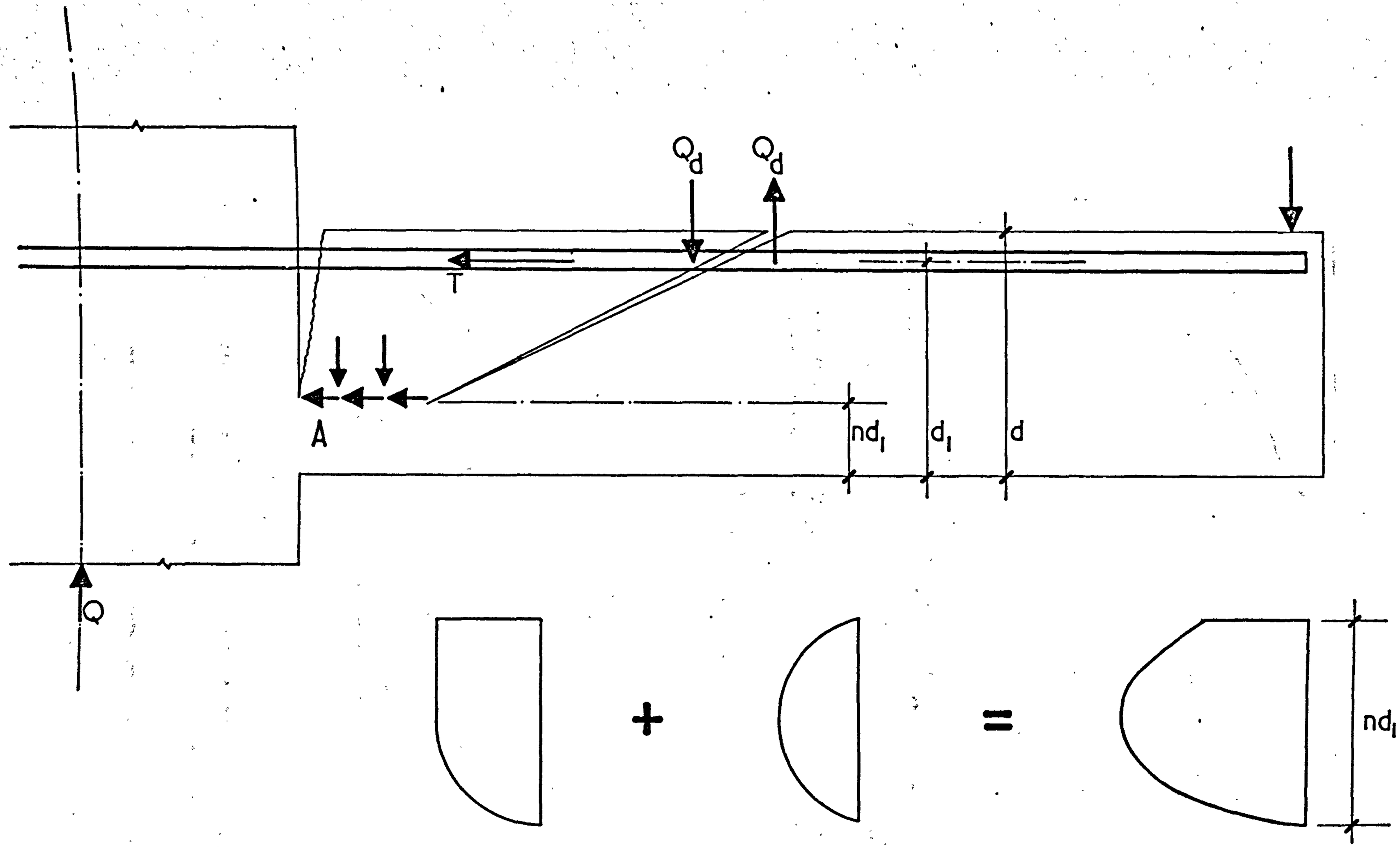

Fig. 52. VERTICAL SHEAR STRESS DISTRIBUTION AT CRITICAL SECTION 'A'.

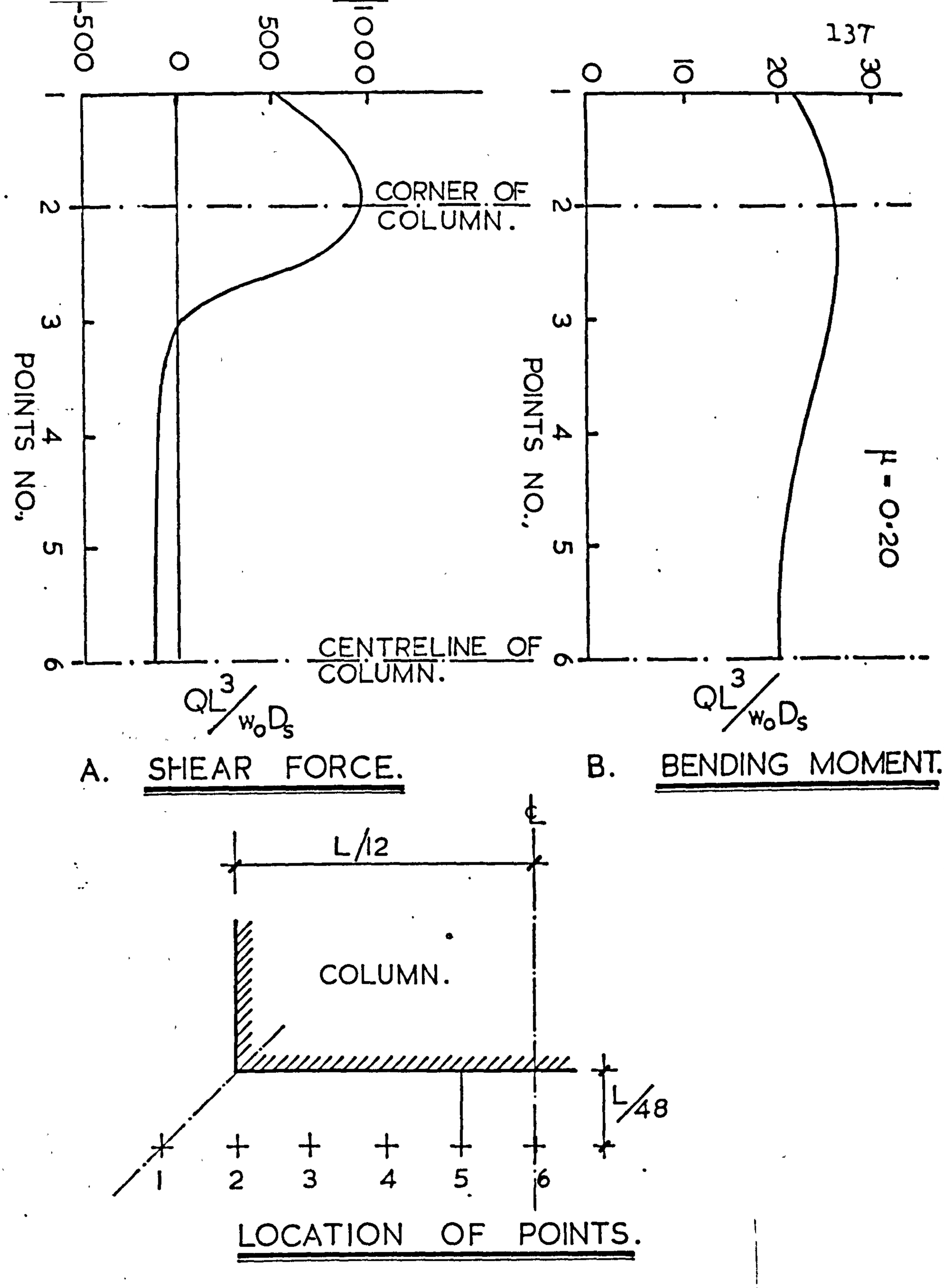

Fig. 53. THEORETICAL DISTRIBUTION OF MOMENT & SHEAR FORCE AT A DISTANCE OF L/48 FROM THE COLUMN.

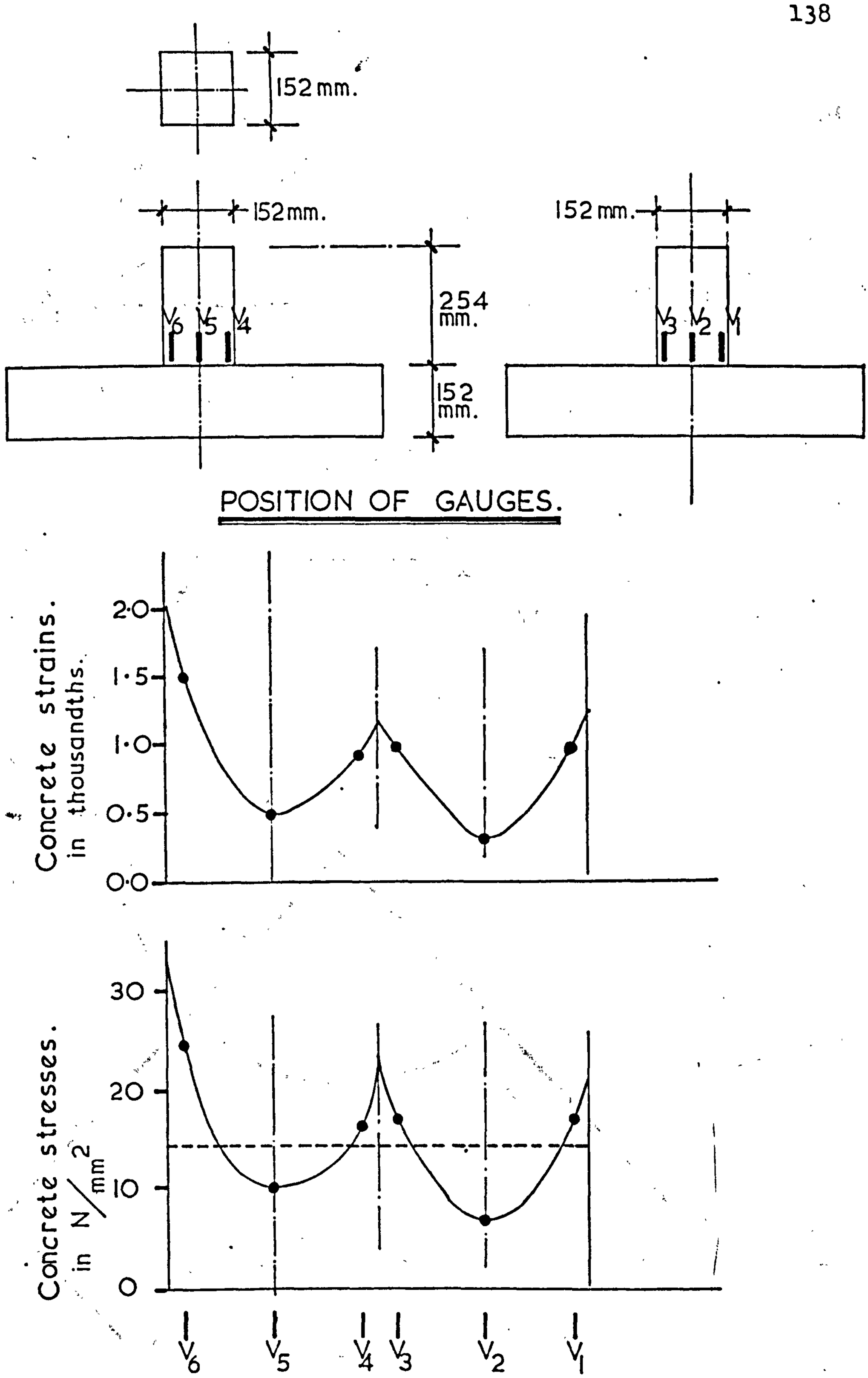

Fig. 54. VERTICAL STRESSES & STRAINS IN COLUMN OF SLAB R-2 ACCORDING TO MOE.

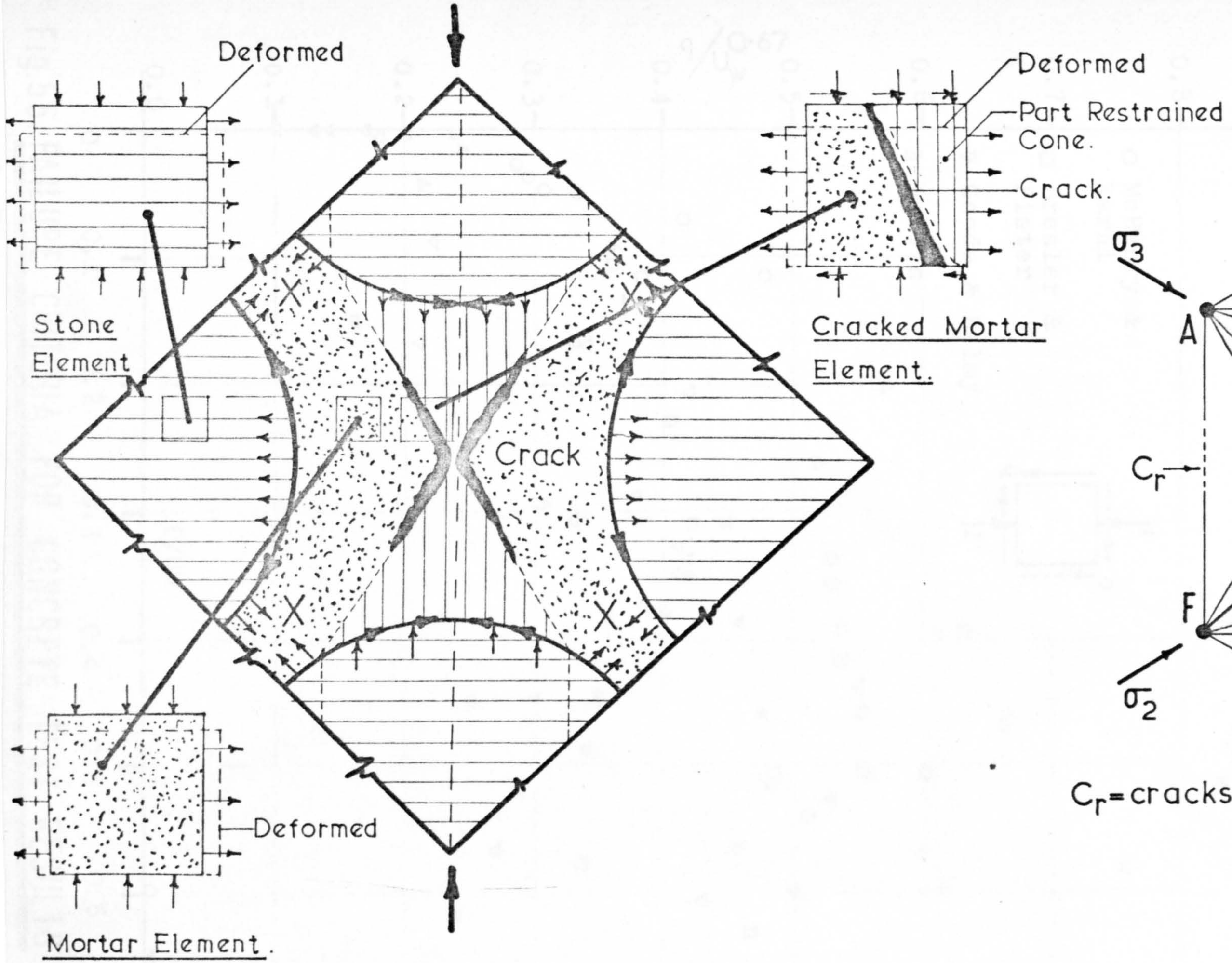

IDEALISED CONCRETE ELEMENT.

Fig.55.

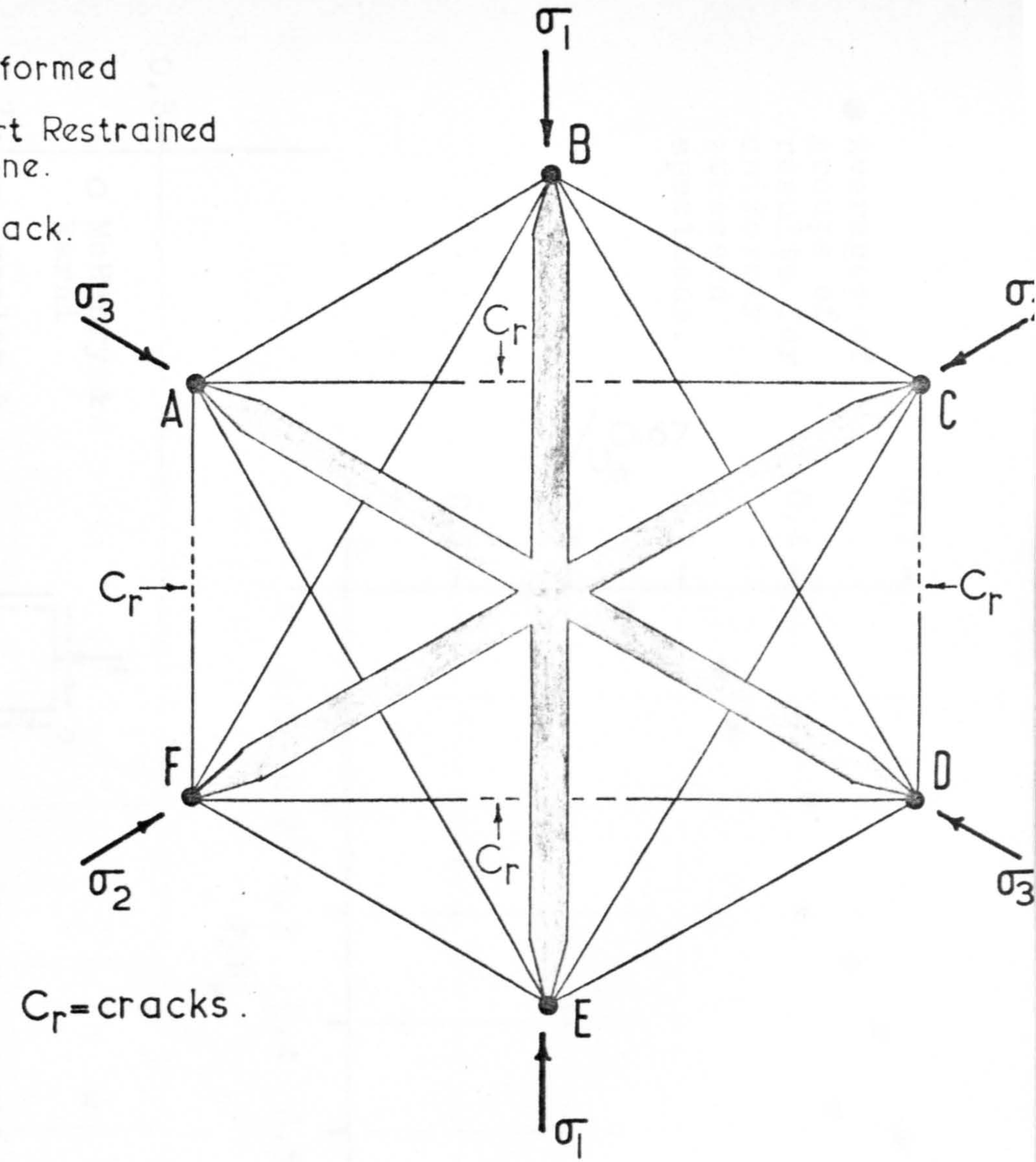

ISOMETRIC OF TETRAHEDRAL MODEL.

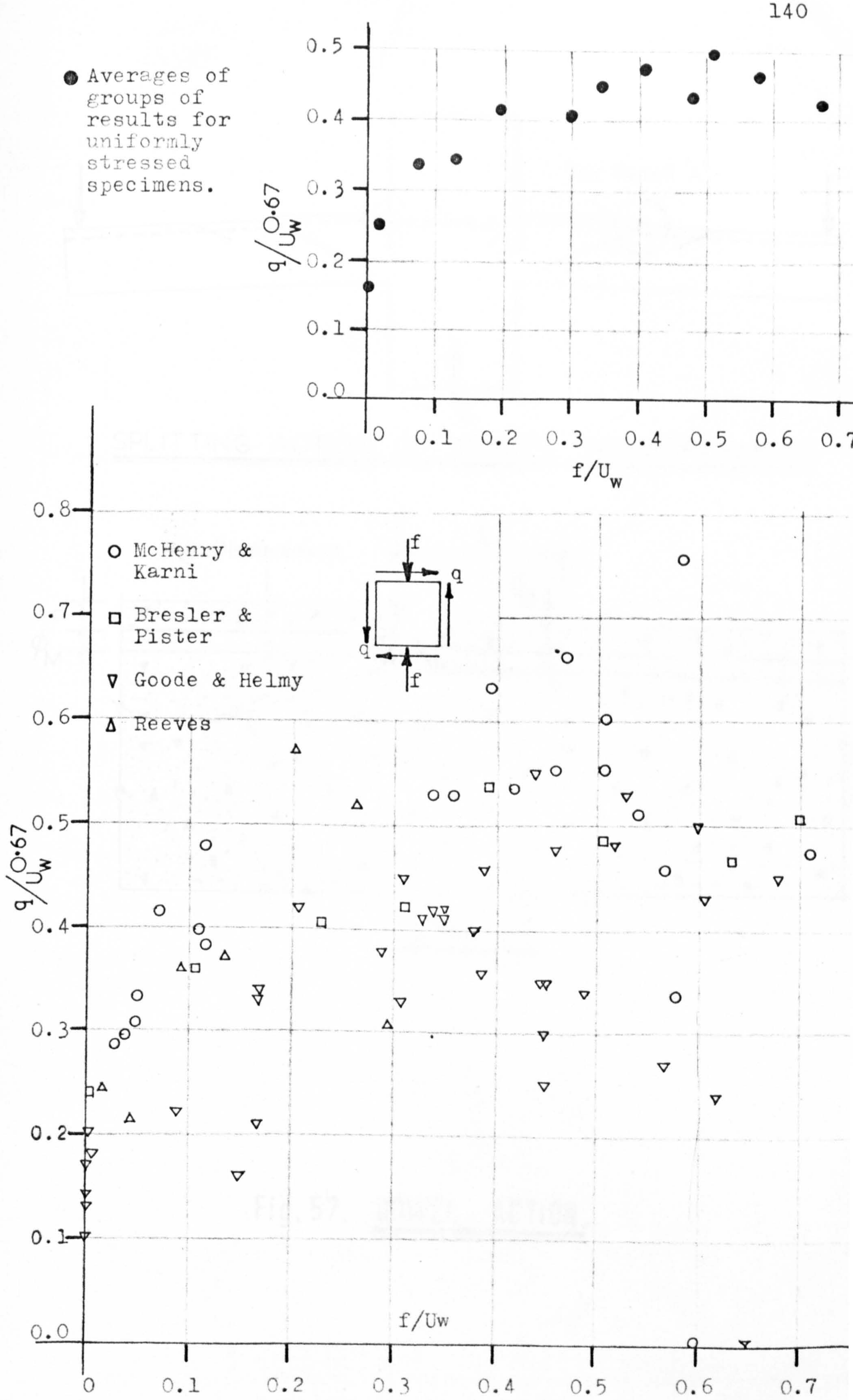

Fig.56. FAILURE CRITERIA FOR CONCRETE TEST RESULTS.

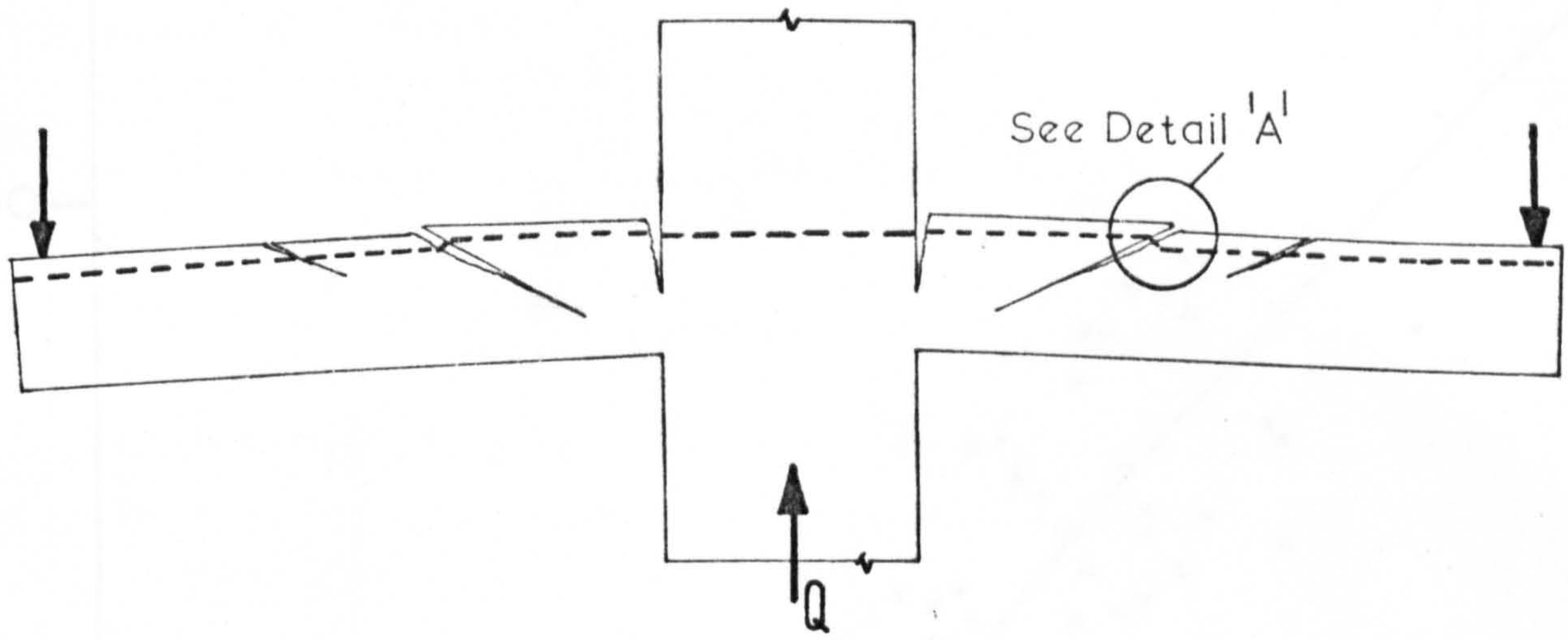

SPLITTING ACTION OF TENSILE REINFORCEMENT.

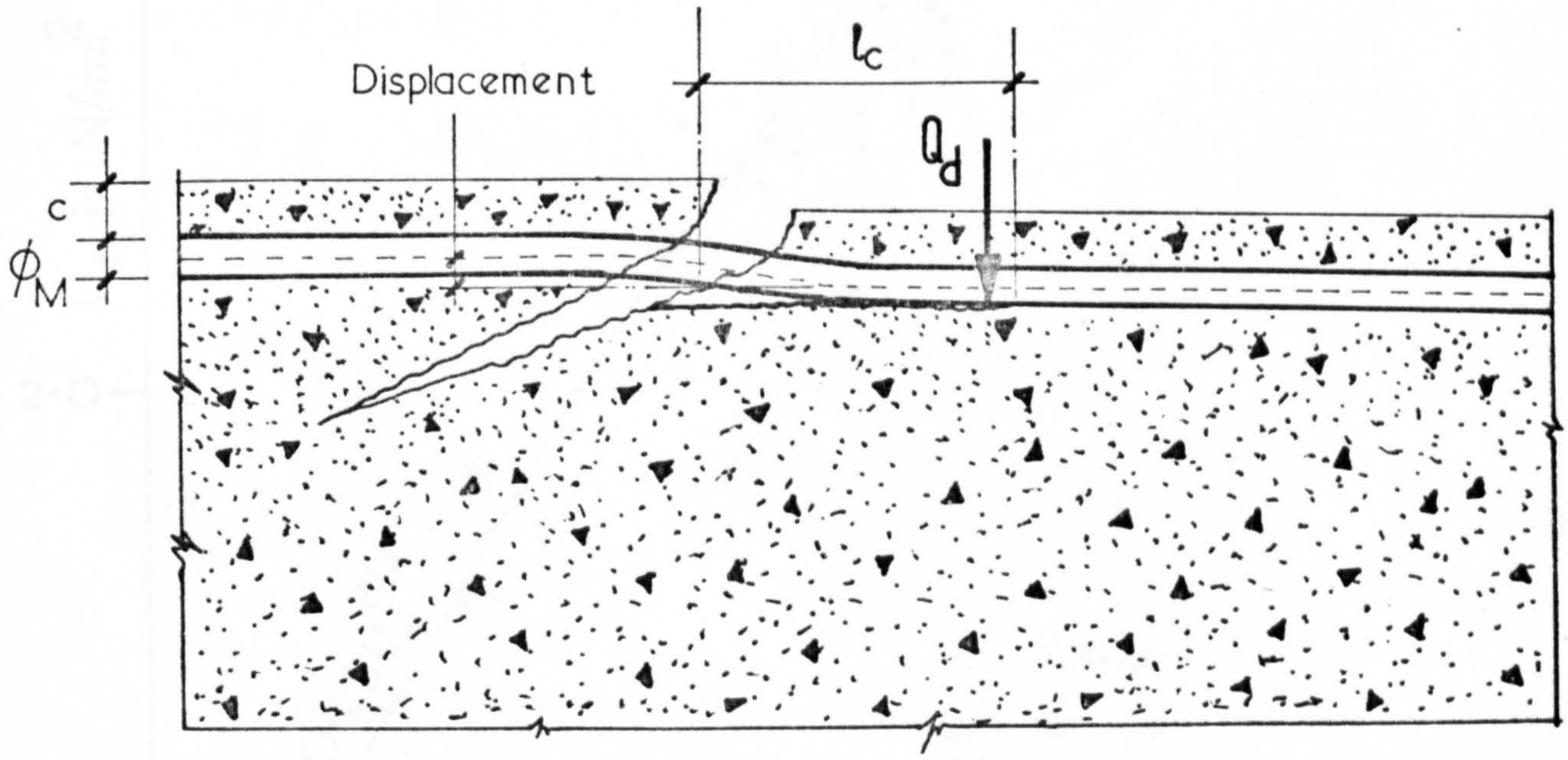

DETAIL 'A'.

Fig. 57. DOWEL ACTION.

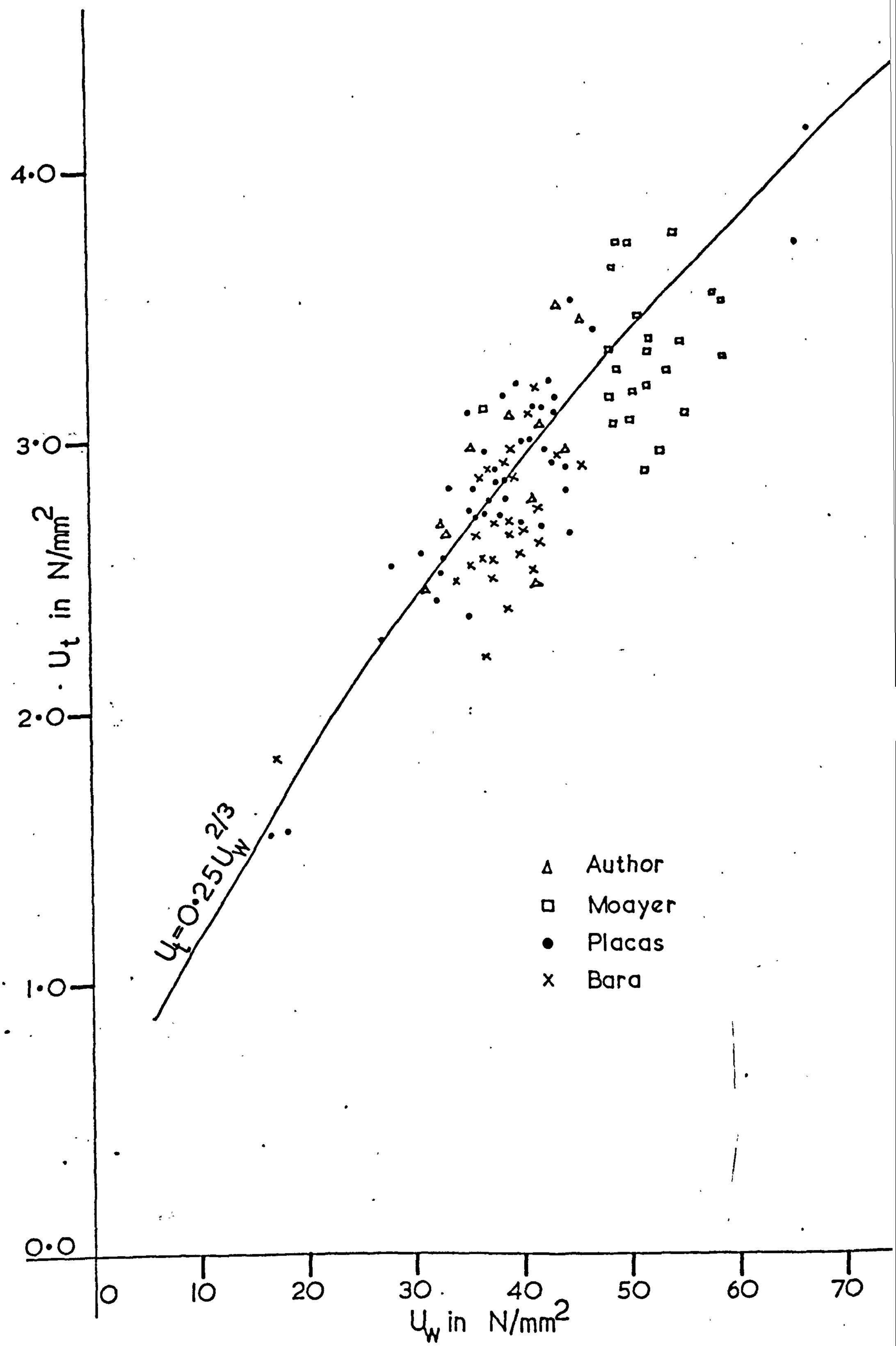

Fig. 58. RELATIONSHIP BETWEEN TENSILE SPLITTING AND COMPRESSIVE STRENGTH OF CONCRETE.

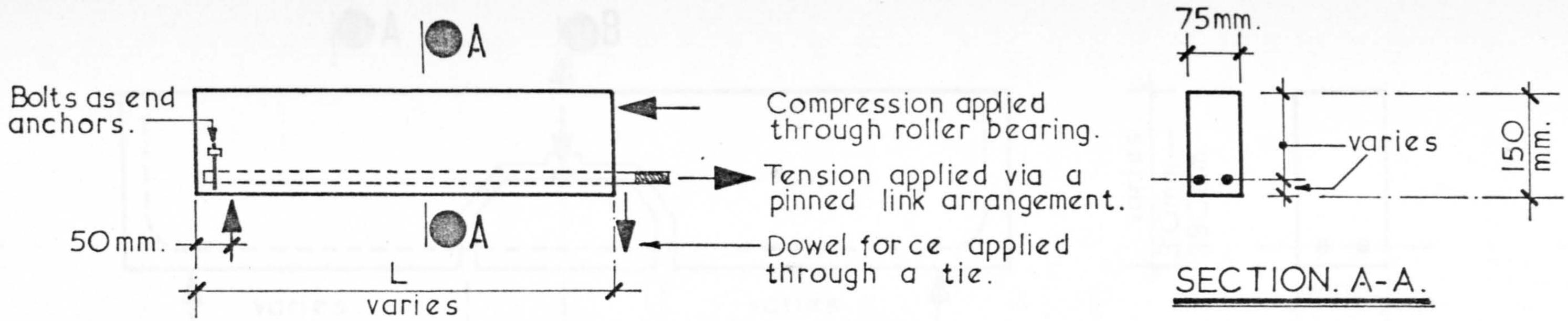

DOWEL TEST SPECIMEN — ROY.

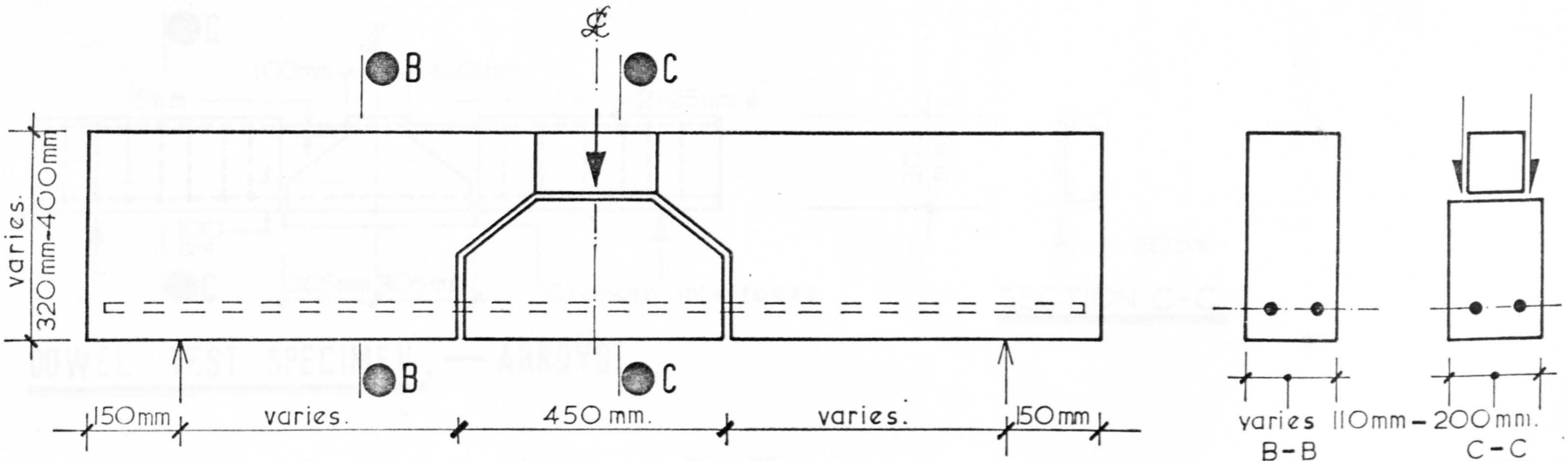

DOWEL TEST SPECIMEN — BAUMANN.

Fig. 59.

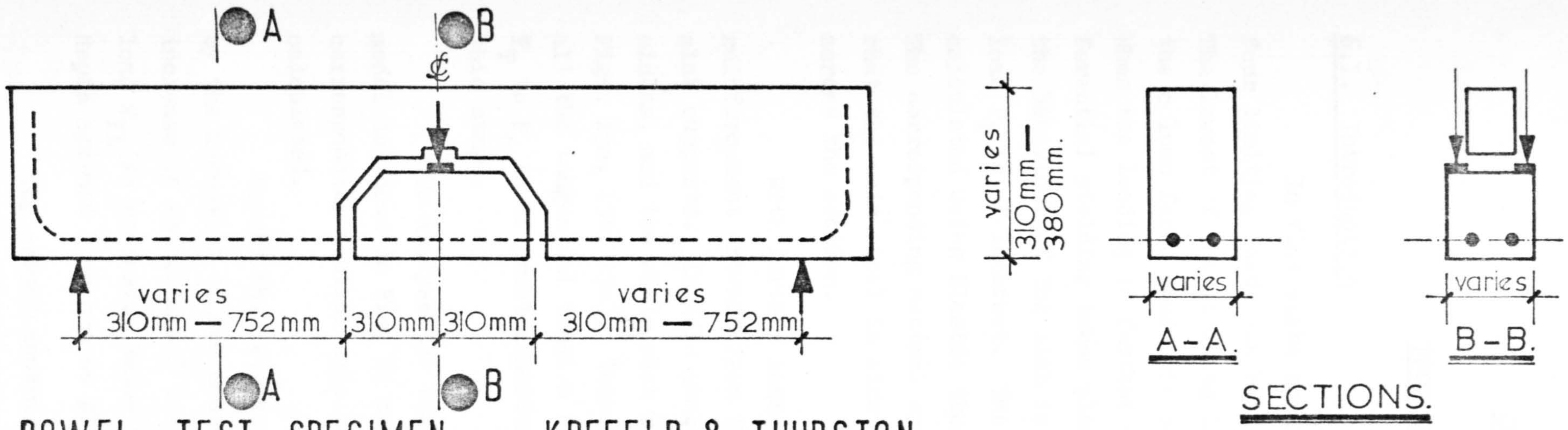

DOWEL TEST SPECIMEN. — KREFELD & THURSTON.

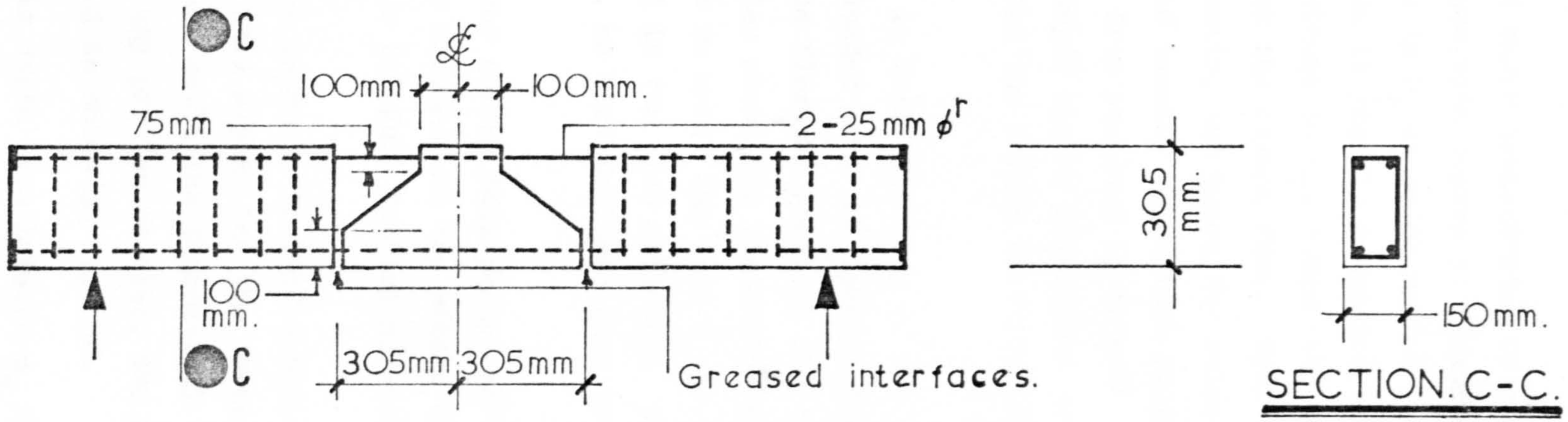

DOWEL TEST SPECIMEN. — ARROYO.

Fig. 60.

CHAPTER VI

PROPOSED SOLUTION.

6.1. Introduction.

In flat slabs analysed under concentrated or combined loads, four limiting loads can be defined with regard to flexural behaviour. The lowest of the limiting loads is P_r at which radial yield begins at the column face, where the column is rigidly connected to the slab. When the loading is further continued to P_T, tangential or circumferential yielding takes place at the column face. Upto this load the behaviour of the slab is elastic, and hence the value of this load P_T is of interest. The load causing tangential yield can be calculated using Elastic theory from standard books such as Timoshenko[51]. The corresponding neutral axis depth can be calculated on the assumption that the main steel is elastic and the strain distribution is linear across the section.

With further increase in load, yielding of the tension reinforcement extends from the loaded area and spreads towards the slab supports. In this phase the flexural crack at the column face widens, and the whole slab rotates about the flexural crack (see Figs. 15a, 15b, 15c). This goes on until the load P_o is reached with all the tangential tension steel in the slab yielding. The stage from P_T to P_o is of great importance, as most failures seem to occur in this stage.

To analyse the behaviour during this phase, an idealised model as shown in Fig. 61 can be assumed and the values of P_o and the corresponding neutral axis factor (at full tangential yield) can be calculated.

Beyond this stage, some increase in load can be obtained by the reduction of the neutral axis depth, and the corresponding increase of the internal lever arm until the theoretical 'yield line' load P_{YL} is reached. Hence for any particular slab, the neutral axis depth against load can be plotted as shown in Fig. 62.

The actual neutral axis depth lies between n_e and n_{YL} at failure. Once the actual neutral axis depth is known, then the failure load can be obtained from the n V_s P diagram or vice versa. Again the

punching resistance is provided by the dowel action of the main reinforcement and the concrete compressive zone. The dowel force and strength of the compressive zone can be determined as outlined in sections 5.3 and 5.4, chapter V.

In the following pages the loads P_T, P_o, P_{YL} and the corresponding neutral axis factors n_e, n_o, n_{YL} are determined for the simple case of a circular slab with a circular column (with special reference to two-way reinforcement). A method of predicting the failure load based on the above and on the failure criterion (see section 5.3), is outlined.

6.2 ELASTIC NEUTRAL AXIS FACTOR n_e.

The neutral axis depth is not strictly a constant for stages at which the reinforcement is elastic. However it can be assumed to be a constant, and a particular elastic value n_e can be selected. For this purpose it is convenient to take the limiting case when the stress block is fully developed, (i.e.) when the extreme fibre strain is equal to the limiting strain for concrete, which may be taken as 0.0035 according to the C.E.B. Recommendations[49] and the steel is taken as unyielding.

Using a parabolic rectangular stress-strain relationship for concrete as shown in Fig. 63 with a maximum stress of $2.35\ U_w^{2/3}$, the average stress in the compression zone is $1.9\ U_w^{2/3}$ [43].

Assuming a linear strain distribution across the section,

$$\frac{e_c}{e_s} = \frac{n_e}{1-n_e} \quad \ldots\ldots\ldots\ldots\ldots\ldots\ldots (32)$$

where e_c and e_s are the strains in the concrete and steel respectively.

Force in concrete, $F_c = f_{av} \cdot b \cdot n_e \cdot d_1$

$= 1.9\ U_w^{2/3} \cdot b \cdot n_e \cdot d_1$

Force in steel, $F_{st} = e_s \cdot E_{st} \cdot r_{st} \cdot b \cdot d_1$

where E_{st} = Young's modulas of steel.

Equating forces,

$$1.9U_w^{2/3} \cdot b \cdot n_e \cdot d_1 = e_s \cdot E_{st} \cdot r_{st} \cdot b \cdot d_1$$

$$e_s = \frac{1.9U_w^{2/3} \cdot n_e}{E_{st} \cdot r_{st}} \quad \ldots\ldots\ldots\ldots\ldots\ldots (33)$$

assuming $E_{st} = 200 \times 10^3$ N/mm^2 and substituting the values of e_s and e_c in equation (32)

$$\frac{n_e^2}{1-n_e} = \frac{700}{1.9} \; r_{st}/U_w^{2/3} \quad \ldots\ldots\ldots\ldots\ldots\ldots (34)$$

$n_e^2/1-n_e$ can be approximated to $2.85\, n_e^{2.5}$ (see Fig.64). Equation (34) can then be written as,

$$2.85\, n_e^{2.5} = \frac{700}{1.9} \; r_{st}/U_w^{2/3}$$

$$\text{or} \quad n_e = \frac{1.1(r_{st})^{0.4}}{U_w^{0.27}} \quad \ldots\ldots\ldots\ldots\ldots\ldots (35)$$

Values of n_e for various values of U_w and r_{st} are given in table VI-1.

6.3. CALCULATION OF THE LOAD P_T.

This is the load at which the tangential steel yields adjacent to the column face. There is a definite increase in load, between the stage at which the radial steel yields around the column face, and the stage at which the tangential yield occurs. Hence the first step is to calculate the load corresponding to radial yielding. If m_r and m_t are the moments per unit width of slab in the radial and tangential directions respectively, they can be expressed in terms of deflection w[51] as:

$$m_r = -D\,(d^2w/dr^2 + v/r \cdot dw/dr) \quad \ldots\ldots\ldots\ldots (36)$$

TABLE VI-1

U_w N/mm^2	15.0	22.5	30.0	37.5	45.0	52.5	60.0	67.5
r_{st} %	ELASTIC NEUTRAL AXIS DEPTH FACTOR n_e							
0.15	0.224	0.200	0.185	0.174	0.166	0.158	0.153	0.148
0.25	0.304	0.273	0.252	0.237	0.226	0.217	0.209	0.203
0.50	0.401	0.360	0.333	0.313	0.298	0.286	0.276	0.267
0.75	0.472	0.423	0.391	0.368	0.351	0.336	0.325	0.314
1.00	0.529	0.475	0.439	0.413	0.394	0.378	0.364	0.353
1.25	0.579	0.519	0.480	0.452	0.430	0.413	0.398	0.386
1.50	0.623	0.558	0.516	0.486	0.463	0.444	0.428	0.415
1.75	0.662	0.594	0.549	0.517	0.492	0.472	0.456	0.441
2.00	0.699	0.626	0.579	0.546	0.519	0.498	0.481	0.465
2.25	0.732	0.656	0.607	0.572	0.544	0.522	0.504	0.488
2.50	0.764	0.685	0.633	0.596	0.568	0.545	0.525	0.509

and

$$n_t = -D\left(\frac{1}{r}\frac{dw}{dr} + v \cdot \frac{d^2w}{dr^2}\right) \quad \ldots\ldots\ldots (37)$$

where D is the flexural rigidity of the slab and r the radius under consideration.

The deflection of the slab (built in along the inner edge and uniformly loaded along the outer edge) is due to a combination of systems (1) and (2) as shown in Fig. 65 up to radial yield. Beyond this stage any further increase in load is purely due to system (2).

$$w \text{ for systems (1) + (2)} = \frac{b^2 m_1 (a^2 - r^2)}{2(1+v)(a^2 - b^2)D} + \frac{a^2 b^2 m_1}{(1-v)(a^2 - b^2)} \log r/a + \frac{P.r^2}{8.\pi.D}(\text{Log } r/a - 1) - \frac{C_1.r^2}{4} - C_2 \text{ Log } r/a + C_3 \quad \ldots\ldots\ldots (38)$$

$$w \text{ for system (2)} = \frac{P.r^2}{8.\pi.D}(\text{Log } r/a - 1) - \frac{C_1 r^2}{4} - C_2 \text{Log } r/a + C_3 \quad \ldots\ldots\ldots (39)$$

where $m_1 = \dfrac{P}{4.\pi(1+v)a^2/b^2 + (1-v)} \; (1-v).\left(\dfrac{a^2}{b^2} - 1\right) + 2(1+v)\dfrac{a^2}{b^2} \text{ Log } a/b$

$$C_1 = \frac{-2b^2.m_1}{(1+v)\,D\,(a^2 - b^2)}$$

$$C_2 = \frac{-a^2.\,b^2.\,m_1}{(1-v)(a^2 - b^2).D}$$

$$C_3 = \frac{a^2 b^2 .m_1}{2(1+v)(a^2 - b^2)D}$$

and $a/b = B/L$

From the above it can be seen that the derivatives of the deflection are functions of B/L and P. Values of m_r and m_t calculated for various values of B/L in terms of P are tabulated in Table VI - 2. Only values of B/L between 0.1 and 0.2 are considered as these are the limits normally used in practice.

A typical calculation for obtaining P_T from m_r, m_{t1} upto radial yield, and m_{t2} upto tangential yield is indicated below for $B/L = 0.1$. Using equations (36) and (37)

Corresponding to radial yield,

$$m_r = 0.4247\ P = m_y \text{ and} \quad \ldots\ldots\ldots\ldots\ldots \quad (40a)$$

$$m_{t1} = 0.0601\ P \quad \ldots\ldots\ldots\ldots\ldots\ldots\ldots \quad (40b)$$

If (dP) is the further increase upto tangential yield then

$$m_{t2} = 0.4934\ (dP) \quad \ldots\ldots\ldots\ldots\ldots\ldots\ldots \quad (41)$$

From equations (40a) and (40b),

$$\frac{m_{t1}}{0.0601} = \frac{m_y}{0.4247}$$

$$\text{(i.e.)}\ m_{t1} = \frac{0.0601}{0.4247}\ \cancel{P}\ m_Y$$

$$\text{and} \quad P = m_y/0.4247 = 2.36\ m_y \quad \ldots\ldots\ldots\ldots \quad (42)$$

$$\text{Since} \quad m_{t2} = m_y - m_{t1} \quad \text{(seeFig. 66)}$$

$$= m_y - \frac{0.0601}{0.4247}\ m_y$$

$$= 0.86\ m_y \quad \ldots\ldots\ldots\ldots\ldots\ldots\ldots\ldots \quad (43)$$

TABLE VI-2

B/L	n_r in terms of P	m_{t1} in terms of P	m_{t2} in terms of (dP)	P_T in terms of n_y
0.10	0.425	0.060	0.493	4.095
0.11	0.409	0.057	0.477	4.248
0.12	0.395	0.055	0.461	4.398
0.13	0.382	0.052	0.448	4.546
0.14	0.370	0.050	0.435	4.693
0.15	0.359	0.047	0.423	4.838
0.16	0.349	0.045	0.412	4.983
0.17	0.339	0.043	0.402	5.128
0.18	0.329	0.041	0.392	5.273
0.19	0.320	0.039	0.383	5.417
0.20	0.312	0.036	0.374	5.563

Equating equations (41) and (43)

$$0.4934\ (dP) = 0.86\ m_y$$

$$\text{or} \quad (dP) = 1.74\ m_y \quad \ldots\ldots\ldots\ldots\ldots\ldots\ldots (44)$$

Total load P_T at tangential yield $= P + dP$

$$= 2.36\ m_y + 1.74\ m_y$$

$$= 4.1\ m_y$$

m_y is known in terms of r_{st}, f_y, d_1 and n_e

$$\text{(i.e.)} \quad m_y = r_{st} \cdot f_y \cdot d_1^2 \cdot (1 - 0.42\ n_e)$$

$$P_T = 4.1\ m_y$$

$$= 4.1\ r_{st} \cdot f_y \cdot d_1^2 \cdot (1 - 0.42\ n_e) \ldots\ldots (45)$$

or in general

$$P_T = k_T \cdot j_T \cdot r_{st} \cdot f_y \cdot d_1^2 \ldots\ldots\ldots\ldots\ldots (46)$$

where k_T = constant depending on B/L ratio,

and j_T = lever arm factor corresponding to n_e.

The method outlined so far is mainly applicable to circular slabs. For square slabs in the absence of an exact solution, it is proposed to use the coefficients $(1/k_T)$ given by Table 20[51], with values modified for Poissons ratio of $\nu = 0.15$ instead of 0.3. The values can be modified using:

$$m_x' = \frac{1}{(1-v^2)} (1-vv_1)\, n_x + (v_1-v).m_y \quad \text{where}$$

$$n_x = n_y \text{ for a square slab.}$$

$$v = 0.30, \; v_1 = 0.15$$

The above gives a multiplication factor of 0.885. Hence the values given in Table 20[51] must be multiplied by 0.885 and then their reciprocals give the required values of k_T. (See Table VI-3 for values of k_T).

6.4. CALCULATION OF P_o AND THE CORRESPONDING NEUTRAL AXIS FACTOR 'n_o'

6.4.1. Introduction:

For the purpose of assessing the various forces acting on the slab, when the slab is in an elasto-plastic state, an idealised model as shown in Fig. 61 is assumed.

During the tests, it was observed (see chapter IV) that the first wide crack to appear was the flexural crack adjacent to the column face, and the whole slab seemed to rotate about this crack. This can be seen from the typical deflection diagrams shown in Figs. 15a, 15b and 15c.

The expressions for the various forces produced by the rotation of the slab are deduced as shown subsequently. From the conditions of compatability and equilibrium the load P_o and the corresponding neutral axis factor for the condition all the tangential steel yielding are obtained. It is assumed that the neutral axis depth varies linearly from n_e (elastic) to n_o. The same is justified in section 6.4.6.

6.4.2. Forces in the Flexural Steel:

The two-way reinforcement in the slab is assumed to be isotropic (i.e.) to have the same properties in all directions and is subjected to a force per unit length corresponding to that in the actual reinforcement, in calculating the forces in the steel.

TABLE VI-3

VALUES OF K_T FOR SQUARE SLABS

$\frac{b_y}{L}$ \ $\frac{b_x}{L}$	0	0.1	0.2	0.3	0.4
0	00	3.60	4.51	5.40	6.30
0.1	3.00	3.98	4.88	5.70	6.66
0.2	3.68	4.45	5.30	6.15	7.00
0.3	4.30	5.01	5.80	6.73	7.50
0.4	4.88	5.56	6.30	7.15	8.02

Note: b_x and b_y are the side lengths of a rectangular column.

The tensile strain in the tangential direction can be written as:

$$e_{st} = \frac{\psi.(1-n).d_1}{r} \quad \ldots\ldots\ldots\ldots\ldots\ldots\ldots (47)$$

where ψ is the rotation at the column face

and r is the radius, measured from the centre of the column (used in place of the distance from column face to simplify the expression and to avoid infinite strains at the column face).

Then r_s, the radius upto which the steel yields can be written as,

$$r_s = \frac{\psi \times (1-n)\, d_1}{e_s} \quad \ldots\ldots\ldots\ldots\ldots\ldots\ldots (48)$$

where e_s is the 0.2% proof strain.

The projection in the radial direction of the forces in the steel over a sector element subtending an angle $\Delta\phi$ at centre is,

$$T \text{ sector} = \int_0^{r_s} r_{st}.d_1.dr.\Delta\phi.f_y + \int_{r_s}^{L/2} r_{st}.d_1.dr\Delta\phi.f_y.r_s/r$$

$$= r_{st}.d_1.f_y.\Delta\phi.\left[\int_0^{r_s} dr + \int_{r_s}^{L/2} \frac{dr.r_s}{r}\right]$$

$$= r_{st}.d_1 f_y.\Delta\phi \quad (r_s + r_s \operatorname{Log}_e \frac{L}{2r_s})$$

$$= r_{st}.f_y.d_1.\Delta\phi.\frac{r_s}{L}.\ L\ (1 + \operatorname{Log}_e \frac{L}{2r_s})$$

when all the tangential steel has yielded,

$$r_s/L = 0.5$$

$$\therefore \quad T \text{ sector} = 0.5 \cdot r_{st} \cdot f_y \cdot d_1 \cdot L \cdot \Delta\phi \quad \ldots\ldots (49)$$

or

$$\frac{T \text{ sector}}{d_1 L . \Delta\phi \sigma_{CT}} = 0.50 \cdot \frac{r_{st} . f_y}{\sigma_{CT}} \quad \ldots\ldots\ldots\ldots (50)$$

6.4.3. Tangential Forces C_T in concrete.

For the purpose of calculating the forces in the concrete the stress strain relationship is simplified to that shown in Fig.67.

$$\text{Now} \quad \sigma = \frac{\sigma_{CT}}{e_{pl}} \cdot e_c \quad \ldots\ldots\ldots\ldots (51)$$

where e_{pl} is the concrete strain at which state of plastification is reached.

Again the concrete compressive strain in the tangential direction is inversely proportional to the distance from centre line of column (see section 4.5.1) and proportional to rotation. Hence,

$$e_c = \psi \cdot \frac{nd_1}{r} \quad \ldots\ldots\ldots\ldots (52)$$

Substituting the value of ψ from equation (48) the radius C_{pl} upto which concrete is in a plastic state will be,

$$C_{pl} = \frac{r_s . e_s}{(1-n) . d_1} \cdot \frac{nd_1}{e_{pl}}$$

$$= r_s \cdot \frac{n}{(1-n)} \cdot \frac{f_y}{E_{st} . e_{pl}}$$

$$\text{or} \quad C_{pl} = \frac{n}{1-n} \cdot r_s \cdot a \quad \ldots\ldots\ldots\ldots (53)$$

$$\text{putting} \quad \frac{f_y}{E_{st} . e_{pl}} = a$$

The projection of the summed compressive forces in a radial direction will be,

$$C_{T\ sector} = \frac{\sigma_{CT}}{e_{pl}} \cdot \frac{nd_1}{2} \cdot \left[\int_{B/2}^{L/2} e_c . dr - \int_{B/2}^{C_{pl}} (e_c - e_{pl})(1 - \frac{e_{pl}}{e_c}) dr \right] \Delta \phi$$

Substituting the value e_c from equation (52) and integrating,

$$C_{T\ sector} = \sigma_{CT} \cdot \frac{nd_1}{2} \cdot C_{pl} (\mathrm{Log}_e \frac{L}{2C_{pl}} + 1.5 + \frac{1}{8} \cdot \frac{B^2}{C_{pl}^{\ 2}} - \frac{B}{C_{pl}}) \Delta \phi \quad \ldots\ldots\ldots\ldots\ldots (54)$$

Substituting the value of C_{pl} from equation (53), in equation (54)

$$C_{T\ sector} = \sigma_{CT} \cdot \frac{nd_1}{2} \cdot \frac{n}{(1-n)} \cdot r_s \cdot a \cdot \Delta \phi \cdot C_4 \ldots\ldots (55)$$

$$\text{where } C_4 = \mathrm{Log}_e \frac{L(1-n)}{2n.r_s.a} + 1.5 + \frac{1}{8} \cdot \frac{B^2(1-n)^2}{n^2.r_s^{\ 2}.a^2} - \frac{B(1-n)}{n.r_s.a}$$

$$= \mathrm{Log}_e \frac{(1-n)}{2.n.a.r_{s/L}} + 1.5 + \frac{1}{8a^2} \cdot \frac{B^2}{L^2} \cdot \frac{(1-n)^2}{n^2} \cdot \frac{1}{r_{s/L}^{\ 2}} - \frac{1}{a} \cdot$$

$$\frac{B}{L} \cdot \frac{1-n}{n} \cdot \frac{1}{r_{s/L}}$$

For $r_{s/L} = 0.5$, $a = f_y / E_{st} . e_{pl} = 1$ and $n = n_o$,

$$C_4 = \text{Log}_e \frac{(1-n_o)}{n_o} + 1.5 + \frac{1}{2}.\frac{B^2}{L^2}.\frac{(1-n_o)^2}{n_o^{\,2}} - 2.\frac{B}{L} \cdot \frac{(1-n_o)}{n_o}$$

and $C_{T\ sector} = 0.25 \cdot \sigma_{CT} \cdot \frac{n_o^{\,2}}{1-n_o} \cdot d_1 \cdot L \cdot C_4 \cdot \Delta\phi$ . . . . . (55a)

or $\frac{C_{T\ sector}}{\sigma_{CT}.L.d_1.\Delta\phi} = 0.25 \cdot n_o^{\,2} \cdot C_4 /_{(1-n_o)}$ . . . . . (55b)

6.4.4. Radial Forces C_R in Concrete.

$C_{R\ sector}$ = Perimeter of the sector at column face . $nd_1.k.\sigma_{CT}$

for fully developed stress block $k = 0.714$

Perimeter at column face $= \frac{B}{2} \cdot \Delta\phi$

For $r_{s/L} = 0.5$, $n = n_o$

$$C_{R\ sector} = \frac{B}{2} \cdot \Delta\phi \cdot n_o d_1 \cdot (0.714 \cdot \sigma_{CT})$$

$$= 0.357 \cdot n_o d_1 \cdot B \cdot \sigma_{CT} \cdot \Delta\phi \quad . . . . . (56)$$

or $\frac{C_{R\ sector}}{L.\sigma_{CT}.d_1.\Delta\phi} = 0.357\, n_o \cdot \frac{B}{L}$ . . . . . (57)

6.4.5. Conditions of Equilibrium.

For horizontal equilibrium,

Forces in concrete = Forces in steel

$C_R + C_T = T$

$$\text{or} \quad \left(\frac{0.25\, n_o^2}{1-n_o} \cdot C_4 + 0.357 \cdot n_o \cdot \frac{B}{L}\right) . L . d_1 . \sigma_{CT} . \Delta\phi = 0.50 \frac{r_{st} f_y}{\sigma_{CT}} . d_1 . L . \sigma_{CT} . \Delta\phi$$

$$\text{(i.e.)} \quad \left(0.50 \frac{n_o^2}{1-n_o} \cdot C_4 + 0.714\, n_o \cdot \frac{B}{L}\right) = \frac{r_{st} . f_y}{2.66 U_w^{2/3}} \quad \ldots\ldots\ldots (58)$$

Fig. 68 shows n_o against L.H.S. of equation (58) for various values of B/L. Hence for any slab, with a particular B/L and knowing $r_{st} . f_y / U_w^{2/3}$ the value of n_o can be obtained. However from the graph, taking $B/L = 0.1$ as a standard one could write the expression for 'n_o' as

$$n_o = \frac{0.45}{U_w^{1/3}} \cdot \sqrt{r_{st} . f_y} \quad \ldots\ldots\ldots\ldots\ldots\ldots (59)$$

Table VI.4 gives n_o values for various values of $r_{st} . f_y$ and U_w. For moment equilibrium,

$$\frac{P_o}{2\pi} . \Delta\phi . \left(\frac{L}{2} - \frac{B}{2}\right) = T(d_1 - 0.42\, n_o d_1) \Delta\phi$$

$$P_o = 2\pi \cdot r_{st} \cdot f_y \cdot d_1^2 . \frac{(1-0.42 n_o)}{(1 - B/L)} \quad \ldots\ldots (60)$$

6.4.6. Variation of Neutral Axis Depth from n_e to n_o.

The above values of P_o and n_o are based on the assumption that all the tangential steel is yielding. In order to check the error involved in assuming that the neutral axis factor varies linearly from n_e to n_o, values of n_o against $\frac{C_R + C_T}{\sigma_{CT} . L . d_1 . \Delta\phi}$ ($= 0.50\, r_{st} . f_y / \sigma_{CT}$ for $C_R + C_T = T$) for various values of r_s/L are plotted as shown in Fig. 69. If we choose two slabs such that $\frac{r_{st} . f_y}{\sigma_{CT}} = 0.125$ and 0.2, n_o against r_s/L can be plotted from Fig. 69, as shown in Fig. 69a.

TABLE VI-4.

U_w in N/mm^2	15.0	22.5	30.0	37.5	45.0	52.5	60.0	67.5
$r_{st} \cdot f_y$	NEUTRAL AXIS DEPTH FACTOR AT OVERALL TANGENTIAL YIELD n_o							
1	0.184	0.161	0.146	0.136	0.128	0.122	0.116	0.112
2	0.26	0.228	0.207	0.192	0.181	0.172	0.165	0.158
3	0.319	0.279	0.254	0.236	0.222	0.211	0.202	0.194
4	0.368	0.322	0.293	0.272	0.256	0.244	0.233	0.224
5	0.412	0.36	0.327	0.304	0.286	0.272	0.261	0.251
6	0.451	0.394	0.359	0.333	0.314	0.298	0.285	0.274
7	0.487	0.426	0.387	0.360	0.339	0.322	0.308	0.296
8	0.521	0.456	0.414	0.385	0.362	0.344	0.33	0.317
9	0.552	0.483	0.439	0.408	0.384	0.365	0.349	0.336
10	0.582	0.509	0.463	0.430	0.405	0.385	0.368	0.354
11	0.611	0.534	0.486	0.451	0.425	0.404	0.386	0.372
12	0.638	0.558	0.507	0.471	0.444	0.422	0.404	0.388
13	0.664	0.581	0.528	0.491	0.462	0.439	0.420	0.404
14	0.689	0.603	0.548	0.509	0.479	0.456	0.436	0.419

From the figure it can be seen that the error in assuming a linear variation in neutral axis depth from elastic state to all tangential steel yielding is not significant and hence the simplification is justified.

6.5 CALCULATION OF LOAD P_{YL} AND NEUTRAL AXIS FACTOR n_{YL}

The value of P_{YL} can be calculated from the standard equation $P = k_{YL} \cdot n$, where $k_{Y.L}$ depends on the configuration and loading of the slab in question.

$$n = r_{st} \cdot f_y \cdot d_1^2 \left(1-0.219\, r_{st}\, f_y/U_w^{2/3}\right) \text{ for the}$$

assumed stress strain diagram as shown in Fig. 63.

$$\therefore\ P_{YL} = \frac{k_{YL}}{(1-B/L)} \cdot r_{st} \cdot f_y \cdot d_1^2 \left(1-0.219\, r_{st} f_y/U_w^{2/3}\right) \quad \ldots\ldots (61)$$

$$\text{and } n_{YL} = \frac{C \text{ or } T}{1.9\, U_w^{2/3} \cdot d_1} = \frac{r_{st} \cdot f_y \cdot d_1}{1.9\, U_w^{2/3} d_1} = \frac{r_{st} \cdot f_y}{1.9 U_w^{2/3}} \quad \ldots\ldots (62)$$

Values of n_{YL} for various values of U_w and $r_{st} \cdot f_y$ are tabulated in Table VI-5.

Having obtained the various values of n_e, P_T, n_o, P_o, n_{YL} and P_{YL} the next step is to plot n against P.

6.6 CALCULATION OF THE FAILURE LOAD.

Since Failure load $Q = Q_c + Q_d$

$$Q_d = K_d \cdot b_d \cdot \phi_M \cdot U_w^{1/3} \quad \text{(see chapter V)}$$

(shear force carried by dowel)

$$Q_c = b_c \cdot n \cdot d_1 \cdot q_c$$

(shear carried by concrete compression zone)

TABLE VI-5

U_w N/mm^2	15.0	22.5	30.0	37.5	45.0	52.5	60.0	67.5
$r_{st}.f_y$	NEUTRAL AXIS DEPTH FACTOR - YIELD LINE $n_{Y.L.}$							
1	0.086	0.065	0.054	0.046	0.041	0.037	0.034	0.031
2	0.171	0.131	0.108	0.093	0.082	0.074	0.068	0.063
3	0.257	0.196	0.162	0.139	0.123	0.111	0.102	0.094
4	0.343	0.261	0.216	0.186	0.164	0.148	0.135	0.125
5	0.429	0.327	0.269	0.232	0.205	0.185	0.169	0.156
6	0.514	0.392	0.323	0.278	0.246	0.222	0.203	0.188
7	0.600	0.457	0.377	0.325	0.287	0.259	0.237	0.219
8	0.686	0.523	0.431	0.371	0.329	0.296	0.271	0.250
9	0.771	0.588	0.485	0.418	0.370	0.330	0.305	0.282
10	-	0.6536	0.539	0.464	0.411	0.370	0.339	0.313
11	-	0.719	0.593	0.510	0.452	0.407	0.373	0.344
12	-	0.784	0.647	0.557	0.493	0.445	0.406	0.375
13	-	-	0.707	0.603	0.534	0.482	0.44	0.407
14	-	-	0.755	0.65	0.575	0.519	0.474	0.438

From section 5.3 chapter V,

$$q_c = 0.3\ U_w^{2/3}$$

$$\therefore \quad Q = Q_d + (b_c \cdot d_1 \cdot 0.3 U_w^{2/3}) \cdot n$$

$$\text{or } Q = Q_d + K.n \quad \ldots\ldots\ldots\ldots\ldots\ldots\ldots \quad (63)$$

where K = constant = $(b_c \cdot d_1 \cdot q_c)$

Q lies between P_T and P_{YL}.

The intersection of the line $Q = Q_d + Kn$ and the curve $P\ V_s\ n$ gives the required values of n and Q. (See Fig. 70)

6.7 COMBINED LOAD.

So far we have been concerned only with junctions subjected to concentric loads. This is not always the case. A certain amount of eccentricity can be introduced into the junction by lateral forces, wind, uneven distributions of live load or uneven spacing of columns. The slab junction is then subjected to a vertical load and a moment, and consequently an uneven shear distribution.

The distribution of the stresses around the column is very complex, and certain simplifying assumptions have to be made in order to estimate the load carrying capacity of a connection subjected to combined loads. It is assumed that at the approximately circular perimeter of contraflexure there exist neither flexural nor torsional moments. The resultant moment about the column (or centroid of perimeter of contraflexure) may thus be assumed to cause a shear stress distribution governed by the classic $(Q/A \pm \frac{M_y}{I})$ expression from which the ratio between the maximum shear and the average can be calculated.

$$A = \frac{22}{7} \cdot L \cdot 1$$

$$I \quad \frac{22}{7} \cdot (\frac{L}{2})^3 \cdot 1$$

$$z = I/y = \frac{\frac{22}{7} \cdot L^3}{8 \cdot L/2} = 22L^2/28$$

$$M = Q \cdot EC$$

$$\therefore \quad V_{max} = \frac{Q}{A} + \frac{Q.EC}{Z}$$

$$= \frac{Q}{A} \left(1 + {}^{4.EC}/_{L}\right)$$

$$\frac{V_{max}}{V_{avg}} = \left(1 + {}^{4.EC}/_{L}\right) \quad \ldots\ldots\ldots\ldots\ldots\ldots (64)$$

where the symbols are those defined under notations and the distance from the column to the line of contraflexure is taken as approximately $0.2L$ [44].

At perimeters closer to the column the moment is progressively taken over by flexural and torsional moments, but the "maximum/average" shear ratio remains constant, so long as no shear is transferred across radial sections.

For large eccentricities, the $\left({}^{Q}/_{A} \pm {}^{M.y}/_{I}\right)$ expression gives negative boundary reactions on part of the perimeter. It is only applicable there, so long as the boundary is held down as is the case in real slabs and was the case in tests done by the author. If the slab is free to lift at the perimeter, this can be dealt with in the context of this approach, if a no tension formula replaces, $\left(\frac{Q}{A} \pm \frac{M_y}{I}\right)$.

Hence based on the above the reduced strength of the connection due to a combined load will be,

$$Q_u = Q_{concentric} \cdot \frac{1}{\left(1 + 4.0\,\frac{EC}{L}\right)} \quad \ldots\ldots\ldots\ldots (65)$$

provided the corners of the slab are not free to lift. $Q_{concentric}$ is obtained from equation (63)

6.8 SHEAR REINFORCEMENT.

Having obtained a method of calculating the load which could be carried concentrically or with a particular eccentricity EC,

the next step is to examine whether or not the slab's capacity is lower than the flexural value. It very often is, unless the slab is very lightly reinforced in flexure. There is then scope for increasing its carrying capacity by means of shear reinforcement.

The required area should be equal to (Flexural capacity - Punching load, without shear reinforcement) ÷ Yield stress of shear reinforcement. This amount is to be provided all round the perimeter of the column. The effect of the combined load or eccentricity is to heavily load part of the column perimeter, but in the absence of certain knowledge of the exact distribution of the load, it is safer to provide the required reinforcement all round.

The simplest way to include the contribution due to shear reinforcement is to treat the reinforcement as fully effective (i.e.) all the reinforcement yielding with $Q_v = A_{sq}.f_{yq}.\text{Sin}\ \theta$. The term Q_v, added to the concrete term Q_c, at the column face + the dowel term Q_d ($2d_1$ out) at the dowel perimeter, gives the total load.

The above is true only as long as the shear failure plane cuts the shear reinforcement (i.e.) the section is not over re-inforced in shear. Once the section is over-reinforced in shear, the failure plane falls outside the shear reinforcement, and the critical perimeters as far as the concrete term and the dowel term are concerned, are increased. The contributing perimeters are at the head and tail of the failure plane (i.e.) for design purposes $d_{1/2}$ inwards from the anchorage of the shear reinforcement in the compressive zone and $2d_1$ out from there. Means of obtaining further increase of load by the provision of subsequent layers has already been discussed in chapter V.

The effectiveness of the shear reinforcement depends to a large extent on the anchorage which can be achieved. Anchorage can be developed by transferring the force from the shear bar to other reinforcement, e.g., by passing stirrups round longitudinal re-inforcement. The other way to develop anchorage is by transferring the force from the shear bar to the concrete by bond. Anchorage by bond is confined to the compression zone. In the case of thin slabs the depth of compression zone is small and hence anchorage cannot be achieved by the latter method. However, there is no reason why the anchorage cannot be achieved by wrapping the shear reinforcement

around the longitudinal steel. This method of obtaining the anchorage worked quite successfully in the slabs tested by the author where the slab thickness was 178 mm.

A further assumption that only that reinforcement which crosses the 1:2 surface (shear failure plane) in its central half is effective, guards against the inefficiency of reinforcement crossing the plane in the compressive zone at one end, and the possibility of a rather dubious anchorage to bent bars crossing the plane too near the level of the main steel. Since some reliance must be placed on bond in addition to practical end anchorages, it may be necessary to limit the bar diameter (ϕ_v) based on the depth of the slab. The following seemed to have worked satisfactorily in the various tests.

for vertical bars $\phi_v \leq d/30$

for inclined bars $\phi_v \leq d/20.$

where d is the total depth of the slab.

The increased diameter for inclined bars is justified by the greater bond length available between the crack and the anchorage.

6.9 ANALYSIS OF EXISTING RESULTS.

To verify the proposed solution the existing data was analysed. Knowing the values of r_{st}, f_y and U_w, the various values of neutral axis factors are calculated using,

Equation 35 where $n_e = 1.1\, r_{st}^{0.4} / U_w^{0.27} = n_1$ (say)

Equation 59 where $n_o = 0.45\, (r_{st}\, f_y)^{0.5} / U_w^{0.33}$ (approx.) $= n_2$ and

Equation 62 where $n_{YL} = r_{st} \cdot f_y / 1.9\, U_w^{2/3} = n_3$

The corresponding loads P_T, P_o and P_{YL} divided by a common denominator $\dfrac{r_{st} \cdot f_y \cdot d_1^2}{1 - B/L}$ are given by Equations (46), (60) and (61).

$$\text{ALPHA 1} = \frac{P_T}{r_{st} \cdot f_y \cdot d_1^2} (1 - B/L) = k_T \cdot (1 - B/L) \cdot (1 - 0.42\ n_1) \quad . \ . \ (66)$$

where k_T depends on the ratio of B/L (Table VI-6 gives values of ALPHA 1 for various B/L and n_e values).

$$\text{ALPHA 2} = \frac{P_o\ (1 - B/L)}{r_{st} \cdot f_y \cdot d_1^2}$$

$$= k_o\ (1 - 0.42\ n_2) \quad . \ . \ . \ . \ . \ . \ . \ . \ . \ . \ . \ . \ . \ . \ . \ . \ . \ (67)$$

where k_o = 6.28 for circular columns and 8.0 for square columns.

$$\text{ALPHA 3} = \frac{P_{YL}(1 - B/L)}{r_{st} \cdot f_y \cdot d_1^2}$$

$$= k_{YL}\ (1 - 0.42\ n_3) \quad . \ . \ . \ . \ . \ . \ . \ . \ . \ . \ . \ . \ . \ . \ . \ . \ . \ (68)$$

where k_{YL} = 6.28 for circular columns and 8.0 for square columns (Table VI-7 gives values of ALPHA 2 and 3 for various values of n). Figure 71 shows a typical curve for n against ALPHA (curve ABCD).

The equation for the curve ABCD can be written in three parts, line AB, line BC and line CD taking O as the origin.

The equation for the line AB joining co-ordinates (o, n_1) and (ALPHA 1, n_1) is

$$y = n_1 \quad . \ . \ . \ . \ . \ . \ . \ . \ . \ . \ . \ . \ . \ . \ . \ . \ . \

n_e \ B/L	0.10	0.11	0.12	0.13	0.14	0.15	0.16	0.17	0.18	0.19	0.20
0.10	3.530	3.622	3.708	3.789	3.866	3.940	4.010	4.077	4.142	4.204	4.263
0.11	3.515	3.606	3.691	3.772	3.849	3.923	3.993	4.060	4.124	4.185	4.245
0.12	3.499	3.590	3.675	3.756	3.832	3.905	3.975	4.042	4.106	4.167	4.226
0.13	3.484	3.574	3.659	3.739	3.815	3.888	3.957	4.024	4.087	4.149	4.207
0.14	3.469	3.558	3.643	3.722	3.798	3.871	3.940	4.006	4.069	4.130	4.189
0.15	3.453	3.542	3.626	3.706	3.781	3.853	3.922	3.988	4.051	4.112	4.170
0.16	3.438	3.526	3.610	3.689	3.765	3.836	3.905	3.970	4.033	4.093	4.151
0.17	3.422	3.510	3.594	3.673	3.748	3.819	3.887	3.952	4.015	4.075	4.133
0.18	3.407	3.495	3.578	3.656	3.731	3.802	3.869	3.934	3.997	4.056	4.114
0.19	3.391	3.479	3.561	3.639	3.714	3.784	3.852	3.917	3.978	4.038	4.095
0.20	3.376	3.463	3.545	3.623	3.697	3.767	3.834	3.899	3.960	4.020	4.077
0.21	3.360	3.447	3.529	3.606	3.680	3.750	3.817	3.881	3.942	4.001	4.058
0.22	3.345	3.431	3.513	3.590	3.663	3.733	3.799	3.863	3.924	3.983	4.039
0.23	3.329	3.415	3.496	3.573	3.646	3.715	3.782	3.845	3.906	3.964	4.020
0.24	3.314	3.399	3.480	3.556	3.629	3.698	3.764	3.827	3.888	3.946	4.002
0.25	3.298	3.383	3.464	3.540	3.612	3.681	3.746	3.809	3.870	3.927	3.983
0.26	3.283	3.368	3.448	3.523	3.595	3.663	3.729	3.791	3.851	3.909	3.964
0.27	3.267	3.352	3.431	3.507	3.578	3.646	3.711	3.774	3.833	3.891	3.946
0.28	3.252	3.336	3.415	3.490	3.561	3.629	3.694	3.756	3.815	3.872	3.927
0.29	3.236	3.320	3.399	3.473	3.544	3.612	3.676	3.738	3.797	3.854	3.908
0.30	3.221	3.304	3.382	3.457	3.527	3.594	3.658	3.720	3.779	3.835	3.890
0.31	3.205	3.288	3.366	3.440	3.510	3.577	3.641	3.702	3.761	3.817	3.871
0.32	3.190	3.272	3.350	3.423	3.493	3.560	3.623	3.684	3.742	3.798	3.852
0.33	3.174	3.256	3.334	3.407	3.476	3.543	3.606	3.666	3.724	3.780	3.834
0.34	3.159	3.241	3.317	3.390	3.459	3.525	3.588	3.648	3.706	3.762	3.815
0.35	3.143	3.225	3.301	3.374	3.442	3.508	3.571	3.630	3.688	3.743	3.796
0.36	3.128	3.209	3.285	3.357	3.426	3.491	3.553	3.613	3.670	3.725	3.777
0.37	3.113	3.193	3.269	3.340	3.409	3.473	3.535	3.595	3.652	3.706	3.759
0.38	3.097	3.177	3.252	3.324	3.392	3.456	3.518	3.577	3.633	3.688	3.740

TABLE VI-6. Values of ALPHA 1 for various values of B/L ratio and N.A. factor (circular Slabs).

n_e \ B/L	0.10	0.11	0.12	0.13	0.14	0.15	0.16	0.17	0.18	0.19	0.20
0.39	3.082	3.161	3.236	3.307	3.375	3.439	3.500	3.559	3.615	3.669	3.721
0.40	3.066	3.145	3.220	3.291	3.358	3.422	3.483	3.541	3.597	3.651	3.703
0.41	3.051	3.129	3.204	3.274	3.341	3.404	3.465	3.523	3.579	3.633	3.684
0.42	3.035	3.114	3.187	3.257	3.324	3.387	3.448	3.505	3.561	3.614	3.665
0.43	3.020	3.098	3.171	3.241	3.307	3.370	3.430	3.487	3.543	3.596	3.647
0.44	3.004	3.082	3.155	3.224	3.290	3.353	3.412	3.470	3.525	3.577	3.628
0.45	2.989	3.066	3.139	3.208	3.273	3.335	3.395	3.452	3.506	3.559	3.609
0.46	2.973	3.050	3.122	3.191	3.256	3.318	3.377	3.434	3.488	3.540	3.591
0.47	2.958	3.034	3.106	3.174	3.239	3.301	3.360	3.416	3.470	3.522	3.572
0.48	2.942	3.018	3.090	3.158	3.222	3.283	3.342	3.398	3.452	3.504	3.553
0.49	2.927	3.002	3.074	3.141	3.205	3.266	3.324	3.380	3.434	3.485	3.534
0.50	2.911	2.987	3.037	3.124	3.188	3.249	3.307	3.362	3.416	3.467	3.516
0.51	2.896	2.971	3.041	3.108	3.171	3.232	3.289	3.344	3.397	3.448	3.497
0.52	2.880	2.955	3.025	3.091	3.154	3.214	3.272	3.327	3.379	3.430	3.478
0.53	2.865	2.939	3.009	3.075	3.137	3.197	3.254	3.309	3.361	3.411	3.460
0.54	2.849	2.923	2.992	3.058	3.120	3.180	3.237	3.291	3.343	3.393	3.441
0.55	2.834	2.907	2.976	3.041	3.103	3.163	3.219	3.273	3.325	3.374	3.422
0.56	2.818	2.891	2.960	3.025	3.087	3.145	3.201	3.255	3.307	3.356	3.404
0.57	2.803	2.875	2.944	3.008	3.070	3.128	3.184	3.237	3.288	3.338	3.385
0.58	2.787	2.859	2.927	2.992	3.053	3.111	3.166	3.219	3.270	3.319	3.366
0.59	2.772	2.844	2.911	2.975	3.036	3.093	3.149	3.201	3.252	3.301	3.348
0.60	2.757	2.828	2.895	2.958	3.019	3.076	3.131	3.184	3.234	3.282	3.329
0.61	2.741	2.812	2.879	2.942	3.002	3.059	3.113	3.166	3.216	3.264	3.310
0.62	2.726	2.796	2.862	2.925	2.985	3.042	3.096	3.148	3.198	3.245	3.291
0.63	2.710	2.780	2.846	2.909	2.968	3.024	3.078	3.130	3.179	3.227	3.273
0.64	2.695	2.764	2.830	2.892	2.951	3.007	3.061	3.112	3.161	3.209	3.254
0.65	2.679	2.748	2.814	2.875	2.934	2.990	3.043	3.094	3.143	3.190	3.235
0.66	2.664	2.732	2.797	2.859	2.917	2.973	3.026	3.076	3.125	3.172	3.217

TABLE VI-6 (Contd) Values of ALPHA 1 for various values of B/L ratio and N.A. factor. (Circular Slabs).

n_e \ B/L	0.10	0.11	0.12	0.13	0.14	0.15	0.16	0.17	0.18	0.19	0.20
0.67	2.648	2.717	2.781	2.842	2.900	2.955	3.008	3.058	3.107	3.153	3.198
0.68	2.633	2.701	2.765	2.825	2.883	2.938	2.990	3.041	3.089	3.135	3.179
0.69	2.617	2.685	2.749	2.809	2.866	2.921	2.973	3.023	3.071	3.116	3.161
0.70	2.602	2.669	2.732	2.792	2.849	2.903	2.955	3.005	3.052	3.098	3.142
0.71	2.586	2.653	2.716	2.776	2.832	2.886	2.938	2.987	3.034	3.080	3.123
0.72	2.571	2.637	2.700	2.759	2.815	2.869	2.920	2.969	3.016	3.061	3.105
0.73	2.555	2.621	2.684	2.742	2.798	2.852	2.903	2.951	2.998	3.043	3.086
0.74	2.540	2.605	2.667	2.726	2.781	2.834	2.885	2.933	2.980	3.024	3.067
0.75	2.524	2.590	2.651	2.709	2.764	2.817	2.867	2.915	2.962	3.006	3.048
0.76	2.509	2.574	2.635	2.693	2.748	2.800	2.850	2.898	2.943	2.987	3.030
0.77	2.493	2.558	2.619	2.676	2.731	2.783	2.832	2.880	2.925	2.969	3.011
0.78	2.478	2.542	2.602	2.659	2.714	2.765	2.815	2.862	2.907	2.951	2.992

TABLE VI-6 (Contd.) Values of ALPHA 1 for various values of B/L ratio and N.A. factor. (Circular Slabs).

TABLE VI-7

VALUES OF ALPHA 2 AND ALPHA 3 FOR CIRCULAR AND SQUARE SLABS FOR VARIOUS VALUES OF NEUTRAL AXIS FACTOR.

NEUTRAL AXIS FACTOR	ALPHA 2 and 3 FOR CIRCULAR SLAB	ALPHA 2 and 3 FOR SQUARE SLAB
0.10	6.01	7.66
0.11	5.99	7.63
0.12	5.97	7.60
0.13	5.93	7.56
0.14	5.91	7.53
0.15	5.88	7.50
0.16	5.86	7.46
0.17	5.83	7.43
0.18	5.81	7.40
0.19	5.78	7.36
0.20	5.75	7.34
0.21	5.73	7.30
0.22	5.70	7.26
0.23	5.68	7.23
0.24	5.65	7.19
0.25	5.63	7.16
0.26	5.60	7.13
0.27	5.57	7.10
0.28	5.54	7.06
0.29	5.51	7.02
0.30	5.48	6.99
0.31	5.46	6.95
0.32	5.44	6.93
0.33	5.41	6.90
0.34	5.38	6.86
0.35	5.35	6.82
0.36	5.33	6.79
0.37	5.30	6.76
0.38	5.28	6.72
0.39	5.25	6.70
0.40	5.22	6.66

NEUTRAL AXIS FACTOR	ALPHA 2 and 3 FOR CIRCULAR SLAB	ALPHA 2 and 3 FOR SQUARE SLAB
0.41	5.20	6.62
0.42	5.17	6.59
0.43	5.15	6.56
0.44	5.11	6.51
0.45	5.08	6.48
0.46	5.06	6.45
0.47	5.04	6.42
0.48	5.01	6.38
0.49	4.98	6.35
0.50	4.96	6.32
0.51	4.94	6.28
0.52	4.91	6.25
0.53	4.88	6.22
0.54	4.86	6.19
0.55	4.82	6.15
0.56	4.80	6.12
0.57	4.78	6.09
0.58	4.75	6.05
0.59	4.72	6.02
0.60	4.69	5.99
0.61	4.67	5.95
0.62	4.65	5.92
0.63	4.62	5.89
0.64	4.59	5.85
0.65	4.57	5.82
0.66	4.54	5.78
0.67	4.51	5.75
0.68	4.49	5.72
0.69	4.46	5.68
0.70	4.43	5.65

where

$$m_1 = \frac{n_1 - n_2}{\text{ALPHA 2} - \text{ALPHA 1}}$$

$$\text{and} \quad c_1 = n_2 + \frac{\text{ALPHA 2}\ (n_1 - n_2)}{\text{ALPHA 2} - \text{ALPHA 1}}$$

Similarly the equation for the line CD joining co-ordinates (ALPHA 2, n_2) and (ALPHA 3, n_3), is

$$y = -m_2 x + c_2 \quad \ldots\ldots\ldots\ldots\ldots\ldots\ldots \quad (71)$$

$$m_2 = \frac{n_2 - n_3}{\text{ALPHA 3} - \text{ALPHA 2}}$$

$$c_2 = n_3 + \frac{\text{ALPHA 3}\ (n_2 - n_3)}{\text{ALPHA 3} - \text{ALPHA 2}}$$

Hence, if the shear force carried by the dowel, shear reinforcement and concrete in the compression zone are divided by the same common denominator $\frac{r_{st}.f_y.d_1^2}{1-B/L}$ (say = H),

we have,

a) In the case of slabs with shear failure planes passing through shear reinforcement,

$$\frac{Q_{CAL}}{H} = \frac{Q_d + Q_v + Q_c}{H} \quad \ldots\ldots\ldots\ldots\ldots\ldots \quad (72)$$

$$\text{ALPHA} = \text{ALPHA d} + \text{ALPHA v} + \text{ALPHA c} \quad \ldots\ldots\ldots \quad (73)$$

Here ALPHA d and ALPHA v are in terms of known quantities, whilst ALPHA c is in terms of n, as can be seen from their values.

$$\text{ALPHA d} = \frac{K_d.\phi_M.b_d.U_w^{1/3}}{H} \quad \ldots\ldots\ldots\ldots\ldots\ldots \quad (74)$$

where b_d is the perimeter $2d_1$ out from the column face

$$\text{ALPHA v} = \frac{A_{sq}.f_{yq}.\sin\theta}{H} \quad \ldots\ldots\ldots\ldots\ldots\ldots \quad (75)$$

and $\text{ALPHA c} = \dfrac{0.3.b_c.d_1.U_w^{2/3}.n}{H}$ . . . . . (76)

where b_c is the perimeter at column face.

or $\dfrac{n}{\text{ALPHA c}} = \dfrac{H}{0.3\ b_c.d_1.U_w^{2/3}} = \text{HS}$ . . . . . (77)

Plotting OP along the x axis to represent (ALPHA d + ALPHA v), then a line PQ, drawn from here at a slope of 'HS' intersects the curve ABCD at Q. The co-ordinates of Q give the required values of n and ALPHA (Q_{CAL} = ALPHA.H). The co-ordinates of P and Q being (ALPHA d + ALPHA v, o) and (x,y) with a slope 'HS' then the equation of PQ is

$$y = \text{HS}\ (x - \text{ALPHA d} - \text{ALPHA v}) \quad . . . . . (78)$$

Solving equations (70) and (78) gives a value of x. This is reasonably equal to the exact value of x. Now that the appropriate part of the curve is known, the solution of this equation with equation (78) will give the values of n and x.

$$\text{Now } x = \frac{Q_{CAL}}{H}$$

$$\text{or } Q_{CAL} = \frac{x.r_{st}.f_y.d_1^2}{1 - B/L} \quad . . . . . (79)$$

The load so obtained is compared with the actual test load.

b) In the case of slabs where the shear failure plane falls outside the shear reinforcement, the value of b_c and b_d are to be modified: b_c will be now taken as the perimeter just outside the shear reinforcement and b_d, $2d_1$ further out from there. The term Q_v has zero value since its direct contribution no longer exists. The rest of the calculation remains exactly the same as before.

c) If the slab is subjected to combined loading then a reduction factor of $\dfrac{1}{1 + 4\ EC/L}$ is applied to the load calculated as outlined above, to obtain the ultimate load.

Table VI-8 shows the comparison between the actual loads and the calculated loads for slabs tested by the author and others.

Fig. 72 shows the same method tackled graphically.

6.10 SIMPLIFIED FORMULA.

The calculation of the ultimate load can further be simplified if the value of the neutral axis depth is taken as the elastic one, rather than the actual one, in calculating Q_c. The total load can then be calculated using,

$$Q_{CAL} = \frac{0.33\ b_{col}(r_{st}\%.U_w)^{0.4}d_1 + K_d.b_d.\phi_M.U_w^{0.33} + A_{sq}.f_{yq}.\sin\theta}{1 + 4.EC/L} \quad . . (80)$$

Figure 73 shows the perimeter b_{col} and b_d to be used for various shapes of column. In principle the above equation would be unsafe in case of slabs where n is less than n_e. The error caused by this is not serious. For widely spaced bars b_d should be limited to that specified in section 5.4.

The loads calculated using the above formula for various test results showed very reasonable agreement with the actual loads obtained during testing (see chapter VII).

6.11 EDGE COLUMNS WITH ECCENTRIC LOAD PERPENDICULAR TO THE FREE EDGE.

The conditions of equilibrium in the case of these edge columns are different from those of internal ones. The location of the column creates torsional stresses across the slab. Even when the load is concentric with respect to the centre line of the column the distribution of the load along the periphery of the support is non-uniform. This is due to the fact that the geometric centre of the slab periphery and column are not one and the same. The overall behaviour of the slab is affected by the eccentricity of the load from the geometric centre of the slab, while local behaviour is affected by the eccentricity from the column centre.

Let us consider a slab under combined load (a load Q with an eccentricity EC to the column centre line and perpendicular to

Slab No.	r_{st} %	f_y N/mm^2	ϕ_M mm	U_w N/mm^2	b mm	d_1 mm	Q_{TEST} M.N.	Q_d M.N.	n_1	n_2	n_3
A-1a	1.15	332	19	16.5	254	117.5	0.302	0.155	0.545	0.349	0.307
A-1b	1.15	332	19	29.6	254	117.5	0.364	0.188	0.466	0.287	0.208
A-1c	1.15	332	19	34.1	254	117.5	0.356	0.197	0.449	0.274	0.189
A-1d	1.15	332	19	43.3	254	117.5	0.351	0.213	0.421	0.254	0.161
A-1e	1.15	332	19	23.8	254	117.5	0.356	0.175	0.494	0.309	0.240
A-2a	2.47	321	25	16.0	254	114.0	0.335	0.202	0.747	0.507	-
A-2b	2.47	321	25	22.8	254	114.0	0.400	0.227	0.678	0.451	-
A-2c	2.47	321	25	44.1	254	114.0	0.470	0.282	0.568	0.363	0.330
A-7b	2.47	321	25	32.8	254	114.0	0.511	0.256	0.615	0.400	0.400
A-3a	3.70	321	25	15.0	254	114.0	0.356	0.198	0.892	0.633	-
A-3b	3.70	321	25	26.6	254	114.0	0.445	0.239	0.765	0.525	-
A-3c	3.70	321	25	31.2	254	114.0	0.534	0.252	0.733	0.498	-
A-3d	3.70	321	25	40.7	254	114.0	0.547	0.275	0.682	0.456	-
A-4	1.15	321	19	30.7	356	117.5	0.400	0.222	0.461	0.279	0.196
A-5	2.47	321	25	32.7	356	114.0	0.534	0.298	0.616	0.401	0.401
A-6	3.70	321	25	29.4	356	114.0	0.498	0.288	0.745	0.508	-

TABLE VI-8a Slabs tested by HOGNESTAD(4) - Concentric load.

Slab No.	ALPHA 1	ALPHA 2	ALPHA 3	ALPHA d	HS	ALPHA	Q_{CAL} M.N.	$\frac{Q_{CAL}}{Q_{TEST}}$
A-1a	2.99	6.82	6.97	2.54	0.261	4.37	0.265	0.88
A-1b	3.12	7.04	7.30	3.08	0.177	5.18	0.317	0.87
A-1c	3.14	7.07	7.36	3.22	0.161	5.37	0.328	0.92
A-1d	3.19	7.15	7.46	3.49	0.137	5.84	0.356	1.01
A-1e	3.07	6.95	7.19	2.86	0.204	4.86	0.298	0.84
A-2a	2.66	6.30	-	1.68	0.526	3.05	0.365	1.09
A-2b	2.77	6.47	-	1.90	0.417	3.42	0.409	1.02
A-2c	2.95	6.76	6.89	2.36	0.272	4.10	0.490	1.04
A-7b	2.87	6.65	6.65	2.14	0.330	3.84	0.459	0.90
A-3a	2.42	5.87	-	1.10	0.834	2.20	0.394	1.10
A-3b	2.63	6.23	-	1.33	0.590	2.62	0.470	1.05
A-3c	2.68	6.31	-	1.40	0.526	2.78	0.500	0.95
A-3d	2.76	6.46	-	1.53	0.435	3.04	0.545	0.99
A-4	3.44	7.06	7.34	3.51	0.127	6.09	0.385	0.96
A-5	3.16	6.65	6.65	2.33	0.254	4.40	0.562	1.06
A-6	2.93	6.30	-	1.50	0.417	3.22	0.577	1.16

TABLE VI-8a (Contd.)

Slab No.	r_{st} %	f_y N/mm^2	ϕ_M mm	U_w N/mm^2	EC mm	b mm	Q_{TEST} M.N.	Q_d M.N.	n_1	n_2	n_3
M1A	1.50	481	19	24.2	0	305	0.433	0.187	0.547	0.422	-
M2A	1.50	481	19	18.3	185.5	305	0.213	0.171	0.590	0.463	-
M4A	1.50	481	19	20.7	485.0	305	0.144	0.178	0.760	0.444	-
M2	1.50	481	19	30.3	195.5	305	0.294	0.202	0.515	0.392	0.386
M3	1.50	481	19	26.7	338.0	305	0.209	0.194	0.533	0.409	-
M6	1.34	327	16	31.1	168.0	254	0.239	0.158	0.489	0.303	0.231
M7	1.34	327	16	29.4	61.0	254	0.315	0.155	0.496	0.309	0.240
M8	1.34	327	16	29.0	437.0	254	0.149	0.155	0.498	0.310	0.242
M9	1.34	327	16	27.3	127.0	254	0.267	0.152	0.506	0.316	0.252
M10	1.34	327	16	24.8	308.0	254	0.178	0.147	0.520	0.327	0.267

Note: d_1 = 114 mm, L = 1830 mm, K_d = 1.3, k_T = 4.87 k_o = k_{YL} = 8.0

TABLE VI-8b Slabs tested by Moe[19] - Combined Load.

Slab No.	ALPHA 1	ALPHA 2	ALPHA 3	ALPHA d	HS	ALPHA	Q_{CAL} M.N.	$\frac{Q_{CAL}}{Q_{TEST}}$
M1A	3.13	6.46	-	1.67	0.319	3.35	0.375	0.87
M2A	3.05	6.45	-	1.52	0.384	3.05	0.240	1.12
M4A	3.09	6.50	-	1.58	0.353	3.00	0.174	1.20
M2	3.18	6.69	6.70	1.79	0.274	3.60	0.282	0.96
M3	3.15	6.62	-	1.72	0.299	3.25	0.209	1.00
M6	3.33	6.98	7.22	2.39	0.191	4.60	0.222	0.93
M7	3.32	6.96	7.19	2.35	0.198	4.55	0.265	0.84
M8	3.32	6.95	7.19	2.34	0.199	4.52	C.151	1.01
M9	3.30	6.92	7.15	2.29	0.208	4.40	0.236	0.89
M10	3.28	6.90	7.10	2.22	0.204	4.45	0.177	0.99

TABLE VI-8b (Contd.)

Slab No.	U_w N/mm^2	EC mm	Q_{TEST} M.N.	A_{sq} mm^2	f_{yq} N/mm^2	θ deg	Q_d M.N.	Q_v M.N.	n_1	n_2	n_3
L1	32.9	305.0	0.399	-	-	-	0.284	-	0.428	0.283	0.202
L2	39.2	0	0.867	1710	309	45	0.384	0.373	0.408	0.267	0.179
L3	33.1	305.0	0.499	1710	309	45	0.364	0.373	0.428	0.283	0.201
L4	45.9	305.0	0.568	775	338	45	0.317	0.185	0.391	0.254	0.161
L5	35.6	305.0	0.499	3040	355	45	0.373	0.763	0.419	0.276	0.191
L6	42.1	152.5	0.598	1190	355	45	0.394	0.299	0.401	0.261	0.171
L7	44.4	0	0.687	-	-	-	0.314	-	0.395	0.257	0.165
L9	41.4	0	0.588	-	-	-	0.307	-	0.402	0.263	0.173
L.10	41.9	152.5	0.638	1190	355	30	0.308	0.210	0.401	0.262	0.171

Note: r_{st} = 1.0%, b = 305 mm, f_y = 398 N/mm^2, ϕ_M = 16 mm, d_1 = 151 mm,

L = 2010 mm, K_d = 1.8, k_T = 4.55, k_o = k_{YL} = 8.0

TABLE VI-8c Slabs tested by Author - Combined loading + shear reinforcement.

Slab No.	ALPHA 1	ALPHA 2	ALPHA 3	ALPHA d	ALPHA v	HS	ALPHA	Q_{CAL} M.N.	$\frac{Q_{CAL}}{Q_{TEST}}$
L1	3.16	7.01	7.32	2.66	-	0.186	4.65	0.310	0.78
L2	3.20	7.06	7.40	3.60	(3.49)	0.097	6.60	0.709	0.81
L3	3.17	7.01	7.32	3.40	(3.49)	0.109	6.25	0.417	0.83
L4*	3.22	7.11	7.46	2.97	1.73	0.149	6.73	0.450	0.79
L5	3.18	7.05	7.36	3.48	(7.13)	0.103	6.39	0.426	0.86
L6	3.21	7.00	7.43	3.68	(2.79)	0.092	6.65	0.546	0.91
L7	3.22	7.11	7.45	2.93	-	0.153	5.06	0.543	0.90
L9	3.21	7.00	7.42	2.87	-	0.160	4.96	0.530	0.90
L10*	3.21	7.00	7.42	2.88	1.97	0.158	6.60	0.541	0.85

* Shear failure plane through shear reinforcement.

TABLE VI-8c (Contd.)

the free edge). The resultant of the forces must be in equilibrium with the applied load. Assuming uniform vertical reactions on edges perpendicular to the free edge and a downward reaction at the parallel edge, the resultant reactions acting at the centres of supports are $V_1 \uparrow$ and $V_2 \downarrow$. In addition to the vertical forces the sides B1C1 and E1D1 are subjected to torsional moments say T_r (see Fig. 74). Then for equilibrium, taking moments about AA,

$$2T_r + \frac{Y}{2} \cdot V_2 = Q(\frac{Y}{2} - \frac{b_y}{2} \pm EC) \quad \ldots\ldots\ldots\ldots\ldots (81)$$

If $T_r \propto QY$ then $T_r = K.QY$

putting $e = (\frac{Y}{2} - \frac{b_y}{2} \pm EC)$, equation (81) can be written as

$$V_2 = \frac{2Q}{Y} \cdot e - 4KQ$$

$$= 2Q(e/Y - 2K) \quad \ldots\ldots\ldots\ldots\ldots\ldots\ldots (82)$$

For vertical equilibrium,

$$2V_1 = V_2 + Q$$

$$= 2Q(e/Y - 2K) + Q$$

$$V_1 = Q(e/Y + 0.5 - 2K) \quad \ldots\ldots\ldots\ldots\ldots\ldots (83)$$

(ie) $V_1 = Q(\text{constant } K_1 + K_2\, e/Y)$ (say)

and $V_2 = Q(2K_1 + 2K_2 e/Y - 1)$

The shear distribution around the column is dependent on the value of EC, the eccentricity of the applied load from the centre line of column. The column faces, parallel to the resultant applied moment, will be predominantly in torsion. The torsional shear stresses can be calculated using $q_t = \frac{M_v}{b_y . d^2/4}$. This is assuming a

distribution as shown in Fig. 74b. The distribution as shown (Fig.74a) cannot occur once the slab is cracked and hence the above is justified.

Since the above ignores the contribution of the torsional stresses in resisting vertical shear, it is logical to assume that the shear is going to be resisted by the concrete compression zone at the head of the shear crack, and the dowel force at the level of the tensile reinforcement.

Hence based on the above,

$$V_1 = (Q_c + Q_d) \text{ at the faces BC or ED}$$

$$\text{and} \quad V_2 = (Q_c + Q_d) \text{ at face CD.}$$

Depending on the ratio of applied moment/applied load, one of the above will be critical and determines the load-carrying capacity.

$$\therefore \quad Q = \frac{V_1}{K_1 + K_2 e/Y} = \frac{(Q_c + Q_d)_{BC \text{ or } ED}}{K_1 + K_2 e/Y}$$

$$\text{or} \quad Q = \frac{V_2}{(2K_1 + 2K_2 - 1)} = \frac{(Q_c + Q_d)_{CD}}{(2K_1 + 2K_2 - 1)}$$

From the author's test results the values of K_1 and K_2 were 0.29 and 0.22, and substituting these values in the equation for Q gives,

$$Q_{CAL} = \frac{(Q_c + Q_d)_{BC \text{ or } ED}}{0.29 + 0.22\, e/y}$$

$$\approx \frac{3.5(Q_c + Q_d)_{BC \text{ or } ED}}{1 + e/Y} \quad \ldots\ldots\ldots\ldots\ldots\ldots (84)$$

for slabs failing at faces perpendicular to the free edge (BC or ED).

$$\text{and} \quad Q_{CAL} = \frac{(Q_c + Q_d)_{CD}}{(.57 + .44\, e/Y - 1)}$$

$$\approx \frac{2.2\,(Q_c + Q_d)_{CD}}{(e/Y - 1)} \quad \ldots\ldots\ldots\ldots\ldots\ldots (85)$$

for slabs failing on the internal face (CD).

The lower of the values given by equations (84) and (85) gives the punching load for design purposes.

In calculating the value of Q_c, the same failure criterion as in the case of internal columns can be used (i.e.) that "failure occurs when the shear stress reaches a limiting value". Based on the above lines punching loads were calculated and compared with test results.

The provision of shear reinforcement increases the load-carrying capacity as in the case of internal columns. The expressions to be used for slabs with shear reinforcement are,

$$Q = \frac{3.5(Q_c + Q_d + Q_v)_{BC \text{ or } ED}}{1 + e/Y} \quad \ldots\ldots\ldots\ldots (86)$$

for slabs failing at faces perpendicular to the free edge,

where $Q_v = A_{sq}.f_{yq}.\sin\theta \left(\frac{b_y}{b_x + 2b_y}\right)$

$$\text{and } Q = \frac{2.2(Q_c + Q_d + Q_v)CD}{e/Y - 1} \quad \ldots\ldots\ldots\ldots\ldots\ldots (87)$$

for slabs failing on the internal face (CD)

where $Q_v = A_{sq}.f_{yq}.\sin\theta \left(\frac{b_x}{b_x + 2b_y}\right)$

The effect of the eccentricity in the case of these slabs was less pronounced than the internal ones. Table VI-9 gives the comparison between the actual loads and the calculated loads for the slabs tested by the author and others. The available results are of limited scope, and hence no definitive conclusions can be drawn, (though the predicted values are reasonable). The validity of the constants used, is questionable for different ratios of X and Y, different amounts of top and bottom steel and differing column shapes.

In view of the above and the fact that the eccentricity has less effect on external columns (with moments perpendicular to

TABLE VI-9

EDGE COLUMNS WITH NORMAL MOMENT.

Slabs tested by author.

Slab No.	U_w N/mm^2	EC mm.	Q_{TEST} M.N.	A_{sq} mm^2	f_{yq} N/mm^2	θ deg	Q_c MN.	Q_d MN.	Q_r MN.	Q_{CAL} MN.	Q_{CAL}/Q_{TEST}
ES1	33.8	0	0.309	-	-	-	0.059	0.051	-	0.282	0.91
ES2	32.8	228.5	0.342	-	-	-	0.059	0.048	-	0.320	0.93
ES3	51.3	228.5	0.442	517	238	45	0.070	0.056	0.027	0.447	1.01
ES4*	50.0	228.5	0.508	1140	309	45	0.094	0.065	0.078	0.478	0.94
ES5	37.6	-228.5	0.264	-	-	-	0.062	0.050	-	0.250	0.95
ES6	40.4	0	0.370	517	238	45	0.064	0.051	0.027	0.364	0.99
ES7*	45.8	-228.5	0.310	517	238	45	0.092	0.065	0.027	0.419	1.35

Note:- $r_{st} = 1.0\%$, $f_y = 398\ N/mm^2$, $d_1 = 144$ mm, $\phi_M = 16$ mm,

$b_x = b_y = 305$ mm, $X = 2010$ mm, $Y = 1155$ mm and $K_d = 1.8$

* Failure outside shear reinforcement.

Average Q_{CAL}/Q_{TEST} = 0.98,

Standard deviation = 0.075

Coefficient of variation = 7.61%

TABLE VI-9 (contd.)

Slabs Tested by Anderson[17]

Slab No.	r_{st} %	f_y N/mm^2	U_w N/mm^2	d_1 mm	Y mm	EC mm	Q_{test} M.N	Q_c M.N	Q_d M.N	Q_{CAL} M.N	$\frac{Q_{CAL}}{Q_{TEST}}$
1a	1.08	427	27.6	120	700	370	0.155	0.038	0.034	0.136	0.88
1b	1.30	437	33.0	122	600	295	0.203	0.044	0.036	0.156	0.77

Note: ϕ_M = 10 mm, X = 1600 mm, K_d = 1.8

Slabs Tested by Stamenkovic'[20]

Slab No.	U_w N/mm^2	EC mm	Q_{TEST} M.N	Q_c M.N	Q_d M.N	Q_{CAL} M.N	$\frac{Q_{CAL}}{Q_{TEST}}$
V/E/1	35.8	0	0.075	0.010	0.010	0.047	0.63
C1/E/1	38.5	75	0.073	0.011	0.010	0.051	0.70
C1/E/2	32.4	168	0.055	0.010	0.010	0.054	0.99

Note: r_{st} = 1.17%, f_y = 495 N/mm^2, ϕ_M = 8 mm, d_1 = 56 mm, $b_x = b_y$ = 127mm

X = Y = 890 mm, K_d = 1.8

the free edge), than on internal column-connections, it may be reasonable to ignore the effect of eccentricity in calculating the ultimate load. Comparison of loads calculated ignoring eccentricity, with the actual loads obtained during testing are given in Table VII-22, Chapter VII.

Before judging the accuracy of the calculated loads, it is required to know the local moment strength of the connection, in order to eliminate the slabs which were not shear failures. Since two of the column faces (perpendicular to the free edge) are predominantly in torsion with the internal face in bending, it is reasonable to assume that the total resistance is

$$M_{CAL} = 2T + M_b \quad \ldots\ldots\ldots\ldots\ldots\ldots \quad (88)$$

where $T = b_x \sqrt{m_x . m_y}$ (see Ref.64)

m_x, m_y = moment per unit length perpendicular to and parallel to the free edge adjacent to the column.

$M_b = A_b \cdot f_y \cdot (jd_1)$

A_b = area of bars passing through the inner face of column

and (jd_1) = lever arm.

Values of M_{CAL} were calculated using the above. Fig. 75 shows the interaction diagram Q_{TEST}/Q_{CAL} V_s M_{TEST}/M_{CAL}.

6.12 EDGE COLUMNS WITH TANGENTIAL MOMENTS.

Tests carried out by Stamenkovi[(20)] and Tankut[(63)] show that the effect of eccentricity is quite considerable in this case. Conditions around the column are comparable to those around the internal column. The reduction in the carrying capacity of the connection due to the absence of one column face can be adequately

taken care of by using reduced perimeters b_c and b_d in equation 80 (see section 6.10). Hence the formula to be used can be written down as,

$$Q_{CAL} = \frac{0.33\ b_{Col}(U_w.r_{st}/)^{0.4}d_1 + K_d.b_d.\phi_M.T_w^{0.33} + A_{sq}.f_{yq}.\sin\theta}{1 + 4EC/L} \quad \ldots\ldots\ldots\ldots (89)$$

For slabs with no shear reinforcement and slabs with shear reinforcement, where the shear failure plane is through the shear reinforcement,

$$b_{Col} = b_x + 2b_y$$

$$b_d = (b_x + 2b_y) + 2\pi.d_1$$

For slabs with shear reinforcement, where the shear failure plane falls outside the shear reinforcement b_{Col} is taken as the perimeter just outside the shear reinforcement and $b_d = b_{Col} + 2\pi d_1$, (which is $2d_1$ further out from the end of shear reinforcement). Table VII-23 shows the comparison of the calculated loads and the actual loads.

It can be seen that the predicted loads are in good agreement with the actual loads. The effect of the eccentricity which is taken care of by the reduction factor $\frac{1}{1 + 4EC/L}$ is shown to be reasonable in Fig.76 (Q_{TEST}/Q_o v$_s$ EC/L).

6.13 CORNER COLUMNS.

The data available in the case of corner columns is very limited and it is very difficult to see the manner in which they fail, but it seems that moment rather than shear capacities are the governing criteria.

When the moment at the junction is normal to a column face, the local moment strength is the sum of the torsional resistance of the face parallel to the eccentricity and the flexural resistance of the other.

$$P_{cal} = \frac{T + M_b}{\text{effective eccentricity}}$$

where $T = b_x \sqrt{m_x m_y}$

m_x, m_y = moment resistances per unit lengths parallel and perpendicular to the eccentricity

effective eccentricity is eccentricity measured from the centroid of the column perimeter.

$M_b = A_b f_y \, jd_1$

A_b = area of steel passing through the column face perpendicular to the applied moment and anchored in the column.

When the bending is bi-axial the interaction of torsion and bending at the faces should be taken into account by reducing the appropriate 'm' value in the expression for T to take account of the forces in the reinforcement caused by flexure.

Overall moment capacaties depend upon the configurations of loads and supports in the surrounding structure. In the simple case tested by the author and Stamenković in which a concentrated load is applied to the column with no other loads on the slab

$$P_{cal} = 2m$$

where m is the resultant moment resistance per unit length.

Table VI-10 shows the results obtained by applying the above to tests by Stamenković[20] and the author and the agreement can be seen to be reasonable.

The only other available test data is from Tankut[63] who obtained corner panel failures by isolating parts of his 4 bay structures following the failure of the main structural system. The modes of failure are unclear and the structure is a complex one. The results are therefore not presented here but appear to give reasonable agreement with an overall yield pattern of failure.

TABLE VI-10

CORNER COLUMNS.

Slab No.	U_w N/mm^2	EC mm	Q_{TEST} M.N	Q_c M.N	Q_d M.N	Q_{CAL} M.N	$\frac{Q_{TEST}}{Q_{CAL}}$	M_{CAL} Nm	$\frac{M_{TEST}}{M_{CAL}}$
Slabs tested by Stamenković									
V/C/1	40.2	0	0.027	0.019	0.022	0.041	0.66	4240	0.90
C/C/1	38.0	250	0.025	0.023	0.021	0.044	0.57	4240	1.31
C/C/2	35.4	400	0.016	0.021	0.020	0.041	0.39	4230	1.45
C/C/3	32.2	776	0.008	0.020	0.020	0.040	0.20	4210	1.33
Slabs tested by Author									
CS	38.5	0	0.159	0.130	0.105	0.235	0.68	11500	1.05

Note: i) In the slabs tested by Stamenković

$r_{st} = 1.17\%$, $f_y = 448\ N/mm^2$, $\phi_M = 8$ mm, $d_1 = 56$ mm,

$b_x = b_y = 127$ mm, $X = Y = 890$ mm, $K_d = 1.8$

ii) In the slabs tested by Author,

$r_{st} = 1.0$, $f_y = 398\ N/mm^2$, $\phi_M = 16$ mm, $d_1 = 151$ mm,

$b_x = b_y = 305$ mm, $X = Y = 1155$ mm.

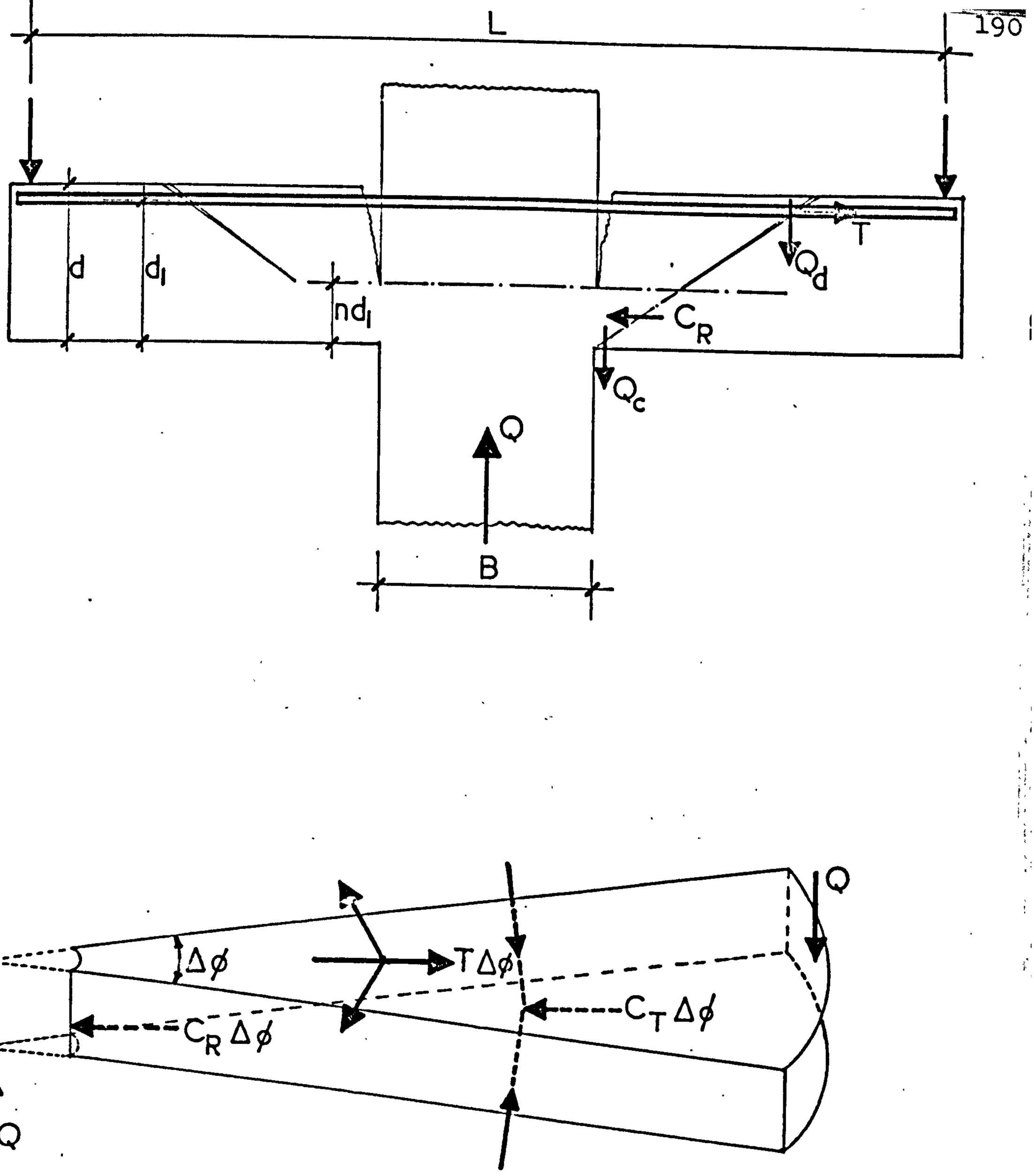

Fig. 61. ASSUMED MODEL WHEN THE SLAB IS IN AN ELASTO PLASTIC STATE.

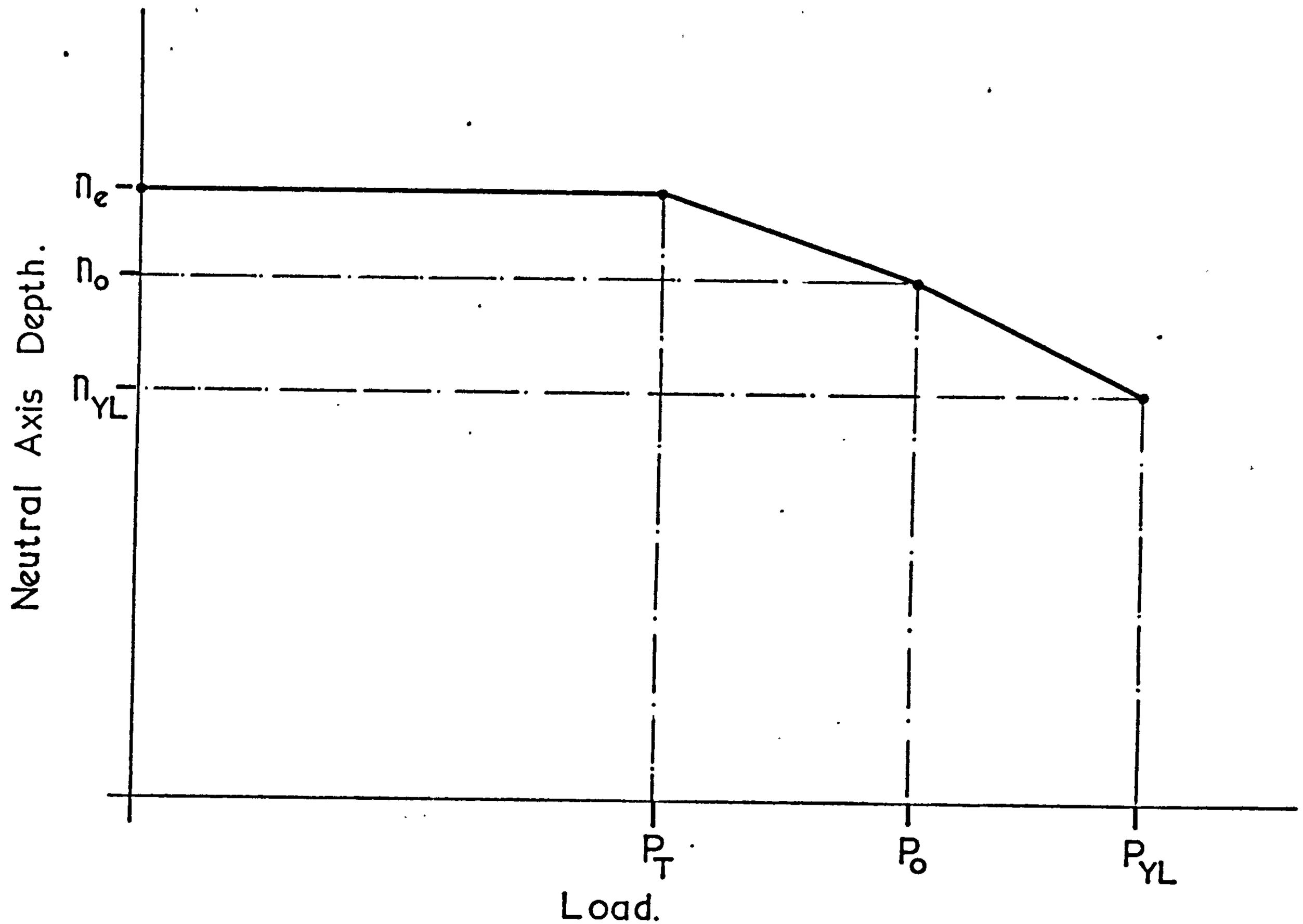

Fig. 62. NEUTRAL AXIS DEPTH vs LOAD.

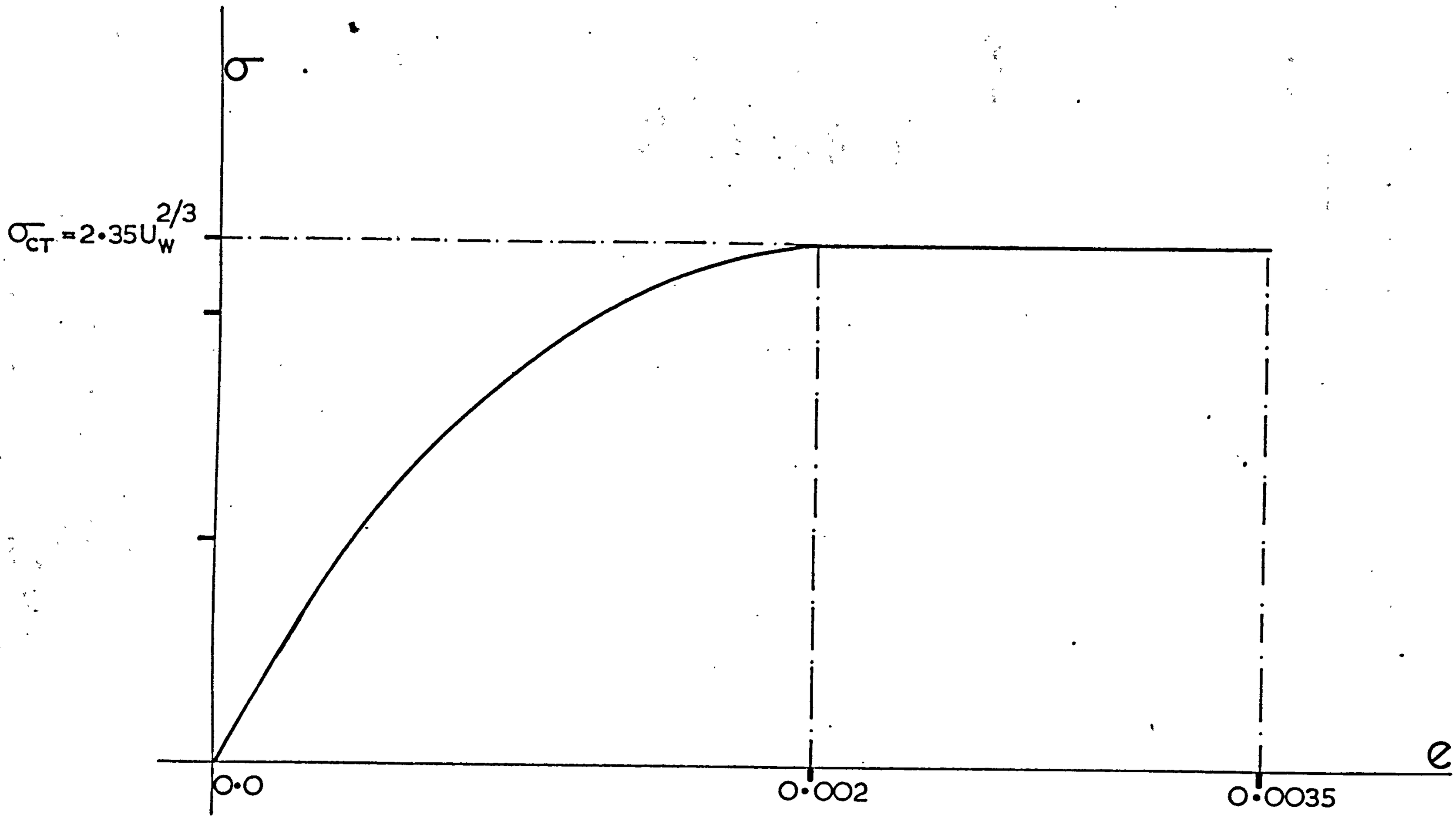

Fig. 63. STRESS-STRAIN CURVE FOR CONCRETE.

n_e	$n_e^2 / (1-n_e)$	$2.8n_e^{5/2}$
0.1	0.0011	0.000895
0.2	0.0500	0.051000
0.3	0.1285	0.138000
0.4	0.2667	0.283000
0.5	0.5000	0.495000

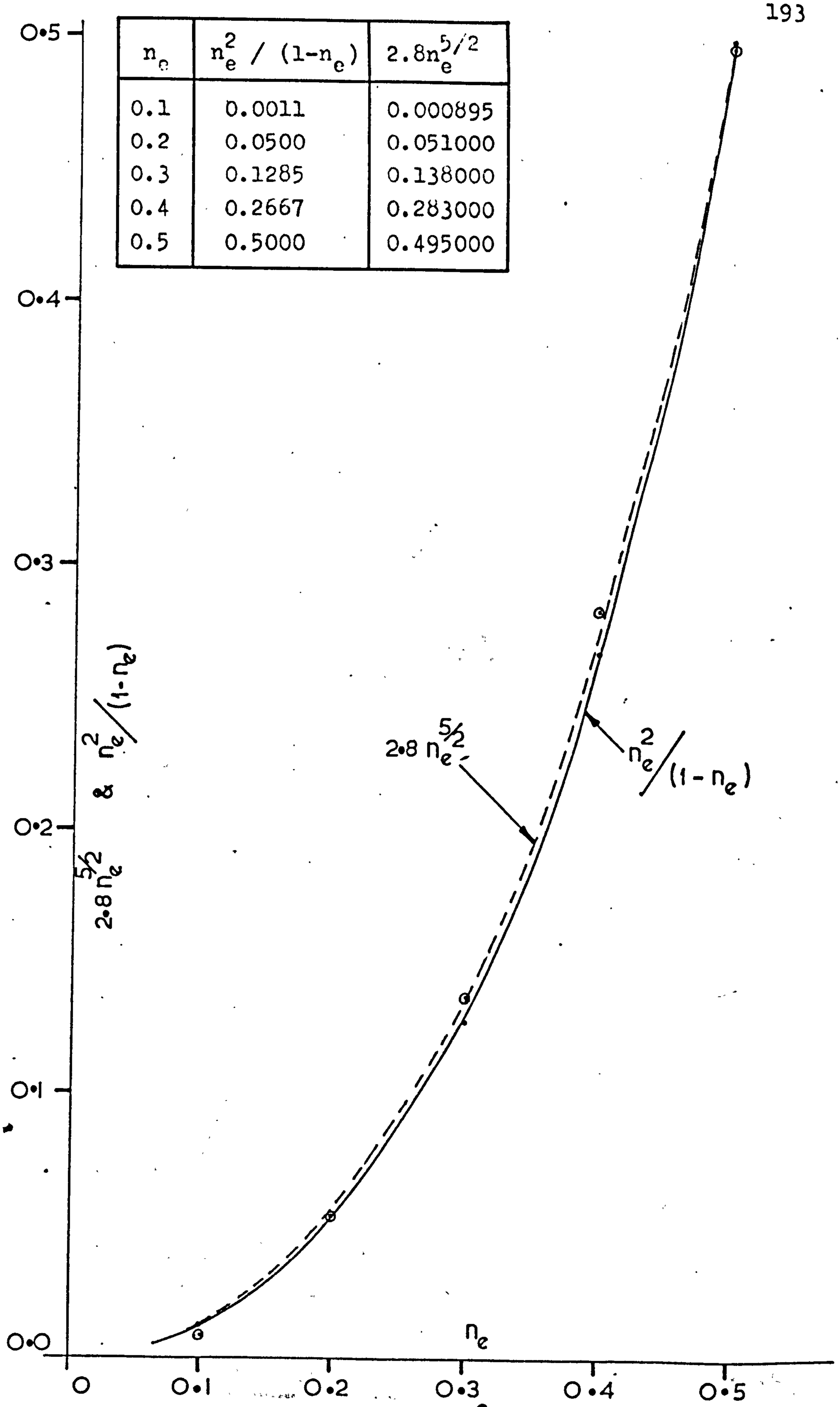

Fig. 64. n_e vs $n_e^2/(1-n_e)$.

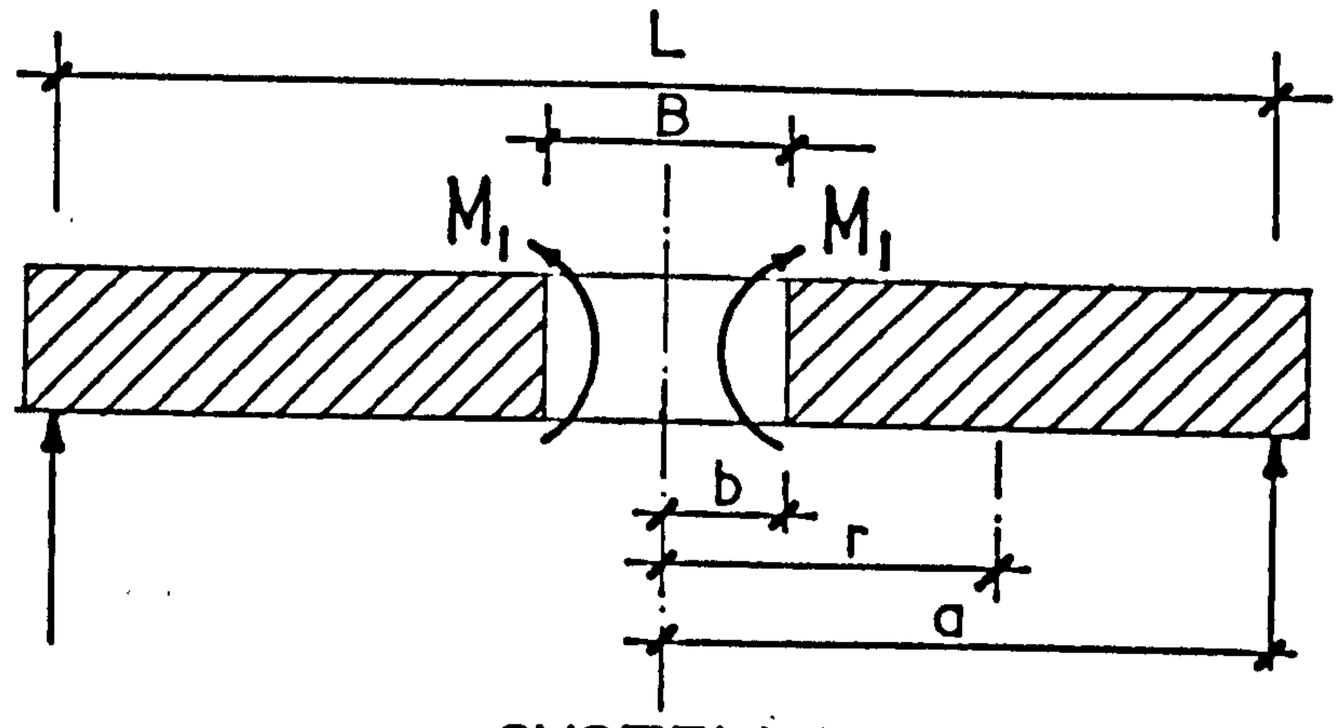

SYSTEM. 1.

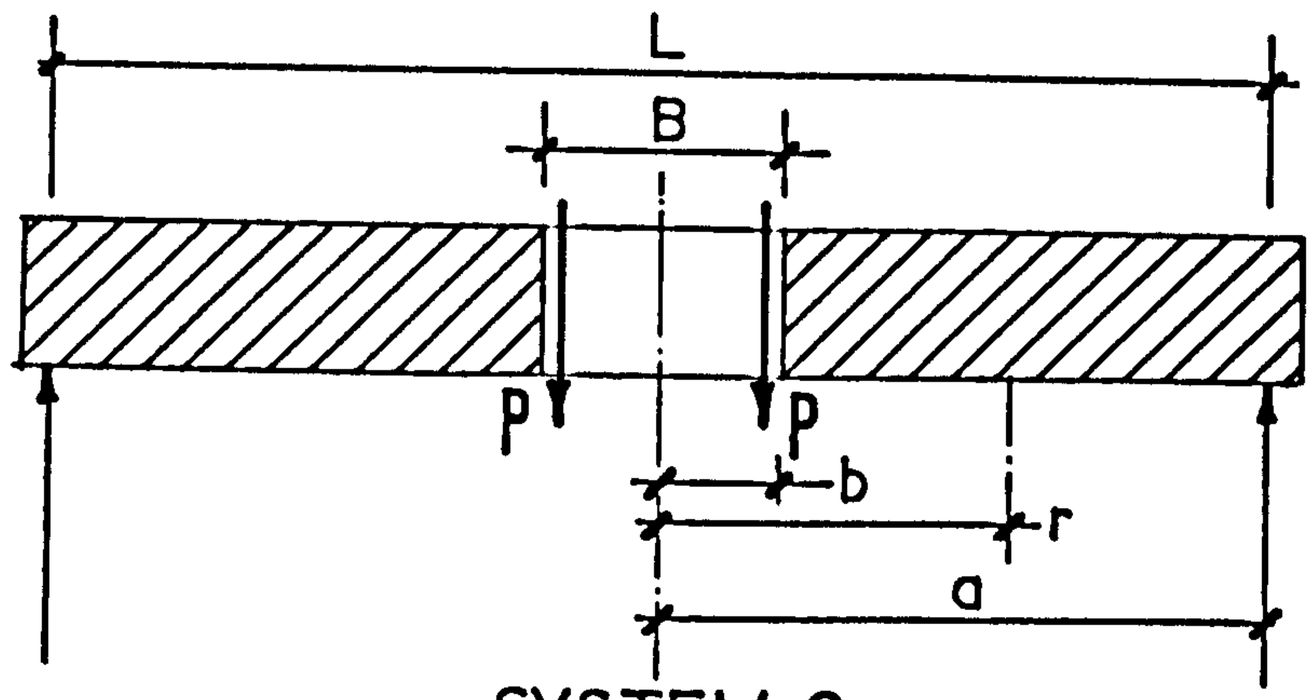

SYSTEM. 2.

Fig. 65.

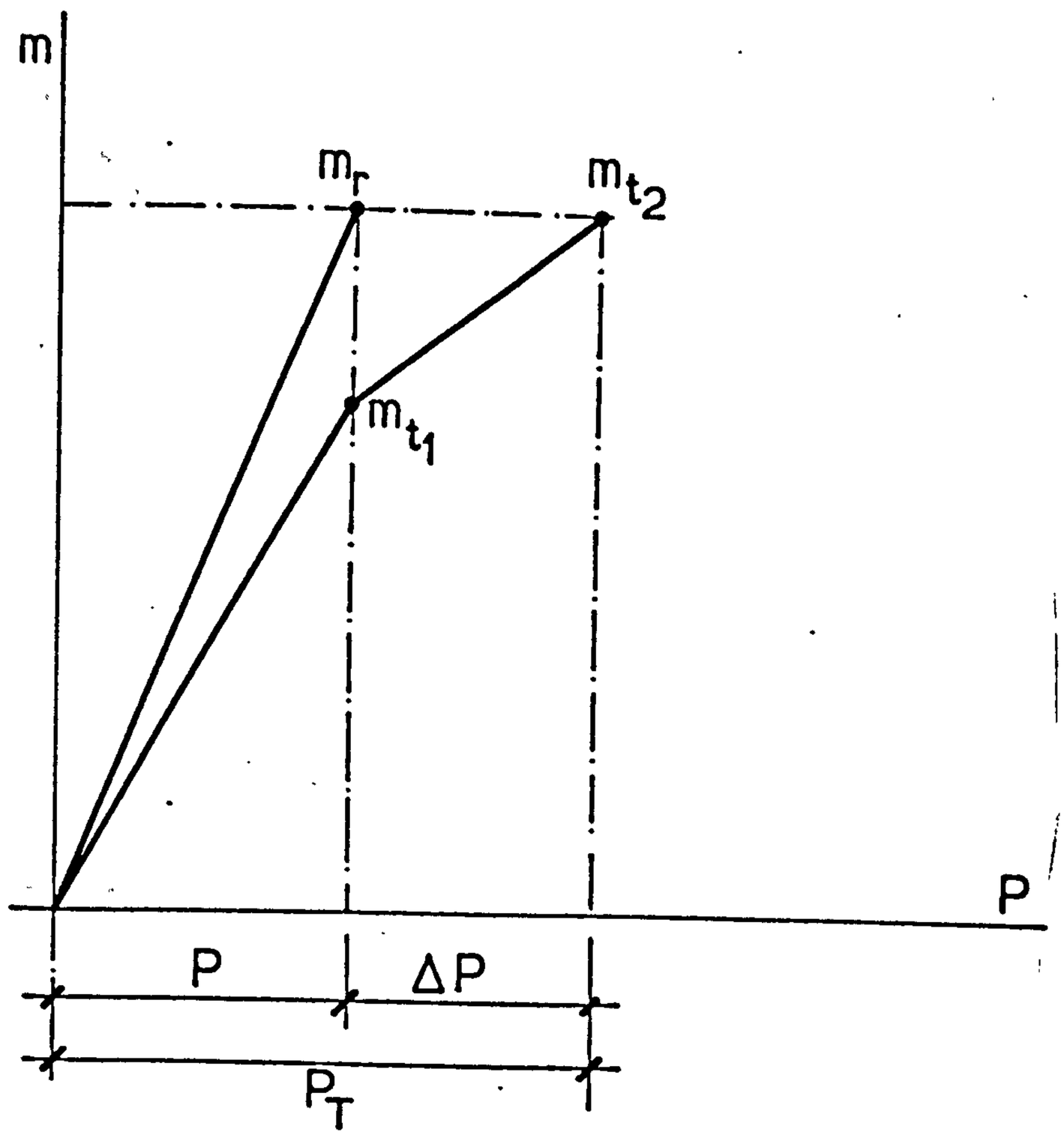

m vs P

Fig. 66.

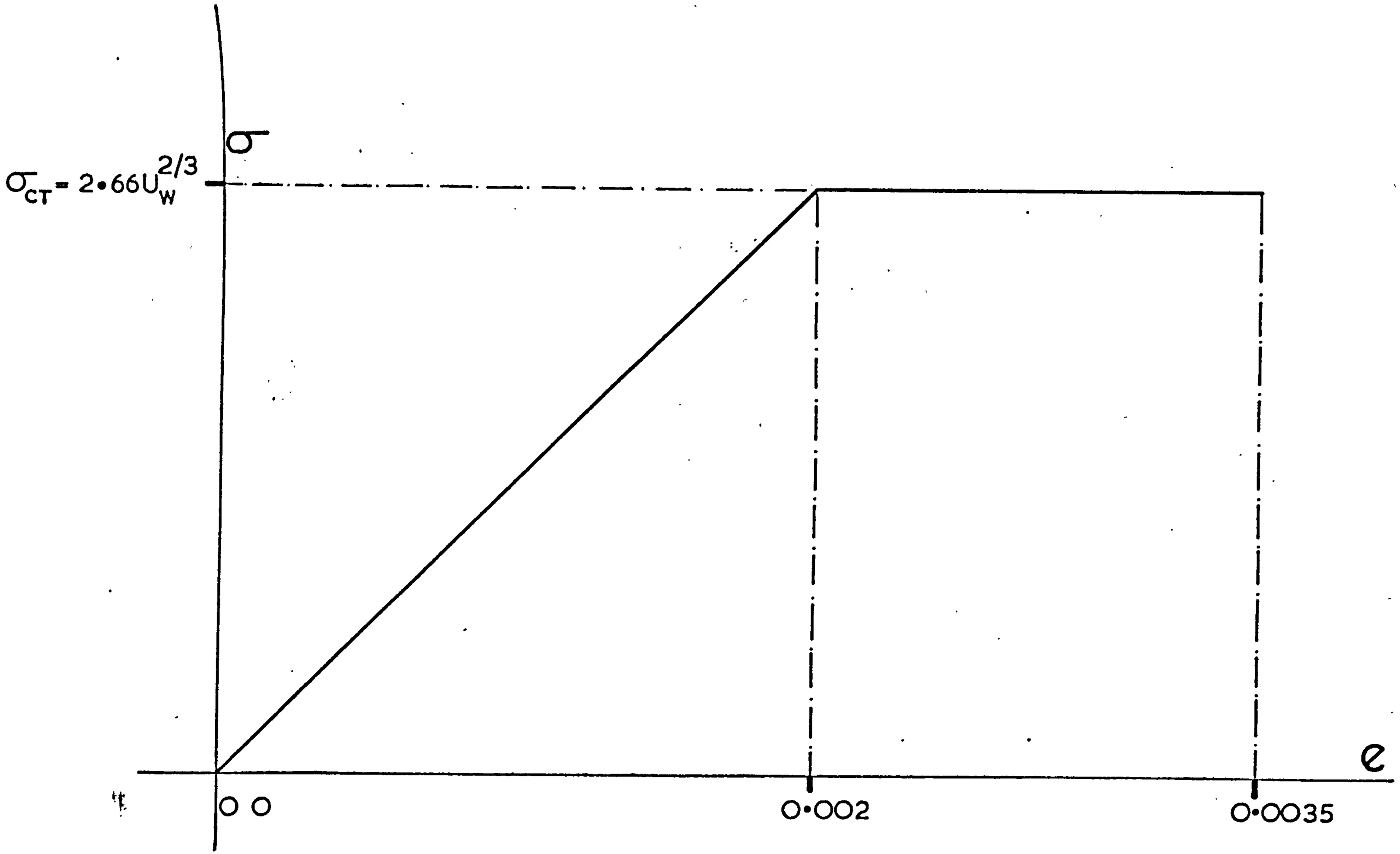

Fig. 67. SIMPLIFIED STRESS-STRAIN CURVE FOR CONCRETE.

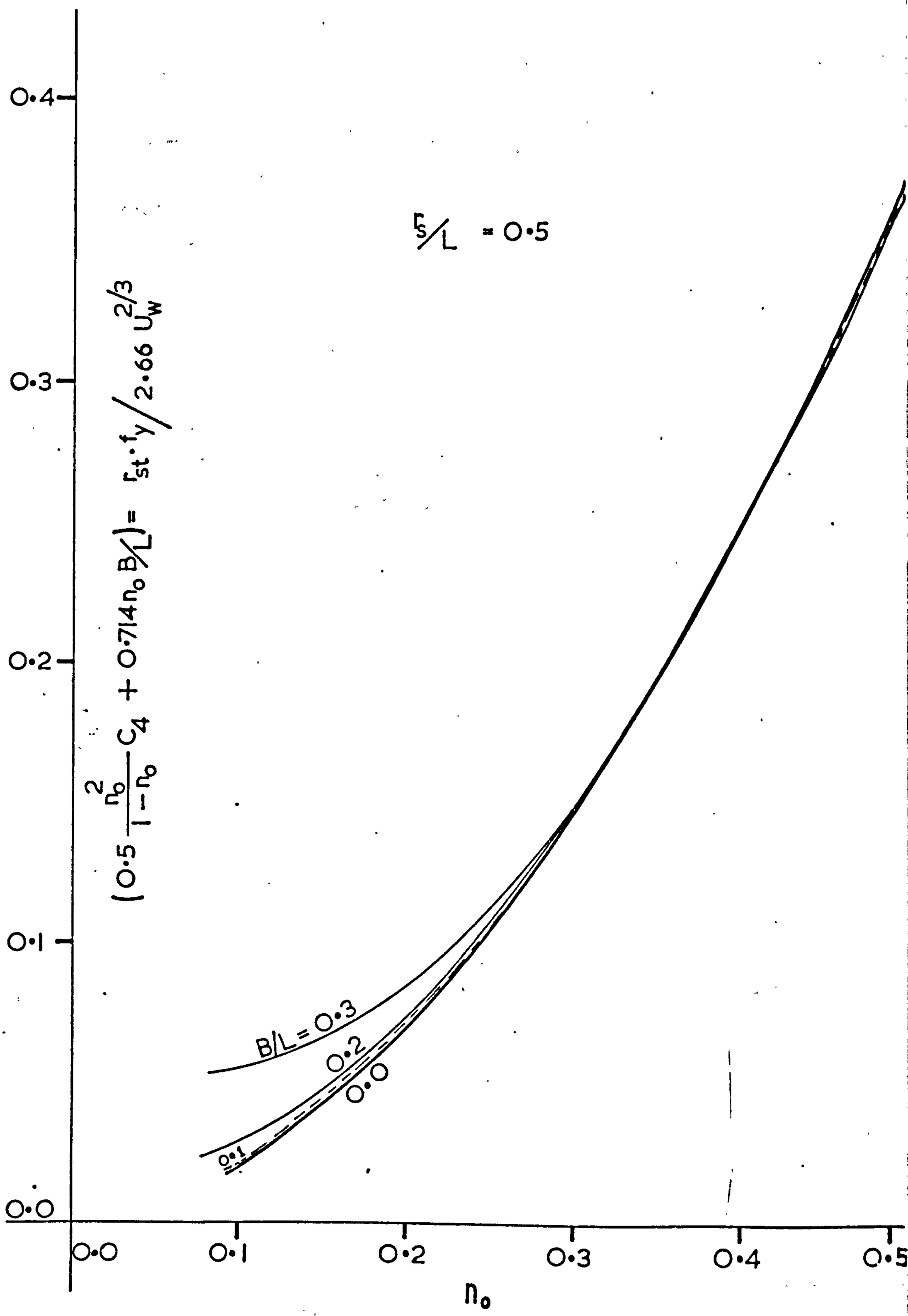
$r_s/L = 0.5$
$\left(0.5\frac{n_o^2}{1-n_o}C_4 + 0.714 n_o B/L\right) = r_{st} \cdot f_y / 2.66\, U_w^{2/3}$
B/L = 0.3
0.2
0.0
0.1
0.0
0.1
0.2
0.3
0.4
0.5
n_o

Fig. 68.

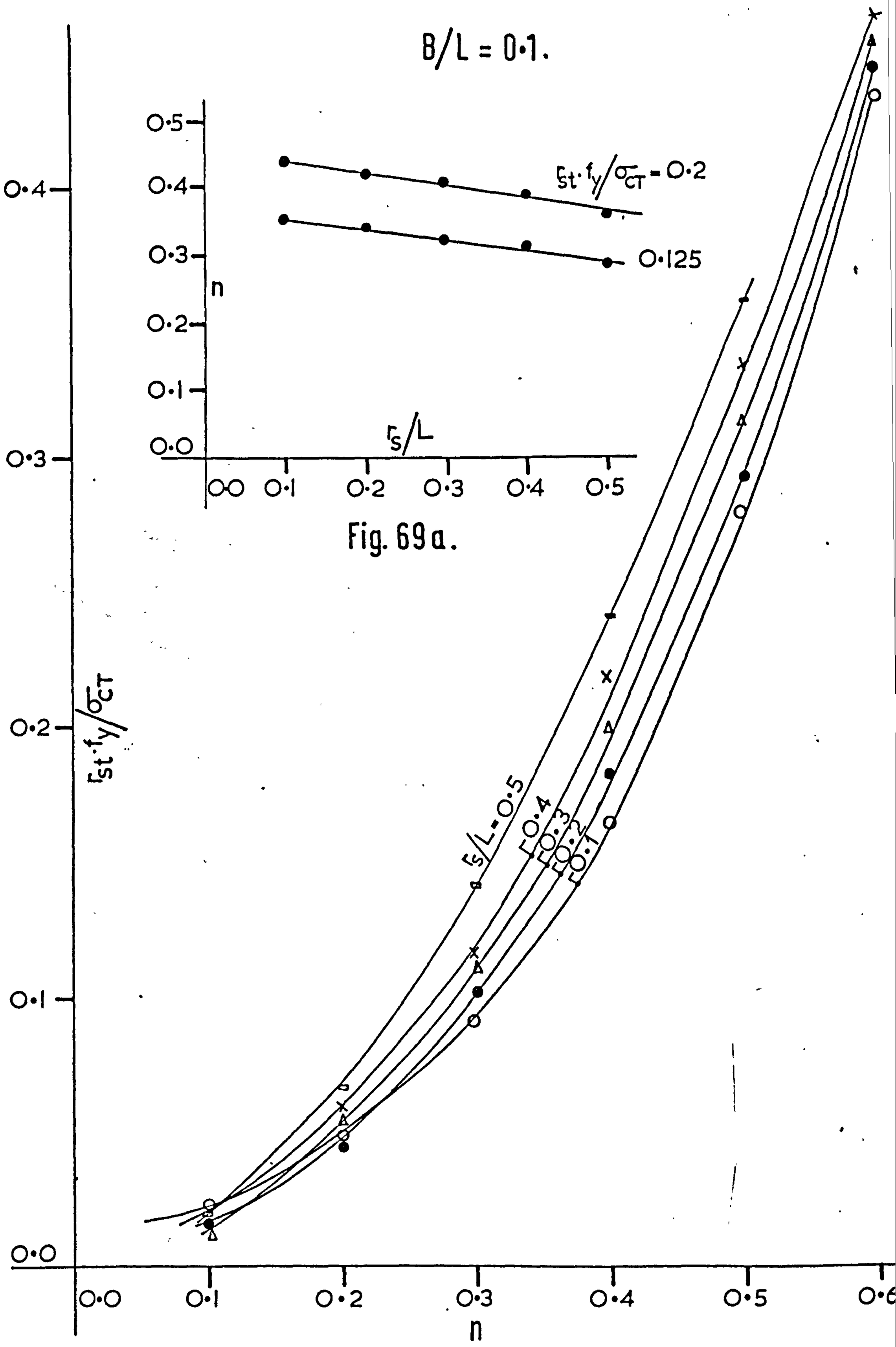

Fig. 69a.

Fig.69. n vs $r_{st}\cdot f_y/\sigma_{CT}$ FOR VARIOUS VALUES OF r_s/L.

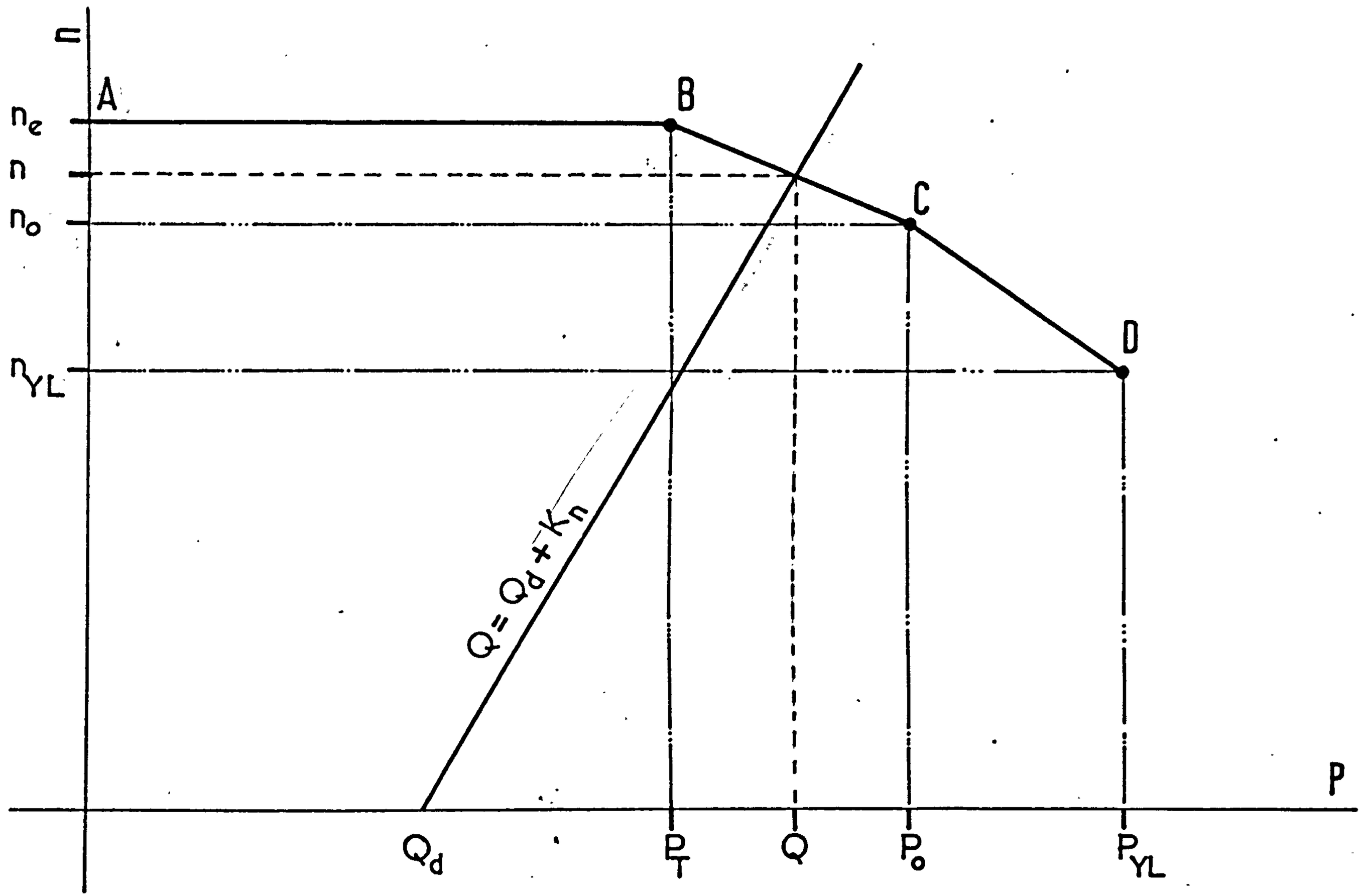

Fig. 70. n vs P

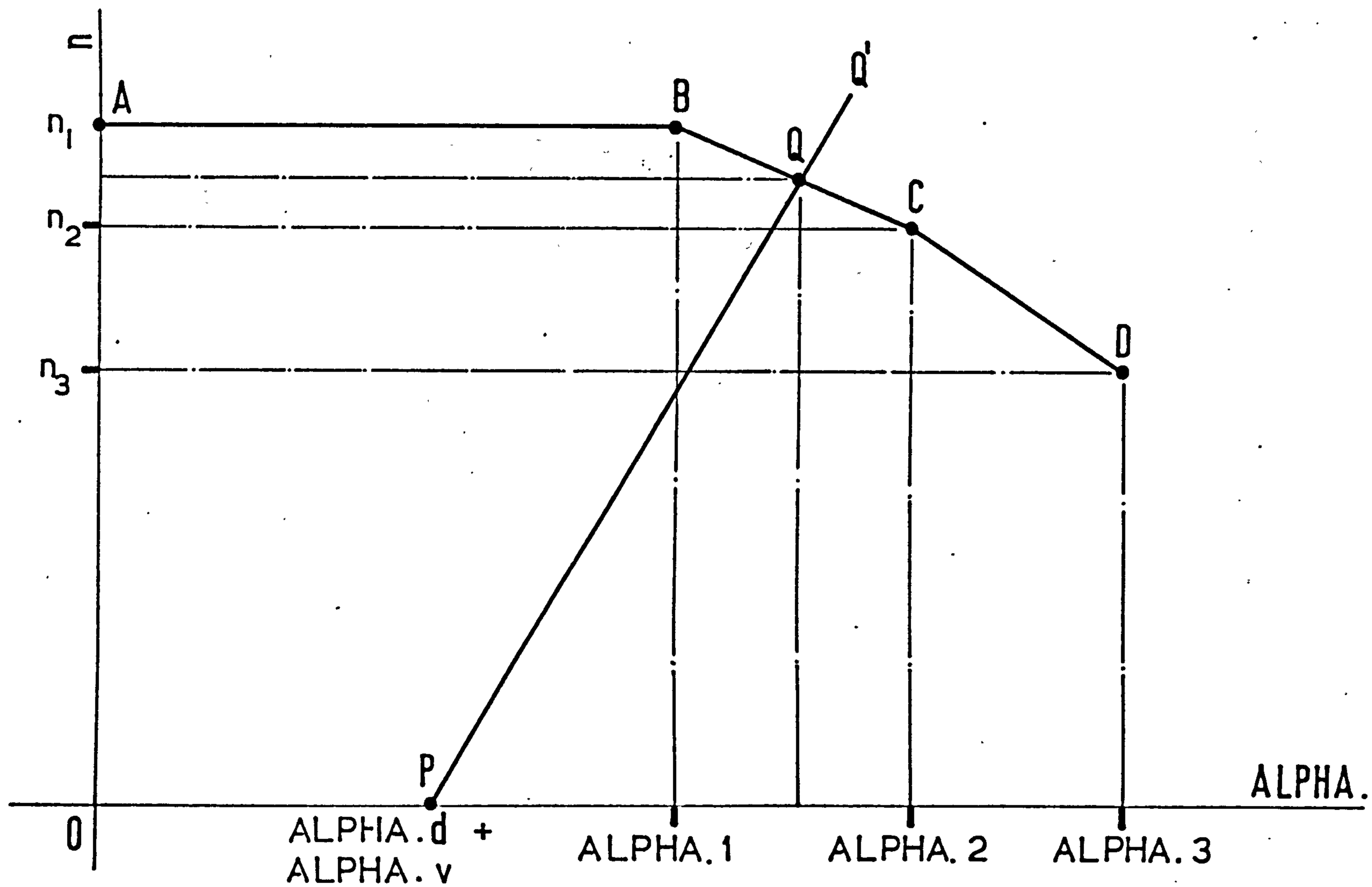

Fig.71. n vs ALPHA.

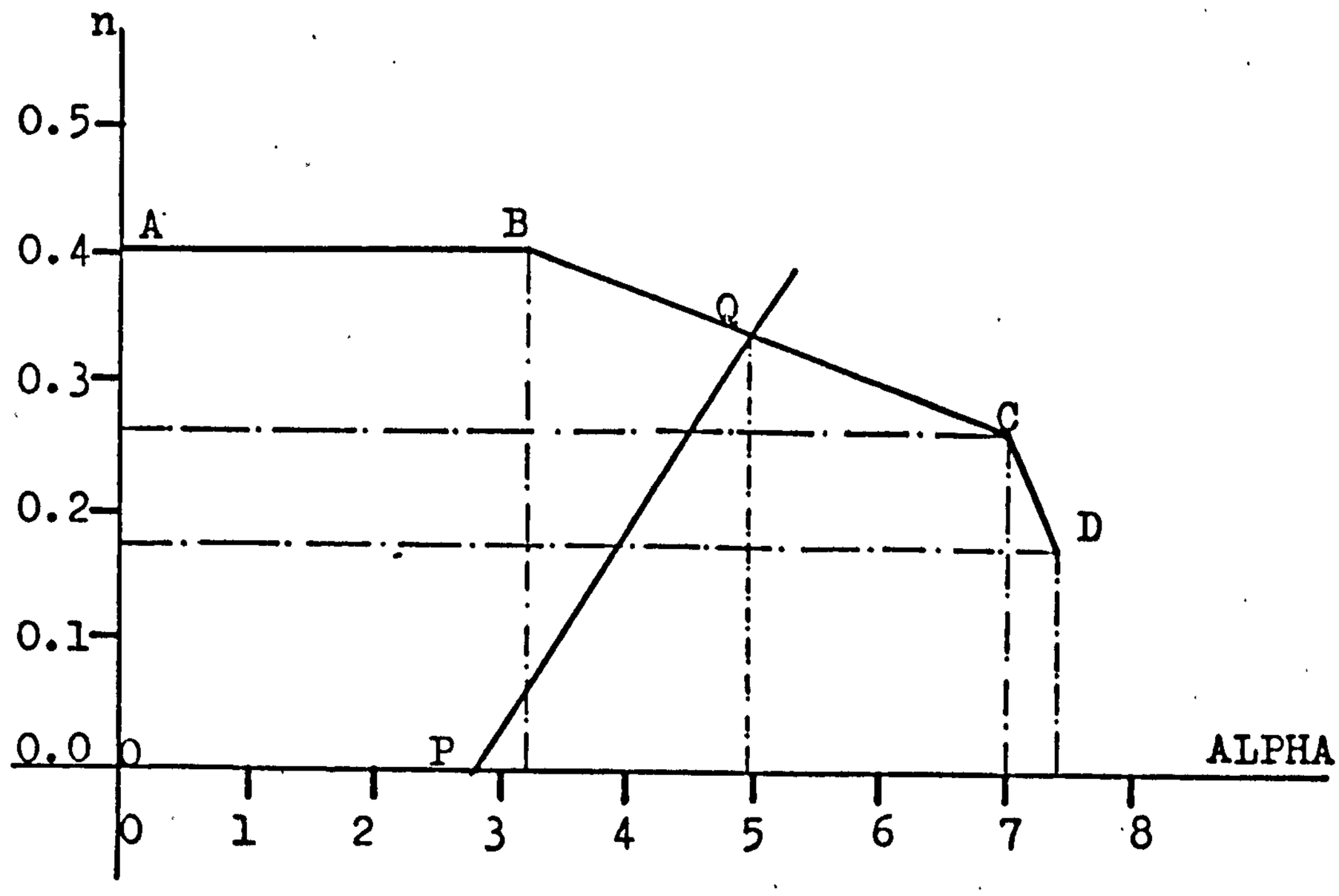

ALPHA d = 2.87; EC = 0; ϕ_v = 0

HS = 0.16; H = 0.107MN; x = 4.96(OP)

Q_{CAL} = 4.96 x 0.107 x 10^6 N = 0.530 MN.

SLAB L9 - CONCENTRIC LOADING.

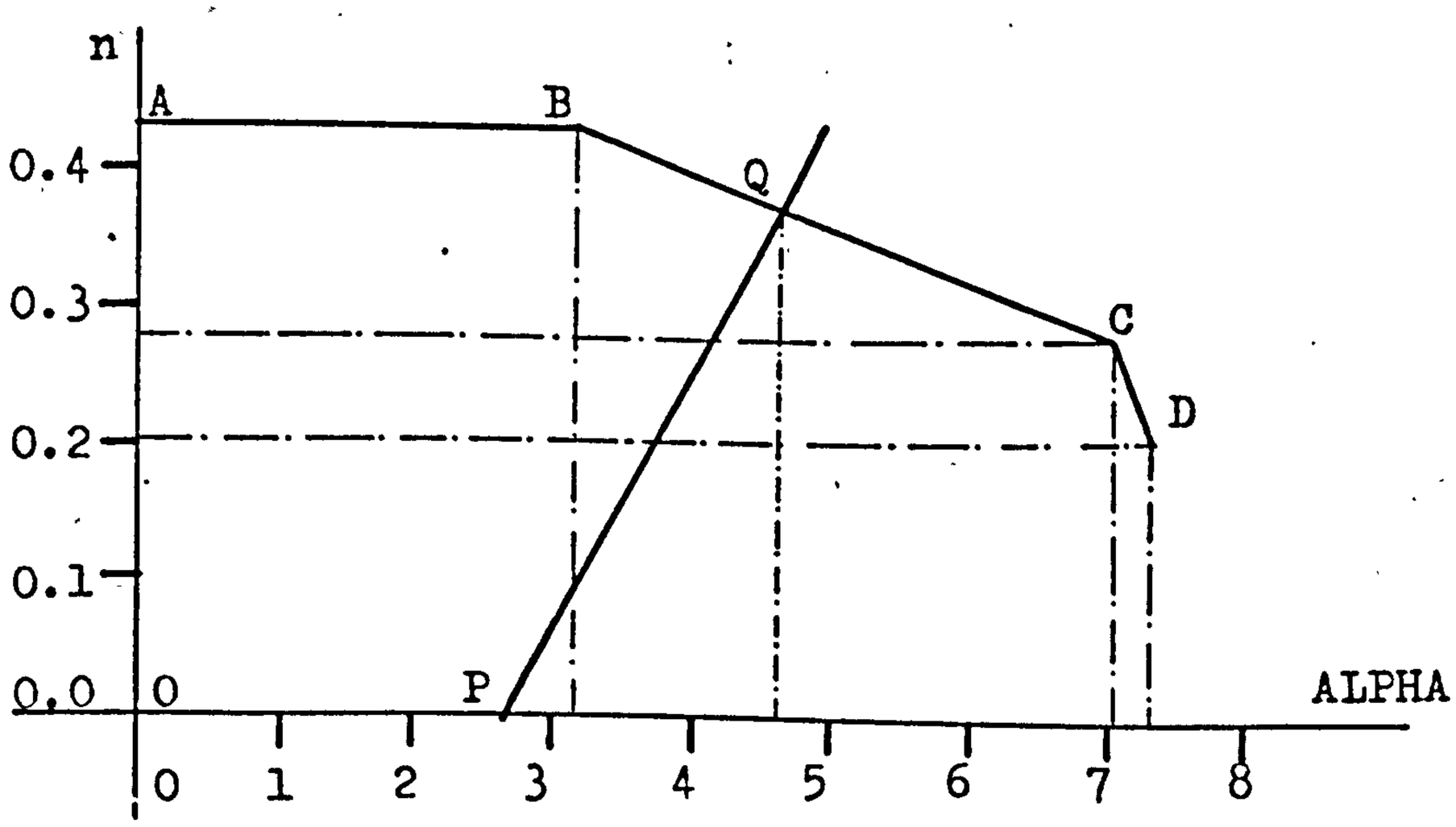

ALPHA d = 2.66; EC = 305 mm; ϕ_v = 0

HS = 0.186; H = 0.107MN; x = 4.65(OP)

$$Q_{CAL} = 4.65 \times 0.107 \times 10^6 \Big/ \left(1 + \frac{4 \times 305}{2010}\right) = 0.310 \text{ MN}$$

SLAB L1 - COMBINED LOADING.

Fig.72. (Sheet 1 of 2)

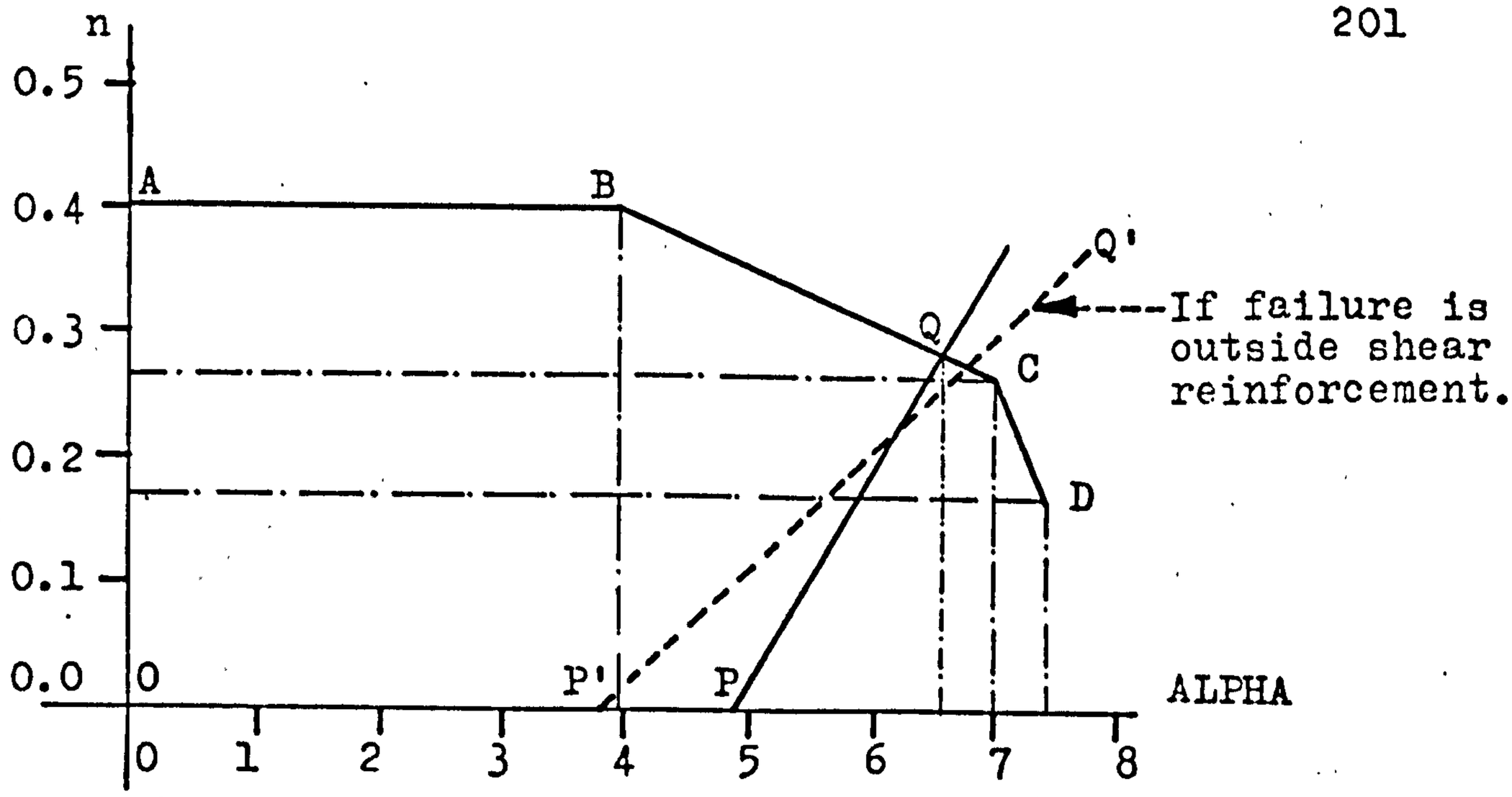

ALPHA d + ALPHA v = 4.85; EC= 305 mm; ϕ_v = 8mm.
HS = 0.158; H = 0.107 MN; x = 6.6 (OP).

$$Q_{CAL} = 6.6 \times 0.107 \times 10^6 \Big/ \left(1 + \frac{4 \times 305}{2010}\right) N = 0.541 \text{ MN.}$$

SLAB L 10 - SLAB WITH COMBINED LOAD + SHEAR REINFORCEMEN
FAILURE PLANE THROUGH SHEAR REINFORCEMENT.

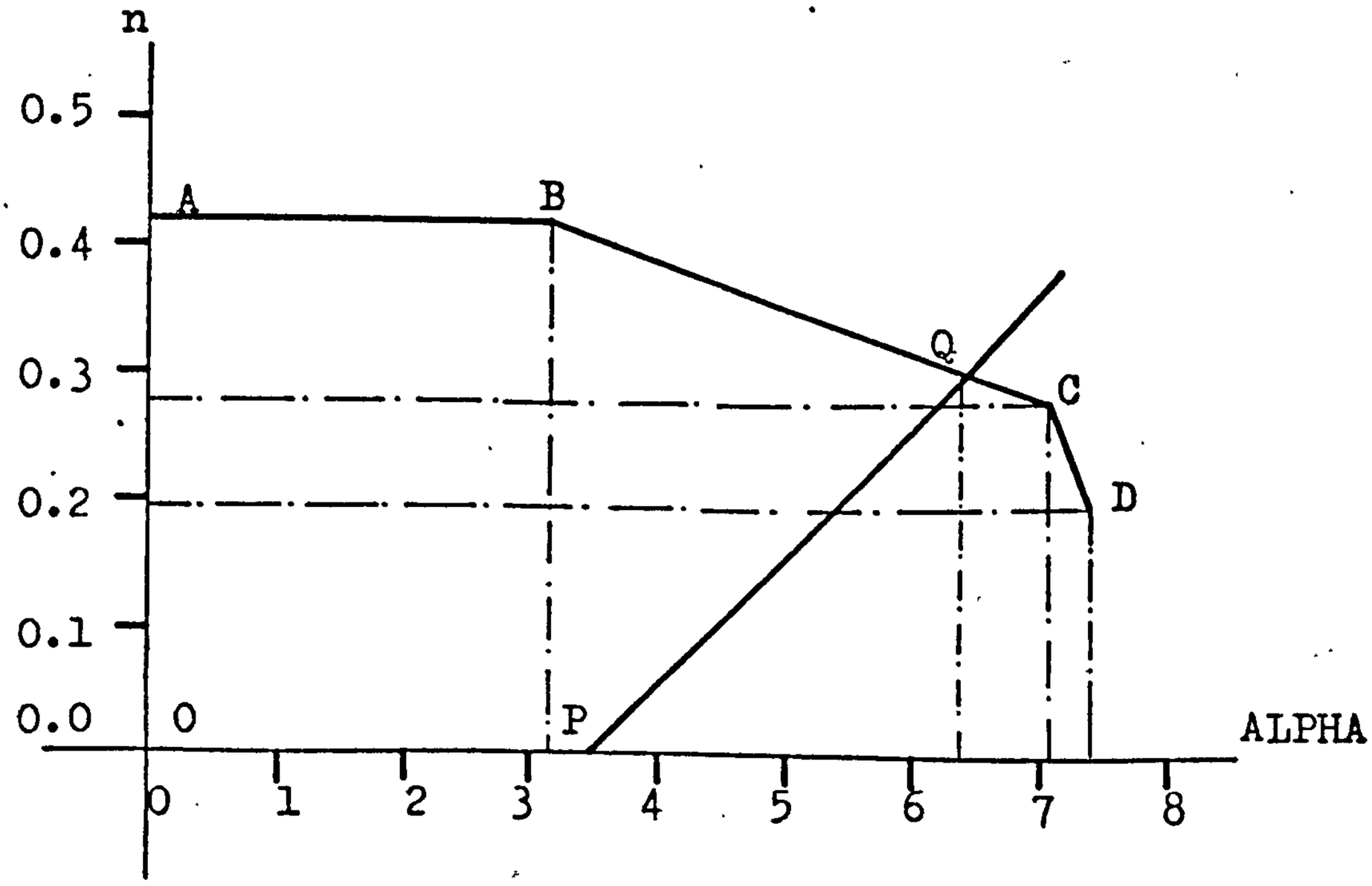

ALPHA d ($2d_1$ outside shear reinforcement) = 3.48
EC=305mm; ϕ_v=13mm; HS=0.103; H=0.107MN; x=6.39(OP).

$$Q_{CAL} = 6.39 \times 0.107 \times 10^6 \Big/ \left(1 + \frac{4 \times 305}{2010}\right) N = 0.426 \text{ MN.}$$

SLAB L5 - SLAB WITH COMBINED LOAD + SHEAR REINFORCEMENT.
FAILURE PLANE OUTSIDE SHEAR REINFORCEMENT.

Fig.72. (Sheet 2 of 2)

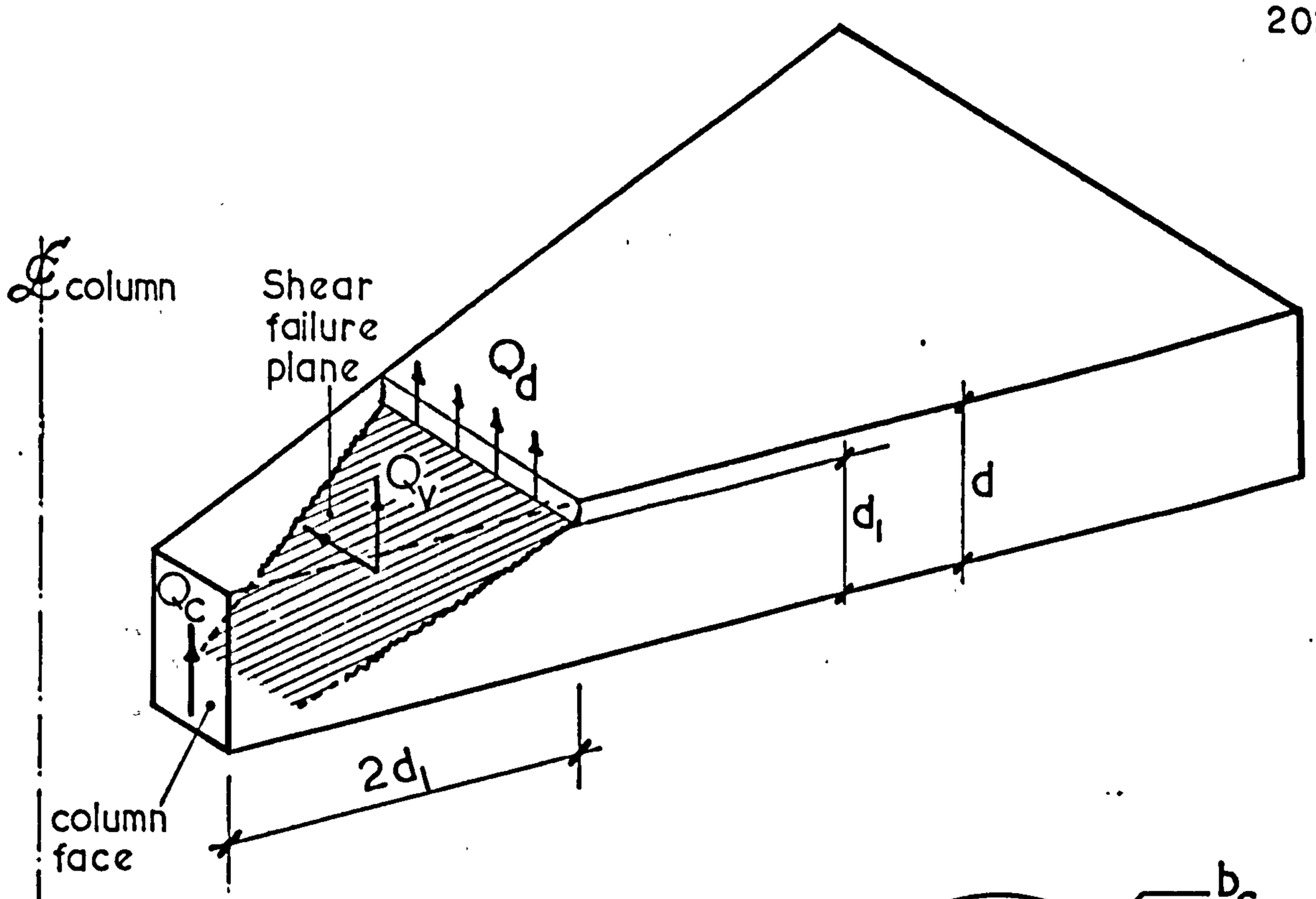

a) Circular column.

$b_c = \pi B$

$b_d = \pi (B + 4d_1)$

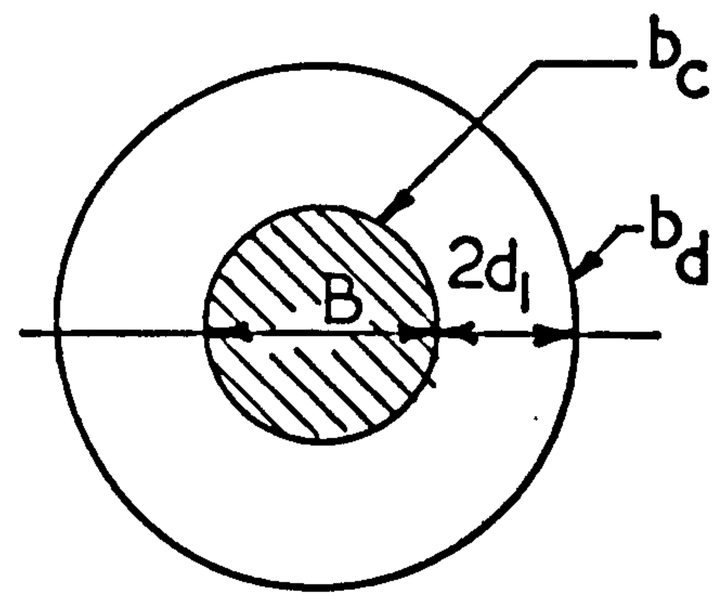

b) Square column.

$b_c = 4b$

$b_d = 4b + 4\pi d_1$

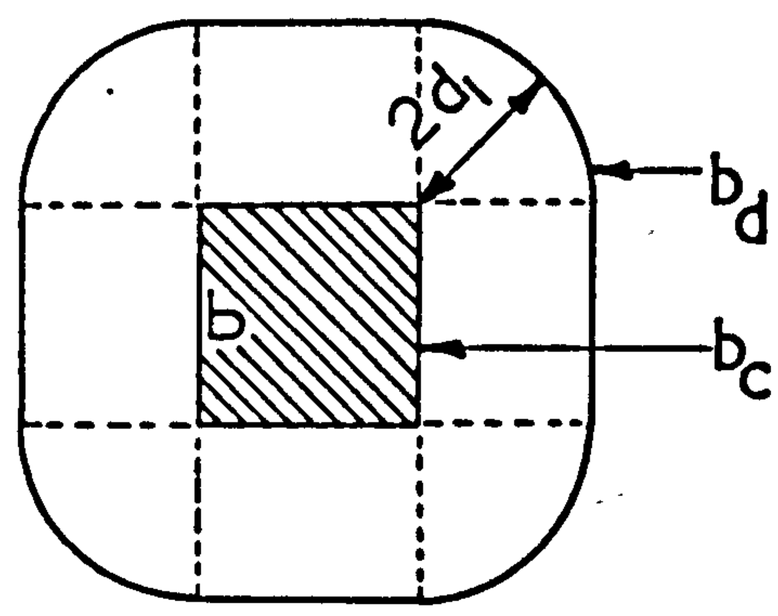

c) Rectangular column.

$b_c = 2(a + b)$

$b_d = 2(a + b) + 4\pi d_1$

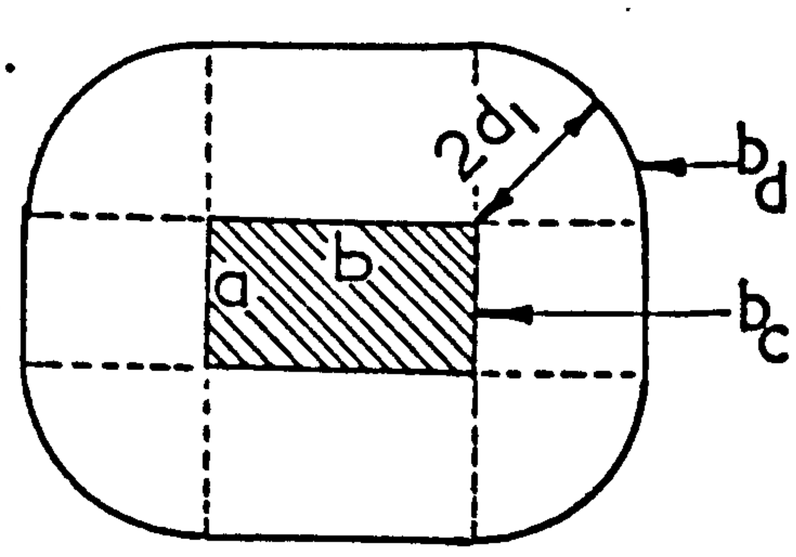

NOTE:

b_c = column or concrete perimeter.

b_d = dowel perimeter.

Fig. 73.

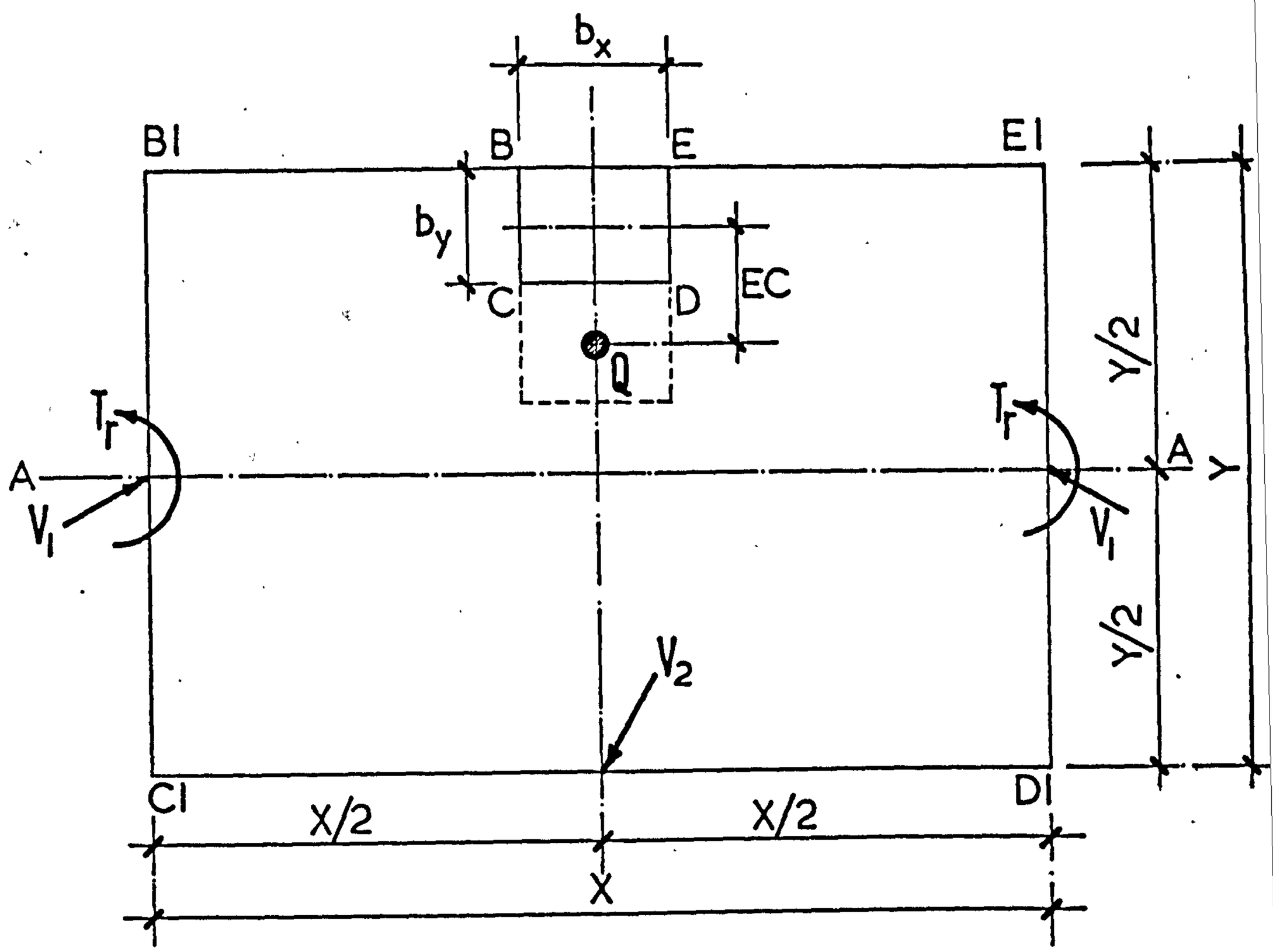

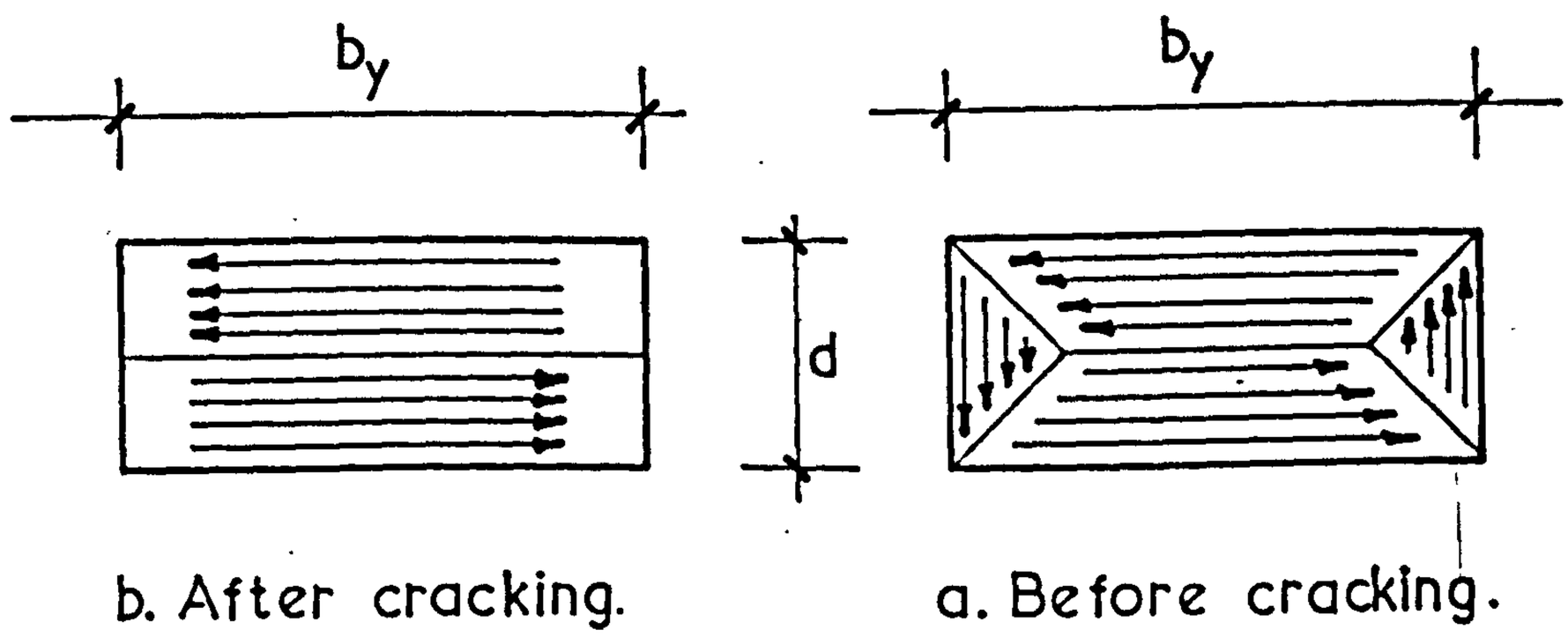

Torsional Shear Stress Distribution.

Fig. 74.

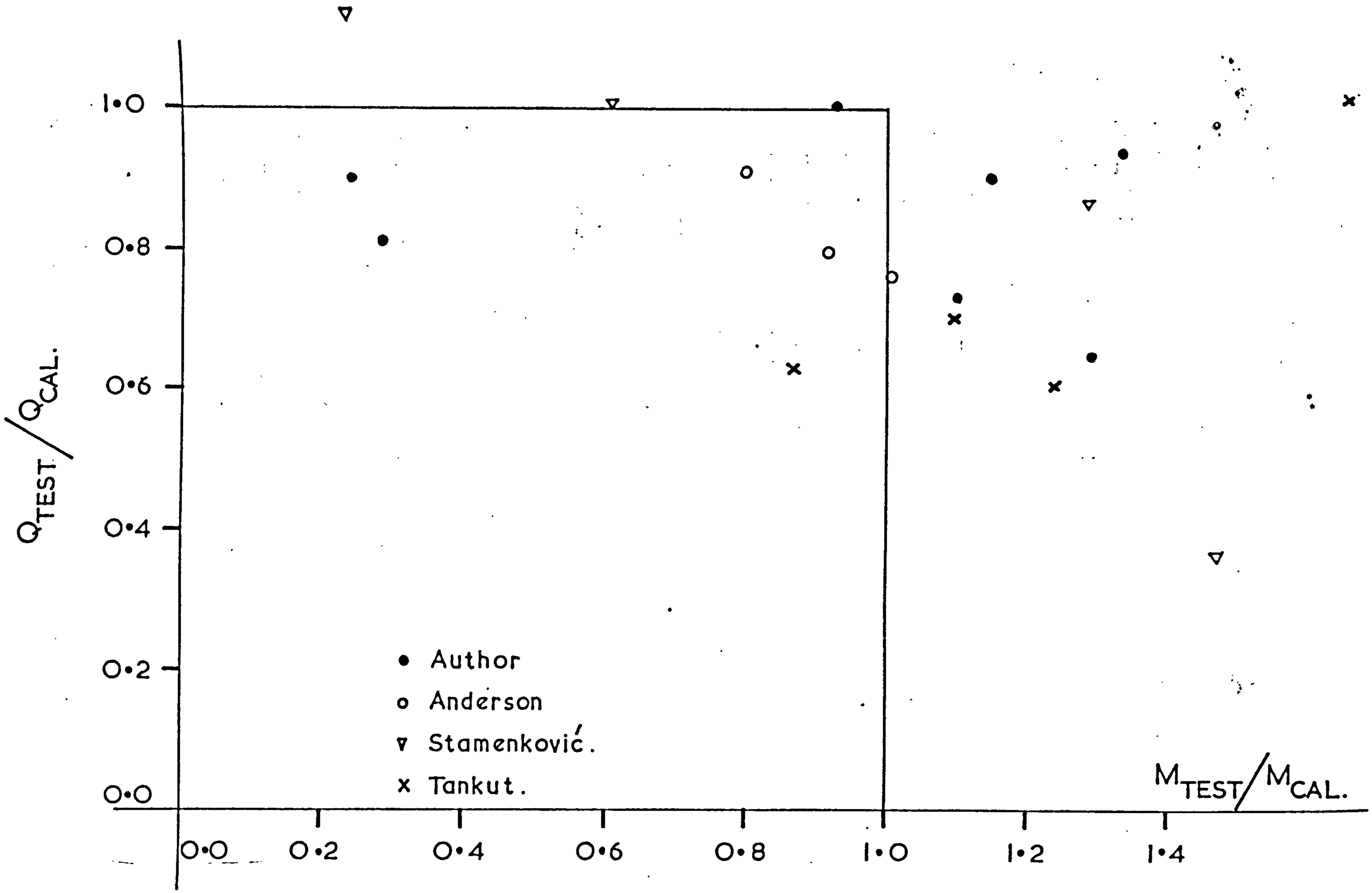

Fig.75. INTERACTION DIAGRAM – EDGE COLUMNS WITH MOMENTS PERPENDICULAR TO THE FREE EDGE.

CHAPTER VII

ANALYSIS OF TEST RESULTS USING PROPOSED SOLUTION.

7.1 Introduction:

Here the test results available from various sources are analysed in the light of proposed solution. Only slabs with two-way reinforcement which failed in shear are considered. Flexural failure loads in the case of internal column connections were calculated as outlined by Anis[18] in order to eliminate slabs which failed in flexure. Some of the test results which lacked sufficient information have not been used. For example, if support conditions are unknown, it is possible that the slabs were laterally restrained, and could carry much higher loads than those predicted by the proposed method or Yield line analysis, for a slab simply supported all round.

The average ratios of Q_{CAL}/Q_{TEST}, standard deviations and coefficient of variation for the slabs tested by the various authors are given independently under each set of results. The overall values for all results together were also calculated and in the case of internal-column connections (total number of slabs - 163) the average Q_{CAL}/Q_{TEST} is 0.938, the standard deviation 0.129 and the coefficient of variation being 13.729%.

It can be seen that the ratios of $\frac{Q_{CAL}}{Q_{TEST}}$, in the case of circular slabs with circular columns, are considerably less than unity, predicting loads well on the safe side, whilst in the case of square slabs with square columns, the ratio of loads is closer to unity. This may be due to the fact that the same average shear stress at failure is assumed in both cases, while actually it may not be so. In the case of square columns a non uniform distribution of shear stress around the column exists (see chapter V), while in the case of circular columns it is uniform. Under these circumstances, the limiting shear stress that can be attained in the case of a circular column may be higher than the one for a square column at failure. This justifies the low values of $\frac{Q_{CAL}}{Q_{TEST}}$ in the case of circular columns.

The moment strength of the connections in the case of edge columns (with normal moment and corner columns) were calculated as outlined in chapter VI, sections 6.11 and 6.13. The values are tabulated along with the predicted shear failure loads in Table VII-22 and VII-10.

7.1.1. Effect of Eccentricity of the load:

In the case of internal column connections and edge columns subjected to tangential moment, a reduction factor of $\frac{1}{1 + 4.\frac{EC}{L}}$ applied to the calculated concentric load, Q_o, gave excellent predictions. Figure 77 shows Q/Q_o values against EC/L values for internal columns and Figure 76 shows the same for external columns subjected to tangential moments.

7.1.2. Effect of column size to slab depth:

Slabs with small columns seem to have higher unit shearing strengths, than those with a large ratio of column size to depth. Figure 78 shows Q_{CAL}/Q_{TEST} against b/d, ratio for internal columns. b was taken as $\frac{\text{column perimeter}}{4}$ in the case of circular columns. No appreciable data is available for external and corner columns.

7.1.3. Effect of main reinforcement:

The influence of main reinforcement, on the shear strength, is felt through its control of deformation and cracking of the structure, and through dowel action. Dowel forces are dependent on the bar diameter provided the spacing is not too great, but not much affected by the number of bars in a given width of concrete. Concentration of reinforcement near a column is thus unlikely to have much effect on the dowel action. The control of the deformation is a function of all the reinforcement within the contraflexure perimeter, approximately the column strip. Thus concentration of reinforcement is unlikely to achieve anything.

This lack of benefit due to concentration of reinforcement, has been already established by tests by Moe[19]. The reinforcement over the whole width of the slab was used in determining the value of r_{st} in the proposed solution. It could be seen from Table VII-16 that

the predicted loads are in reasonable agreement with the test load.

7.1.4. Effect of openings:

The loss of strength when openings are present near the column, seems to be adequately taken into account by deducting the width of the holes from the perimeters b_c and b_d in the case of internal columns. The predicted loads give good agreement with the actual loads as can be seen from Table VII-17. Figure 79 shows $\frac{Q_{TEST}}{Q_{CAL}}$ V$_s$ $\frac{\text{width of opening}}{\text{column perimeter}}$ in the case of internal columns. However in the case of edge columns, in the absence of adequate data it is not possible to draw such conclusions.

7.1.5. Effect of shear reinforcement:

The contribution of the shear reinforcement added to the concrete and dowel terms, in the case of slabs where the shear failure plane cuts the shear reinforcement gives good prediction of the ultimate load. However there is the other possibility that it could fall outside the shear reinforcement. In cases where the exact location of the failure plane is not known, two sets of calculation are required to obtain the required value, 1) Q_c at the column perimeter + Q_d, perimeter $2d_1$ out from column face + Q_v and 2) Q_c, at a perimeter just outside the end of shear reinforcement + Q_d, a perimeter $2d_1$ out from the concrete perimeter.

The lower of the above two, is taken as Q_{CAL} in the foregoing tables.

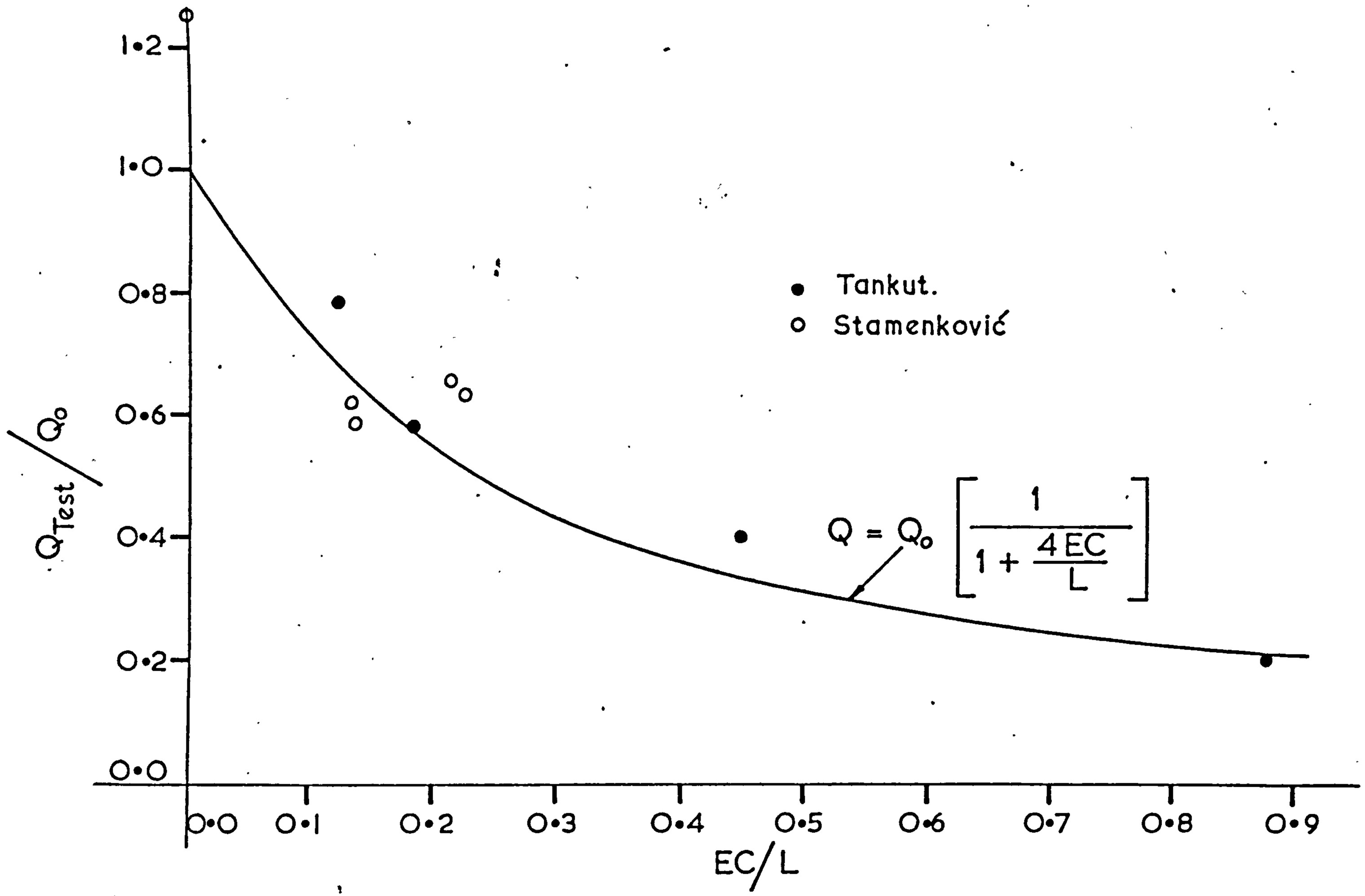

Fig.76. EFFECT OF ECCENTRICITY - EDGE COLUMNS WITH TANGENTIAL MOMENTS.

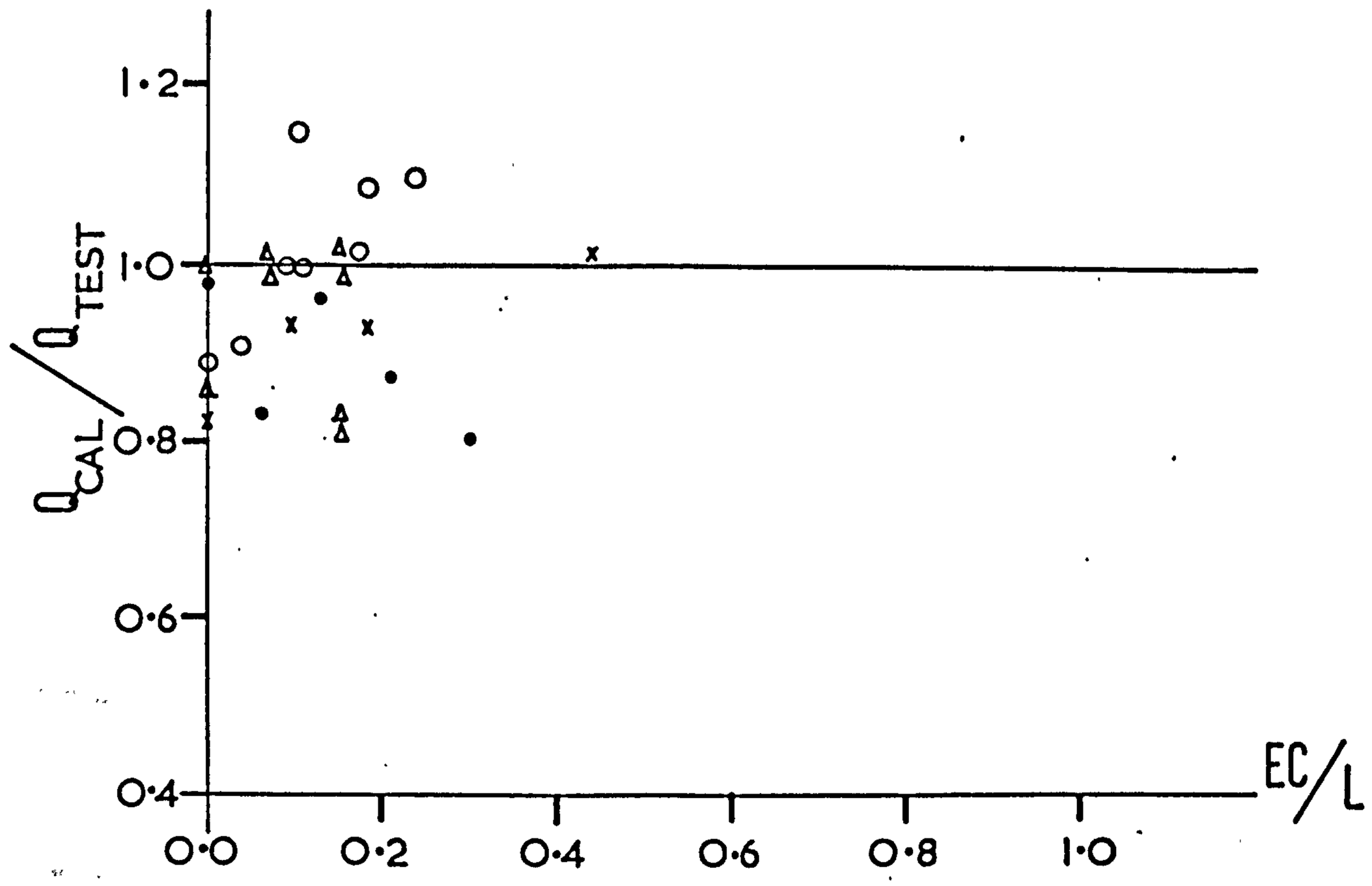

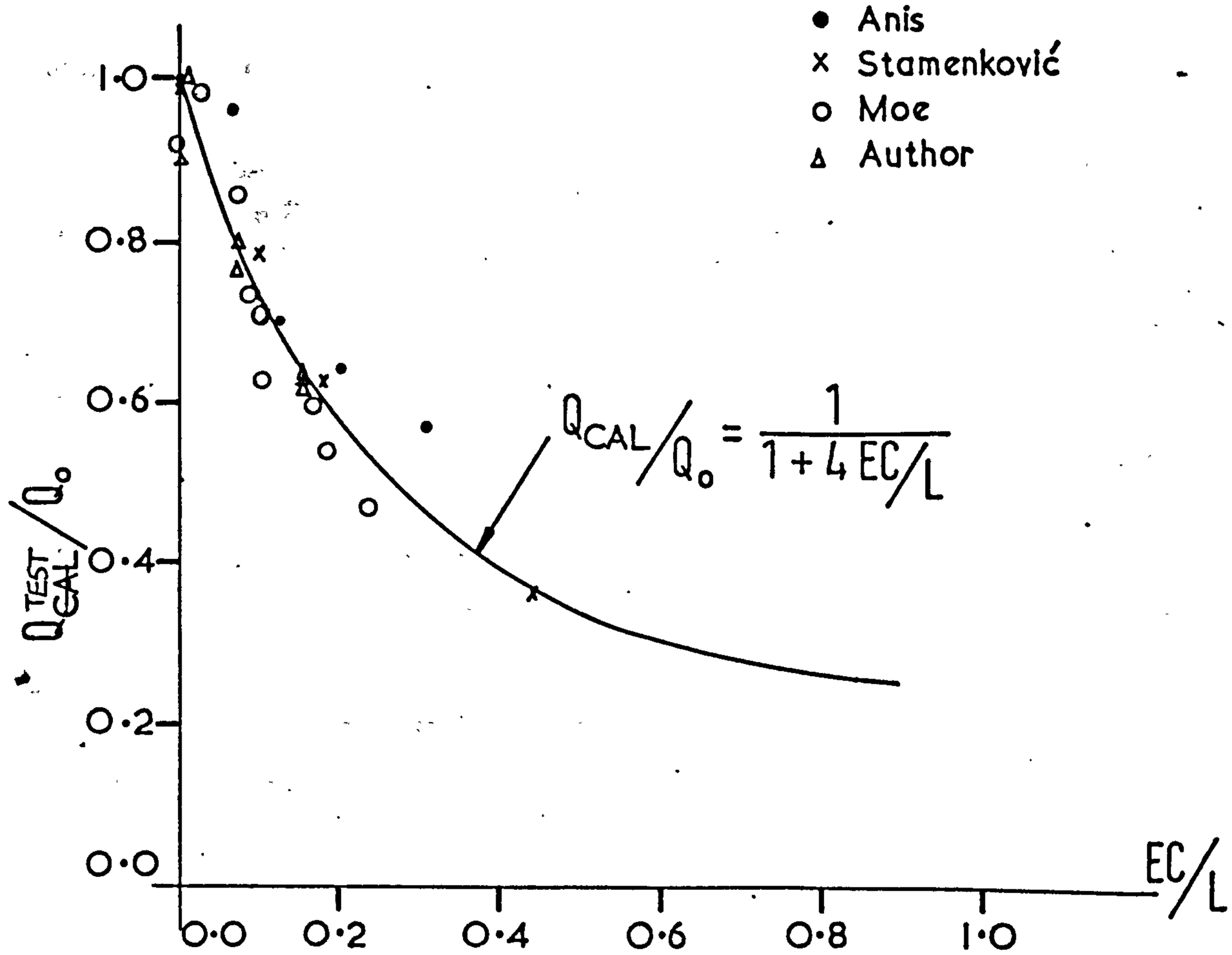

Fig. 77. EFFECT OF ECCENTRICITY.

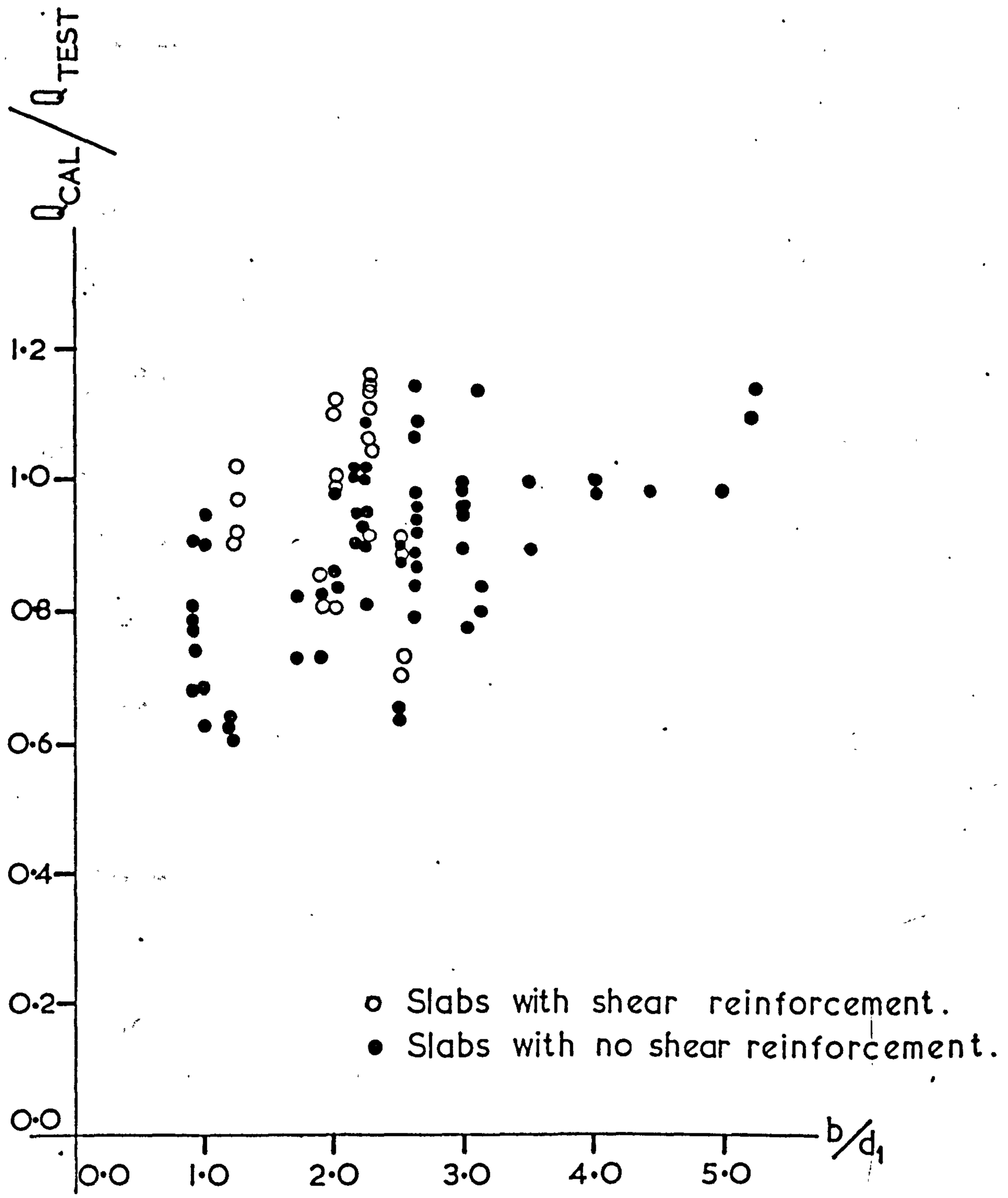

Fig. 78. INFLUENCE OF b/d_1 RATIO.

(Column side/effective depth)

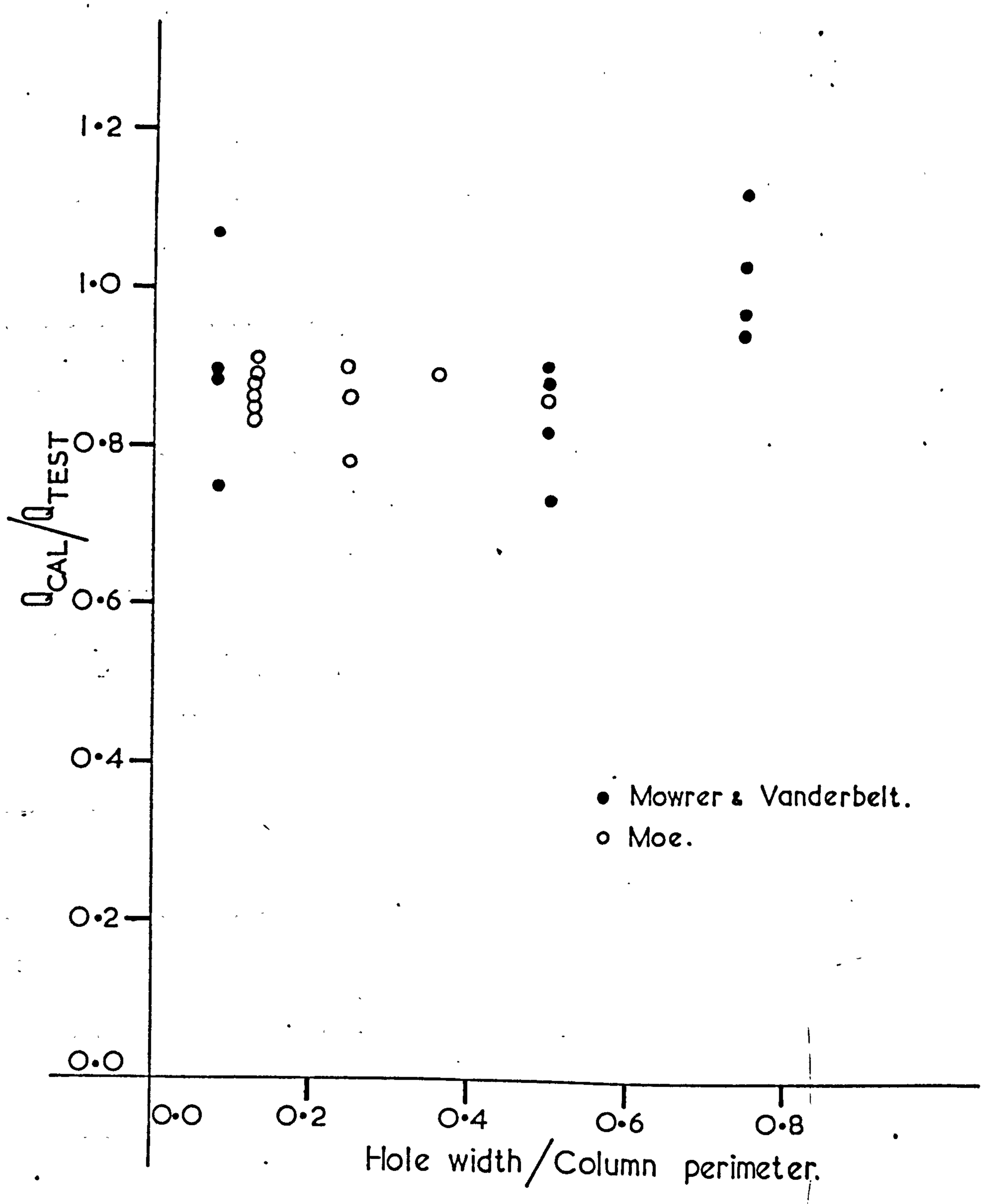

Fig.79. EFFECT OF HOLE WIDTH.

Slab No.	r_{st} %	f_y N/mm^2	U_w N/mm^2	b mm	ϕ_M mm	d_1 mm	Q_{TEST} M.N.	Q_o M.N.	Q_D M.N.	Q_{CAL} M.N.	$\frac{Q_{CAL}}{Q_{TEST}}$
A-1a	1.15	332	16.5	254	19	117.5	0.302	0.128	0.155	0.283	0.94
A-1b	1.15	332	29.6	254	19	117.5	0.364	0.162	0.188	0.350	0.96
A-1c	1.15	332	34.1	254	19	117.5	0.356	0.171	0.197	0.368	1.03
A-1d	1.15	332	43.3	254	19	117.5	0.351	0.188	0.213	0.384	1.14
A-1e	1.15	332	23.8	254	19	117.5	0.356	0.148	0.175	0.323	0.91
A-2a	2.47	321	16.0	254	25	114.0	0.334	0.166	0.202	0.368	1.10
A-2b	2.47	321	22.8	254	25	114.0	0.400	0.192	0.227	0.419	1.05
A-2c	2.47	321	44.1	254	25	114.0	0.470	0.249	0.282	0.531	1.13
A-7b	2.47	321	32.8	254	25	114.0	0.511	0.222	0.256	0.478	0.93
A-3a	3.70	321	15.1	254	25	114.0	0.356	0.191	0.198	0.389	1.09
A-3b	3.70	321	26.6	254	25	114.0	0.445	0.240	0.239	0.479	1.08
A-3c	3.70	321	31.2	254	25	114.0	0.534	0.255	0.252	0.507	0.95
A-3d	3.70	321	40.7	254	25	114.0	0.547	0.284	0.275	0.559	1.02
A-4	1.15	321	30.7	356	19	117.5	0.400	0.230	0.221	0.451	1.13
A-5	2.47	321	32.7	356	25	114.0	0.534	0.310	0.298	0.608	1.14
A-6	3.70	321	29.4	356	25	114.0	0.498	0.341	0.288	0.629	1.26
B-9	2.0	341	51.7	254	22	114.0	0.505	0.244	0.260	0.504	1.00
B-11	3.0	408	15.9	254	25	114.0	0.329	0.179	0.201	0.381	1.16
B-14	3.0	326	59.5	254	25	114.0	0.578	0.304	0.311	0.615	1.06

Note: All slabs were 1830mm square and dowel constant $K_d = 1.3$

Average $Q_{CAL}/Q_{TEST} = 1.055$

Standard Deviation = 0.091

Coefficient of variation = 8.64%

TABLE VII-1 Slabs tested by HOGNESTAD(4) - Concentric Load.

Slab No.	r_{st} %	f_y N/mm^2	U_w N/mm^2	b mm	ϕ_M mm	d_1 mm	Q_{TEST} M.N.	Q_c M.N.	Q_d M.N.	Q_{CAL} M.N.	$\frac{Q_{CAL}}{Q_{TEST}}$
H1-11A6 IV	1.15	355	26.6	254	16	114	0.280	0.150	0.127	0.277	0.99
H1-11A6 VIII	1.15	355	33.3	254	16	114	0.311	0.164	0.137	0.301	0.97
H1-12A6 I	1.15	355	40.9	254	16	114	0.328	0.178	0.147	0.325	0.99
H1-13A6 VI	1.15	355	35.6	254	16	114	0.324	0.169	0.140	0.309	0.95

Note: All slabs were 1830 mm square. Dowel constant K_d = 1.1

Average Q_{CAL}/Q_{TEST} = 0.975

Standard Deviation = 0.019

Coefficient of variation = 1.964%

TABLE VII-2 Slabs tested by IVY[44] - Concentric Load.

Slab No.	r_{st} %	f_y N/mm^2	U_w N/mm^2	b mm	d_1 mm	Q_{TEST} M.N.	Q_c M.N.	Q_d M.N.	Q_{CAL} M.N.	$\frac{Q_{CAL}}{Q_{TEST}}$
IA 15a 5	0.80	441	32.8	150	117	0.255	0.067	0.133	0.200	0.78
IA 15a 6	0.79	454	33.1	150	118	0.274	0.068	0.134	0.202	0.74
IA 15b 9	1.59	446	31.8	150	117	0.274	0.088	0.131	0.219	0.80
IA 15b 10	1.59	448	31.8	150	117	0.274	0.088	0.131	0.219	0.80
IA 30a 24	1.01	455	32.4	300	128	0.429	0.161	0.173	0.334	0.78
IA 30b 25	1.04	451	30.8	300	124	0.407	0.155	0.167	0.322	0.79

Note: All slabs were 1710 mm diameter. Dowel constant K_d = 1.8, ϕ_M = 12 mm

Average Q_{CAL}/Q_{TEST} = .780

Standard Deviation = .026

Coefficient of variation = 3.343%

TABLE VII-3 Slabs tested by KINNUNEN and NYLANDER(14) - Concentric Load.

Slab No.	r_{st} %	f_y N/mm^2	U_w N/mm^2	b mm	L mm	Q_{TEST} M.N.	Q_c M.N.	Q_d M.N.	Q_{CAL} M.N.	$\frac{Q_{CAL}}{Q_{TEST}}$
M2-1-0	1.1	386	33.6	101	1220	0.085	0.029	0.041	0.070	0.82
M2-2-0	2.2	386	28.2	101	1220	0.101	0.035	0.039	0.074	0.73
M3-1-0	1.1	386	24.8	150	1220	0.079	0.038	0.044	0.082	1.04
M3-2-0a	2.2	386	21.2	150	1220	0.099	0.047	0.042	0.089	0.90
M3-2-0b	2.2	386	63.2	150	1220	0.171	0.072	0.060	0.132	0.77
M4-1-0	1.1	386	18.2	203	1220	0.092	0.047	0.045	0.092	1.00
M4-2-0	2.2	386	32.0	203	1220	0.132	0.075	0.056	0.131	0.99
M5-2-0	2.2	386	26.9	254	1220	0.151	0.087	0.061	0.148	0.98
M6-2-0	2.2	386	31.0	305	1220	0.158	0.111	0.071	0.182	1.14
M7-2-0	2.2	386	29.4	356	1220	0.185	0.126	0.078	0.204	1.10
JL-0-1.7a	1.7	352	16.5	152	915	0.081	0.038	0.033	0.071	0.88
JL-0-2.2a	2.2	352	14.3	152	915	0.084	0.041	0.031	0.072	0.86
JL-0-1.7b	1.7	352	31.3	152	915	0.096	0.050	0.041	0.091	0.94
JL-0-2.2b	2.2	352	22.0	152	915	0.079	0.048	0.036	0.084	1.07
JL-0-1.1	1.1	352	45.3	152	915	0.103	0.049	0.046	0.095	0.92

Note: Dowel constant K_d = 1.3, ϕ_M = 9.5 mm and d_1 = 51 mm.

Average Q_{CAL}/Q_{TEST} = 0.949

Standard Deviation = 0.119

Coefficient of variation = 12.58%

TABLE VII-4. Slabs tested by MOWRER and VANDERBELT[45] - Concentric Load.

TABLE VII-5 Slabs Tested by MANTEROLA[53] - Concentric Load.

Slab No.	r_{st} %	f_y N/mm^2	U_w N/mm^2	b mm	Q_{TEST} M.N.	Q_c M.N.	Q_d M.N.	Q_{CAL} M.N.	$\frac{Q_{CAL}}{Q_{TEST}}$
P1-S1	0.92	304	30.1	100	0.216	0.053	0.116	0.169	0.78
P1-S2	0.92	324	28.5	100	0.196	0.052	0.114	0.166	0.85
P1-S3	0.92	324	46.7	100	0.184	0.063	0.134	0.197	1.07
P2-S3	1.22	324	42.1	100	0.211	0.068	0.129	0.198	0.94

Note: All slabs were 3000 mm square, Dowel constant K_d = 1.8, d_1 = 107 mm
ϕ_M = 12 mm

Average Q_{CAL}/Q_{TEST} = 0.910

Standard deviation = 0.125

Coefficient of variation = 13.75%

TABLE VII-6 Slabs Tested by HOGNESTAD, ELSNER AND HANSON[60]

Slab No.	U_w N/mm^2	b mm	Q_{TEST} M.N.	Q_c M.N.	Q_d M.N.	Q_{CAL} M.N.	$\frac{Q_{CAL}}{Q_{TEST}}$
H1 L3	35.3	254	0.311	0.123	0.167	0.290	0.93
H1 L4	32.3	254	0.311	0.112	0.162	0.274	0.88
H6	33.4	254	0.245	0.058	0.130	0.188	0.77
H6 L3	32.1	254	0.210	0.056	0.128	0.184	0.88
H6 L4	31.7	254	0.200	0.055	0.127	0.182	0.91

Note: All slabs were 1830 mm square. Dowel constant $K_d = 1.3$

$r_{st} = 1.15\%$, $f_y = 328\ N/mm^2$, $d_1 = 114$ mm and $\phi_M = 16$ mm

Average $Q_{CAL}/Q_{TEST} = 0.874$

Standard deviation = 0.062

Coefficient of variation = 7.081%

Slab No.	r_{st} %	f_y M/mm^2	U_w N/mm^2	b mm	ϕ_M mm	EC mm	Q_{TEST} M.N.	Q_c M.N.	Q_d M.N.	Q_{CAL} M.N.	$\frac{Q_{CAL}}{Q_{TEST}}$
M-1A	1.50	481	24.2	305	19	0	0.433	0.193	0.187	0.381	0.88
M-2A	1.50	481	18.3	305	19	185	0.213	0.173	0.171	0.244	1.15
M-4A	1.50	481	20.7	305	19	435	0.144	0.182	0.178	0.182	1.28
M-2	1.50	481	30.3	305	19	195	0.294	0.211	0.202	0.289	0.98
M-3	1.50	481	26.7	305	19	338	0.209	0.201	0.194	0.227	1.09
M-6	1.34	327	31.1	254	16	168	0.239	0.170	0.158	0.240	1.00
M-7	1.34	327	29.4	254	16	61	0.315	0.166	0.155	0.284	0.90
M-8	1.34	327	29.0	254	16	437	0.149	0.165	0.155	0.164	1.10
M-9	1.34	327	27.3	254	16	127	0.267	0.161	0.152	0.245	0.92
M-10	1.34	327	24.8	254	16	308	0.178	0.155	0.147	0.181	1.01

Note: All slabs were 1830 mm square, Dowel constant K_d = 1.3 and d_1 = 114 mm.

Average Q_{CAL}/Q_{TEST} = 1.031

Standard deviation = 0.125

Coefficient of variation = 12.13%

TABLE VII-7 Slabs tested by MOE[19] - Combined Load.

Slab No.	U_w N/mm^2	b mm	d_1 mm	EC mm	Q_{TEST} M.N.	Q_c M.N.	Q_d M.N.	Q_{CAL} M.N.	$\frac{Q_{CAL}}{Q_{TEST}}$
V/I/1	47.3	127	56	0	0.120	0.047	0.062	0.109	0.91
V/I/2	32.4	127	56	0	0.117	0.040	0.055	0.095	0.81
V/II/1	45.5	127	56	0	0.104	0.046	0.061	0.107	1.03
V/I2/1	66.4	127	56	0	0.130	0.053	0.070	0.123	0.95
C/I/1	45.0	127	56	87	0.084	0.046	0.061	0.077	0.93
C/I/2	37.1	127	56	168	0.062	0.042	0.057	0.057	0.93
C/I/3	31.8	127	56	404	0.034	0.040	0.055	0.034	1.01

Note: All slabs were 915 mm square, Dowel constant K_d = 1.8, r_{st} = 1.17%,

f_y = 435 N/mm^2, ϕ_M = 8 mm.

Average Q_{CAL}/Q_{TEST} = 0.94

Standard deviation = 0.072

Coefficient of variation = 7.67%

TABLE VII-8 Slabs tested by STAMENKOVIĆ[20] - Combined Load.

TABLE VII-9 Slabs tested by ANIS[18] - Combined Load.

Slab No.	U_w N/mm^2	EC mm	Q_{TEST} M.N.	Q_c M.N.	Q_d M.N.	Q_{CAL} M.N.	$\frac{Q_{CAL}}{Q_{TEST}}$
B-2	47.3	0	0.224	0.131	0.089	0.219	0.98
B-3	38.0	94	0.192	0.120	0.084	0.162	0.84
B-4	37.2	188	0.140	0.119	0.082	0.134	0.96
B-5	36.2	312	0.126	0.117	0.081	0.109	0.87
B-6	39.2	465	0.116	0.121	0.083	0.092	0.79
B-2C	38.8	0	0.094	0	0.083	0.083	0.88

Note: All slabs were 1525 mm square with 203 mm square column stubs.

r_{st} = 2.19%, f_y = 331 N/mm^2, d_1 = 76 mm, ϕ_M = 13 mm.

Average Q_{CAL}/Q_{TEST} = 0.886

Standard deviation = 0.072

Coefficient of variation = 8.12%

Slabs Tested by TANKUT[63] - Combined Load

Slab No.	r_{st} %	f_y N/mm^2	U_w N/mm^2	EC mm	K_d	Q_{TEST} M.N.	Q_c M.N.	Q_d M.N.	Q_{CAL} M.N.	$\frac{Q_{CAL}}{Q_{TEST}}$
E/1	1.44	404	42.7	71	1.3	0.164	0.103	0.074	0.144	0.88
E/2	1.96	310	46.1	105	1.1	0.185	0.120	0.064	0.137	0.77

Note: L = 1220 mm, b = 200 mm square, d_1 = 75 mm and ϕ_M = 9.5 mm

Slab No.	r_{st} %	f_y N/mm^2	U_w N/mm^2	ϕ_M mm	A_{sq} mm^2	f_{yq} N/mm^2	θ deg	Q_{TEST} M.N.	Q_v M.N.	Q_c M.N.	Q_d M.N.	Q_{CAL} M.N.	$\frac{Q_{CAL}}{Q_{TEST}}$
B-5	2.0	420	16.9	16	516	331	45	0.378	0.121	0.156	0.248	0.404	1.07
B-6	2.0	380	19.9	16	1033	331	45	0.468	0.242	0.167	0.262	0.429	0.92
B-10	2.0	334	54.5	16	1033	331	45	0.533	0.242	0.249	0.366	0.615	1.16
B-12	3.0	331	53.9	16	1420	323	90	0.787	0.459	0.400	0.436	0.836	1.06
B-13	3.0	328	56.5	16	4040	372	20	0.777	0.515	0.385	0.450	0.835	1.07
B-15	3.0	331	57.5	16	-	-	-	0.689	-	0.299	0.426	0.726	1.05
B-16	3.0	339	53.3	16	2065	331	45	0.746	0.483	0.379	0.444	0.823	1.10

Note: i) All slabs were 1830 mm square with 254 mm square column stubs, d_1 = 114 mm, K_d = 1.3

ii) For details of shear reinforcement see Fig. 81.

Average Q_{CAL}/Q_{TEST} = 1.064

Standard deviation = 0.073

Coefficient of variation = 6.837%

TABLE VII-10. Slabs tested by HOGNESTAD[4] - Concentric Load + Shear Reinforcement.

Slab No.	r_{st} %	f_y N/mm^2	U_w N/mm^2	B mm	d_1 mm	A_{sq} mm^2	f_{yq} N/mm^2	θ deg	Q_{TEST} M.N.	Q_v M.N.	Q_c M.N.	Q_d M.N.	Q_{CAL} M.N.	$\frac{Q_{CAL}}{Q_{TEST}}$
IIIA 15a S2 66	0.78	437	33.4	150	119	905	294	90	0.275	0.266	0.146	0.173	0.319	1.16
IIIA 15a S2 67	0.77	435	34.2	150	121	905	294	90	0.250	0.266	0.149	0.176	0.325	1.30
IIIA 15a S3 68	0.775	439	32.1	150	120	680	294	45	0.273	0.141	0.067	0.132	0.340*	1.24
IIIA 15a S3 69	0.77	447	31.0	150	121	680	294	45	0.293	0.141	0.066	0.136	0.343*	1.16
IIIA 30a S2 82	1.08	442	33.9	300	120	1290	294	90	0.460	0.379	0.231	0.201	0.432	0.94
IIIA 30a S2 83	1.09	442	29.3	300	119	1290	294	90	0.460	0.379	0.219	0.191	0.410	0.89
IIIA 30a S3 84	1.05	447	30.9	300	123	905	294	45	0.412	0.188	0.253	0.220	0.450	1.13
IIIA 30a S3 85	1.06	437	31.2	300	122	905	294	45	0.393	0.188	0.253	0.218	0.450	1.15

Note: i) All slabs were 1710 mm diameter, Dowel constant K_d = 1.8, ϕ_M = 12 mm

ii) For details of shear reinforcement see Fig. 81.

iii) * Shear Failure plane through shear reinforcement.

Average Q_{CAL}/Q_{TEST} = 1.121

Standard deviation = 0.140

Coefficient of variation = 12.44%

TABLE VII-11. Slabs tested by ANDERSON[16] - Concentric Load + Shear Reinforcement.

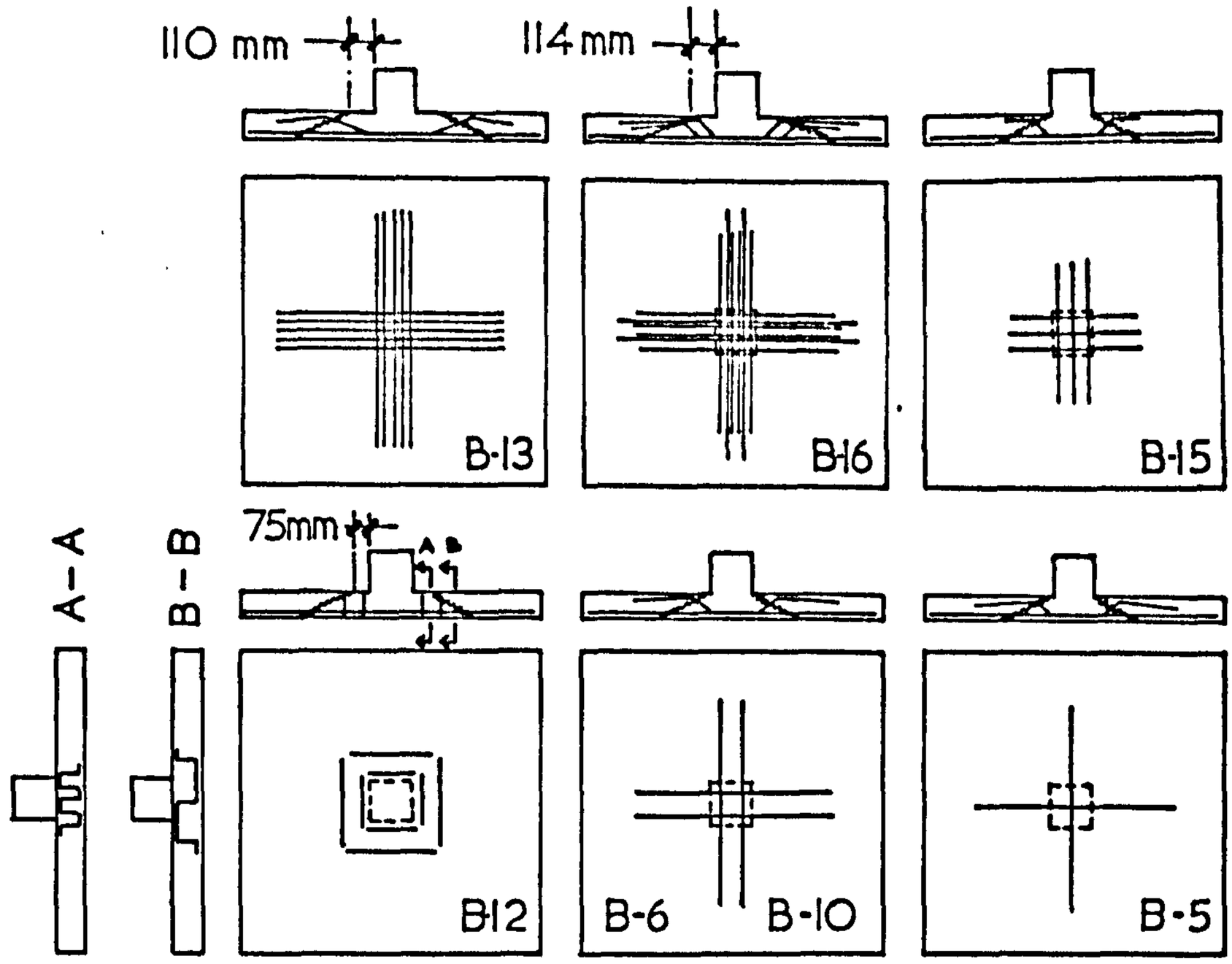

Fig. 80. SLABS TESTED BY HOGNESTAD.

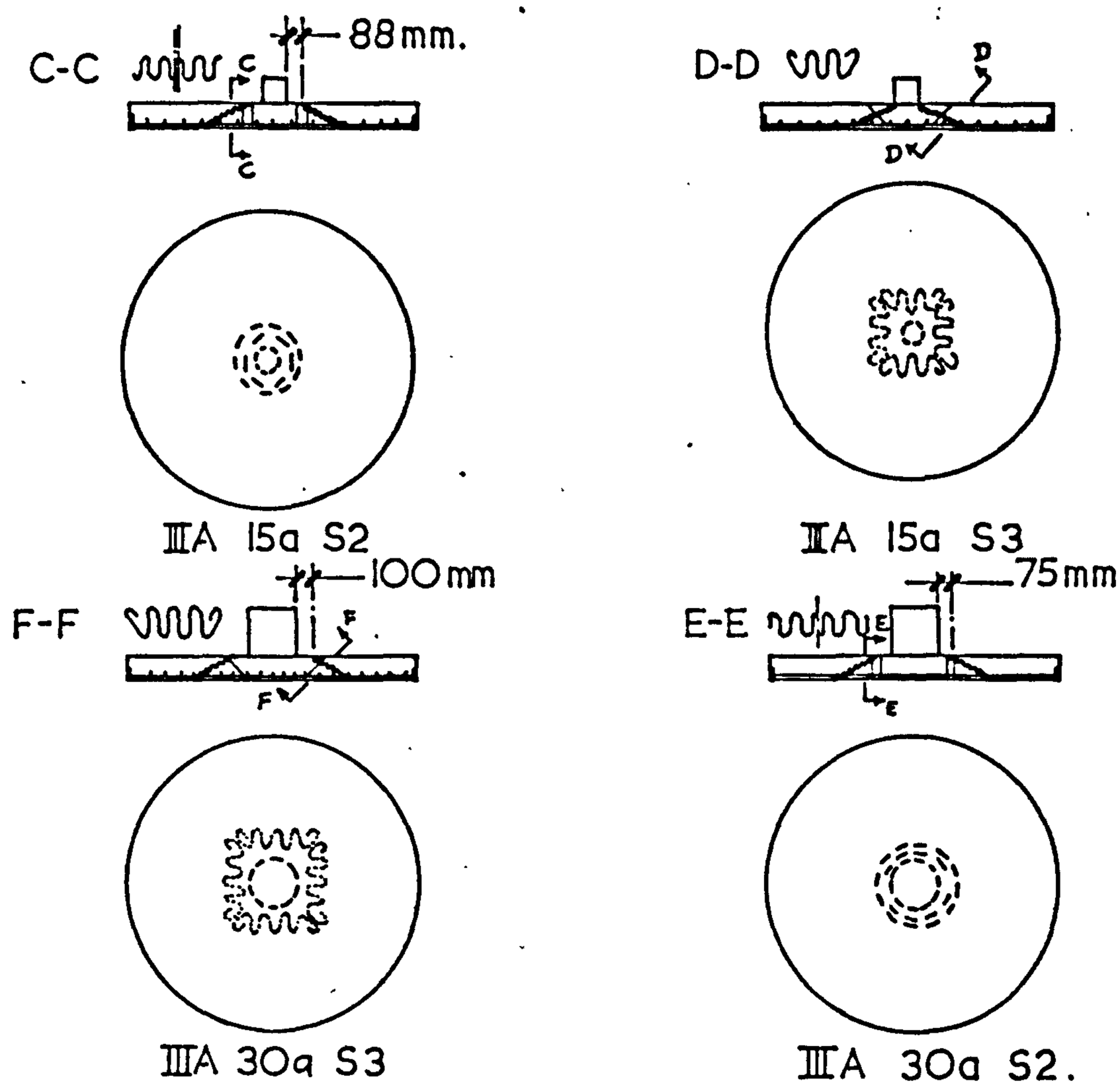

SLABS TESTED BY ANDERSON.

represents failure plane.

Fig. 81. DETAILS OF SHEAR REINFORCEMENT.

Slab No.	r_{st} %	f_y N/mm^2	U_w N/mm^2	b mm	Shear reinforcement details.	Q_{TEST} M.N.	Q_c M.N.	Q_d M.N.	Q_{CAL} M.N.	$\frac{Q_{CAL}}{Q_{TEST}}$
S5-60	1.06	398	26.1	203	None	0.342	0.114	0.138	0.252	0.74
S6-60	1.06	398	25.2	203	254 x 254 mm PLATE	0.320*	0.141	0.149	0.290	0.91
S7-60	1.06	398	27.1	203	305 x 305 mm PLATE	0.421*	0.174	0.166	0.340	0.81
S5-70	1.06	482	27.1	203	None	0.378	0.116	0.141	0.257	0.68
S6-70	1.06	482	28.5	203	254 x 254 mm PLATE	0.378*	0.147	0.155	0.302	0.80
S1-60	1.06	398	27.4	254	None	0.389	0.146	0.153	0.299	0.77
S1-70	1.06	482	28.8	254	None	0.392	0.149	0.156	0.305	0.78

Note: i) All slabs were 1830 mm square, Dowel constant K_d = 1.3, ϕ_M = 16 mm and d_1 = 114 mm

ii) * Failure plane outside shear reinforcement.

Average Q_{CAL}/Q_{TEST} = 0.781

Standard deviation = 0.073

Coefficient of variation = 9.34%

TABLE VII-12. Slabs tested by MOE[19] - Concentric Load + Shear Reinforcement.

SLAB NO.	r_{st} %	U_w N/mm^2	ϕ_M mm	A_{sq} mm^2	f_{yq} N/mm^2	θ deg	Q_{TEST} M.N.	Q_v M.N.	Q_c M.N.	Q_d M.N.	Q_{CAL} M.N.	$\frac{Q_{CAL}}{Q_{TEST}}$
1	0.85	35.9	12	-	-	-	0.220	-	0.070	0.089	0.159	0.72
4	1.06	34.5	12	-	-	-	0.239	-	0.075	0.083	0.163	0.68
5	1.06	35.6	12	414	302	90	0.271*	0.128	0.076	0.089	0.290	1.08
6	1.06	38.0	12	414	302	90	0.275*	0.128	0.078	0.091	0.297	1.08
8	1.06	37.0	12	630	284	90	0.275	0.179	0.141	0.115	0.256	0.93

Note: i) All slabs were 1500 mm in diameter, with 180 mm diameter column stubs.
$f_y = 464\ N/mm^2$, $d_1 = 95$ mm and dowel constant $K_d = 1.3$

ii) * Shear failure plane through first layer of shear reinforcement.

iii) For details of shear reinforcement see Fig. 82

Average $\frac{Q_{CAL}}{Q_{TEST}} = 0.898$

TABLE VII-13. Slabs tested by WANTHUR[46] - Concentric Load + Shear Reinforcement.

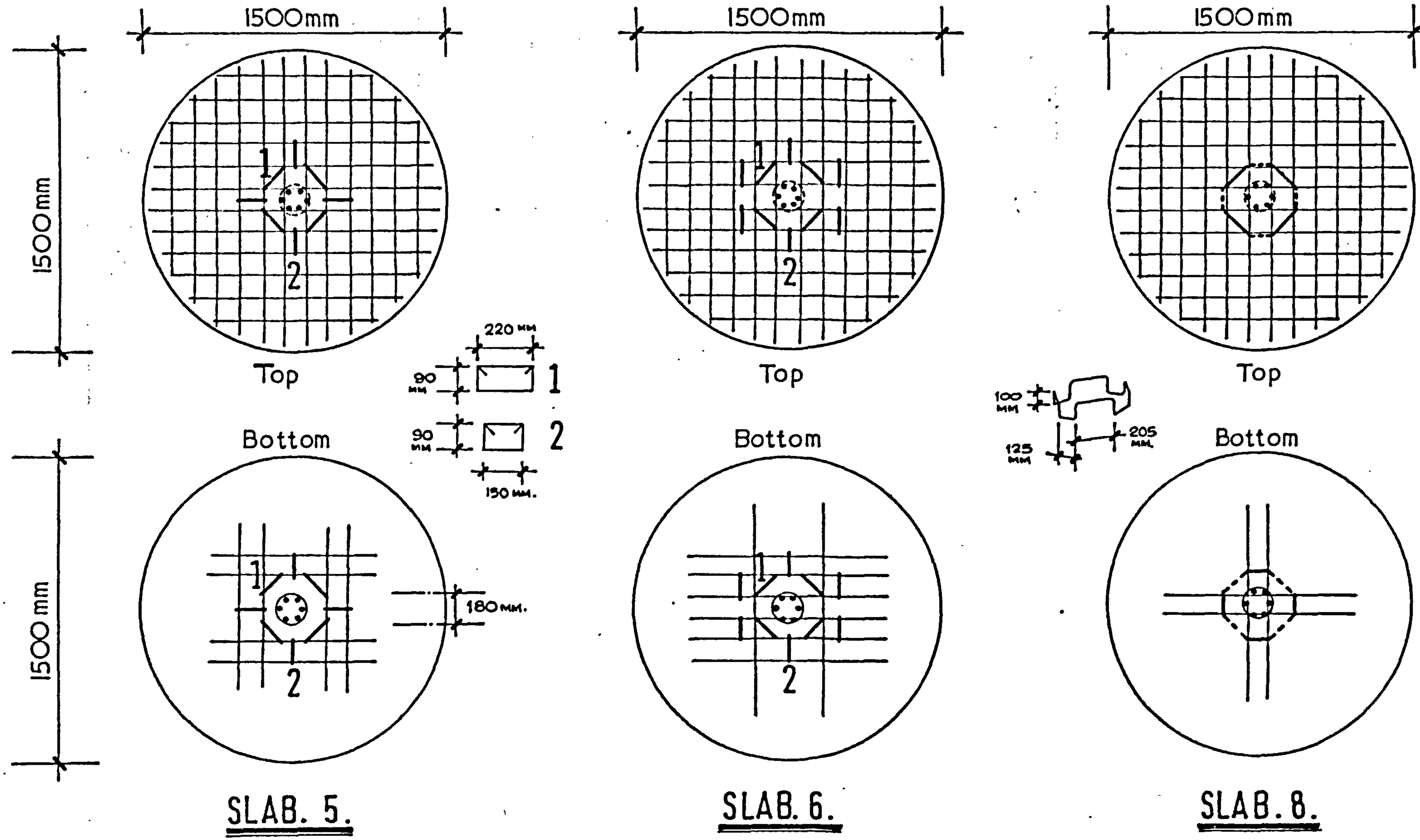
1500mm
1500mm
1
2
Top
Bottom
220 MM
90 MM
1
90 MM
2
150 MM.
180 MM.
SLAB. 5.
1500mm
1500mm
1
2
Top
Bottom
SLAB. 6.
1500mm
Top
100 MM
125 MM
205 MM.
Bottom
SLAB. 8.

Fig. 82.

Slab No.	U_w N/mm^2	A_{sq} mm^2	f_{yq} N/mm^2	θ deg.	EC mm	Q_{TEST} M.N.	Q_c M.N.	Q_d M.N.	Q_v M.N.	Q_{CAL} M.N.	$\frac{Q_{CAL}}{Q_{TEST}}$
L_1	32.9	-	-	-	305.0	0.399	0.284	0.246	-	0.330	0.83
L_3	33.1	1710	309	45	0	0.499	0.364	0.421	0.373	0.488	0.98
L_4*	45.9	775	338	45	305.0	0.568	0.317	0.281	0.185	0.487	0.86
L_5	35.6	3040	355	45	305.0	0.499	0.372	0.433	0.760	0.502	1.01
L_6	42.1	1190	355	45	152.5	0.598	0.394	0.463	0.298	0.658	1.10
L_7	44.4	-	-	-	0	0.687	0.314	0.277	-	0.591	0.86
L_9	41.4	-	-	-	0	0.588	0.306	0.269	-	0.576	0.98
L_{10}*	41.9	1190	355	30	152.5	0.638	0.308	0.271	0.211	0.606	0.95

Note:- i) All slabs were 2010 mm square with 305 mm square column stubs.

ii) r_{st} = 1.0% $f_y = 398\ N/mm^2$, ϕ_M = 16 mm, d_1 = 151 mm, K_d = 1.8

iii) * Shear failure plane through shear reinforcement.

Average Q_{CAL}/Q_{TEST} = 0.939, Standard Deviation = 0.101 Coefficient of variation = 10.79%

TABLE VII-14 Slabs tested by Author - combined load + shear reinforcement.

TABLE VII-15

Slabs tested by Graf[3] - Concentric load + Shear Reinforcement.

Slab No.	r_{st} %	f_y N/mm^2	U_w N/mm^2	d_1 mm	L mm	Q_{TEST} M.N.	A_{sq} mm^2	f_{yq} N/mm^2	θ deg	Q_v M.N.	Q_c M.N.	Q_d M.N.	Q_{CAL} M.N.	$\frac{Q_{CAL}}{Q_{TEST}}$
1355	0.83	276	19.8	273	1300	1.20	3700	270	45	0.705	0.219	0.216	1.140	0.95
1356	0.82	276	18.5	273	1300	1.28	3680	270	45	0.700	0.212	0.213	1.125	0.88
1376	0.50	276	18.2	472	1500	2.25	6700	267	60	1.550	0.304	0.246	2.10	0.93
1377	0.50	276	17.6	472	1500	2.20	6700	267	60	1.550	0.294	0.246	2.09	0.95
1361	1.17	269	17.0	273	1300	1.72	5180	265	60	0.974	0.352	0.233	1.56	0.91
1363	0.70	268	16.8	472	1500	3.01	8940	262	60	2.075	0.497	0.270	2.84	0.94

Note:- i) For slabs 1355, 1356, 1376 and 1377, b = 200 mm and ϕ_M = 14 mm

ii) For slabs 1361 and 1363, b = 300 mm and ϕ_M = 16 mm.

iii) For details of shear reinforcement see Fig. 83.

Average Q_{CAL}/Q_{TEST} = 0.926

Standard deviation = 0.027

Coefficient of variation = 2.949%

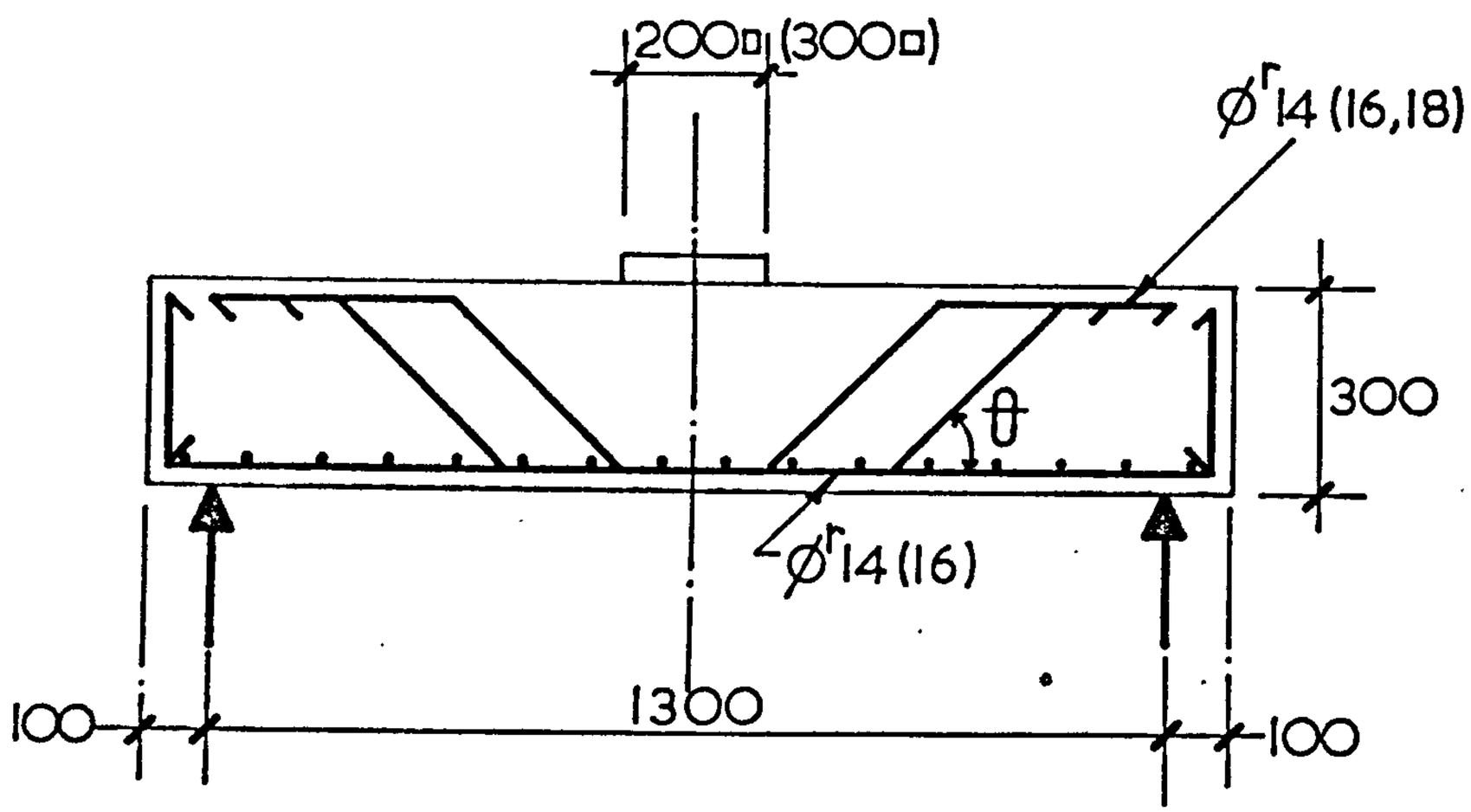

SLABS - 1355, 1356, 1351.

All dimensions are in Millimetres.

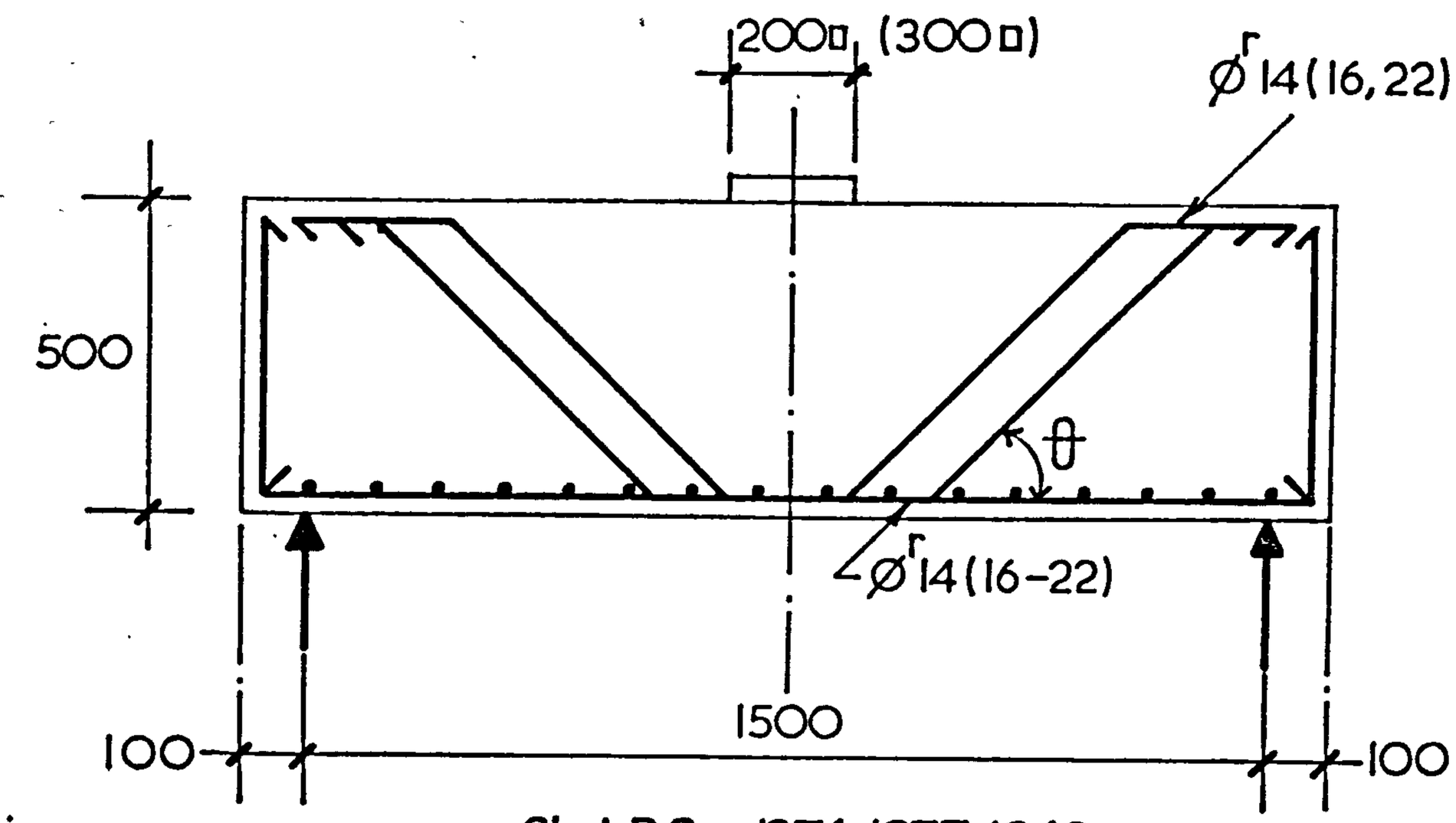

SLABS - 1376, 1377, 1363.

Fig. 83. DETAILS OF SHEAR REINFORCEMENT.

(Reproduced from Reference 46)

TABLE VII-16

Slabs Tested by Moe[19] - Concentration of Reinforcement Near Column.

Slab No.	r_{st} %	f_y N/mm^2	U_w N/mm^2	ϕ_M mm	Q_{TEST} M.N.	Q_c M.N.	Q_d M.N.	Q_{CAL} M.N.	$\frac{Q_{CAL}}{Q_{TEST}}$
S2-60	1.06	398	26.0	16	0.366	0.144	0.149	0.293	0.80
S3-60	1.06	398	26.6	16	0.364	0.145	0.150	0.296	0.81
S4-60	1.06	398	28.0	16	0.334	0.148	0.153	0.301	0.90
S3-70	1.06	482	29.9	16	0.378	0.152	0.156	0.309	0.82
S4-70	1.06	482	41.4	16	0.374	0.173	0.174	0.347	0.93
S4A-70	1.06	482	24.1	16	0.314	0.140	0.145	0.285	0.92

Note: i) All slabs were 1830 mm square with 254 mm square column stubs.

ii) r_{st} taken as the average value over the full width of the slab. (For reinforcement layout see Fig. 84.)

iii) Effective depth of slab = 114 mm and dowel constant Kd = 1.3

Average $\frac{Q_{CAL}}{Q_{TEST}}$ = 0.863

Standard deviation = 0.060

Coefficient of variation = 6.898%

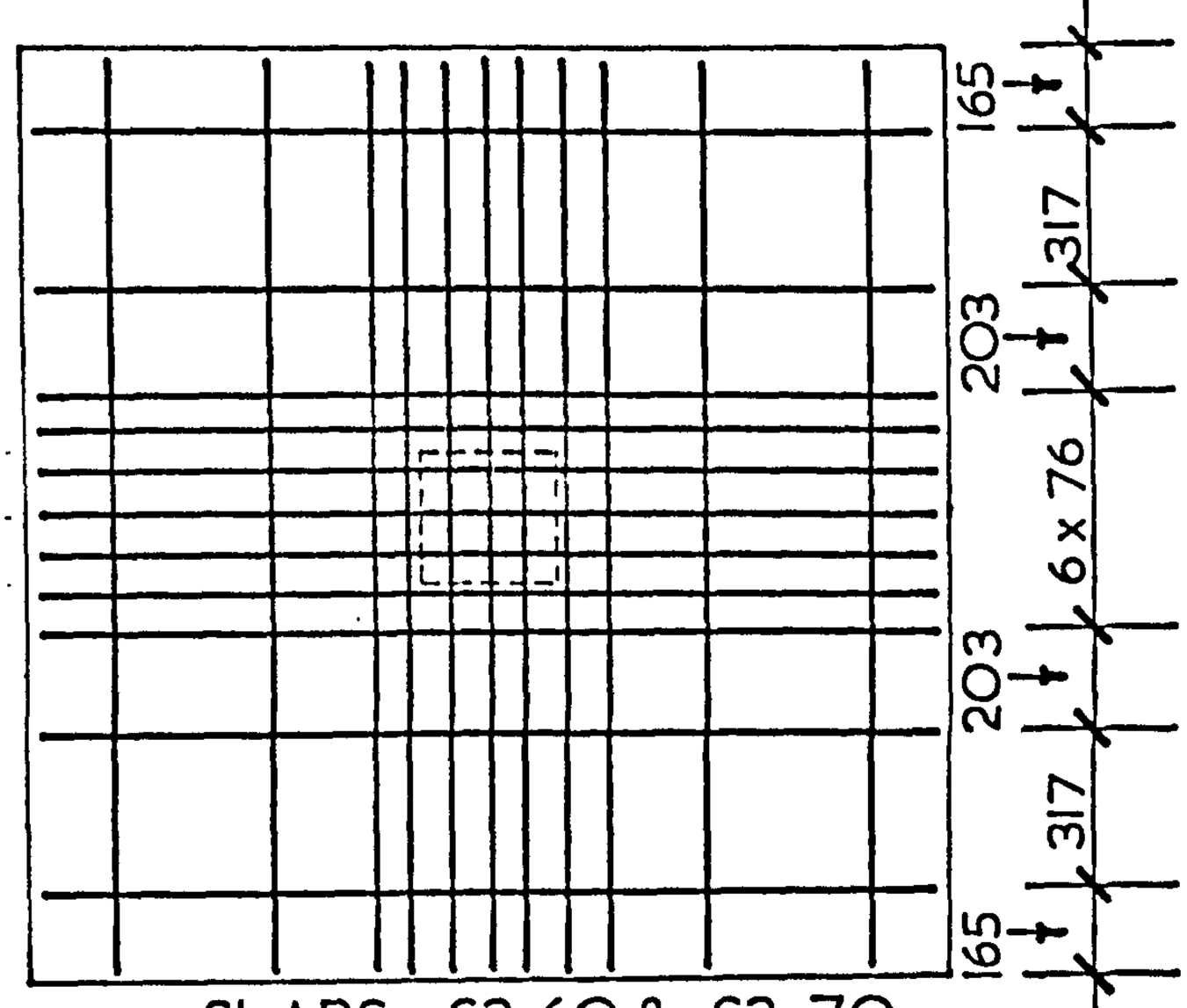

SLABS. S3-60 & S3-70.

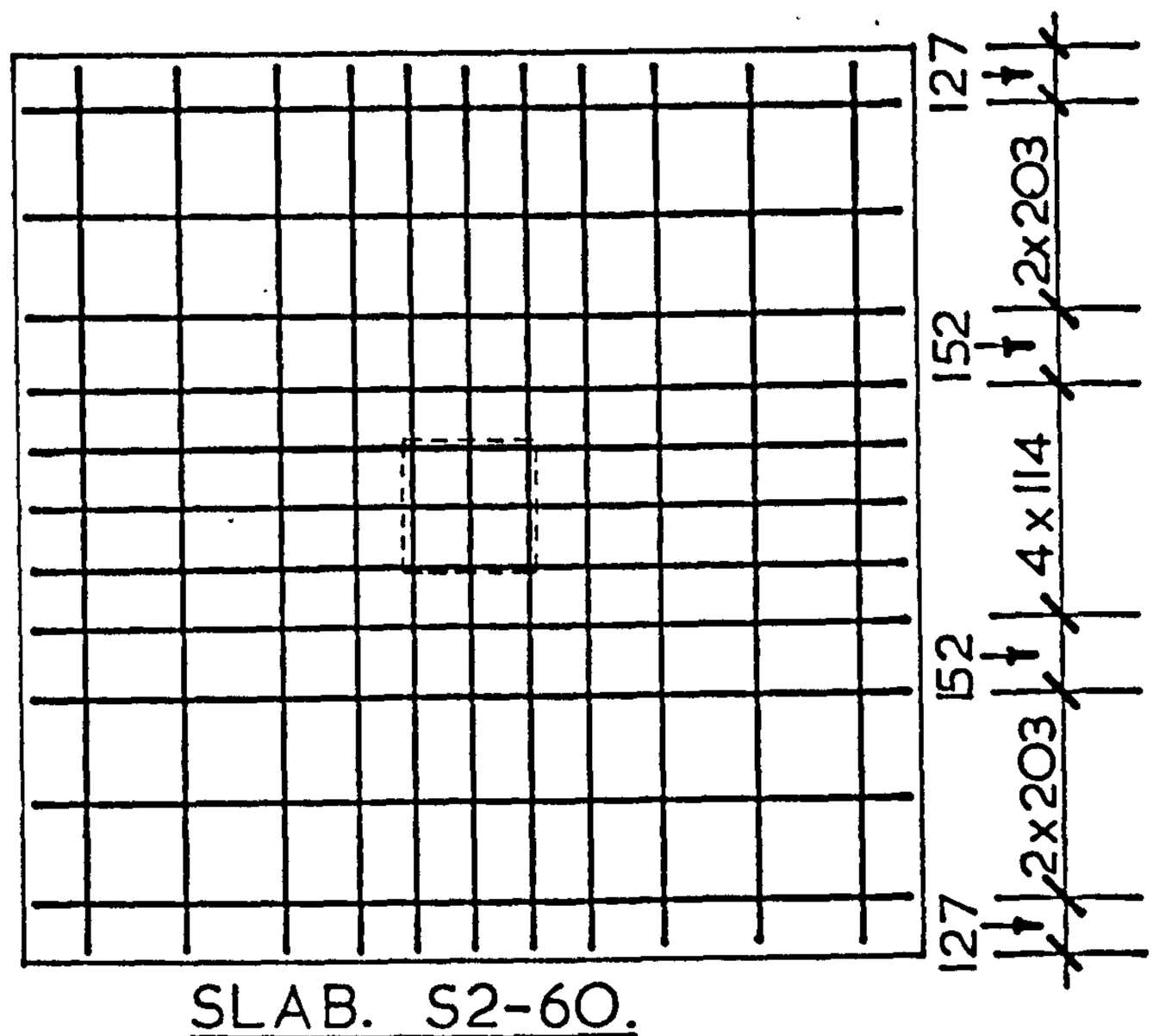

SLAB. S2-60.

All dimensions shown are in millimetres.

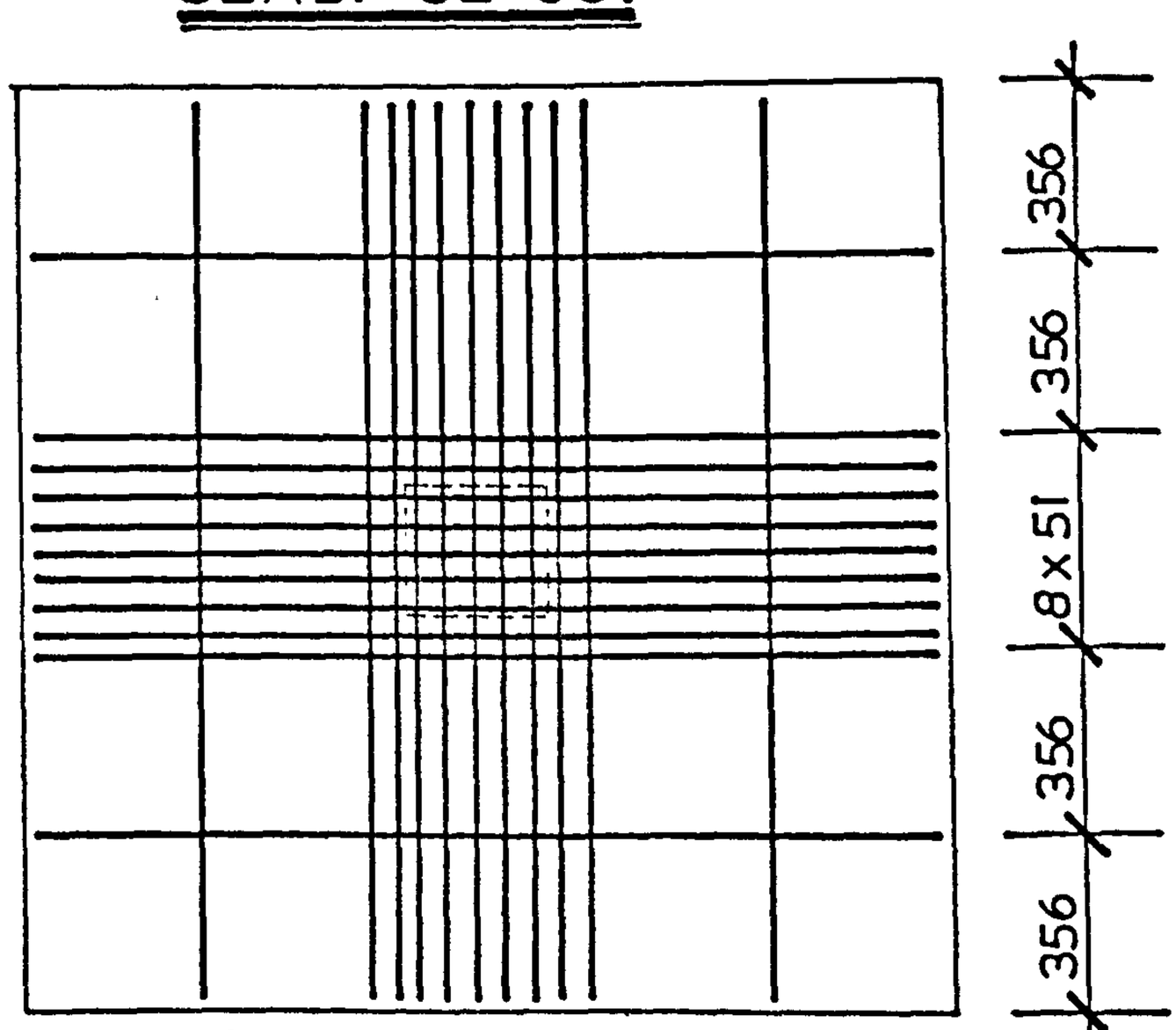

SLABS. S4-60 & S4-70.

Fig. 84. REINFORCEMENT DETAILS – MOE'S SLABS.

TABLE VII-17

Slabs Tested by Moe[19] - With Holes Near Column.

Slab No.	r_{st} %	f_y N/mm^2	U_w N/mm^2	ϕ_M mm	Q_{TEST} M.N.	Q_c M.N.	Q_d M.N.	Q_{CAL} M.N.	$\frac{Q_{CAL}}{Q_{TEST}}$
H2	1.15	327	29.4	16	0.329	0.135	0.148	0.283	0.86
H3	1.15	327	27.8	16	0.324	0.114	0.137	0.251	0.78
H4	1.15	327	30.2	16	0.289	0.117	0.142	0.259	0.90
H5	1.15	327	29.4	16	0.249	0.097	0.124	0.221	0.89
H6	1.15	327	33.4	16	0.245	0.081	0.130	0.211	0.86
H7	1.15	327	29.6	16	0.311	0.136	0.148	0.284	0.91
H8	1.15	327	33.0	16	0.311	0.121	0.146	0.267	0.86
H9	1.15	327	28.3	16	0.312	0.134	0.145	0.279	0.89
H10	1.15	327	29.3	16	0.334	0.136	0.148	0.284	0.85
H11	1.15	327	30.6	16	0.338	0.137	0.150	0.287	0.85
H15	1.15	327	27.5	16	0.332	0.133	0.144	0.277	0.83

Note: i) All slabs were 1830 mm square with 254 mm square column stubs.

ii) Effective depth of the slab = 114 mm, dowel constant $K_d = 1.3$

iii) For details of holes see Fig. 85.

Average value of Q_{CAL}/Q_{TEST} = 0.862

Standard deviation = 0.037

Coefficient of variation = 4.24%

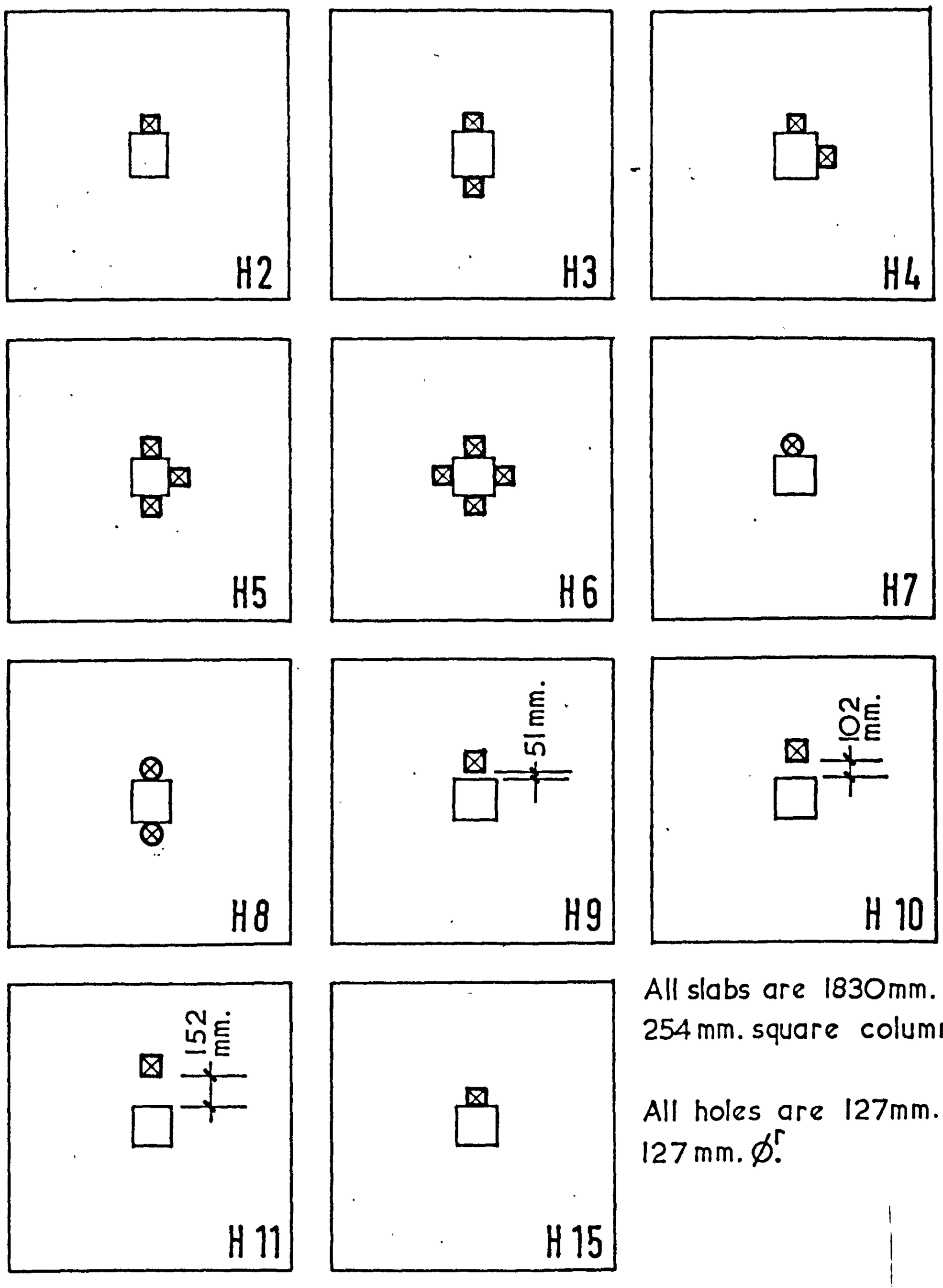

All slabs are 1830mm. square with 254 mm. square columns.

All holes are 127mm. square or 127 mm. Ø.

Fig. 85. PATTERN OF HOLES — MOE'S SLABS.

TABLE VII-17

Slabs Tested by Mowrer and Vanderbelt[45] - With Holes Near Column.

Slab No.	r_{st} %	f_y N/mm^2	U_w N/mm^2	Hole Width mm	Q_c M.N.	Q_d M.N.	Q_{CAL} M.N.	Q_{TEST} M.N.	$\frac{Q_{CAL}}{Q_{TEST}}$
JL.1-1.7a	1.67	352	21.3	152	0.032	0.042	0.074	0.066	1.12
JL.2-1.7a	1.67	352	20.9	305	0.021	0.036	0.057	0.065	0.88
JL.3-1.7a	1.67	352	19.3	38	0.038	0.044	0.082	0.093	0.88
JL.1-2.2a	2.20	352	20.5	152	0.035	0.042	0.077	0.079	0.97
JL.2-2.2a	2.20	352	19.8	305	0.023	0.036	0.059	0.066	0.90
JL.3-2.2a	2.20	352	17.2	38	0.041	0.044	0.085	0.079	1.07
JL.1-1.7b	1.67	352	27.2	152	0.035	0.046	0.081	0.086	0.94
JL.2-1.7b	1.67	352	30.8	305	0.025	0.041	0.066	0.090	0.73
JL.3-1.7b	1.67	352	29.3	38	0.045	0.038	0.083	0.111	0.75
JL.1-2.2b	2.20	352	30.9	152	0.041	0.048	0.089	0.086	1.03
JL.2-2.2b	2.20	352	33.0	305	0.028	0.043	0.071	0.086	0.82
JL.3-2.2b	2.20	352	28.2	38	0.051	0.051	0.102	0.114	0.89

Note: i) d_1 = 51 mm, b = 152 mm square, L = 915 mm square, ϕ_M = 12.7 mm, K_d = 1.3.

ii) For details of holes see Fig. 86.

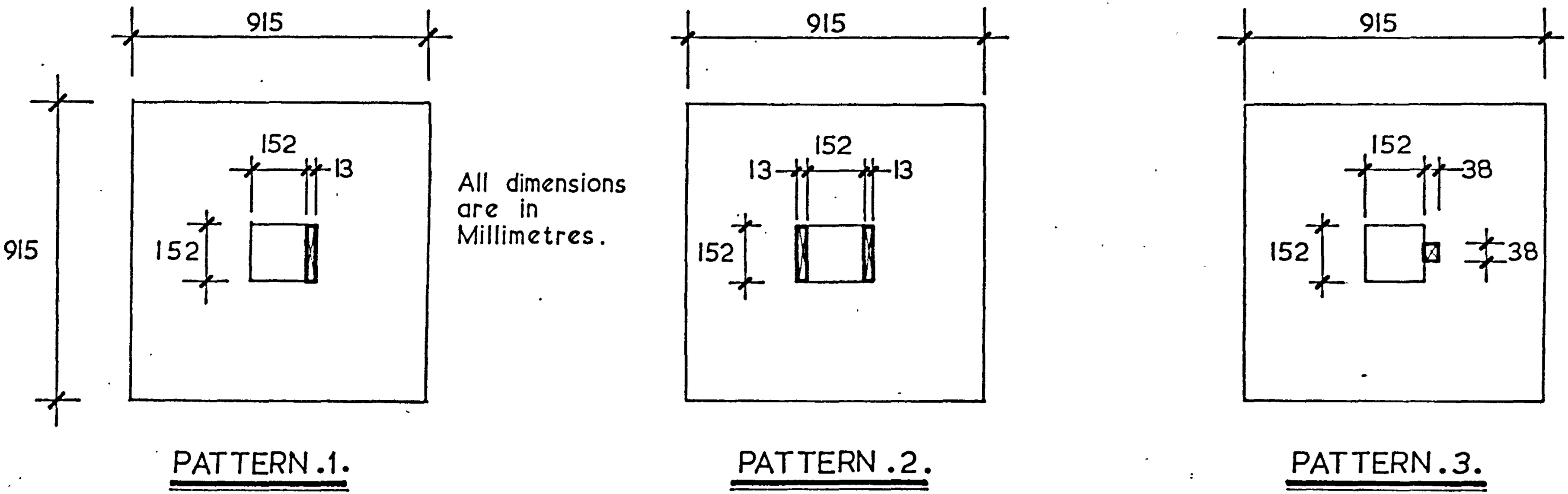
915
915
152
13
152
All dimensions are in Millimetres.
PATTERN .1.
915
152
13
13
152
PATTERN .2.
915
152
38
152
38
PATTERN .3.

Fig. 86.

TABLE VII-18

Slabs Supported on two sides only - Hognestad[4]

Slab No.	U_w N/mm^2	b mm.	d_1 mm	Q_{TEST} M.N.	Q_c M.N.	Q_d M.N.	Q_{CAL} M.N.	$\frac{Q_{CAL}}{Q_{TEST}}$
A.7	33.5	254	114	0.400	0.224	0.162	0.386	0.96
A.8	25.8	356	114	0.435	0.282	0.174	0.456	1.05

Note:- $r_{st} = 2.47\%$, $f_y = 321\ N/mm^2$, $\phi_M = 16$ mm,

$L = 1830$ mm, $K_d = 1.3$

TABLE VII-19

Slabs tested by Richart and Kluge[62] - Isolated load on slab.

Load No.	U_w N/mm^2	B mm	d_1 mm	Q_u M.N.	Q_c M.N.	Q_d M.N.	Q_{CAL} M.N.	$\frac{Q_{CAL}}{Q_{TEST}}$
I/1	30.1	152	140	0.380	0.090	0.195	0.285	0.75
I/2	30.1	152	140	0.342	0.090	0.195	0.285	0.83
I/3	30.1	152	140	0.391	0.090	0.195	0.285	0.73
II/1	34.3	152	140	0.320	0.105	0.214	0.319	1.00
II/2	34.3	152	140	0.369	0.105	0.214	0.319	0,86
II/3	34.3	51	140	0.269	0.035	0.165	0.200	0.75
II/4	34.3	152	140	0.372	0.105	0.214	0.319	0.86

Note:- i) For location of loads see Fig. 87

ii) $r_{st} = 1.13\%$, $f_y = 314\ N/mm^2$, $\phi_M = 12.7$ mm, $K_d = 1.3$

iii) Stiffness of the square bar taken into account in calculating Q_d values.

Average $\frac{Q_{CAL}}{Q_{TEST}} = 0.826$

Standard deviation = 0.094

Coefficient of variation = 11.422%

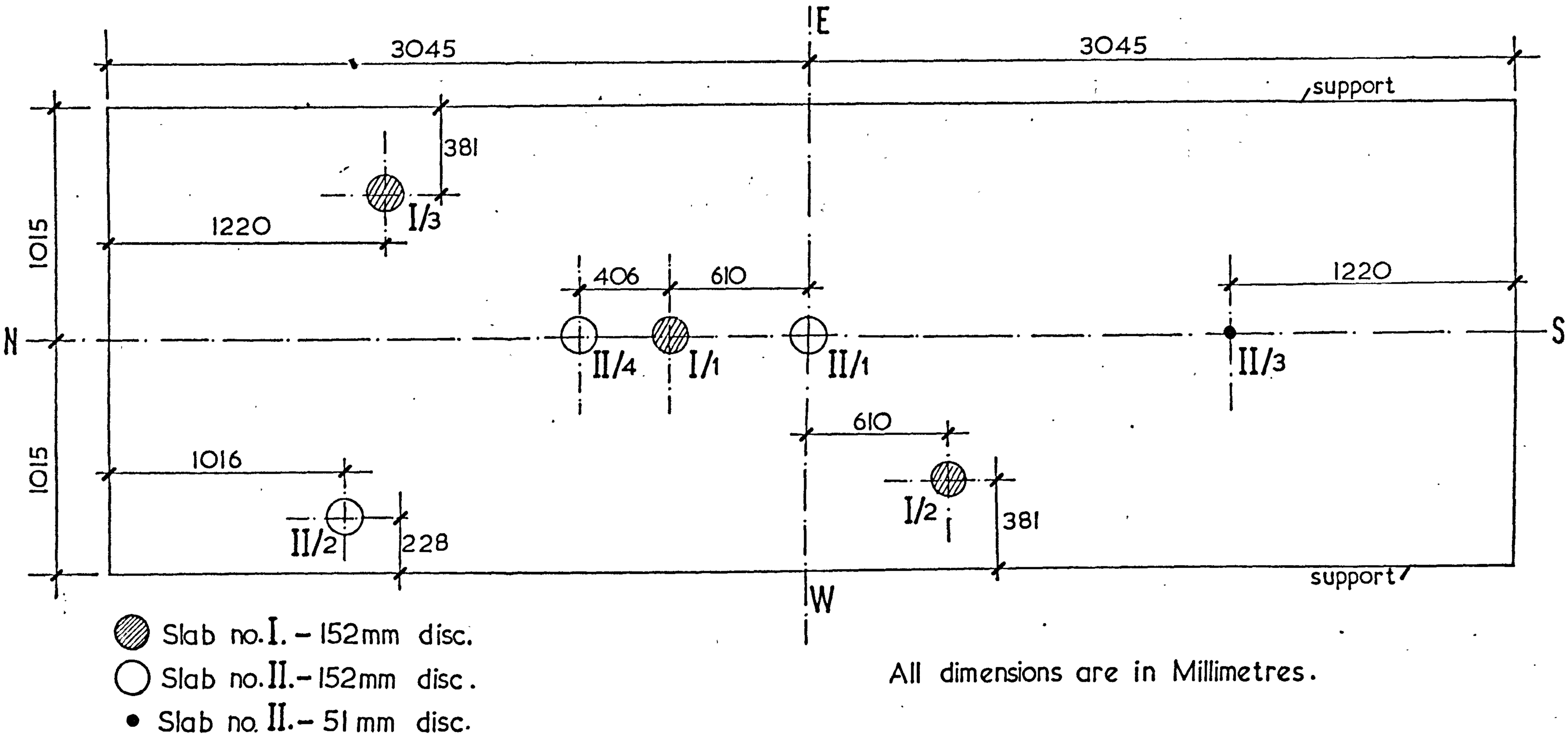

Fig. 87. LOCATION OF ISOLATED LOADS PRODUCING LOCAL FAILURES.

TABLE VII-20.

RECTANGULAR COLUMNS SUBJECTED TO COMBINED LOAD.

Slabs tested by Stamenkovic'[20]

Slab No.	U_w N/mm^2	Q_{TEST} M.N.	EC mm	Q_c M.N.	Q_d M.N.	Q_{CAL} M.N.	$\frac{Q_{CAL}}{Q_{TEST}}$
V/Ir/1	31.4	0.108	0	0.035	0.053	0.088	0.82
C/Ir/1	28.3	0.085	85	0.034	0.051	0.062	0.73
C/Ir/2	36.5	0.067	161	0.038	0.055	0.054	0.81
C/Ir/3	35.7	0.040	394	0.037	0.055	0.033	0.82
C/Ir/4	33.2	0.021	780	0.036	0.054	0.020	1.05

r_{st} = 1.17% f_y = 414 N/mm^2, d_1 = 56 mm, ϕ_M = 8mm,

L = 890 mm, K_d = 1.8, b_y = 152 mm, b_x = 76 mm.

Slab tested by Moc[19]

R1	32.5	0.393	0	0.208	0.175	0.383	0.97

r_{st} = 1.38%, f_y = 328 N/mm^2, d_1 = 114 mm, ϕ_M = 16 mm,

L = 1830 mm, K_d = 1.3, b_y = 457 mm, b_x = 152 mm

TABLE VII-21

Footings tested by RICHART[58]

Slab No.	r_{st} %	f_y N/mm^2	ϕ_M mm	U_w N/mm^2	Q_{TEST} M.N.	Soil Pr. N/mm^2	Q_{NET} M.N.	Q_c M.N.	Q_d M.N.	Q_{CAL} M.N.	$\frac{Q_{CAL}}{Q_{NET}}$
105a	0.393	460	9.5	27.8	2.34	0.515	1.03	0.373	0.211	0.584	0.57
105b	0.393	460	9.5	20.2	1.80	0.395	0.79	0.328	0.190	0.518	0.65
106a	0.391	430	12.7	30.4	2.34	0.515	1.03	0.386	0.290	0.676	0.65
106b	0.391	430	12.7	29.4	2.11	0.467	0.92	0.381	0.287	0.668	0.72
107a	0.395	412	16.0	29.4	2.11	0.467	0.92	0.382	0.361	0.744	0.80
107b	0.395	412	16.0	27.6	1.89	0.416	0.83	0.373	0.354	0.727	0.87
108a	0.374	364	19.0	33.7	2.12	0.466	0.93	0.395	0.449	0.844	0.91
108b	0.374	364	19.0	26.5	2.01	0.422	0.93	0.359	0.415	0.774	0.83
109a	0.561	530	9.5	24.4	2.40	0.527	1.06	0.407	0.201	0.608	0.57
109b	0.561	530	9.5	25.0	2.05	0.450	0.90	0.412	0.203	0.616	0.68
110a	0.561	489	12.7	26.0	2.23	0.490	0.98	0.419	0.275	0.694	0.71
110b	0.561	489	12.7	21.9	2.32	0.510	1.02	0.391	0.260	0.651	0.64
111a	0.632	425	16.0	24.4	2.14	0.470	0.94	0.428	0.340	0.768	0.82
111b	0.632	425	16.0	27.6	2.56	0.562	1.13	0.450	0.354	0.804	0.71
112a	0.748	510	19.0	28.1	2.14	0.470	0.94	0.484	0.423	0.907	0.96
112b	0.748	510	19.0	22.9	2.32	0.510	1.02	0.446	0.395	0.842	0.82
109Ra	0.561	456	9.5	33.0	2.55	0.560	1.12	0.460	0.223	0.683	0.61
109Rb	0.561	456	9.5	33.8	2.44	0.535	1.07	0.465	0.225	0.690	0.64
110Ra	0.561	511	12.7	25.6	2.25	0.495	0.99	0.416	0.274	0.690	0.70
110Rb	0.561	511	12.7	28.4	2.61	0.573	1.15	0.433	0.284	0.717	0.62

Note: i) All footings were 2135 mm square with 305 mm square columns.

ii) $d_1 = 356$ mm, $K_d = 1.3$

iii) $Q_{NET} = Q_{TEST} - \text{Soil Pr.}\ (b^2 - 8b.d_1 + 4\pi d_1^2)$

TABLE VII-22

EDGE COLUMNS WITH NORMAL MOMENT

(Q_{CAL}^{*}, calculated ignoring eccentricity)

Slabs tested by Author.

SLAB NO.	Q_c M.N.	Q_d M.N.	Q_v M.N.	Q_{CAL}^{*} M.N.	$\frac{Q_{TEST}}{Q_{CAL}}$	M_{CAL} Nm	$\frac{M_{TEST}}{M_{CAL}}$
ES1	0.178	0.167	-	0.345	0.90	65300	0.24
ES2	0.176	0.165	-	0.341	1.00	65300	0.93
ES3	0.210	0.192	0.087	0.489	0.90	67100	1.15
ES4	0.315	0.240	0.249	0.455	0.92	67100	1.34
ES5	0.185	0.174	-	0.359	0.73	66400	1.11
ES6	0.191	0.178	0.087	0.455	0.81	66700	0.28
ES7	0.201	0.185	0.087	0.473	0.65	66900	1.29

Slabs tested by Anderson[17]

Slab No.	Q_c M.N.	Q_d M.N.	Q_{CAL}^{*} M.N.	$\frac{Q_{TEST}}{Q_{CAL}}$	M_{CAL} Nm	$\frac{M_{TEST}}{M_{CAL}}$
1a	0.115	0.081	0.196	0.79	55300	0.92
1b	0.136	0.086	0.222	0.91	64400	0.80
1c	0.140	0.093	0.233	0.76	60100	1.07

TABLE VII-22 (contd.)

Slabs tested by Stamenkovic'[20]

Slab No.	Q_c M.N.	Q_d M.N.	Q_{CAL}* M.N.	$\frac{Q_{TEST}}{Q_{CAL}}$	M_{CAL} Nm	$\frac{M_{TEST}}{M_{CAL}}$
V/E/1	0.032	0.034	0.066	1.14	6450	0.24
C1/E/1	0.032	0.035	0.067	1.08	6480	0.61
C1/E/2	0.030	0.033	0.063	0.87	6430	1.28
C1/E/3	0.031	0.033	0.064	0.39	6440	1.47

Slabs tested by Tankut[63]

Slab No.	Q_c M.N.	Q_d M.N.	Q_{CAL}* M.N.	$\frac{Q_{TEST}}{Q_{CAL}}$	M_{CAL} Nm	$\frac{M_{TEST}}{M_{CAL}}$
B1	0.079	0.047	0.126	0.70	19800	1.10
H1	0.079	0.047	0.126	0.60	19800	1.24
B2	0.079	0.040	0.119	1.02	19800	1.66
H2	0.079	0.040	0.119	0.63	19800	0.87

TABLE VII-23

EDGE COLUMNS WITH TANGENTIAL MOMENTS.

Slabs tested by Stamenkovic'[20]

Slab No.	U_w N/mm^2	EC mm	Q_{TEST} M.N.	Q_c M.N.	Q_d M.N.	Q_{CAL} M.N.	$\frac{Q_{CAL}}{Q_{TEST}}$
V/E/1	35.8	0	0.075	0.025	0.035	0.060	0.80
C11/E/1	34.8	106	0.046	0.024	0.034	0.041	0.89
C11/E/2	35.5	163	0.035	0.025	0.035	0.035	1.00
C11/E/3	34.8	400	0.024	0.024	0.034	0.021	0.88
C11/E/4	36.6	780	0.013	0.025	0.035	0.013	1.00

Note:- r_{st} = 1.17%, f_y = 448 N/mm^2, d_1 = 56 mm, ϕ_M = 8 mm,

$b_x = b_y$ = 127 mm, X = Y = 890 mm, K_d = 1.8

Slabs tested by Tankut[63]

Slab No.	r_{st} %	f_y N/mm^2	U_w N/mm^2	K_d	EC mm	Q_{TEST} M.N.	Q_c M.N.	Q_d M.N.	Q_{CAL} M.N.	$\frac{Q_{CAL}}{Q_{TEST}}$
D1	1.44	404	42.7	1.3	162	0.074	0.079	0.047	0.082	1.11
F1	1.44	404	42.7	1.3	258	0.079	0.079	0.047	0.068	0.86
D2	1.96	310	46.2	1.1	162	0.074	0.079	0.040	0.077	1.04
F2	1.96	310	46.2	1.1	273	0.079	0.079	0.040	0.063	0.80

Note:- d_1 = 76 mm, ϕ_M = 9.5 mm, $b_x = b_y$ = 203 mm,

X = Y = 1220 mm.

7.2 COMPARISON WITH EXISTING FORMULAE - INTERNAL COLUMNS.

7.2.1 Introduction:

The Ratios of Q_{CAL}/Q_{TEST} obtained using some of the existing formulae and those obtained using the proposed solution are compared. The available test results are sub divided into four catagories as some of the existing formulae do not cater for combined loading and slabs with shear reinforcement.

7.2.2 Slabs with concentric loading and no shear reinforcement.

The slabs were analysed using methods given by Hognestad[4], Moe[19], Anis[18], A.C.I.[23], C.P.114[22] and the proposed solution. Table No. VII-24 shows the comparison. In using the British Code of Practice[22] for comparison, a load factor is necessary, to enable the design stresses given in the code to be converted to ultimate values. It is assumed that the intended load factor is 2.0 and the lever arm factor is taken as a constant 0.85.

The results of a statistical treatment of the comparison are given below, 63 tests involved.

METHOD BY	HOGNESTAD	MOE	A.C.I.	*ANIS	C.P.114	PROPOSED SOLUTION
Average $\frac{Q_{CAL}}{Q_{TEST}}$	1.036	0.946	0.756	0.916	0.690	0.946
Standard Deviation	0.143	0.158	0.151	0.117	0.199	0.121
Coefficient of variation %	13.822	16.705	20.021	12.84	28.853	12.83

* Average of 40 tests only.

TABLE VII-24

Slabs with Concentric Loads.

FORMULA BY	Hognestad	Moe	A.C.I.	Anis*	C.P.114	Proposed Solution
SLAB NO.	Value of Q_{CAL}/Q_{TEST}					
Slabs tested by Hognestad(4)						
A-1a	1.05	1.00	0.72	0.79	0.68	0.94
A-1b	1.01	1.02	0.80	0.85	0.79	0.96
A-1c	1.07	1.10	0.88	0.94	0.83	1.03
A-1d	1.17	1.20	1.00	1.04	0.85	1.09
A-1e	0.97	0.97	0.73	0.78	0.70	0.91
A-2a	1.03	1.09	0.62	0.80	0.53	1.10
A-2b	0.98	0.99	0.61	0.83	0.61	1.05
A-2c	1.05	1.11	0.73	1.04	0.64	1.13
A-7b	0.86	0.90	0.57	0.81	0.58	0.93
A-3a	1.03	0.95	0.56	0.79	0.46	1.09
A-3b	1.01	1.02	0.60	0.94	0.60	1.08
A-3c	0.90	0.91	0.52	0.86	0.56	0.95
A-3d	0.98	1.01	0.60	0.98	0.54	1.02
A-4	1.21	1.09	0.94	1.02	0.91	1.13
A-5	1.07	1.03	0.73	1.02	0.69	1.14
A-6	1.21	1.15	0.74	1.17	0.71	1.26
B-9	0.99	1.04	0.73	0.96	0.59	1.00
B-11	1.08	1.06	0.62	0.84	0.54	1.16
B-14	1.03	1.06	0.68	1.07	0.51	1.06

TABLE VII-24 (Contd)

Formula By	Hognestad	Moe	A.C.I.	Anis*	C.P.114	Proposed Solution
Slab No.	Value of Q_{CAL}/Q_{TEST}					
Slabs tested by Mowrer and Vanderbelt(45)						
M-2-1.0	0.88	0.83	0.63	-	0.43	0.82
M-2-2.0	0.75	0.79	0.50	-	0.34	0.73
M-3-1.0	1.08	0.96	0.79	-	0.54	1.04
M-3-2.0a	0.94	0.88	0.58	-	0.39	0.90
M-3-2.0b	0.80	0.78	0.58	-	0.28	0.77
M-4-1.0	1.10	0.80	0.73	-	0.45	1.00
M-4-2.0	1.01	0.87	0.67	-	0.46	0.99
M-5-2.0	1.00	0.75	0.65	-	0.45	0.98
M-6-2.0	1.16	0.76	0.78	-	0.63	1.14
M-7-2.0	1.12	0.62	0.74	-	0.52	1.10
JL-0-1.7a	1.02	0.91	0.65	-	0.37	0.88
JL-0-2.2a	0.96	0.85	0.57	-	0.31	0.86
JL-0-1.7b	1.04	0.99	0.75	-	0.52	0.94
JL-0-2.2b	1.16	1.10	0.75	-	0.50	1.07
JL-0-1.1	0.95	0.84	0.81	-	0.47	0.92
Slabs tested by Stamenkovic'(20)						
V/I/1	0.89	0.93	0.72	-	0.65	0.91
$V/I_1/1$	0.81	0.83	0.60	-	0.75	1.03
$V/I_2/1$	1.01	1.05	0.80	-	0.60	0.95
V/I/2	0.92	0.95	0.78	-	0.67	0.81
Slabs tested by Manterola(53)						
P1S1	0.71	0.48	0.71	-	0.71	0.78
P1S2	0.80	0.52	0.78	-	0.74	0.85
P1S3	1.02	0.59	0.96	-	0.80	1.07
P2S3	0.81	0.51	0.89	-	0.72	0.94
Slabs tested by Ivy(44)						
H1 11A6IV	1.19	1.16	0.94	0.95	1.05	0.99
H1 11A6VIII	1.13	1.12	0.96	0.98	0.89	0.97
H1 12A6I	1.14	1.13	1.00	1.03	0.95	0.99
H1 13A6VI	1.11	1.09	0.96	0.98	0.91	0.95

TABLE VII-24 (Contd)

Formula by	Hognestad	Moe	A.C.I.	Anis**	C.P.114	Proposed Solution.
Slab No.	Values of Q_{CAL}/Q_{TEST}					
Slabs tested by Moe[19]						
H2	1.10	0.98	0.88	0.85	0.86	0.86
H3	1.07	0.88	0.82	0.84	0.85	0.78
H4	1.23	1.02	0.98	1.00	1.0	0.90
H5	1.41	1.03	1.12	1.12	1.14	0.89
H6	1.49	0.95	1.20	1.23	1.21	0.86
H7	1.13	1.06	0.88	0.91	0.91	0.91
H8	1.17	1.02	0.95	0.96	0.95	0.86
H9	1.12	1.05	0.88	0.89	0.89	0.89
H10	1.05	1.05	0.82	0.84	0.85	0.85
H11	1.05	1.05	0.82	0.86	0.86	0.85
H15	1.04	0.96	0.81	0.81	0.82	0.83
Slabs tested by Kinnunen and Nylander[14]						
IA 15a 5	-	0.93	0.68	0.72	0.87	0.78
IA 15a 6	-	0.87	0.63	0.76	0.81	0.74
IA 15b 9	-	0.94	0.62	0.85	0.81	0.80
IA 15b10	-	0.95	0.62	0.85	0.81	0.80
IA 30a24	-	1.04	0.70	0.85	0.78	0.78
IA 30b25	-	1.02	0.55	0.83	0.82	0.79

Note: ** Values taken from reference (18)

7.2.3. Slabs with combined loading and no shear reinforcement.

The slabs were analysed using methods given by Hognestad[4], Moe[19], Anis[18], A.C.I[25] and the proposed solution. Table VII-25 shows the comparison and the results of a statistical treatment are given below:

Method by	Hognestad	Moe	A.C.I.	Anis*	C.P.114	Proposed
Average $\frac{Q_{CAL}}{Q_{TEST}}$	1.559	1.021	1.054	1.038	0.850	0.950
Standard Deviation	0.454	0.277	0.278	0.177	0.395	0.125
Coefficient of variation %	29.101	27.142	26.399	17.074	46.492	13.195

TABLE VII-25

Slabs subjected to combined moment (No shear reinforcement)

Method by	Hognestad	Moe	A.C.I.	Anis*	C.P.114	Proposed Solution
Slab No.	Values of Q_{CAL}/Q_{TEST}					
Slabs tested by Hognestad (4)						
A-11	1.03	0.98	0.63	0.81	0.66	0.80
A-12	1.06	1.02	0.67	0.84	0.70	0.83
Slabs tested by Moe (19)						
M-1A	0.98	1.02	0.67	0.84	0.57	0.88
M-2A	1.79	1.03	1.08	1.08	0.53	1.15
M-4A	2.56	1.09	1.54	1.44	0.58	1.28
M-2	1.54	0.91	1.01	1.03	0.73	1.98
M-3	2.01	0.97	1.26	1.21	0.68	1.09
M-6	1.67	0.99	1.10	1.08	0.66	1.00
M-7	1.10	1.01	0.87	0.92	0.64	0.90
M-8	2.08	1.04	1.51	1.39	0.63	1.1
M-9	1.25	0.97	0.95	0.97	0.61	0.92
M-10	1.75	1.00	1.24	1.19	0.57	1.01
Slabs tested by Anis (18)						
B-2	1.04	1.12	0.80	0.89	0.66	0.98
B-3	1.11	0.82	0.79	0.87	0.77	0.84
B-4	1.49	0.85	1.01	1.07	1.06	0.96
B-5	1.58	0.71	1.03	1.08	1.17	0.87
B-6	1.58	0.61	1.06	1.12	1.28	0.79
Slabs tested by Tankut						
E-1	1.30	1.02	0.99	0.95	0.90	0.88
E-2	1.20	0.83	0.89	0.95	0.80	0.77
Slabs tested by Stamenković						
C/I/1	1.76	1.24	1.39	-	0.93	0.93
C/I/2	2.15	1.14	1.60	-	1.26	0.93
C/I/3	2.29	2.09	1.10	-	2.30	1.01

* Values taken from reference (18)

7.2.4. Slabs with concentric load and shear reinforcement:

The slabs were analysed using methods given by Hognestad[4], Moe[19], A.C.I.[25] and the proposed solution. Table No. VII-26 shows the comparison of $\frac{Q_{CAL}}{Q_{TEST}}$ obtained using different methods. The results of the statistical treatment are given below.

METHOD BY	HOGNESTAD	MOE	ACI	PROPOSED SOLUTION.
Average $\frac{Q_{CAL}}{Q_{TEST}}$	1.037	1.111	0.948	1.044
Standard deviation	0.328	0.348	0.261	0.139
Coefficient of variation %	31.665	31.280	28.14	13.329

TABLE VII-26

Slabs with shear reinforcement subjected to concentric load.

Method by	Hognestad	Moe	ACI	Proposed Formula
Slab No.	Values of Q_{CAL}/Q_{TEST}			
Slabs tested by Anderson[16]				
IIIA 15a S2 66	0.72	0.85	1.07	1.16
IIIA 15a S2 67	0.72	0.84	0.93	1.30
IIIA 15a S3 68	0.77	0.89	0.89	1.24
IIIA 15a S3 69	0.83	0.96	0.96	1.16
IIIA 30a S2 82	0.81	0.88	0.89	0.94
IIIA 30a S2 83	0.81	0.86	0.85	0.86
IIIA 30a S3 84	0.94	1.01	0.90	1.10
IIIA 30a S3 85	0.99	1.06	0.95	1.15
Slabs tested by Hognestad[4]				
B.5	1.02	0.94	0.72	1.07
B.6	1.04	0.98	0.73	0.92
B.10	0.96	1.05	0.93	1.16
B.13	0.98	1.07	0.75	1.06
B.15	0.96	1.05	0.83	1.05
B.16	1.01	1.08	0.75	1.10
Slabs* tested by Moe[19]				
S6-60	-	1.08	0.81	0.91
S7-60	-	0.92	0.70	0.81
S6-70	-	1.02	0.73	0.80
Slabs tested by Wanthur[46]				
5	1.69	1.89	1.49	1.08
6	1.70	1.91	1.50	1.08
8	1.68	1.89	1.58	0.93

* Note: Column size assumed to be that of plate provided.

7.2.5. Slabs with combined load and shear reinforcement:

The only set of results available in this case are those tested by the Author. Table No.VII-27 shows the comparison of $\frac{Q_{CAL}}{Q_{TEST}}$ obtaining using formulae given by Hognestad(4), Moe(19), ACI(25) and the proposed solution. The results of the statistical treatment are given below.

METHOD BY	HOGNESTAD	MOE	ACI	PROPOSED.
Average $\frac{Q_{CAL}}{Q_{TEST}}$	1.219	0.782	0.886	0.939
Standard deviation	0.321	0.175	0.080	0.101
Coefficient of variation %	26.320	22.415	9.066	10.790

TABLE VII-27

Slabs with combined load and shear reinforcement.

FORMULA BY	HOGNESTAD	MOE	ACI	PROPOSED
Slab No.	Values of Q_{CAL}/Q_{TEST}			
Slabs tested by Author				
L1	1.50	0.78	0.73	0.83
L3	1.37	0.65	0.88	0.98
L4	1.16	0.62	0.91	0.80
L5	1.82	0.66	0.91	1.01
L6	0.91	0.76	1.00	1.10
L7	0.92	0.97	0.82	0.8[illegible]
L9	1.06	1.12	0.92	0.98
L.10	1.01	0.70	0.92	0.95

7.3 Comparison with existing methods - Edge columns with moments perpendicular to free edge.

The available test results from Anderson[17], Stamenković[20] and author were analysed using the formulae given by Anderson and ACI[25] (see chapter II for details). In calculating the load according to Anderson, the allowable shear stresses given in the Swedish Code[27] are used with a factor of safety of 1.8. Comparison of $\frac{Q_{CAL}}{Q_{TEST}}$ values obtained using the methods outlined by Anderson, ACI and with the proposed method are given in Table VII-28. Means of calculating the local moment strength and shear strength of the connections are already outlined in section 6.11, chapter VI.

TABLE VII-28

Comparison of $\frac{Q_{CAL}}{Q_{TEST}}$ for Edge Columns.

METHOD BY / SLAB NO.	ANDERSON	ACI	PROPOSED SOLUTION
Slabs tested by Anderson[17]			
1a	1.08	0.51	1.09
1b	0.95	0.32	1.10
1c	1.01	0.48	0.93
Slabs tested by Stamenkovic'[20]			
V/E/1	0.61	0.54	0.88
C1/E/1	0.61	0.41	0.93
C1/E/2	0.63	0.31	0.78
C1/E/3	1.03	0.35	0.67
Slabs tested by Author			
ES1	0.97	0.76	1.10
ES2	0.77	0.44	1.00
ES3	0.97	0.63	0.87
ES4	0.85	0.60	0.75
ES5	0.67	0.46	0.90
ES6	0.85	1.04	1.23
ES7	0.86	0.65	0.77

CHAPTER VIII

CONCLUSIONS AND SUGGESTIONS FOR FUTURE RESEARCH.

8.1. Conclusions.

Based on the observations during tests and the analysis of the test results the following conclusions are drawn.

1. Shear failure occurs on planes inclined at 1:2 (one vertical to two horizontal) starting along the perimeter of the loaded area.

2. The contribution of the dowel in carrying the shear force is considerable and hence cannot be ignored.

3. The effect of combined load is to decrease the ultimate load of the connection.

4. Increase of shear capacity, up to the flexural capacity of the slab can be achieved by the provision of shear reinforcement.

5. Successful anchorage of shear reinforcement can be obtained by tying the shear reinforcement round the main steel.

6. The punching strength can be predicted using the formula,

$$Q_{CAL} = \frac{K_d.b_d.\phi_M.U_w^{0.33} + 0.33(r_{st}\%.U_w)^{0.4}.b_{col}.d_1}{1 + \frac{4EC}{L}}$$

for internal column connections and external column connections with moments parallel to the free edge, and without shear reinforcement.

7. In the case of external column connections with moments normal to the free edge, and corner columns, the punching strength can be predicted using,

$$Q_{CAL} = K_d.b_d.\phi_M.U_w^{0.33} + 0.33(r_{st}\%.U_w)^{0.4}.b_{col}.d_1$$

A more accurate method of calculating the punching strength taking the eccentricity into account is outlined in 6.11 chapter VI. The same formulae may also be applicable to corner columns, but the existing data is insufficient to substantiate this.

8. The required area f shear reinforcement can be calculated using the formula,

$$A_{sq} = \frac{(Q_{flex} - Q_{CAL})}{f_{yq}.\sin\theta} \cdot \left(1 + \frac{4EC}{L}\right)$$

for internal columns and external columns subjected to tangential moments. If conditions are also critical with respect to shear on perimeters beyond the first layer of shear reinforcement additional shear reinforcement should be provided and the area required determined using the above equation with Q_{CAL} modified accordingly.

9. If the local moment strength calculated as outlined in section 6.11, for external columns with moments perpendicular to free edge, is greater than the value of Q_{CAL} given under (7), then shear reinforcement can be provided to increase the strength of the connection. The required area here would be,

$$A_{sq} = \frac{Q_{flex} - Q_{CAL}}{f_{yq}.\sin\theta}$$

$$\text{where } Q_{flex} = \frac{\text{local moment strength}}{\text{eccentricity of the load about the centroid of column perimeter.}}$$

8.2. Recommendations for design:

The design formulae given under section 8.1 are based on the analysis of test specimens representing the column strips, or approximately the line of contraflexure around the column-slab connection. Based on the assumption that the line of contraflexure is at 0.2 times the span length l ; from the centre line of the column (see Fig. 88 - 'l' is the distance between column centres), the corresponding formulae for estimating the punching strength can be obtained by replacing $L = 0.4\,l$ for internal column connections and by replacing $X = 0.4\,l$ and $Y = 0.2\,l$ in the case of edge column connections.

The required shear reinforcement calculated using the proposed equation is to be provided all round the column. Perimeter outside the shear reinforcement should be checked for carrying capacity (Q_{CAL}, calculated taking the appropriate values of b_c and b_d), and further shear reinforcement provided accordingly.

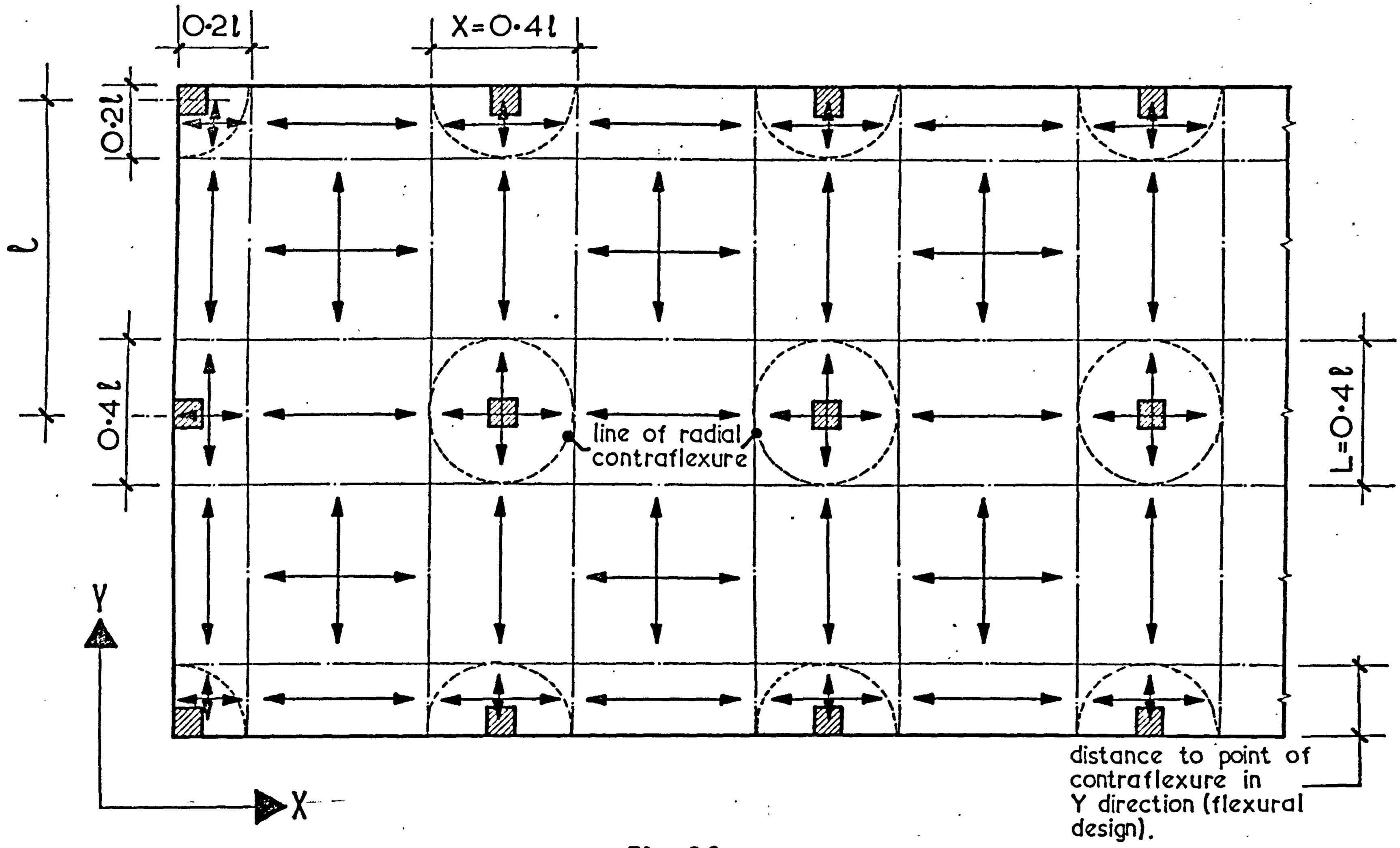
0·2l
X=0·4l
0·2l
l
0·4l
line of radial contraflexure
L=0·4l
Y
X
distance to point of contraflexure in Y direction (flexural design).

Fig. 88.

The procedure is to be repeated for successive perimeters. From the practical point of view, a slab with heavy shear reinforcement, extending a long way from columns, would be a singularly unattractive solution. Under such circumstances, when it required to provide more than two layers of shear reinforcement to achieve a particular punching strength, it is preferable to use a thicker slab. Particular attention must be paid to anchorage requirements in the use of shear reinforcement, and the limitation for diameter of the shear reinforcement must be adhered to as outlined in section 6.9 chapter VI.

8.3. Suggestion for future research.

In order to complete the picture of behaviour of slabs under concentric and combined loading, more work should be done on slabs with different types of reinforcing bars to estimate the exact contribution of dowel force for the various types of steel.

Also more experimental work is needed on external columns (particularly corner columns) subjected to concentric and combined loading with and without shear reinforcement.

REFERENCES.

(1) TALBOT, A.N. "Reinforced concrete wall footings and column footings", University of Illinois Engineering Experiment Station, Bulletin No. 67, March 1913.

(2) GRAF, O. "Tests of reinforced concrete slabs under concentrated load applied near one support", ("Versuche über die Wiederstandfähigkeit von Eisenbetonplattern under konzen trierter Last nahe einem Auflager"), (In German), Deutcher Ausschuss für Eisenbeton (Berlin) Heft 73, 1933.

(3) GRAF, O. "Strength tests of thick reinforced concrete slabs supported on all sides under concentrated loads", ("Versuche über die Wiederstandsfähigkeit von allseitigen aufliegenden dicken Eisenbetonplatten under Einzellasten"), (In German), Deutscher Ausschuss für Eisenbeton (Berlin) Heft 88, 1938.

(4) ELSTNER, R.C. and HOGNESTAD, E., "Shearing strength of Reinforced concrete slabs", Journal of the American Concrete Institute (July, 1956); Proceedings, 53, 29-58 (1956).

(5) ELSTNER, E.C., and HOGNESTAD, E., "An investigation of reinforced concrete slabs failing in shear", University of Illinois, Department of Theoretical and Applied Mechanics. Mimeographed Report, March 1953.

(6) KEEFE, R.A., "An investigation on the effectiveness of diagonal tension reinforcement in flat slabs", Thesis, Massachusetts Institute of Technology, June 1954.

(7) WHITNEY, C.S.,"Ultimate Shear Strength of Reinforced Concrete Flat Slabs, Footings, Beams and Frame Members without Shear Reinforcement", Journal of the American Concrete Institute (October 1957); Proceedings, 54, (1957).

(8) BASE, G.D., "Some Tests on the Punching Shear Strength of Reinforced Concrete Slabs". Technical Report, July, 1959, Cement and Concrete Association, London.

(9) ROSENTHAL, I., "Experimental Investigation of Flat Plate Floors". Journal of the American Concrete Institute, Proceedings, Vol. 56. (1959).

(10) YITZHAKI, D., "Punching Strength of Reinforced Concrete Slabs", Journal of the American Concrete Institute, Proceedings V.63, No. 5, May 1966.

(11) DI STASIO, J and VAN BUREN, M.P. "Transfer of Bending Moment between Flat Plate Floor and Column". Journal of the American Concrete Institute, Proceedings V.32, No. 3, Sept., 1960.

(12) BERESFORD, F.D., "Tests of Edge Column Connections of a Flat Plate Structure". Civil Engineering Transactions, The Institute of Engineers Australia. Vol CE9, No.2, October 1967.

(13) LONG, A.E. and BOND, D. "Punching Failure of Reinforced Concrete Slabs". Paper No. 7002, Proceedings, The Institution of Civil Engineers, Vol. 37, May 1967.

(14) KINNUNEN, S. and NYLANDER, H, 1960 "Punching of Concrete Slabs Without Shear Reinforcement." Transactions of the Royal Institute of Technology, No. 158, Stockholm, 1960.

(15) KINNUNEN, S., "Punching of Concrete Slabs with Two-way Reinforcement, with special reference to Dowel Effect and Deviation of Reinforcement from Polar symmetry". Transactions of the Royal Institute of Technology, No. 198, Stockholm, 1963.

(16) ANERSSON, J.L., "Punching of Concrete Slabs with Shear Reinforcement", Paper No. 212, Transactions of the Royal Institute of Technology, Stockholm, 1963.

(17) ANERSSON, J.L., "Punching of Slabs Supported on Columns at Free Edge. Nordisk Betong, No. 2, 1966.

(18) ANIS, N.N., "Shearing Strength of Reinforced Concrete Flat Slabs without Shear Reinforcement". Ph.D. Thesis, University of London, 1970.

(19) MOE, J., "Shearing Strength of Reinforced Concrete Slabs and Footings under Concentrated Loads". Bulletin D.49, Development Department, Portland Cement Association, Illinois (1961).

(20) STAMENKOVIĆ, A., "Local Strength of Flat Slabs at Column Heads". Ph.D. Thesis, University of London, 1969.

(21) HANSON, N.W. and HANSON, J.M., "Shear and Moment Transfer Between Concrete Slabs and Columns". Journal of the Portland Cement Association, Research and Development Laboratories, Vol. 10, No. 1, January 1968.

(22) B.S.I. "The Structural use of Reinforced Concrete in Building" - British Standard Code of Practice, C.P.114, London 1957.

(23) A.C.I. Standards, "Building Code Requirements for Reinforced Concrete." A.C.I.318-63, 1963.

(24) A.C.I. Committee 318, "Commentary on Building Code Requirements for Reinforced Concrete A.C.I.318-63." A.C.I. Manual of Concrete Practice, Part 2, pp.318-145 to 318-239 (1967).

(25) "Proposed Revision of A.C.I.318-63, Building Code requirements for Reinforced Concrete". Journal of the American Concrete Institute, Proceedings, V.67, February 1970.

(26) Standards Association of Australia 1963 - Code of Practice for Concrete Buildings (CA2-1963).

(27) Kl-1964 "Förslag Till Bestämmelser För Dimensionering Av Betongplattor Pa Pelare Jämte Utdrag Ur Kommentarer" (In Swedish - English Translation by Dr. P.E.Regan).

(28) BAUMANN, T., "An Experimental Study of Dowel Action by the main Reinforcement of Reinforced Concrete Beams". A synopsis of "Versuche zum Studium der Verdübelungswirkung der Bericht Nr. 77, Materialprüfungsamt für des Bauwesen der Technischen Hochschule München.

(29) KREFELD, W.J. and THURSTON, C.W., "Contribution of Longitudinal Steel to Shear Resistance of Reinforced Concrete Beams". Journal of the American Concrete Institute, Proceedings, March 1966.

(30) ROY, M.K., "A Study of Dowel Force Resistance in Reinforced Concrete Beams in relation to the Effects of Shear", M.Sc. Dissertation, Department of Structural Engineering, Manchester College of Science and Technology, May 1965.

(31) ARROYO, J., "Study of Dowel Action by the Main Reinforcement of Reinforced Concrete Beams", A Thesis submitted for the Diploma of Membership of Imperial College, London, December 1969.

(32) TAYLOR, N.P.J., "Investigation of the Dowel Shear Force carried by the Tensile Steel in Reinforced Concrete Beams". TRA/431, Cement and Concrete Association, November, 1967.

(33) FRIBERG, B.F., "Design of Dowels in Transverse Joints of Concrete Pavements". Paper No. 2091, Transactions of A.S.C.E., Vol. 105, 1940.

(34) BRANDTZAEG, A., "Failure of a Material Composed of Non-isotropic Elements: an Analytical Study with Special Application to Concrete". Det Konge lige Norske Videnskabers Selskabs. Shrifter. No. 2, 1927.

(35) REINIUS, E., "A Theory of theDeformation and the Failure of Concrete". C & C.A. Library Translation from Betong 1955. No. 1 Cj.63 (3/57).

(36) BAKER, A.L.L., "An Analysis of Deformation and Failure Characteristics of Concrete". Mag. Concr. Res. 1959, 11, No.33.

(37) BAKER, A.L.L., "A Criterion of Concrete Failure" - Institution of Civil Engineers, Proceedings, Feb. 1970.

(38) BRESLER, B and PISTER, K.S., "Failure of Plain Concrete Under Combined Stresses". Proceedings, American Society of Civil Engineers, 81 Separate No. 674, April, 1955.

(39) BRESLER, B and PISTER K.S., "Strength of Concrete under Combined Stresses". Journal of the American Concrete Institute (September, 1958); Proceedings, 55, Vol. 30, No. 3.

(40) McHENRY, D. and KARNI, J., "Strength of Concrete Under Combined Tensile and Compressive Stresses", Journal of the American Concrete Institute (April, 1958), Proceedings, Vol. 29, No. 10 (1958).

(41) REEVES, J.S., "The Strength of Concrete Under Combined Direct and Shear Stresses". Technical Report TRA/365, November 1962, Cement and Concrete Association, London.

(42) GOODE, C.D. and HELMY, M.A., "The Strength of Concrete under Combined Shear and Direct Stress". Mag. of Conc. Research, Vol. 19, No. 59, June 1967.

(43) REGAN, P.E., "Shear in Reinforced Concrete (An Analytical Study)" Civil Engineering Department, Imperial College, Report to C.I.R.I.A., 1971.

(44) IVY, C.B., "The Diagonal Tension Resistance of Structural Lightweight Concrete Slabs", Ph.D. Dissertation, Graduate College of the Texas A & M University, January 1966.

* (45) MOWRER, R.D. and VANDERBILT, M.D., "Shear Strength of Lightweight Aggregate Reinforced Concrete Flat Plates". A.C.I. Journal, November 1967.

(46) WANTHUR, H.Z., "Dimensioning of Flat Slabs in the Column Region with Simultaneous Consideration of the Bending and Vertical Reinforcement". Dissertation au der Rijksuniversiteit Gent, 1969.

(47) JOHANSEN, K.W., "Yield Line Theory". Cement and Concrete Association, London, April 1962.

(48) WOOD, R.H., "Plastic and Elastic Design of Slabs and Plates". Thames and Hudson, London 1961.

(49) "Recommendations for an International Code of Practice for Reinforced Concrete". Comite Europeen du Beton, Cement and Concrete Association.

(50) NEWMAN, K., "Criteria for the Behaviour of Plain Concrete under Complex States of Stress". International Conference on the structure of Concrete. Paper F.1, Imperial College, London, 1965.

(51) TIMOSHENKO, S.P., WOINOWSKY-KRIEGER, S., "Theory of Plates and Shells". McGraw Hill Company, Inc.

(52) Bulletin D'Information No. 57, Comite Europeen du Beton. Septembre 1966.

(53) MANTEROLA, M.J., "Poinconnement de dalles sans armature d'effort trenchant". - Bulletin D'Information No. 58, Comite Europeen du Beton. Octobre 1966.

(54) BARA, H.C., "Investigation of the Effect of Axial Loads on the Shear Strength of Reinforced Concrete Beams", Ph.D. Thesis to be submitted to London University, 1971.

(55) PLACAS, A., "Shear Failure of Reinforced Concrete Beams", Ph.D., Thesis, University of London, November 1969.

(56) MOAYER, M., "Shear and Torsion in Prestressed Concrete Beams", Ph.D. Thesis to be submitted to London University, 1971.

(57) FORSELL, C., and HOLMBERG, A., "Concentrated Load on Concrete Slabs" (Stämpellast pa plattor av belong"), (In Swedish), Betong (Stockholm), 31, No. 2, 1946.

(58) RICHART, F.E., "Reinforced Concrete Wall and Column Footings", Journal of the American Concrete Institute (October - November, 1948); Proceedings, 45, 97-127, 237-260 (1948).

(59) HOGNESTAD, E., "Shearing Strength of Reinforced Concrete Column Footings", Journal of the American Concrete Institute (Nov. 1953); Proceedings, 50, (1953).

(60) HOGNESTAD, E., ELSNER, R AND HANSON, J., "Shear Strength of Reinforced Structural Lightweight Concrete Slabs", Journal of the American Concrete Institute, Proceedings, 61, June 1964.

(61) GURALNICK, S.A., and LAFRAUGH, R.W., "Laboratory Study of a 45 sq.ft. Square Flat Plate Structure". Journal of the American Concrete Institute, Proceedings, 60, September 1963.

(62) RICHART, F.E. and KLUGE, R.W., "Tests of Reinforced Concrete Slabs Subjected to Concentrated Loads". University of Illinois Bulletin Vol. XXXVI No. 85 (1939).

(63) TANKUT, A.T.,"The Behaviour of the Reinforced Concrete Flat Plate Structure Subjected to Various Combinations of Vertical and Horizontal Loads". Ph.D. Thesis, University of London, November, 1969.

(64) NIELSEN, M.P., "Om jernbeton skivers styrke, (On the strength of reinforced concrete plates) Tekn Dr Thesis, Denmarks Terniske Hojskole 1967, Polyteknisk Forlag, Aalborg, Denmark 1969.